TNF

Technisch-Naturwissenschaftliche
Fakultät

The Multiharmonic Finite Element and Boundary Element Method for Simulation and Control of Eddy Current Problems

DISSERTATION

zur Erlangung des akademischen Grades

Doktor

im Doktoratsstudium der

Technischen Wissenschaften

Eingereicht von:
Dipl.-Ing. Michael Kolmbauer Bakk.techn.

Angefertigt am:
Institut für Numerische Mathematik

Beurteilung:
O. Univ.Prof. Dipl.-Ing. Dr. Ulrich Langer (Betreuung)
Prof. Dr. Fredi Tröltzsch

Linz, August, 2012

Abstract

This thesis deals with the simulation and control of time-dependent, but time-periodic eddy current problems in unbounded domains in $\mathbb{R}^3$. In order to discretize such problems in the full space-time cylinder, we use a non-standard space-time discretization method, namely, the *multiharmonic finite element and boundary element method*. This discretization technique yields large systems of linear algebraic equations, whereas the fast solution of these systems determines the efficiency of this method. Here, suitable preconditioners are needed in order to ensure *efficient* and *parameter-robust* convergence rates of the applied iterative method. Therefore, the main focus of this thesis lies on the construction and analysis of robust and efficient preconditioning strategies for the resulting systems of linear equations.

The basic idea of the *multiharmonic approach* is to use a Fourier series approximation as a discretization technique in time. This allows to switch from the time domain to the frequency domain, and therefore, to replace the solution of a time-dependent problem by the solution of a system of time-independent problems for the Fourier coefficients. Due to the infinite exterior domain on the one hand, and inhomogeneities and the possible presence of sources in the interior domains on the other hand, the symmetric finite element - boundary element coupling method is used to discretize the Fourier coefficients in space.

The main challenge in the construction of *efficient* and *parameter-robust* preconditioners for the resulting frequency domain equations is indicated by the full range of crucial model, regularization and discretization parameters, that imping on the convergence rate of any iterative method. We use matrix and operator interpolation techniques to construct parameter-robust, block-diagonal preconditioners in a straightforward fashion. Furthermore, we prove rigorous bounds for the condition numbers of the preconditioned frequency domain equations, that are independent of all involved model, regularization, and discretization parameters. Numerical examples illustrate the robustness of these block-diagonal preconditioners.

In order to obtain efficient preconditioners, the diagonal blocks have to be replaced by efficient (and robust) preconditioners. The individual diagonal blocks rely on the solution of standard H^1 or $\mathbf{H}(\mathbf{curl})$ problems, for which efficient and robust preconditioners are already available.

First, we consider and analyze the eddy current problem. We start by investigating the pure multiharmonic finite element approach on a bounded domain, before we tackle the case of unbounded domains in terms of the multiharmonic finite element - boundary element coupling method. For both, we construct block-diagonal preconditioners for various types of variational formulations.

Second, we consider the eddy current optimal control problem with distributed control. Again we apply the multiharmonic finite element - boundary element coupling method to discretize in time and space. After deriving the optimality system, efficient and parameter-robust preconditioners are constructed for the resulting system of linear equations.

A challenging topic in optimal control problems is the incorporation of various constraints imposed on the state or control variables in the optimization procedure. These constraints render the resulting system of equations nonlinear. There, the semi-smooth Newton linearization leads to problems, where our constructed block-diagonal preconditioners can also be useful.

Zusammenfassung

Diese Dissertation befasst sich mit der Simulation und Steuerung von zeitabhängigen, aber zeit-periodischen Wirbelstromproblemen auf unbeschränkten Gebieten in $\mathbb{R}^3$. Wir verwenden die *multi-harmonische Finite Elemente und Rand Elemente Methode*, um eine volle Diskretisierung des Pro-blems in Zeit und Raum durchzuführen. Dieses Diskretisierungsverfahren führt zu großdimensionier-ten, linearen Gleichungssystemen, deren schnelle Lösung ganz wesentlich die Effizienz dieser nume-rischen Methoden bestimmt. Hier werden Vorkonditionierer benötigt, um zu gewährleisten, dass die Konvergenz eines iterativen Verfahrens, angewendet auf dieses Gleichungssystem, nicht von der Größe des Problems, oder von anderen Parametern beeinflusst wird. Das Hauptaugenmerk liegt daher auf der Konstruktion und Analyse von robusten und effizienten Vorkonditionierungsstrategien.

Der *multiharmonische Ansatz* basiert auf der grundlegenden Idee, die Zeitdiskretisierung durch eine Fourierreihenapproximation durchzuführen. Dieser Ansatz ermöglicht eine Berechnung im Frequenz-bereich, d.h., ein zeitabhängiges Problem wird durch ein System von zeitunabhängigen Problemen in den Fourierkoeffizienten ersetzt. Aufgrund des unbeschränkten Außenraumes einerseits, und In-homogenitäten und der möglichen Präsenz von Quelltermen im Innenraum andererseits, verwenden wir eine symmetrische Finite Elemente - Rand Elemente Kopplungsstrategie um eine Diskretisierung der Fourierkoeffizienten im Raum vorzunehmen.

Die Herausforderung in der Konstruktion von effizienten und parameter-robusten Vorkonditionierern liegt in der richtigen Behandlung einer Serie von kritischen Modell-, Regularisierungs- und Diskre-tisierungsparametern. Wir verwenden Operator- und Matrixinterpolationstechniken um parameter-robuste, block-diagonale Vorkonditionierer zu konstruieren. Weiters zeigen wir explizite Schranken für die Konditionszahlen der vorkonditionierten Gleichungssysteme, welche nicht von den Modell-, Regularisierungs- oder Diskretisierungsparametern abhängen. Unsere theoretischen Ergebnisse be-züglich der Robustheit der block-diagonalen Vorkonditionierer werden in numerischen Experimenten bestätigt. Die Konstruktion von effizienten und robusten Vorkonditionierern wird durch den Aus-tausch der diagonalen Blöcke durch weitere effiziente (und robuste) Standard-Vorkonditionierer kom-plettiert.

Zunächst betrachten wir das Wirbelstromproblem. Wir analysieren zunächst den multiharmonischen Ansatz für den Spezialfall einer Finite Elemente Diskretisierung im Falle eines beschränkten Gebietes, bevor der allgemeine Fall eines unbeschränkten Gebietes mit Hilfe der symmetrischen Kopplung in Angriff genommen wird. Für beide Fälle, den beschränkten und den unbeschränkten, konstruieren und analysieren wir block-diagonale Vorkonditionierer für verschiedene Arten von Variationsformu-lierungen.

Weiters betrachten wir das optimale Steuerungsproblem für das Wirbelstromproblem. Auch hier wird die multiharmonische Finite Elemente - Rand Elemente Methode als Zeit- und Raumdiskreti-sierungstechnik angewendet. Für das Optimalitätssystem wiederum konstruieren wir effiziente und parameter-robuste, block-diagonale Vorkonditionierer.

Eine weitere Herausforderung in der Behandlung von optimalen Steuerungsproblemen stellen zusätz-liche Nebenbedingungen an die Kontrolle oder die Steuerung dar. Die numerische Behandlung die-ser Nebenbedingungen führt auf nichtlineare Gleichungssysteme. Hier führt die semiglatte Newton-Linearisierung auf Problemstellungen, welche durch block-diagonale Vorkonditionierungsstrategien effizient gelöst werden können.

Preface

This thesis covers results that were achieved within my research at the Institute of Computational Mathematics and the Doctoral Program "Computational Mathematics" at the Johannes Kepler University Linz. I would like to express my gratitude to many people for assisting me during this dissertation.

First of all, I would like to express my thanks to my supervisor Prof. Ulrich Langer, for his support, guidance and encouragement throughout my thesis work with his curiosity, ideas and questions.

At the same time I would like to thank Prof. Fredi Tröltzsch for showing so much interest in my work and for co-refereeing this thesis.

I owe special thanks to Prof. Walter Zulehner for introducing me to the topic of robust preconditioning techniques for saddle point problems. In this context I also want to thank my colleague Dipl.-Ing. Markus Kollmann for his valuable contributions and for many fruitful and enlightening discussions concerning this topic. Also, I am much obliged to the authors of ParMax, and especially to Dr. Clemens Pechstein, for being able to implement my program codes for the numerical experiments in their framework.

Furthermore I acknowledge the Institute of Computational Mathematics and the Doctoral Program "Computational Mathematics" at the Johannes Kepler University of Linz for the environment and technical support.

I am eternally thankful to my parents, Alois and Elfriede Kolmbauer, for the life long assistance and trust, which stretched all the way through my schooling and university, during the diploma thesis, as well as during this dissertation. Many thanks go out to my sisters Angelika and Veronika and my brothers Markus and Johannes. Furthermore my special thanks go to Anja for many years of love, fun and laughter as well as her constant support and understanding.

<div align="right">

Michael Kolmbauer
Linz, August 2012

</div>

Contents

Introduction

State of the Art

Electromagnetic processes are present everywhere in our daily life. Classical applications include generators, transformers and motors. Typically, electromagnetic phenomena are modeled by partial differential equations, namely Maxwell's equations, which are the basis for the mathematical analysis and numerical treatment.

Eddy current problems

A special class of electromagnetic problems arises, when at least one of the electromagnetic fields varies only slowly in time. Indeed, this simplified model has a high practical significance in low frequency applications, such as in the numerical simulation of electric motors, relays and transformers. In this case, the magnetic induction is the dominant factor, and the contribution of the displacement currents is negligible in comparison to the currents. Therefore, the eddy current model is well-established in the engineering literature.

Deriving the vector potential formulation, one ends up with a partial differential equation of the type

$$\sigma \frac{\partial \mathbf{y}}{\partial t} + \mathbf{curl}\,(\nu\,\mathbf{curl}\,\mathbf{y}) = \mathbf{u}, \quad \text{in } \Omega \times (0, T), \tag{1}$$

with the unknown function $\mathbf{y}$, the given coefficients σ and ν, the source term $\mathbf{u}$, the computational domain $\Omega \subset \mathbb{R}^3$ and a prescribed time interval $(0, T)$. The coefficient ν refers to the reluctivity. In general ν depends on the magnetic induction $|\mathbf{curl}\,\mathbf{y}|$, which renders (1) to be nonlinear, but in many cases it is sufficient to model ν by a linear function. In particular, in non-conductors, ν is constant. The coefficient σ refers to the electric conductivity. In typical applications (e.g. electrical machines), the computational domain Ω consist of conductors, e.g. iron parts, and non-conductors, e.g. air regions, wherein the conductivity is positive and is identical zero, respectively. Due to this specific regime, (1) is sometimes referred as *parabolic-elliptic eddy current equation*. Therefore, the analysis of these kinds of equations is a challenging issue, since we are dealing with two totally different equations in the conducting and non-conducting domains, respectively. Beside many approaches, we mention the works [3, 10, 17, 97], that provide a rigorous analysis for the elliptic-parabolic eddy current problem, including existence and uniqueness results.

For a comprehensive mathematical theory on Maxwell's equations and eddy current problems see, e.g., the monographs [91, 153, 118] and [6], respectively.

Optimal control problems

During recent years, the importance of solving optimization problems with constraints in form of partial differential equations has been growing. In typical optimal control problems, one wants to determine the *control* $\mathbf{u}$, and the corresponding *state* $\mathbf{y}$, such that a given cost functional is minimized. In the research area of optimal control of electromagnetic fields the basic interest is on

the minimization of problems of the following type: Find $(\hat{\mathbf{y}}, \hat{\mathbf{u}})$, such that

$$\mathcal{J}(\hat{\mathbf{y}}, \hat{\mathbf{u}}) = \min_{(\mathbf{y}, \mathbf{u})} \mathcal{J}(\mathbf{y}, \mathbf{u}), \quad \text{subject to the state equation} \quad (1), \tag{2}$$

with the unknown functions $\mathbf{y}$ and $\mathbf{u}$, and a prescribed cost functional $\mathcal{J}$, which we want to minimize. Usually, the partial differential equation (PDE), also called *state equation*, is treated as a constraint. Using this approach, one can solve the optimization problem by solving the corresponding system of optimality conditions, called the Karush-Kuhn-Tucker system (KKT system). In this setting, we are dealing with a state equation of parabolic-elliptic type. Therefore, the optimality system of partial differential equations is of parabolic-elliptic type as well.

Recently, the consideration of time-periodic optimal control problems, i.e, the minimization of a functional with respect to a time-periodic parabolic partial differential equation, has also seen an increasing interest, see e.g., [1, 65, 95, 133, 145].

Beside the PDE constraints, in some applications, inequality or box constraints imposed on the state or control are also of importance. Indeed, in the case of Maxwell's equations, box constraints imposed on the state are important to filter out singularities in the solution. In the standard approach, these constraints can be handled by a simple projection to the box [108] leading to a nonlinear optimality system that can be solved by superlinearly convergent, semi-smooth Newton methods [76, 89].

For a comprehensive introduction in optimal control problems we refer to [151]. Furthermore, for works on optimal control of electromagnetic fields, we mention [52, 64, 65, 158, 159].

FEM, BEM and FEM-BEM coupling

In general, it is not possible to solve the partial differential equations arising from electromagnetic problems analytically. Therefore, one aims at finding approximate solutions, which solve a discrete system stemming from the infinite-dimensional one. The most common approaches for the discretization of PDEs are the finite element method (FEM) and the boundary element method (BEM). Each of these methods has its own advantages accompanied by some weakness.

FEM The finite element method (FEM) is based on the weak formulation of partial differential equations and has certainly been established as the most powerful tool in the discretization of linear and nonlinear partial differential equations. Its main advantage is probably the fact that it is applicable to a huge class of problems, be they linear or nonlinear, with varying coefficients, on complex domains with different types of boundary conditions.

In *Computational Electromagnetics* the natural function space is $\mathbf{H}(\mathbf{curl})$, which has a lower smoothness as H^1, since only tangential continuities over material interfaces are required. The classical $\mathbf{H}(\mathbf{curl})$-conforming finite element spaces have been introduced by Nédélec in [120, 121].

A rather complete overview on finite element methods for Maxwell's equations can be found in [49, 79, 118, 160].

BEM In the past decades, the method of boundary integral equations has become a versatile and powerful tool for numerical modeling of physical systems. Using the fundamental solution of a differential operator, one can derive integral equations that completely describe the underlying boundary value problem involving the unknown function only on the boundary of the computational domain. The discretization of these boundary integral equations is called boundary element method (BEM). An obvious advantage is, that only the boundary of the computational domain has to be discretized. This allows, on the one hand, a reduction of dimension, and, on the other hand to treat unbounded domains. Unfortunately, due to the requirement of the knowledge of a fundamental solution, the application of BEM is restricted to specific settings.

Indeed, in eddy current computations the fundamental solution is known for the case of constant coefficients (conductivity, reluctivity). Furthermore, the description of suitable boundary element spaces for Maxwell's equation is a very delicate part. Recently, the appropriate trace spaces for

Maxwell's equation have been introduced by Buffa and Ciarlet in [33, 34]. Based on these results, the boundary element method has been made available also for Maxwell's equations and especially eddy current problems in Lipschitz domains, see e.g. [35, 81]. The boundary element method for Maxwell's equations is also addressed in [36, 37, 84].

FEM-BEM coupling In many situations, it is of interest to couple FEM and BEM to exploit the advantages of both methods, also known as *marriage a la mode - the best of both worlds* [163]. For instance, the finite element method is suitable for heterogeneous coefficients, source terms, and nonlinearities, whereas the boundary element method can be used to model subdomains with constant coefficients (such as large air regions) and even unbounded regions. These properties are very typical for eddy current problems: In the conducting parts, due to the presence of nonlinearities in the reluctivity, highly varying conductivity and possible source terms, a finite element scheme based on edge elements is the preferable choice. In the non-conducting parts (e.g. air), the unbounded domains can be tackled by BEM, since there we are dealing with a homogeneous problem with constant coefficients. Based on the remarkable work of Costabel [42] on the symmetric coupling method, a symmetric FEM and BEM coupling for the time-harmonic eddy current problem in the frequency domain has been performed and analyzed in [80]. Even more recent, FEM and BEM coupling for the time-dependent eddy current problem posed in the whole space-time domain are analyzed in [2, 134, 135]. The main advantage of the latter approaches is that they allow a great flexibility for the choice of the discretization techniques in space and mainly in time.

Indeed, the coupling of FEM and BEM has been widely used for the numerical simulation of electromagnetic fields, see e.g. [83, 111, 137, 144].

Fourier series approximation techniques

Fourier series approximation methods are a well established tool in the discretization of partial differential equations. One has to distinguish between two fundamentally different kinds of application. In some regimes the spatial dimension is approximated in terms of a Fourier series, e.g., [22, 27, 71], while in other application, the issue of interest is to discretize in time, e.g., [17, 95]. The latter mentioned approach expands a time-dependent function $u(t)$ in terms of a Fourier series, i.e.,

$$u(t) = \sum_{k=0}^{\infty} \left[u_k^c \cos(k\omega t) + u_k^s \sin(k\omega t) \right],$$

where ω is the frequency, k is referred as the mode and u_k^c, u_k^s are the amplitudes associated to the mode k. For numerical approximation, the infinite series are truncated at a finite index $N \in \mathbb{N}$. Due to this expansion into several *harmonics*, the name *multiharmonic approach* is also very popular. Indeed, for time-dependent problems, this means that we can switch from a time-dependent problem in the full time domain, to a time-independent problem in the frequency domain.

One special regime is the *time-harmonic* one, meaning that only one frequency mode is taken into account, e.g., time-harmonic full Maxwell's equations, time-harmonic eddy current problems, time-harmonic wave equations (Helmholtz problems) and others.

Time-harmonic problems In many practical applications, e.g. in *Computational Electromagnetics*, the excitation is time-harmonic. For instance, if the source $\mathbf{u}$ in (1) is provided by an alternating current in terms of sine and cosine terms, it has the structure

$$\mathbf{u}(\mathbf{x}, t) = \mathbf{u^c}(\mathbf{x}) \cos(\omega t) + \mathbf{u^s}(\mathbf{x}) \sin(\omega t). \tag{3}$$

Under the assumption, that (1) is linear, the solution $\mathbf{y}$ exhibits the same time-harmonic behavior as well. This allows to switch from the time domain to the frequency domain, and, therefore, to replace a time-dependent problem by a system of time-independent problems. Furthermore, the unknown amplitudes $\mathbf{y^c}$ and $\mathbf{y^s}$ of the solution $\mathbf{y}$ can be approximated by spatial discretization techniques, like

the finite element method. In general, it turns out, that when dealing with nonlinear problems, the time-harmonic approximation is not enough, since due to the nonlinearity, the solution depends on higher harmonics as well. This leads to the framework of harmonic balance method in time-periodic settings.

Multiharmonic FEM   It is quite common to combine the multiharmonic approach as a discretization technique in time with the finite element method as a discretization technique in space, leading to the well-known *harmonic balanced finite element method* (HB-FEM) also called *multiharmonic finite element method* (MH-FEM). The idea is to discretize in time in terms of a truncated Fourier series and perform a discretization of the Fourier coefficients in terms of the finite element method. Indeed, in this case an approximation of the solution **y** in terms of

$$\mathbf{y}(\mathbf{x},t) \approx \mathbf{y}_{\mathbf{N},\mathbf{h}}(\mathbf{x},t) = \sum_{k=0}^{N} \left[\mathbf{y}_{\mathbf{k},\mathbf{h}}^{\mathbf{c}}(\mathbf{x}) \cos(k\omega t) + \mathbf{y}_{\mathbf{k},\mathbf{h}}^{\mathbf{s}}(\mathbf{x}) \sin(k\omega t) \right] \tag{4}$$

is used. The *harmonic balance finite element method* (HB-FEM) was introduced in 1988 by Yamada and Bessho in [155] for the first time by simply combining the harmonic balance method [43, Chapter 6] and the finite element method. They applied HB-FEM to the two-dimensional quasi-stationary Maxwell's equations in order to compute the time-periodic solution, when an alternating current is applied. There followed a sequence of papers by this group, e.g. [113, 114, 115, 156, 157]. In these works the main focus is on the application of HB-FEM, therefore no theoretical results or proofs are given. Furthermore, the issue of solving the corresponding system of linear equations is not addressed either.
The first rigorous analysis of MH-FEM applied to the time-periodic eddy current problem is provided in [16, 17, 18]. Beside the numerical analysis, including existence and uniqueness results and error estimates, also an efficient solver is stated without any theoretical analysis. Indeed, the development of robust and efficient solvers is crucial for the competitiveness of the MH-FEM method.
The issue of developing fast solution procedures for the resulting huge systems of equations is addressed, e.g., in [40, 48, 51, 58].
For other pioneering works on HB-FEM, we refer to [11, 12, 13, 66, 67, 92].

Solving techniques

After an arbitrary discretization in space and time, systems of linear algebraic equations have to be solved. Focusing on computational time, one heads for developing solvers of *optimal complexity*, i.e., the operations required to solve the problem is proportional to the number of unknowns. While in small scale applications, direct solvers, e.g. PARDISO[1] or UMFPACK[2], are the methods of choice, in large scale computations the application of those is illusive, and, therefore, iterative solution methods have to be taken into account.

Saddle point problems and preconditioning   The system of linear equations stemming from harmonic balance approximations, optimal control problems or FEM-BEM coupling methods typically obtain saddle point structures of the form

$$\text{Find } \mathbf{x}: \quad \underbrace{\begin{pmatrix} A & B^T \\ B & -C \end{pmatrix}}_{=:\mathcal{A}} \mathbf{x} = \mathbf{f}, \tag{5}$$

where, due to the properties of the underlying matrices, the system matrix $\mathcal{A}$ in (5) is symmetric and indefinite. One of the most famous iterative method is the *conjugate gradient* (CG) method, cf. [74],

---

[1] http://www.pardiso-project.org/
[2] http://www.cise.ufl.edu/research/sparse/umfpack/

but due to the indefiniteness of the system matrix $\mathcal{A}$ it may fail if applied to (5). One way out is to apply the Bramble Pasciak CG [30] or Zulehner CG [143], that require the construction of appropriate inner products, such that $\mathcal{A}$ as given in (5) becomes positive definite and self-adjoint with respect to the new inner product. Other very common choices for iterative methods are Krylov subspace methods such as the *minimal residual method* (MinRes) [128], that is suitable for solving symmetric systems of linear equations, or the *generalized minimal residual method* (GmRes) [139], that is suitable for solving even general regular systems. Nevertheless the convergence of these iterative methods applied to (5) suffers from the number of unknowns (mesh size) and possibly crucial parameters, like discretization, regularization, model or cost parameters. Anyhow, in the situation, where only a few isolated eigenvalues lie outside an otherwise nice spectrum, the MinRes method can deal with these kind of problems efficiently, see e.g. [124, 126]. In general, there is a full range of isolated eigenvalues, e.g. due to the presence of large jumps in material parameters, and therefore, preconditioning is an important issue. Among the works that are concerned with this topic we mention the review article [23]. Recently, it was discovered, that the choice of the preconditioners is equivalent to choosing the right inner product in the underlying Hilbert space, see e.g., [117, 164]. This leads to the framework of block-diagonal and operator preconditioning. For early works, see e.g., [8, 82, 112].

Interpolation technique   Recently, the work of Zulehner [164] builds a bridge, that strongly relates the subject of finding parameter-robust and block-diagonal preconditioners for saddle point problems of the form (5) and the topic of Hilbert space and matrix interpolation. Indeed Zulehner's theory provides the fantastic breakthrough, that the appropriate scalar products for the underlying Hilbert spaces can be derived by interpolating between the well-known Schur complement preconditioners [109, 119] for (5), given by

$$\mathcal{P}_0 = \begin{pmatrix} A & 0 \\ 0 & C + BA^{-1}B^T \end{pmatrix}, \qquad \mathcal{P}_1 = \begin{pmatrix} A + B^TC^{-1}B & 0 \\ 0 & C \end{pmatrix}.$$

In order to perform this interpolation, the abstract space and matrix interpolation technique, developed e.g. in [4, 24], emerges as an important tool.

Standard preconditioners and solvers   In practical applications, the blocks of the theoretical block-diagonal preconditioners have to be replaced by robust and (almost) optimal preconditioners. In many applications, the diagonal blocks correspond to standard $\mathbf{H}(\mathbf{curl})$ or H^1 problems like

$$(\alpha\,\mathbf{curl}\,\mathbf{u}, \mathbf{curl}\,\mathbf{v})_\mathbf{0} + (\beta\mathbf{u}, \mathbf{v})_\mathbf{0} \quad \text{and} \quad (\alpha\nabla p, \nabla q)_\mathbf{0} + (\beta p, q)_0,$$

for the FEM part. The coefficient α and β are usually positive, piecewise constant functions, that may have large jumps. For these kinds of problems, there is a full zoo of solvers and preconditioners available. Depending on the properties of the coefficients α and β, these standard problems can be handled by these well-known robust and (almost) optimal preconditioners and/or solvers like multigrid preconditioners [9, 78], auxiliary space preconditioners [85, 154], and domain decomposition preconditioners [87, 147, 149] in the $\mathbf{H}(\mathbf{curl})$ setting and multigrid or multilevel preconditioners [31, 55, 104, 105, 106, 125] and domain decomposition preconditioners [131, 149] in the H^1 setting, respectively. For the boundary integral equations, robust and optimal preconditioners for the vectorial single layer potential are required. Indeed, this problem can be reduced to scalar boundary integral operators, where again efficient solvers and preconditioners are available. Here, we mention domain decomposition or multilevel methods [75, 150], multipole methods [62, 63] and purely algebraic approaches like $\mathcal{H}$-matrices approximations [20, 69, 70] and adaptive cross approximation methods [19].

Furthermore, we refer, e.g., to the software projects *hypre*[3], *NgSolve*[4], and *Dune*[5], where some of these solvers and preconditioners are available.

---

[3]`https://computation.llnl.gov/casc/hypre/software.html`
[4]`http://www.hpfem.jku.at/ngsolve/`
[5]`http://www.dune-project.org/`

On this Work

The main aims of this work are to combine the multiharmonic approach and the FEM-BEM coupling method in a unified framework as a discretization technique for time-dependent, but time-periodic eddy current problems of parabolic-elliptic type and time-dependent, but time-periodic eddy current optimal control problems in three dimensions. The main innovations in this context are the construction, analysis and verification of parameter-robust solvers for the resulting systems of linear algebraic equations in all the considered settings.

Main achievements

The main emphasis of this thesis is not on computations but on the analysis and numerical analysis. Nevertheless we have also confirmed our theoretical results by numerical experiments. Our main achievements are the following ones.

Existence and uniqueness results We provide existence and uniqueness results for the eddy current problem stated in $\mathbb{R}^3$ for both, the initial value setting and the time-periodic setting. These results are carried over to the eddy current optimal control problem, where again existence and uniqueness results are provided for both the initial value setting and the time-periodic setting. These existence and uniqueness results provide the mathematical basis of the following discretization and solution schemes.

Multiharmonic approach We provide a uniform framework for the application of the multiharmonic approach to time-dependent partial differential equations and optimal control problems.

Treatment of possibly unbounded domains The combination of the multiharmonic approach as a time discretization technique with a FEM-BEM coupling method as a space discretization technique, leads to a powerful method that we call MH-FEM-BEM.

Robust solvers and preconditioners In contrast to previous works, we provide a rigorous mathematical justification of the robustness and optimality of our proposed solvers for the MH-FEM-BEM equations. One of our main focus is to provide theoretical convergence results and quantitative convergence rates. Depending on the setting, our solvers obtain nice robustness qualities with respect to the involved model, regularization or cost parameters not only in theory but also in practice. Furthermore, we use an interpolation technique to derive the block-diagonal preconditioners in a constructive fashion. Although this interpolation can be carried out only in specific regimes, these intermediate results teach us how to choose the preconditioners in the more involving settings. Therein the inf-sup and the sup-sup condition

$$\underline{c}\,\|\mathbf{x}\| \leq \sup_{\mathbf{y}\neq\mathbf{0}} \frac{\mathbf{y}^T \mathcal{A}\,\mathbf{x}}{\|\mathbf{y}\|} \leq \overline{c}\,\|\mathbf{x}\|,$$

that also appears in the Theorem of Babuška-Aziz, plays an important role in the analysis of the block-diagonal preconditioners. In order to apply our constructed block-diagonal preconditioners, only already available preconditioners for standard problems are required. Indeed, this makes our techniques very flexible and easily useable in different environments.
Furthermore, due to the special choice of the discretization technique in combination with the design of our solution algorithm, a parallelization of the proposed methods is straightforward.

Optimal control problem We establish the multiharmonic approach as a powerful discretization technique for solving time-periodic optimal control problems in three dimensions. Indeed, we apply the MH-FEM-BEM coupling method to the optimality system of the optimal control problem, that allows us to consider the full computational domain $\mathbb{R}^3$. Furthermore, a huge range of practical

relevant constraints in optimal control computations are covered by our analysis concerning efficient solution strategies, e.g., control and state constraints, different control and observation domains, observation in certain energy spaces or end time control.

Outline

This dissertation is structured as follows.

- In Chapter 1 we introduce the eddy current problem. We pay special attention to the vector potential formulation, and consider both, time-domain and frequency domain equations.

- Chapter 2 provides some preliminaries, like variational methods and existence and uniqueness results for both, time-dependent and time-independent problems. Furthermore, we recall the natural function spaces and their properties for eddy current problems. Based on those, we introduce FEM, BEM and FEM-BEM couplings.

- Chapter 3 provides existence and uniqueness results for time-dependent eddy current problems and time-dependent eddy current optimal control problems.

- In Chapter 4 we explain and analyze the application of the multiharmonic approach as a time discretization technique for both, forward and optimal control problems.

- Chapter 5 briefly overviews the basic concepts of parameter-robust preconditioning for saddle point problems.

- In Chapter 6 we apply the MH-FEM-BEM method to eddy current problems and construct parameter-robust and block-diagonal preconditioners for the resulting systems of linear equations.

- In Chapter 7 we discuss the application of the MH-FEM-BEM method to eddy current optimal control problems and construct parameter-robust and block-diagonal preconditioners for the resulting systems of linear equations.

- Chapter 8 is devoted to the discussion of parameter-robust and efficient realization of the standard $\mathbf{H}(\mathbf{curl})$ and H^1 problems, appearing in the diagonal blocks of our preconditioners.

- In Chapter 9 we provide numerical experiments including some settings, that are relevant in practice.

- In Chapter 10 we give some final comments and discuss open questions and possible continuations of this work.

Parts of this work have already been published by the author (and co-authors) in peer-reviewed international journals or proceedings of international conferences:

- Parts of Chapter 5 have been addressed in

[95] M. Kollmann, M. Kolmbauer, U. Langer, M. Wolfmayr, and W. Zulehner. A robust finite element solver for a multiharmonic parabolic optimal control problem. *Computers and Mathematics with Applications*, 2012. DOI: 10.1016/j.camwa.2012.06.012.

- Parts of Chapter 6 have been addressed in

[100] M. Kolmbauer and U. Langer. A frequency-robust solver for the time-harmonic eddy current problem. In *Scientific Computing in Electrical Engineering SCEE 2010*, volume 16 of *Mathematics in Industry*, pages 97–106. Springer, 2011.

[102] M. Kolmbauer and U. Langer. A robust FEM-BEM solver for time-harmonic eddy current problems. In *Domain Decomposition Methods in Science and Engineering XX*, Lecture Notes in Computational Science and Engineering. Springer, 2012. (to appear).

[103] M. Kolmbauer and U. Langer. A robust preconditioned MinRes solver for time-periodic eddy current problems. *Comput. Methods Appl. Math.*, 2012. DOI: 10.2478/cmam-2012-0023.

- Parts of Chapter 7 and Chapter 8 have been addressed in

[98] M. Kolmbauer. Efficient solvers for multiharmonic eddy current optimal control problems with various constraints and their analysis. *IMA J. Numer. Anal.*, 2012. (to appear).

[99] M. Kolmbauer. A robust FEM-BEM MinRes solver for distributed multiharmonic eddy current optimal control problems in unbounded domains. *Electronic Transactions on Numerical Analysis*, 39:231–252, 2012.

[101] M. Kolmbauer and U. Langer. A robust preconditioned MinRes solver for distributed time-periodic eddy current optimal control problems. NuMa-Report 2011-04, Institute of Computational Mathematics, Linz, May 2011. (submitted).

Chapter 1

Introduction to eddy current computations

In the first part of this chapter, we briefly introduce the classical Maxwell's equations, describing the electromagnetic field equations. This system of equations is completed by constitutive laws. Furthermore we introduce the *eddy current model* for magneto-quasi-static fields and derive the *vector potential formulation*. Finally, we introduce the problem settings under consideration in this work, namely the eddy current problem and the eddy current optimal control problem.

For a comprehensive study of the Maxwell equations, we refer to [153].

1.1 Maxwell's equations

Maxwell's equations describe the interaction of electric and magnetic fields in dependence of space $\mathbf{x} \in \mathbb{R}^3$ and time t. The classical formulation in differential form is given as follows.

$$\mathbf{curl\, E} + \frac{\partial \mathbf{B}}{\partial t} = \mathbf{0}, \qquad \text{(Faraday's induction law)} \qquad (1.1a)$$

$$-\mathbf{curl\, H} + \frac{\partial \mathbf{D}}{\partial t} = -\mathbf{j}, \qquad \text{(Ampere's law)} \qquad (1.1b)$$

$$\operatorname{div} \mathbf{D} = \rho, \qquad \text{(Electric Gauss law)} \qquad (1.1c)$$

$$\operatorname{div} \mathbf{B} = 0. \qquad \text{(Magnetic Gauss law)} \qquad (1.1d)$$

Here, the four time- and space-dependent vector fields are given by the electric field intensity denoted by $\mathbf{E}$, the magnetic field intensity $\mathbf{H}$, the electric displacement field (electric flux) $\mathbf{D}$, and the magnetic induction field (magnetic flux) $\mathbf{B}$. The sources of electromagnetic fields are electric charges and currents, described by the scalar charge density ρ, and the vectorial current density function $\mathbf{j}$.

An important physical property can be derived by taking the divergence in the Ampere's law. Using the Electric Gauss law yields the continuity equation

$$\operatorname{div} \mathbf{j} + \frac{\partial \rho}{\partial t} = 0 \qquad (1.2)$$

that reflects the *conservation of charges*.

The system (1.1) is completed by appropriate constitutive laws, taking care of the material properties. The magnetic and electric field intensities are related with the corresponding fluxes by

$$\mathbf{D} = \epsilon \, \mathbf{E}, \qquad (1.3a)$$

$$\mathbf{B} = \mu \, \mathbf{H}. \qquad (1.3b)$$

Furthermore, in conducting materials the electric field induces a conduction current, which is given by Ohm's law

$$\mathbf{j} = \sigma \, \mathbf{E} + \mathbf{j_i}, \tag{1.4}$$

where $\mathbf{j}$ and $\mathbf{j_i}$ denote the total and the impressed current densities, respectively. Hence, the electric and magnetic properties of a material are characterized by the electric permittivity ϵ, the magnetic permeability μ, and the electric conductivity σ. Although in general, μ and σ are tensors, they are scalars in the case of isotropic materials. In the main part of this work, we only consider homogeneous and isotropic materials, where μ and σ are piecewise constant. The conductivity σ is positive in conductors and zero in non-conductors. In general, these coefficients do not only depend on the coordinates in space, but also on the magnetic and/or electric field. Indeed, the permeability μ depends also on the magnetic field $\mathbf{H}$ in ferromagnetic materials (e.g. steel), i.e., $\mu = \mu(|\mathbf{H}|)$. Furthermore, we also use the reluctivity, the inverse of the magnetic permeability, given by $\nu = \mu^{-1}$. Neglecting the effects of hysteresis, we have $\mathbf{H} = \nu(|\mathbf{B}|)\mathbf{B}$ with some strictly monotone function $s \mapsto \nu(|s|)s$ in ferromagnetic materials. In practical application, this relation is given by a discrete set of data points, cf. [132].

1.2   Magneto quasi-static fields: eddy current problems

For slowly varying electric fields, the displacement currents are very small in comparison with the impressed currents and eddy currents, i.e.,

$$\left| \frac{\partial \mathbf{D}}{\partial t} \right| \ll |\mathbf{j}|.$$

This leads to the so-called quasi-static model, where the time derivative of the electric flux is neglected. Therefore, we are dealing with the *eddy current model*, given by

$$\mathbf{curl}\,\mathbf{E} + \frac{\partial \mathbf{B}}{\partial t} = \mathbf{0}, \qquad \text{(Faraday's induction law)} \tag{1.5a}$$

$$\mathbf{curl}\,\mathbf{H} = \mathbf{j}, \qquad \text{(reduced Ampere's law)} \tag{1.5b}$$

$$\mathrm{div}\,\mathbf{D} = \rho, \qquad \text{(Electric Gauss law)} \tag{1.5c}$$

$$\mathrm{div}\,\mathbf{B} = 0. \qquad \text{(Magnetic Gauss law)} \tag{1.5d}$$

In this setting, due to (1.5b), the *conservation of charges law* reads as $\mathrm{div}\,\mathbf{j} = 0$. A rigorous justification of the eddy current model as an approximation of the full Maxwell's equations is given in [7, 141].

Typically, the equations (1.5) are considered in $\Omega = \mathbb{R}^3$. The behavior of the magnetic field $\mathbf{H}$ and the electric $\mathbf{E}$ at infinity is described by *radiation conditions*, i.e.,

$$\mathbf{E} = \mathcal{O}\left(|\mathbf{x}|^{-1}\right), \quad \mathbf{H} = \mathcal{O}\left(|\mathbf{x}|^{-1}\right), \quad \text{for } \mathbf{x} \to \infty.$$

Additionally, the system (1.5) is completed by a prescribed initial condition

$$\mathbf{B}|_{t=0} = \mathbf{B_0}, \quad \text{in } \bar{\Omega}.$$

1.3   Vector potential formulation

There exists a full range of formulations for the eddy current problem (1.5). These different formulations are basically the consequence of different potentials, introduced for the $\mathbf{E}$ field or the $\mathbf{H}$ field. Throughout this work, we use the approach of a *vector potential formulation*, that has been derived, e.g., in [160]. Let Ω be a bounded, simply connected domain in $\mathbb{R}^3$. Then due to $\mathrm{div}\,\mathbf{B} = 0$, we know,

that $\mathbf{B}$ can be expressed as a *vector potential* $\tilde{\mathbf{y}}$, i.e., $\mathbf{B} = \mathbf{curl}\,\tilde{\mathbf{y}}$. Substituting into Faraday's law (1.5a), we obtain

$$\mathbf{curl}\left(\mathbf{E} + \frac{\partial \tilde{\mathbf{y}}}{\partial t}\right) = \mathbf{0}.$$

Therefore, there exists a scalar potential φ, such that

$$\mathbf{E} = -\frac{\partial \tilde{\mathbf{y}}}{\partial t} - \nabla\varphi.$$

Using this representation, Ampere's law (1.5b) can be expressed as follows:

$$\sigma \frac{\partial \tilde{\mathbf{y}}}{\partial t} + \mathbf{curl}\left(\nu(|\,\mathbf{curl}\,\tilde{\mathbf{y}}|)\,\mathbf{curl}\,\tilde{\mathbf{y}}\right) = \mathbf{j_i} - \sigma\nabla\varphi.$$

By choosing another vector potential $\mathbf{y} = \tilde{\mathbf{y}} + \int_0^t \nabla\varphi\,\mathrm{d}t$, we have $\mathbf{curl}\,\mathbf{y} = \mathbf{curl}\,\tilde{\mathbf{y}}$ and $\mathbf{E} = -\frac{\partial\mathbf{y}}{\partial t}$, and consequently, we obtain the following vector potential formulation of the eddy current problem

$$\sigma \frac{\partial \mathbf{y}}{\partial t} + \mathbf{curl}\left(\nu(|\,\mathbf{curl}\,\mathbf{y}|)\,\mathbf{curl}\,\mathbf{y}\right) = \mathbf{j_i}, \tag{1.6}$$

which is the type of equation whose numerical solution we will investigate in detail in this work. Indeed in Chapter 3, we discuss the existence and uniqueness of solutions for (1.6).

1.4 Time-harmonic eddy current problems

When dealing with alternating currents, the imposed current density shows a harmonic dependence on time, i.e., for a given alternating current $I(t)$, with frequency ω, the time-dependence can be expressed in terms of the time-harmonic ansatz $I(t) = I_0 \sin(\omega t)$. This motivates the usage of time-harmonic excitations of the form $\mathbf{j_i}(\mathbf{x}, t) = \hat{\mathbf{j}}_\mathbf{i}(\mathbf{x})e^{\mathrm{i}\omega t}$, with the complex number $\mathrm{i} = \sqrt{-1}$, some base frequency $\omega > 0$, and complex amplitude $\hat{\mathbf{j}}$. For the special case of linear material laws in (1.3), one obtains a time-harmonic representation of the vector potential $\mathbf{y}$, i.e.,

$$\mathbf{y}(\mathbf{x}, t) = \mathrm{Re}\left[\hat{\mathbf{y}}(\mathbf{x})e^{\mathrm{i}\omega t}\right], \tag{1.7}$$

with the complex amplitude $\hat{\mathbf{y}}$, and the same base frequency ω. Using this ansatz, the time-harmonic eddy current problem can be transformed from the time domain to the frequency domain, and therefore, a time-dependent problem is transformed into a complex valued time-independent problem. The corresponding vector potential formulation reads as follows:

$$i\omega\sigma\hat{\mathbf{y}} + \mathbf{curl}(\nu\,\mathbf{curl}\,\hat{\mathbf{y}}) = \hat{\mathbf{j}}_\mathbf{i}.$$

In some applications, e.g. [17, 129], it is advantageous to use a real reformulation of (1.7), in terms of

$$\mathbf{y}(\mathbf{x}, t) = \mathbf{y^c}(\mathbf{x})\cos(\omega t) + \mathbf{y^s}(\mathbf{x})\sin(\omega t),$$

with the real valued amplitudes $\mathbf{y^c} = \mathrm{Re}[\hat{\mathbf{y}}]$ and $\mathbf{y^s} = -\mathrm{Im}[\hat{\mathbf{y}}]$. Using this real reformulation, the time-harmonic eddy current problem obtains the following structure as a system of two partial differential equations:

$$\begin{cases} \omega\sigma\mathbf{y^s} + \mathbf{curl}(\nu\,\mathbf{curl}\,\mathbf{y^c}) = \mathbf{j_i^c}, \\ -\omega\sigma\mathbf{y^c} + \mathbf{curl}(\nu\,\mathbf{curl}\,\mathbf{y^s}) = \mathbf{j_i^s}. \end{cases}$$

In Chapter 4, we revisit the idea of time-harmonic approximation and provide a suitable extension of this approach, that even fits in the case of nonlinear material laws, i.e., $\mathbf{H} = \nu(|\mathbf{B}|)\mathbf{B}$.

Time-harmonic eddy current problems have been analyzed, e.g., in [5, 17, 38, 110].

1.5   Problem settings in eddy current computations

In typical applications of eddy current problems, there is a distinction between two main computational regimes:

1. Determine the vector potential $\mathbf{y}$ under some prescribed $\mathbf{j_i}$ as the solution of (1.6).

2. Determine $\mathbf{j_i}$ and the corresponding vector potential $\mathbf{y}$ as the solution of (1.6), such that the vector potential $\mathbf{y}$ is driven to some prescribed target.

While the first problem setting is referred as the *forward* problem, the second is referred as the *inverse* problem. Typically, the *forward* problem is a well-posed problem, and the *inverse* problem is an ill-posed problem. Due to the ill-posedness of the inverse problem one needs the machinery developed for *inverse* or *optimal control* problems in order to clarify the solvability. In the field of optimal control problems, one deals with minimization problems of the following type: Find $(\hat{\mathbf{y}}, \hat{\mathbf{j}}_\mathbf{i})$, such that

$$\mathcal{J}(\hat{\mathbf{y}}, \hat{\mathbf{j}}_\mathbf{i}) = \min_{(\mathbf{y}, \mathbf{j_i})} \mathcal{J}(\mathbf{y}, \mathbf{j_i}), \quad \text{subject to (1.6).} \tag{1.8}$$

The minimization functional is chosen in such a way, that either $\mathbf{y}$ or the magnetic induction field $\mathbf{B} = \mathbf{curl}\,\mathbf{y}$ are steered to a prescribed desired state in the whole time interval $(0, T)$, or a specific time point $t \in (0, T)$, e.g., $t = T$. Typical choices for the minimization functional $\mathcal{J}$ are the following ones:

$$\mathcal{J}(\mathbf{y}, \mathbf{j_i}) := \mathcal{J}_1(\mathbf{y}) + \mathcal{J}_2(\mathbf{y}) + \mathcal{J}_3(\mathbf{y}) + \mathcal{J}_4(\mathbf{y}) + \mathcal{G}(\mathbf{j_i}), \tag{1.9}$$

where the functionals $\mathcal{J}_i$, $i = 1, 2, 3, 4$, and $\mathcal{G}$ are given by

$$\mathcal{J}_1(\mathbf{y}) := \frac{\tau_1}{2} \int_{\Omega_1} |\mathbf{y}(\mathbf{x}, T) - \mathbf{y_{d,T}}(\mathbf{x})|^2 \mathrm{d}\mathbf{x},$$

$$\mathcal{J}_2(\mathbf{y}) := \frac{\tau_2}{2} \int_{\Omega_2} |\,\mathbf{curl}\,\mathbf{y}(\mathbf{x}, T) - \mathbf{y_{c,T}}(\mathbf{x})|^2 \mathrm{d}\mathbf{x},$$

$$\mathcal{J}_3(\mathbf{y}) := \frac{\tau_3}{2} \int_{\Omega_3 \times (0,T)} |\mathbf{y}(\mathbf{x}, t) - \mathbf{y_d}(\mathbf{x}, t)|^2 \mathrm{d}\mathbf{x}\,\mathrm{d}t,$$

$$\mathcal{J}_4(\mathbf{y}) := \frac{\tau_4}{2} \int_{\Omega_4 \times (0,T)} |\,\mathbf{curl}\,\mathbf{y}(\mathbf{x}, t) - \mathbf{y_c}(\mathbf{x}, t)|^2 \mathrm{d}\mathbf{x}\,\mathrm{d}t,$$

$$\mathcal{G}(\mathbf{j_i}) := \frac{\lambda}{2} \int_{\Omega_5 \times (0,T)} |\mathbf{j_i}(\mathbf{x}, t)|^2 \mathrm{d}\mathbf{x}\,\mathrm{d}t,$$

with some prescribed desired states $\mathbf{y_{d,T}}, \mathbf{y_{c,T}}, \mathbf{y_d}, \mathbf{y_c}$, cost parameters $\tau_1, \tau_2, \tau_3, \tau_4 \geq 0$ and the regularization parameter $\lambda > 0$. Here, the task of the functionals $\mathcal{J}_i, i = 1, \ldots, 4$, is to steer the *state* $\mathbf{y}$ or the magnetic induction field $\mathbf{B} = \mathbf{curl}\,\mathbf{y}$ to some desired state in a required setting. Furthermore, the functional $\mathcal{G}$ plays the role of a Tikhonov regularization term, that can also be interpreted as the cost for the control $\mathbf{j_i}$.

Chapter 2

Mathematical basics

In the previous chapter we discussed the eddy current problem in both regimes, the time domain and the frequency domain. The main purpose of this chapter is to provide the functional analytical framework for the analysis and solution of the resulting partial differential equations. Beside abstract existence and uniqueness results for both, time-dependent and time-independent problems, we also introduce the natural function spaces for the variational formulation of the partial differential equations under consideration.

In Section 2.1 we briefly discuss abstract variational methods, including existence and uniqueness results and Galerkin discretizations. Section 2.2 deals with the functional analytical setting for eddy current problems. In Section 2.3 we recall the framework of boundary integral operators and Calderon's projection for eddy current problems. Section 2.4 briefly covers two discretization techniques, the finite element method (FEM) and the boundary element method (BEM). In Section 2.4 the abstract setting and existence and uniqueness results for time-dependent problems of parabolic type are provided. Finally, Section 2.5 is devoted to the analysis of optimal control problems.

2.1 Abstract variational methods

Existence and uniqueness Let X be a Hilbert space with the inner product $(\cdot, \cdot)_X$, and the associated norm $\| \cdot \|_X = \sqrt{(\cdot, \cdot)_X}$. We consider the bilinear form $\mathcal{A}(\cdot, \cdot) : X \times X \to \mathbb{R}$, and the linear form $\mathcal{F} \in X^*$. In the following, we investigate the abstract variational problem: Find $z \in X$ such that

$$\mathcal{A}(z, y) = \langle \mathcal{F}, y \rangle, \quad \forall\, y \in X. \tag{2.1}$$

Theorem 2.1 (Babuška-Aziz)**.** *Let X be a Hilbert space and let $\mathcal{F} \in X^*$ be a bounded linear form. Let $\mathcal{A}(\cdot, \cdot) : X \times X \to \mathbb{R}$ fulfill the inf-sup and sup-sup conditions*

$$\underline{c}\, \|z\|_X \leq \sup_{y \in X} \frac{\mathcal{A}(z, y)}{\|y\|_X} \leq \bar{c}\, \|z\|_X, \quad \forall\, z \in X, \tag{2.2}$$

$$\underline{c}\, \|y\|_X \leq \sup_{z \in X} \frac{\mathcal{A}(z, y)}{\|z\|_X} \leq \bar{c}\, \|y\|_X, \quad \forall\, y \in X, \tag{2.3}$$

with constants $\underline{c} > 0$ and $\bar{c} > 0$. Then the variational formulation (2.1) has a unique solution $z \in X$, which fulfills the a priori estimate

$$\frac{1}{\bar{c}}\, \|\mathcal{F}\|_{X^*} \leq \|z\|_X \leq \frac{1}{\underline{c}}\, \|\mathcal{F}\|_{X^*}.$$

Proof. See [14]. □

If the bilinear form $\mathcal{A}$ is symmetric, i.e.,

$$\mathcal{A}(z,y) = \mathcal{A}(y,z), \quad \forall\, y,z \in X,$$

Theorem 2.1, simplifies to the following Corollary.

Corollary 2.2. *Let X be a Hilbert space and let $\mathcal{F} \in X^*$ be a bounded linear form. Let $\mathcal{A}(\cdot,\cdot) :$ $X \times X \to \mathbb{R}$ by symmetric and fulfill the inf-sup and sup-sup condition*

$$\underline{c}\,\|z\|_X \leq \sup_{y \in X} \frac{\mathcal{A}(z,y)}{\|y\|_X} \leq \overline{c}\,\|z\|_X, \quad \forall\, z \in X, \tag{2.4}$$

with constants $\underline{c} > 0$ and $\overline{c} > 0$. Then the variational formulation (2.1) has a unique solution $z \in X$.

Proof. The result immediately follows from Theorem 2.1. □

So far the results hold for general symmetric problems. Next we address the special case of symmetric saddle point problems. Therefore, let V and Q be Hilbert spaces with the inner products $(\cdot,\cdot)_V$ and $(\cdot,\cdot)_Q$. The associated norms are given by $\|\cdot\|_V = \sqrt{(\cdot,\cdot)_V}$ and $\|\cdot\|_Q = \sqrt{(\cdot,\cdot)_Q}$. Furthermore, let X be the product space $X = V \times Q$, equipped with the inner product $((v,q),(w,r))_X = (v,w)_V + (q,r)_Q$ and the associated norm $\|(v,q)\|_X = \sqrt{((v,q),(v,q))_X}$. Consider a mixed variational problem: Find $z = (w,r) \in X$, such that

$$\mathcal{A}(z,y) = \langle \mathcal{F}, y \rangle, \quad \forall\, y = (v,q) \in X. \tag{2.5}$$

Here the mixed bilinear form $\mathcal{A}(\cdot,\cdot)$ is given by

$$\mathcal{A}(z,y) = a(w,v) + b(v,r) + b(w,q), \tag{2.6}$$

where $a(\cdot,\cdot)$ and $b(\cdot,\cdot)$ are bilinear forms, fulfilling the following properties: $a(\cdot,\cdot) : V \times V \to \mathbb{R}$ symmetric and $b(\cdot,\cdot) : V \times Q \to \mathbb{R}$. For mixed variational problems, existence and uniqueness follows from the Theorem of Brezzi.

Theorem 2.3 (Brezzi). *Assume that there exist constants α_1, α_2, β_1 and $\beta_2 > 0$, such that*

1. *$a(w,v) \leq \alpha_2\|w\|_V\|v\|_V, \quad \forall\, w,v \in V,$*

2. *$b(v,r) \leq \beta_2\|v\|_V\|r\|_Q, \quad \forall\, v \in V, \forall\, r \in Q,$*

3. *the inf-sup condition of $a(\cdot,\cdot)$ on kernel of $b(\cdot,\cdot)$ holds, i.e.,*

$$\inf_{v \in V_0} \sup_{w \in V_0} \frac{a(w,v)}{\|w\|_V\|v\|_V} \geq \alpha_1 \quad and \quad \inf_{w \in V_0} \sup_{v \in V_0} \frac{a(w,v)}{\|w\|_V\|v\|_V} \geq \alpha_1,$$

   with $V_0 := \{v \in V : b(v,r) = 0, \forall\, r \in Q\}$

4. *and the inf-sup condition of $b(\cdot,\cdot)$ holds, i.e.,*

$$\inf_{r \in Q} \sup_{v \in V} \frac{b(v,r)}{\|v\|_V\|r\|_Q} \geq \beta_1.$$

Then (2.4) is satisfied with the constants

$$\underline{c} = \frac{\alpha_1}{1 + (\alpha_2/\beta_1)^2} \quad and \quad \overline{c} = \frac{\alpha_2 + \sqrt{\alpha_2^2 + 4\beta_2^2}}{2},$$

and consequently (2.5) has a unique solution $z \in X$.

Proof. See [32]. □

Next we subtract from $\mathcal{A}(\cdot,\cdot)$ in (2.6) a symmetric and positive bilinear form $c(\cdot,\cdot): Q \times Q \to \mathbb{R}$. Consider a mixed variational problem in the product space $X = V \times Q$: Find $z = (w, r) \in X$, such that

$$\mathcal{A}(z, y) = \mathcal{F}(y), \quad \forall\, y = (v, q) \in X, \tag{2.7}$$

with

$$\mathcal{A}(z, y) = a(w, v) + b(v, r) + b(w, q) - c(r, q).$$

For these kinds of mixed variational problems, existence and uniqueness follows by a result of Zulehner, that extends the Theorem of Brezzi.

Theorem 2.4 (Zulehner). *Assume, that there are constants $\underline{c}_w$, $\underline{c}_r$, $\overline{c}_w$, $\overline{c}_r > 0$, such that*

$$\underline{c}_w \|w\|_V^2 \le a(w, w) + \sup_{q \in Q} \frac{b(w, q)^2}{\|q\|_Q^2} \le \overline{c}_w \|w\|_V^2, \quad \forall\, w \in V, \tag{2.8}$$

$$\underline{c}_r \|r\|_Q^2 \le c(r, r) + \sup_{v \in Q} \frac{b(v, r)^2}{\|v\|_V^2} \le \overline{c}_r \|r\|_Q^2, \qquad \forall\, r \in Q. \tag{2.9}$$

Then (2.4) is satisfied with the constants,

$$\underline{c} = -\frac{\left(-3 + \sqrt{5}\right) \min\left(\underline{c}_r^2 \min\left(\frac{1}{2}, \underline{c}_r\right)^2, \underline{c}_w^2 \min\left(\frac{1}{2}, \underline{c}_w\right)^2\right)}{4 \max\left(\sqrt{\overline{c}_r} \max(1, \overline{c}_r), \sqrt{\overline{c}_w} \max(1, \overline{c}_w)\right)},$$

$$\overline{c} = \sqrt{2} \max\left(\sqrt{\overline{c}_r} \max(1, \overline{c}_r), \sqrt{\overline{c}_w} \max(1, \overline{c}_w)\right), \tag{2.10}$$

that only depend on $\underline{c}_w$, $\underline{c}_r$, $\overline{c}_w$, $\overline{c}_r$, and consequently (2.7) has a unique solution $z \in X$.

Proof. See [164, Theorem 2.6]. $\qquad\square$

Furthermore, the conditions (2.8) and (2.9) in Theorem 2.4 are necessary and sufficient, i.e., $\underline{c}$ and $\overline{c}$ only depend on $\underline{c}_w$, $\underline{c}_r$, $\overline{c}_w$, $\overline{c}_r$ and vice versa.

Galerkin's method Let X be a Hilbert space with a closed subspace X_0, and let $g \in X$. We consider the abstract variational problem: Find $z \in X_g = g + X_0$, such that

$$\mathcal{A}(z, y) = \langle \mathcal{F}, y \rangle, \quad \forall\, y \in X_0, \tag{2.11}$$

where the bilinear form $\mathcal{A}(\cdot,\cdot): X \times X \to \mathbb{R}$ fulfills the inf-sup and sup-sup conditions (2.4), and $\mathcal{F} \in X^*$. Take a finite dimensional subspace $X_0^h \subset X_0$, and consider the discrete problem: Find $z_h \in X_g^h = g + X_0^h$, such that

$$\mathcal{A}(z_h, y_h) = \langle \mathcal{F}, y_h \rangle, \quad \forall\, y_h \in X_0^h. \tag{2.12}$$

The following a priori estimate states, that the discretization error is controlled in terms of the approximation error.

Lemma 2.5 (Cea type estimate). *Let $z \in X_g$ be the solution of (2.11) and let $z_h \in X_g^h$ be the solution of (2.12). Then the discretization error estimate*

$$\|z - z_h\|_X \le \frac{\overline{c}}{\underline{c}} \inf_{y_h \in X_g^h} \|z - y_h\|_X$$

holds, where $\underline{c}$ and $\overline{c}$ are the inf-sup and sup-sup constants of $\mathcal{A}(\cdot,\cdot)$ in (2.4), respectively.

Proof. See [14]. $\qquad\square$

2.2   Abstract setting for eddy current computations

The main purpose of this section is to introduce the differential operators, function spaces, trace operators, and trace spaces, that are necessary for investigating eddy current problems.

In the following, let $\Omega_1 \subset \mathbb{R}^3$ be a Lipschitz domain, i.e., a bounded domain with a Lipschitz continuous boundary $\Gamma := \partial\Omega_1$. The unbounded complement of Ω_1 in $\mathbb{R}^3$ is denoted by Ω_2, i.e., $\Omega_2 := \mathbb{R}^3\backslash\bar{\Omega}_1$. Furthermore, we denote the outer unit normal vector on Γ by $\mathbf{n}$, i.e., $\mathbf{n}$ points from Ω_1 to Ω_2. Throughout this section, let Ω denote either Ω_1 or Ω_2.

2.2.1   Differential operators

We start with the definition of the basic operators involved in the formulation of Maxwell's equations. The *gradient* operator of a scalar function q is defined as

$$\nabla q := \left(\frac{\partial q}{\partial x_1}, \frac{\partial q}{\partial x_2}, \frac{\partial q}{\partial x_3} \right)^T,$$

and the *divergence* operator of a vector field $\mathbf{y} = (y_1, y_2, y_3)^T$ is defined as

$$\operatorname{div} \mathbf{y} := \nabla \cdot \mathbf{y} = \sum_{k=1}^{3} \frac{\partial y_k}{\partial x_k}.$$

The *curl* operator of a vector field $\mathbf{y} = (y_1, y_2, y_3)^T$ is defined as

$$\mathbf{curl}\, \mathbf{y} := \nabla \times \mathbf{y} = \left(\frac{\partial y_3}{\partial x_2} - \frac{\partial y_2}{\partial x_3}, \frac{\partial y_1}{\partial x_3} - \frac{\partial y_3}{\partial x_1}, \frac{\partial y_2}{\partial x_1} - \frac{\partial y_1}{\partial x_2} \right)^T.$$

All these operators can be defined by derivatives in a weak sense, cf. [54].

2.2.2   Function spaces

The following function spaces will turn out to provide the natural setting for the investigation of the partial differential equations involved in the Maxwell's equations. Beside the well-known Sobolev spaces $L_2(\Omega)$, $H^1(\Omega)$ for scalar functions and $\mathbf{L_2}(\Omega) := [L_2(\Omega)]^3$, $\mathbf{H^1}(\Omega) := [H^1(\Omega)]^3$ for vector fields, we also need the fractional Sobolev space $H^s(\Omega)$ and $\mathbf{H^s}(\Omega)) := [H^s(\Omega)]^3$ of order $s \in \mathbb{R}$, cf. [54]. The corresponding norms are denoted by $\| \cdot \|_{0,\Omega}$, $\| \cdot \|_{1,\Omega}$, $\| \cdot \|_{\mathbf{0},\Omega}$, $\| \cdot \|_{\mathbf{1},\Omega}$, $\| \cdot \|_{s,\Omega}$, and $\| \cdot \|_{\mathbf{s},\Omega}$. Furthermore, we define

$$\mathbf{H}(\operatorname{div}, \Omega) := \{\mathbf{y} \in \mathbf{L_2}(\Omega) : \operatorname{div} \mathbf{y} \in L_2(\Omega)\},$$
$$\mathbf{H}(\mathbf{curl}, \Omega) := \{\mathbf{y} \in \mathbf{L_2}(\Omega) : \mathbf{curl}\, \mathbf{y} \in \mathbf{L_2}(\Omega)\},$$
$$\mathbf{H}(\mathbf{curl}^2, \Omega) := \{\mathbf{y} \in \mathbf{H}(\mathbf{curl}, \Omega) : \mathbf{curl}\,\mathbf{curl}\, \mathbf{y} \in \mathbf{L_2}(\Omega)\},$$

and the corresponding scalar products by

$$(\mathbf{u}, \mathbf{v})_{\operatorname{div},\Omega} = (\operatorname{div} \mathbf{u}, \operatorname{div} \mathbf{v})_{0,\Omega} + (\mathbf{u}, \mathbf{v})_{\mathbf{0},\Omega},$$
$$(\mathbf{u}, \mathbf{v})_{\mathbf{curl},\Omega} = (\mathbf{curl}\, \mathbf{u}, \mathbf{curl}\, \mathbf{v})_{\mathbf{0},\Omega} + (\mathbf{u}, \mathbf{v})_{\mathbf{0},\Omega},$$
$$(\mathbf{u}, \mathbf{v})_{\mathbf{curl}^2,\Omega} = (\mathbf{curl}\, \mathbf{u}, \mathbf{curl}\, \mathbf{v})_{\mathbf{curl},\Omega} + (\mathbf{u}, \mathbf{v})_{\mathbf{0},\Omega}.$$

The induced norms are denoted by $\| \cdot \|_{\operatorname{div},\Omega}$, $\| \cdot \|_{\mathbf{curl},\Omega}$ and $\| \cdot \|_{\mathbf{curl}^2,\Omega}$. Furthermore, we also use the linear manifolds

$$H_0^1(\Omega) := \{q \in H^1(\Omega) : q = 0 \text{ on } \Gamma\},$$
$$\dot{H}^1(\Omega) := \{q \in H^1(\Omega) : \int_\Omega q \, \mathrm{dx} = 0\},$$
$$\mathbf{H_0}(\mathbf{curl}, \Omega) := \{\mathbf{y} \in \mathbf{H}(\mathbf{curl}, \Omega) : \mathbf{y} \times \mathbf{n} = \mathbf{0} \text{ on } \Gamma\}.$$

Helmholtz decompositions An important tool within the analysis of the Maxwell equations is the *Helmholtz decomposition:* Every vector field in $\mathbf{L_2}(\Omega)$ can be decomposed into a divergence-free function and a gradient function.

Lemma 2.6 (Helmholtz decompositions)**.**

- *Let* $\mathbf{u} \in \mathbf{L_2}(\Omega)$*. There exists a decompositions* $\mathbf{u} = \nabla q + \mathbf{curl}\,\tilde{\mathbf{u}}$ *with* $q \in \dot{H}^1(\Omega)$ *and* $\tilde{\mathbf{u}} \in \mathbf{H}(\mathbf{curl}, \Omega)$*.*

- *Let* $\mathbf{y} \in \mathbf{H}(\mathbf{curl}, \Omega)$*. There exists a decompositions* $\mathbf{y} = \nabla q + \tilde{\mathbf{y}}$ *with* $q \in \dot{H}^1(\Omega)$ *and* $\tilde{\mathbf{y}} \in \mathbf{H}(\mathbf{curl}, \Omega)$*, satisfying* $(\tilde{\mathbf{y}}, \nabla p)_{\mathbf{0}, \Omega} = 0, \forall\, p \in \dot{H}^1(\Omega)$*.*

Proof. See [118]. □

Lemma 2.6 is also valid, if homogeneous Dirichlet boundary conditions are added to the space $\mathbf{H}(\mathbf{curl}, \Omega)$ and $H^1(\Omega)$. Similar decompositions can also be derived in non-standard $\mathbf{L_2}$ inner products. Commonly, inner products of the type $(\sigma \cdot, \cdot)_{0, \Omega}$ are used, where $\sigma > 0$ is some weighting function. Indeed, the Helmholtz decomposition is strongly linked to the De-Rham complex, cf. [118]. For more different kinds of Helmholtz decompositions in both the standard $\mathbf{L_2}$ inner product and weighted $\mathbf{L_2}$ inner products, we refer to [118].

Friedrichs type inequalities Friedrichs type inequalities are powerful tools for the analysis of variational problems and finite element approximations.

Lemma 2.7 (Friedrichs' inequality for $H_0^1(\Omega)$)**.** *Let* Ω *be a simply-connected and bounded Lipschitz domain. There exists a constant* $C_1^F > 0$ *depending only on* Ω*, such that for all* $q \in H_0^1(\Omega)$*, we have*

$$\|q\|_{0,\Omega} \leq C_1^F \|\nabla q\|_{\mathbf{0}, \Omega}.$$

Proof. See [149, Lemma A.14]. □

Lemma 2.8 (Friedrichs' inequality for $\mathbf{H}(\mathbf{curl}, \Omega)$)**.** *Let* Ω *be a simply-connected and bounded Lipschitz domain. Suppose, that* $\mathbf{y} \in \mathbf{H}(\mathbf{curl}, \Omega)$ *is orthogonal to gradient functions, i.e.,*

$$(\mathbf{y}, \nabla q)_{\mathbf{0}, \Omega} = 0, \quad \forall\, q \in H^1(\Omega),$$

then there exists a constant $C_2^F > 0$ *depending only on* Ω*, such that*

$$\|\mathbf{y}\|_{\mathbf{0}, \Omega} \leq C_2^F \|\mathbf{curl}\,\mathbf{y}\|_{\mathbf{0}, \Omega}.$$

Proof. See [60, Lemma 3.4]. □

Lemma 2.9 (Weighted Friedrichs' inequality for $\mathbf{H}(\mathbf{curl}, \Omega)$)**.** *Let* Ω *be a simply-connected and bounded Lipschitz domain and* $\sigma \in L^\infty(\Omega)$ *with* $\sigma \geq \underline{\sigma} > 0$*. Suppose, that* $\mathbf{y} \in \mathbf{H}(\mathbf{curl}, \Omega)$ *is orthogonal to gradient functions in the sense*

$$(\sigma \mathbf{y}, \nabla q)_{\mathbf{0}, \Omega} = 0, \quad \forall\, q \in H^1(\Omega),$$

then there exists a constant $C_2^F > 0$ *depending only on* Ω *and independent of* σ*, such that*

$$\|\sqrt{\sigma}\mathbf{y}\|_{\mathbf{0}, \Omega} \leq C_2^F \|\sqrt{\sigma}\,\mathbf{curl}\,\mathbf{y}\|_{\mathbf{0}, \Omega}.$$

Proof. See [118]. □

Both, Lemma 2.8 and Lemma 2.9, also hold for $\mathbf{H}(\mathbf{curl}, \Omega)$ and $H^1(\Omega)$ replaced by $\mathbf{H_0}(\mathbf{curl}, \Omega)$, and $H_0^1(\Omega)$, respectively.

2.2.3   Traces, trace spaces and trace theorems

In this subsection we introduce the appropriate trace spaces of $\mathbf{H}(\mathbf{curl}, \Omega)$ in the case of polyhedral domains.

For a sufficiently smooth vector function $\mathbf{y}$, we define the *Dirichlet trace operator* (tangential trace) $\gamma_{\mathbf{D}}$ on Γ by $\gamma_{\mathbf{D}}\mathbf{y} := \mathbf{n} \times (\mathbf{y} \times \mathbf{n})$, the *twisted tangential trace operator* $\gamma_{\times}$ on Γ by $\gamma_{\times}\mathbf{y} := \mathbf{y} \times \mathbf{n}$, and the *normal trace operator* $\gamma_{\mathbf{n}}$ by $\gamma_{\mathbf{n}}\mathbf{y} := \mathbf{y} \cdot \mathbf{n}$. In order to derive the trace spaces for vector fields in $\mathbf{H}(\mathbf{curl}, \Omega)$, we consider a polyhedral domain Ω. The boundary Γ is assumed to be separated into m faces Γ_i with $\Gamma = \bigcup_{i=1}^{m} \Gamma_i$. For two faces with a common edge e_{ij} we define $\mathbf{t}_{ij}$ as the unit tangential vector and $\mathbf{t}_{i(j)} := \mathbf{t}_{ij} \times \mathbf{n}_i$, where $\mathbf{n}_i$ denotes the unit normal vector on e_{ij} w.r.t. Γ_i. Furthermore, let $\mathcal{I}_j$ denote the set of those indices i, such that Γ_i shares an edge with Γ_j.

We begin by introducing the spaces $\mathbf{H}_{\perp}^{\frac{1}{2}}(\Gamma)$ and $\mathbf{H}_{\parallel}^{\frac{1}{2}}(\Gamma)$ (cf. [33]), that consist of tangential surface vector fields, which are piecewise in $\mathbf{H}^{\frac{1}{2}}(\Gamma)$ and satisfy weak normal and tangential continuity conditions over non smooth edges of Γ, respectively. In order to characterize these spaces, we first introduce the space of tangential vector fields

$$\mathbf{L}_{\mathbf{t}}^{\mathbf{2}}(\Gamma) := \{\boldsymbol{\lambda} \in \mathbf{L_2}(\Gamma) : \boldsymbol{\lambda} \cdot \mathbf{n} = 0 \text{ a.e. on } \Gamma\},$$

with the duality product

$$\langle \boldsymbol{\lambda}, \boldsymbol{\mu} \rangle_t := \int_{\Gamma} \boldsymbol{\lambda} \cdot \boldsymbol{\mu} \, \mathrm{d}\mathbf{x}, \quad \boldsymbol{\mu}, \boldsymbol{\lambda} \in \mathbf{L}_{\mathbf{t}}^{\mathbf{2}}(\Gamma).$$

Furthermore, we define

$$\mathbf{H}_{\star}^{\frac{1}{2}}(\Gamma) := \{\boldsymbol{\lambda} \in \mathbf{L}_{\mathbf{t}}^{\mathbf{2}}(\Gamma) : \boldsymbol{\lambda}|_{\Gamma_j} \cdot \mathbf{t}_{j(i)} \in H^{\frac{1}{2}}(\Gamma_j), \boldsymbol{\lambda}|_{\Gamma_j} \cdot \mathbf{t}_{ji} \in H^{\frac{1}{2}}(\Gamma_j), \forall i \in \mathcal{I}_j, j = 1, \ldots, m\},$$

and

$$\mathbf{H}_{\perp}^{\frac{1}{2}}(\Gamma) := \{\boldsymbol{\lambda} \in \mathbf{H}_{\star}^{\frac{1}{2}}(\Gamma) : \mathcal{N}_{ij}^{\perp}(\boldsymbol{\lambda}) < \infty, \forall i \in \mathcal{I}_j, j = 1, \ldots, m\},$$
$$\mathbf{H}_{\parallel}^{\frac{1}{2}}(\Gamma) := \{\boldsymbol{\lambda} \in \mathbf{H}_{\star}^{\frac{1}{2}}(\Gamma) : \mathcal{N}_{ij}^{\parallel}(\boldsymbol{\lambda}) < \infty, \forall i \in \mathcal{I}_j, j = 1, \ldots, m\},$$

where we have used the functionals

$$\mathcal{N}_{ij}^{\perp}(\boldsymbol{\lambda}) := \int_{\Gamma_i} \int_{\Gamma_j} \frac{|(\boldsymbol{\lambda} \cdot \mathbf{t}_{ij})(\mathbf{x}) - (\boldsymbol{\lambda} \cdot \mathbf{t}_{ij})(\mathbf{y})|^2}{|\mathbf{x} - \mathbf{y}|^3} \mathrm{dS}_{\mathbf{x}} \mathrm{dS}_{\mathbf{y}},$$
$$\mathcal{N}_{ij}^{\parallel}(\boldsymbol{\lambda}) := \int_{\Gamma_i} \int_{\Gamma_j} \frac{|(\boldsymbol{\lambda} \cdot \mathbf{t}_{i(j)})(\mathbf{x}) - (\boldsymbol{\lambda} \cdot \mathbf{t}_{j(i)})(\mathbf{y})|^2}{|\mathbf{x} - \mathbf{y}|^3} \mathrm{dS}_{\mathbf{x}} \mathrm{dS}_{\mathbf{y}}.$$

The spaces $\mathbf{H}_{\perp}^{-\frac{1}{2}}(\Gamma)$ and $\mathbf{H}_{\parallel}^{-\frac{1}{2}}(\Gamma)$ are then defined as the dual spaces of $\mathbf{H}_{\perp}^{\frac{1}{2}}(\Gamma)$ and $\mathbf{H}_{\parallel}^{\frac{1}{2}}(\Gamma)$ with respect to the pivot space $\mathbf{L}_{\mathbf{t}}^{\mathbf{2}}(\Gamma)$, respectively.

We continue by defining differential operators on surfaces. Let $q \in H^2(\Omega)$ be a scalar function. The *surface gradient* of q on Γ is defined as $\mathbf{grad}_{\Gamma} q := \gamma_{\mathbf{D}}(\nabla q)$ and the *vectorial surface rotation* on Γ by $\mathbf{curl}_{\Gamma} q := \mathbf{grad}_{\Gamma} q \times \mathbf{n}$. Let $\mathbf{y} \in \mathbf{H}^2(\Omega)$ be a vector function with $\mathbf{y} \cdot \mathbf{n} = 0$. The *scalar surface rotation* on Γ is given by $\mathrm{curl}_{\Gamma} \mathbf{y} := \mathbf{curl}\, \mathbf{y} \cdot \mathbf{n}$. The *surface divergence* is defined by $\mathrm{div}_{\Gamma} \mathbf{y} := \mathrm{div}(\gamma_{\mathbf{D}}\mathbf{y}) = -\mathrm{curl}_{\Gamma}(\mathbf{y} \times \mathbf{n})$. The definitions of these operators hold for all regular points of Γ but can be extended to Lipschitz domains. Furthermore, they can be extended to other Sobolev spaces with properties given in the next lemma.

Lemma 2.10. *Let Γ be a Lipschitz domain. Then the surface differential operators $\mathbf{grad}_{\Gamma}$ and $\mathbf{curl}_{\Gamma}$ can be extended to linear and continuous mappings*

$$\mathbf{grad}_{\Gamma} : H^{\frac{1}{2}}(\Gamma) \to \mathbf{H}_{\perp}^{-\frac{1}{2}}(\Gamma), \qquad \mathbf{curl}_{\Gamma} : H^{\frac{1}{2}}(\Gamma) \to \mathbf{H}_{\parallel}^{-\frac{1}{2}}(\Gamma).$$

Their adjoints

$$\mathrm{div}_\Gamma : \mathbf{H}^{\frac{1}{2}}_\perp(\Gamma) \to H^{-\frac{1}{2}}(\Gamma), \qquad \mathrm{curl}_\Gamma : \mathbf{H}^{\frac{1}{2}}_\parallel(\Gamma) \to H^{-\frac{1}{2}}(\Gamma),$$

are linear, continuous and surjective. The following duality pairings hold

$$\langle \mathbf{grad}_\Gamma \varphi, \boldsymbol{\lambda} \rangle_t = -\langle \mathrm{div}_\Gamma \boldsymbol{\lambda}, \varphi \rangle, \quad \forall \varphi \in H^{\frac{1}{2}}(\Gamma), \boldsymbol{\lambda} \in \mathbf{H}^{\frac{1}{2}}_\perp(\Gamma),$$

$$\langle \mathbf{curl}_\Gamma \varphi, \boldsymbol{\lambda} \rangle_t = \langle \mathrm{curl}_\Gamma \boldsymbol{\lambda}, \varphi \rangle, \quad\;\; \forall \varphi \in H^{\frac{1}{2}}(\Gamma), \boldsymbol{\lambda} \in \mathbf{H}^{\frac{1}{2}}_\parallel(\Gamma).$$

Furthermore, there holds

$$\ker(\mathrm{curl}_\Gamma \mathbf{H}^{-\frac{1}{2}}_\perp(\Gamma)) = \mathrm{im}(\mathbf{grad}_\Gamma(H^{\frac{1}{2}})), \qquad \ker(\mathrm{div}_\Gamma \mathbf{H}^{-\frac{1}{2}}_\parallel(\Gamma)) = \mathrm{im}(\mathbf{curl}_\Gamma(H^{\frac{1}{2}})).$$

Proof. See [33, 34]. □

We are now in position to define the following trace spaces

$$\mathbf{H}^{-\frac{1}{2}}_\perp(\mathrm{curl}_\Gamma, \Gamma) := \{\boldsymbol{\lambda} \in \mathbf{H}^{-\frac{1}{2}}_\perp(\Gamma), \mathrm{curl}_\Gamma \boldsymbol{\lambda} \in H^{-\frac{1}{2}}(\Gamma)\},$$

$$\mathbf{H}^{-\frac{1}{2}}_\parallel(\mathrm{div}_\Gamma, \Gamma) := \{\boldsymbol{\lambda} \in \mathbf{H}^{-\frac{1}{2}}_\parallel(\Gamma), \mathrm{div}_\Gamma \boldsymbol{\lambda} \in H^{-\frac{1}{2}}(\Gamma)\}.$$

These spaces are equipped with the corresponding graph norms. Furthermore, $\mathbf{H}^{-\frac{1}{2}}_\perp(\mathrm{curl}_\Gamma, \Gamma)$ is the dual of $\mathbf{H}^{-\frac{1}{2}}_\parallel(\mathrm{div}_\Gamma, \Gamma)$ and vice versa. The corresponding duality product is the extension of the $\mathbf{L}^2_{\mathbf{t}}(\Gamma)$ duality product, and, in the following, it will be denoted with subscript τ, i.e.,

$$\langle \cdot, \cdot \rangle_\tau := \langle \cdot, \cdot \rangle_{\mathbf{H}^{-\frac{1}{2}}_\parallel(\mathrm{div}_\Gamma, \Gamma) \times \mathbf{H}^{-\frac{1}{2}}_\perp(\mathrm{curl}_\Gamma, \Gamma)}.$$

For $\mathbf{y} \in \mathbf{H}(\mathbf{curl}^2, \Omega)$, the *Neumann trace* $\boldsymbol{\gamma}_{\mathbf{N}} \mathbf{y} \in \mathbf{H}^{-\frac{1}{2}}_\parallel(\mathrm{div}_\Gamma, \Gamma)$ is defined through the integration by parts formula (see [80])

$$\langle \boldsymbol{\gamma}_{\mathbf{N}} \mathbf{y}, \boldsymbol{\gamma}_{\mathbf{D}} \mathbf{v} \rangle_\tau = \pm(\mathbf{curl}\,\mathbf{y}, \mathbf{curl}\,\mathbf{v})_{\mathbf{0},\Omega} \mp (\mathbf{curl}\,\mathbf{curl}\,\mathbf{y}, \mathbf{v})_{\mathbf{0},\Omega}, \quad \forall \mathbf{v} \in \mathbf{H}(\mathbf{curl}, \Omega). \tag{2.13}$$

Here, the upper signs are applied to the interior domain $\Omega = \Omega_1$, and the lower signs are used for the exterior domain $\Omega = \Omega_2$. Furthermore there holds the representation $\boldsymbol{\gamma}_{\mathbf{N}} \mathbf{y} = \mathbf{curl}\,\mathbf{y} \times \mathbf{n}$. Finally, we collect the mapping properties of the trace operators.

Lemma 2.11. *The trace operators*

$$\boldsymbol{\gamma}_\times : \mathbf{H}(\mathbf{curl}, \Omega) \to \mathbf{H}^{-\frac{1}{2}}_\parallel(\mathrm{div}_\Gamma, \Gamma),$$

$$\boldsymbol{\gamma}_{\mathbf{D}} : \mathbf{H}(\mathbf{curl}, \Omega) \to \mathbf{H}^{-\frac{1}{2}}_\perp(\mathrm{curl}_\Gamma, \Gamma),$$

$$\boldsymbol{\gamma}_{\mathbf{N}} : \mathbf{H}(\mathbf{curl}^2, \Omega) \to \mathbf{H}^{-\frac{1}{2}}_\parallel(\mathrm{div}_\Gamma, \Gamma),$$

$$\boldsymbol{\gamma}_{\mathbf{n}} : \mathbf{H}(\mathrm{div}, \Omega) \to H^{-\frac{1}{2}}(\Gamma)$$

are linear, continuous and surjective.

Proof. See [80] □

Furthermore, we need the space

$$\mathbf{H}^{-\frac{1}{2}}_\parallel(\mathrm{div}_\Gamma\, 0, \Gamma) := \left\{ \boldsymbol{\mu} \in \mathbf{H}^{-\frac{1}{2}}_\parallel(\mathrm{div}_\Gamma, \Gamma), \mathrm{div}_\Gamma\,\boldsymbol{\mu} = 0 \right\}. \tag{2.14}$$

For more details about the construction of the traces for Maxwell's equation on a Lipschitz polyhedron, we refer to the articles [33, 34].

2.3 Boundary integral equations for eddy current computations

This section introduces potentials and boundary integral operators for the eddy current problem and provides a brief review of the most important properties, as they are used in the numerical analysis of boundary element methods. One of the key results of this section is a Calderon projection in a weak form. Indeed, in the case of the eddy current problem, the Calderon projector in weak form provides an indispensable tool for the coupling of the finite element and the boundary element method.

Therefore, again, $\Omega = \mathbb{R}^3$ is split into two subdomains Ω_1 and Ω_2. Ω_1 is assumed to be a simply connected Lipschitz domain, whereas Ω_2 is the complement of Ω_1 in $\mathbb{R}^3$, i.e., $\mathbb{R}^3\backslash\overline{\Omega}_1$. Furthermore, we denote by Γ the interface of the two subdomains, i.e., $\Gamma = \overline{\Omega}_1 \cap \overline{\Omega}_2$. The exterior unit normal vector of Ω_1 on Γ is denoted by $\mathbf{n}$, i.e., $\mathbf{n}$ points from Ω_1 to Ω_2. We consider the exterior eddy current problem

$$\begin{cases} \mathbf{curl}\,(\mathbf{curl}\,\mathbf{y}) = \mathbf{0}, & \text{in } \Omega_2, \\ \operatorname{div}(\mathbf{y}) = 0, & \text{in } \Omega_2, \end{cases} \tag{2.15}$$

with appropriate decay conditions

$$\mathbf{y} = \mathcal{O}(|\mathbf{x}|^{-1}), \quad \mathbf{curl}\,\mathbf{y} = \mathcal{O}(|\mathbf{x}|^{-1}), \qquad \text{for } |\mathbf{x}| \to \infty. \tag{2.16}$$

The derivation of the boundary integral equations for the eddy current problem emerges from the integration by parts formula (2.13) and the fundamental solution of the Laplace operator in three dimensions, given by the expression

$$E(\mathbf{x}, \mathbf{z}) := \frac{1}{4\pi} \frac{1}{|\mathbf{x} - \mathbf{z}|}, \quad \mathbf{x}, \mathbf{z} \in \mathbb{R}^3, \mathbf{x} \neq \mathbf{z}.$$

Therefore, for any vector field $\mathbf{y}$, fulfilling the decay condition (2.16) the representation formula (*Stratton-Chu formula*) can be derived as follows

$$\begin{aligned} \mathbf{y}(\mathbf{x}) = &\int_\Gamma (\mathbf{n} \times \mathbf{curl}\,\mathbf{y})(\mathbf{z})E(\mathbf{x},\mathbf{z})\,\mathrm{dS}_\mathbf{z} - \mathbf{curl}_\mathbf{x} \int_\Gamma (\mathbf{n} \times \mathbf{y})(\mathbf{z})E(\mathbf{x},\mathbf{z})\,\mathrm{dS}_\mathbf{z} \\ &+ \nabla_\mathbf{x} \int_\Gamma (\mathbf{n} \cdot \mathbf{y})(\mathbf{z})E(\mathbf{x},\mathbf{z})\,\mathrm{dS}_\mathbf{z} + \int_\Omega \mathbf{curl\,curl}\,\mathbf{y}(\mathbf{z})E(\mathbf{x},\mathbf{z})\,\mathrm{d}\mathbf{z} \\ &- \int_\Omega \operatorname{div}\,\mathbf{y}(\mathbf{z})\nabla_\mathbf{x}E(\mathbf{x},\mathbf{z})\,\mathrm{d}\mathbf{z}, \quad \mathbf{x} \in \Omega. \end{aligned} \tag{2.17}$$

Due to the last two contributions from the volume integral over Ω in (2.17), it is crucial to take the information on the divergence and the zero source condition in (2.15) into account. By introducing the scalar single layer potential ψ_V, the vectorial single layer potential $\boldsymbol{\psi}_\mathbf{A}$ and the vectorial double layer potential $\boldsymbol{\psi}_\mathbf{M}$, i.e.,

$$\psi_V(\mathbf{n} \cdot \mathbf{y})(\mathbf{x}) := \int_\Gamma (\mathbf{n} \cdot \mathbf{y})(\mathbf{z})E(\mathbf{x},\mathbf{z})\,\mathrm{dS}_\mathbf{z}, \qquad \text{for } \mathbf{x} \in \Omega\backslash\Gamma,$$

$$\boldsymbol{\psi}_\mathbf{A}(\mathbf{y})(\mathbf{x}) := \int_\Gamma \mathbf{y}(\mathbf{z})E(\mathbf{x},\mathbf{z})\,\mathrm{dS}_\mathbf{z}, \qquad \text{for } \mathbf{x} \in \Omega\backslash\Gamma,$$

$$\boldsymbol{\psi}_\mathbf{M}(\mathbf{n} \times \mathbf{y})(\mathbf{x}) := \mathbf{curl}_\mathbf{x} \int_\Gamma (\mathbf{n} \times \mathbf{y})(\mathbf{z})E(\mathbf{x},\mathbf{z})\,\mathrm{dS}_\mathbf{z}, \quad \text{for } \mathbf{x} \in \Omega\backslash\Gamma,$$

the representation formula (2.17) can be expressed in terms of the potential operators, i.e.,

$$\mathbf{y} = \boldsymbol{\psi}_M[\boldsymbol{\gamma}_\mathbf{D}\mathbf{y}] - \boldsymbol{\psi}_A[\boldsymbol{\gamma}_\mathbf{N}\mathbf{y}] - \nabla\psi_V[\gamma_\mathbf{n}\mathbf{y}]. \tag{2.18}$$

In order to derive the boundary integral equations for the *Cauchy data* $(\boldsymbol{\gamma_D}\mathbf{y}, \boldsymbol{\gamma_N}\mathbf{y}, \gamma_{\mathbf{n}}\mathbf{y})$, the trace operators are applied to (2.18). Indeed, taking the Dirichlet trace $\boldsymbol{\gamma_D}$ and the Neumann trace $\boldsymbol{\gamma_N}$ in the representation formula (2.18) motivates the definition of the scalar boundary integral operator

$$\mathbf{S}(\varphi) := \boldsymbol{\gamma_D}(\nabla\psi_V(\varphi)), \tag{2.19}$$

and the vectorial boundary integral operators

$$\mathbf{A}(\boldsymbol{\lambda}) := \boldsymbol{\gamma_D}\psi_{\mathbf{A}}(\boldsymbol{\lambda}), \quad \mathbf{B}(\boldsymbol{\lambda}) := \boldsymbol{\gamma_N}\psi_{\mathbf{A}}(\boldsymbol{\lambda}), \quad \mathbf{C}(\boldsymbol{\mu}) := \boldsymbol{\gamma_D}\psi_{\mathbf{M}}(\boldsymbol{\mu}), \quad \mathbf{N}(\boldsymbol{\mu}) := \boldsymbol{\gamma_N}\psi_{\mathbf{M}}(\boldsymbol{\mu}). \tag{2.20}$$

The next lemma clarifies the mapping properties of the boundary integral operators.

Lemma 2.12. *The mappings*

$$\mathbf{A} : \mathbf{H}_{\parallel}^{-\frac{1}{2}}(\mathrm{div}_{\Gamma}, \Gamma) \to \mathbf{H}_{\perp}^{-\frac{1}{2}}(\mathrm{curl}_{\Gamma}, \Gamma), \qquad \mathbf{B} : \mathbf{H}_{\parallel}^{-\frac{1}{2}}(\mathrm{div}_{\Gamma}, \Gamma) \to \mathbf{H}_{\parallel}^{-\frac{1}{2}}(\mathrm{div}_{\Gamma}, \Gamma),$$

$$\mathbf{C} : \mathbf{H}_{\perp}^{-\frac{1}{2}}(\mathrm{curl}_{\Gamma}, \Gamma) \to \mathbf{H}_{\perp}^{-\frac{1}{2}}(\mathrm{curl}_{\Gamma}, \Gamma), \qquad \mathbf{N} : \mathbf{H}_{\perp}^{-\frac{1}{2}}(\mathrm{curl}_{\Gamma}, \Gamma) \to \mathbf{H}_{\parallel}^{-\frac{1}{2}}(\mathrm{div}_{\Gamma}, \Gamma),$$

$$\mathbf{S} : H^{-\frac{1}{2}}(\Gamma) \to \mathbf{H}_{\perp}^{-\frac{1}{2}}(\Gamma),$$

are linear and bounded.

Proof. See [80]. $\square$

Consequently, the *Calderon mapping* can be obtained by a straightforward application of the Dirichlet and Neumann traces to the representation formula (2.18), using the boundary integral operators (2.19) and (2.20):

$$\begin{cases} \boldsymbol{\gamma_D}\mathbf{y} = \mathbf{C}(\boldsymbol{\gamma_D}\mathbf{y}) - \mathbf{A}(\boldsymbol{\gamma_N}\mathbf{y}) - \mathbf{S}(\gamma_{\mathbf{n}}\mathbf{y}), \\ \boldsymbol{\gamma_N}\mathbf{y} = \mathbf{N}(\boldsymbol{\gamma_D}\mathbf{y}) - \mathbf{B}(\boldsymbol{\gamma_N}\mathbf{y}). \end{cases} \tag{2.21}$$

Due to the additional term $\mathbf{S}(\gamma_{\mathbf{n}}\mathbf{y})$, including a contribution from the additional Neumann data $\gamma_{\mathbf{n}}\mathbf{y}$, the extraction of a *Calderon projector* is not straightforward. Heading for a Calderon projection in a weak setting, we start by investigating the *correct* space for the Neumann trace $\boldsymbol{\gamma_N}\mathbf{y}$ (see also [80, Section 4]).

Lemma 2.13. *Let* $\mathbf{y} \in \mathbf{H}(\mathbf{curl}^2, \Omega_2)$, *such that* $\mathbf{curl}\,\mathbf{curl}\,\mathbf{y} = 0$ *in* Ω_2, *then there holds*

$$\langle \boldsymbol{\gamma_N}\mathbf{y}, \mathbf{grad}_{\Gamma}\varphi \rangle_{\tau} = 0, \quad \forall\varphi \in H^{\frac{1}{2}}(\Gamma).$$

Proof. By using the definition of the surface operators and Stokes formulas on surfaces, we obtain

$$\int_{\Gamma} \boldsymbol{\gamma_N}\mathbf{y} \cdot \mathbf{grad}_{\Gamma}\varphi\,\mathrm{dS} = \int_{\Gamma} \mathbf{curl}\,\mathbf{y} \cdot (\mathbf{grad}_{\Gamma}\varphi \times \mathbf{n})\,\mathrm{dS} = \int_{\Gamma} \mathbf{curl}\,\mathbf{y} \cdot \mathbf{curl}_{\Gamma}\,\varphi\,\mathrm{dS}$$

$$= \int_{\Gamma} \mathrm{curl}_{\Gamma}\,(\mathbf{curl}\,\mathbf{y})\,\varphi\,\mathrm{dS} = \int_{\Gamma} (\mathbf{curl}\,\mathbf{curl}\,\mathbf{y})|_{\Gamma} \cdot \mathbf{n}\,\varphi\,\mathrm{dS} = 0.$$

$\square$

Consequently, the surface divergence of the Neumann trace vanishes, i.e., $\mathrm{div}_{\Gamma}(\boldsymbol{\gamma_N}\mathbf{y}) = 0$ in a weak sense. Therefore, the Neumann trace $\boldsymbol{\gamma_N}\mathbf{y}$ is even in the gauged subspace $\mathbf{H}_{\parallel}^{-\frac{1}{2}}(\mathrm{div}_{\Gamma}\,0, \Gamma)$ as introduced in (2.14). The advantage of this subspace is, that the following relation can be verified:

$$\langle \boldsymbol{\mu}, \mathbf{grad}_{\Gamma}\varphi \rangle_{\tau} = 0, \quad \forall\boldsymbol{\mu} \in \mathbf{H}_{\parallel}^{-\frac{1}{2}}(\mathrm{div}_{\Gamma}\,0, \Gamma) \quad \forall\varphi \in H^{\frac{1}{2}}(\Gamma).$$

Consequently, more information about the impact of the additional Neumann data $\gamma_{\mathbf{n}}\mathbf{y}$ can be extracted

$$\langle \boldsymbol{\mu}, \mathbf{S}(\varphi) \rangle_{\tau} = \langle \boldsymbol{\mu}, \boldsymbol{\gamma_D}(\nabla\,\psi_V(\varphi)) \rangle_{\tau} = \langle \boldsymbol{\mu}, \mathbf{grad}_{\Gamma}\boldsymbol{\gamma_D}\psi_V(\varphi) \rangle_{\tau} = 0, \quad \forall\boldsymbol{\mu} \in \mathbf{H}_{\parallel}^{-\frac{1}{2}}(\mathrm{div}_{\Gamma}\,0, \Gamma).$$

Using this information, the test space $\mathbf{H}_{\parallel}^{-\frac{1}{2}}(\operatorname{div}_\Gamma 0, \Gamma)$ can be used to get rid of the additional Neumann data $\gamma_{\mathbf{n}}\mathbf{y}$. Testing (2.21) with appropriate test functions $\boldsymbol{\mu}$ and $\boldsymbol{\lambda}$ yields the *Calderon projection* in a weak setting

$$
\begin{cases}
\langle \boldsymbol{\mu}, \gamma_{\mathbf{D}}\mathbf{y} \rangle_\tau = \langle \boldsymbol{\mu}, \mathbf{C}(\gamma_{\mathbf{D}}\mathbf{y}) \rangle_\tau - \langle \boldsymbol{\mu}, \mathbf{A}(\gamma_{\mathbf{N}}\mathbf{y}) \rangle_\tau, & \forall \boldsymbol{\mu} \in \mathbf{H}_{\parallel}^{-\frac{1}{2}}(\operatorname{div}_\Gamma 0, \Gamma), \\
\langle \gamma_{\mathbf{N}}\mathbf{y}, \boldsymbol{\lambda} \rangle_\tau = \langle \mathbf{N}(\gamma_{\mathbf{D}}\mathbf{y}), \boldsymbol{\lambda} \rangle_\tau - \langle \mathbf{B}(\gamma_{\mathbf{N}}\mathbf{y}), \boldsymbol{\lambda} \rangle_\tau, & \forall \boldsymbol{\lambda} \in \mathbf{H}_{\perp}^{-\frac{1}{2}}(\operatorname{curl}_\Gamma, \Gamma).
\end{cases}
\tag{2.22}
$$

The following symmetry and ellipticity properties of the boundary integral operators $\mathbf{A}$, $\mathbf{B}$, $\mathbf{C}$ and $\mathbf{N}$ are essential for the investigation of existence and uniqueness of boundary integral equations.

Lemma 2.14. *The bilinear form on $\mathbf{H}_{\parallel}^{-\frac{1}{2}}(\operatorname{div}_\Gamma 0, \Gamma)$, induced by the operator $\mathbf{A}$, is symmetric and positive definite, i.e.,*

$$
\langle \boldsymbol{\lambda}, \mathbf{A}(\boldsymbol{\lambda}) \rangle_\tau \geq c \, \|\boldsymbol{\lambda}\|^2_{\mathbf{H}_{\parallel}^{-\frac{1}{2}}(\operatorname{div}_\Gamma, \Gamma)}, \qquad \forall \boldsymbol{\lambda} \in \mathbf{H}_{\parallel}^{-\frac{1}{2}}(\operatorname{div}_\Gamma 0, \Gamma),
$$

for some constant $c > 0$.

Proof. See [80, Theorem 6.2]. $\qquad\qquad\qquad\qquad\qquad\qquad\qquad\qquad\qquad\qquad\qquad$ $\square$

Lemma 2.15. *The operators $\mathbf{B}$ and $\mathbf{C}$ fulfill the symmetry property*

$$
\langle \mathbf{B}(\boldsymbol{\mu}), \boldsymbol{\lambda} \rangle_\tau = \langle \boldsymbol{\mu}, (\mathbf{C} - \mathbf{Id})(\boldsymbol{\lambda}) \rangle_\tau, \qquad \forall \boldsymbol{\mu} \in \mathbf{H}_{\parallel}^{-\frac{1}{2}}(\operatorname{div}_\Gamma 0, \Gamma), \forall \boldsymbol{\lambda} \in \mathbf{H}_{\perp}^{-\frac{1}{2}}(\operatorname{curl}_\Gamma, \Gamma),
$$

where $\mathbf{Id} : \mathbf{H}_{\perp}^{-\frac{1}{2}}(\operatorname{curl}_\Gamma, \Gamma) \to \mathbf{H}_{\perp}^{-\frac{1}{2}}(\operatorname{curl}_\Gamma, \Gamma)$ denotes the identity operator.

Proof. See [80, Equation (6.5)]. $\qquad\qquad\qquad\qquad\qquad\qquad\qquad\qquad\qquad\qquad$ $\square$

Lemma 2.16. *The bilinear form on $\mathbf{H}_{\perp}^{-\frac{1}{2}}(\operatorname{curl}_\Gamma, \Gamma)$, induced by the operator $\mathbf{N}$, is symmetric and negative semi-definite, i.e.,*

$$
-\langle \mathbf{N}(\boldsymbol{\mu}), \boldsymbol{\mu} \rangle_\tau \geq c \, \|\operatorname{curl}_\Gamma \boldsymbol{\mu}\|^2_{\mathbf{H}^{-\frac{1}{2}}(\Gamma)}, \qquad \forall \boldsymbol{\mu} \in \mathbf{H}_{\perp}^{-\frac{1}{2}}(\operatorname{curl}_\Gamma, \Gamma),
$$

for some constant $c > 0$.

Proof. See [80, Theorem 6.4]. $\qquad\qquad\qquad\qquad\qquad\qquad\qquad\qquad\qquad\qquad$ $\square$

The following Lemma reflects an important property of the integration by parts formula (2.13).

Lemma 2.17. *For $\gamma_{\mathbf{N}}\mathbf{y} \in \mathbf{H}_{\parallel}^{-\frac{1}{2}}(\operatorname{div}_\Gamma 0, \Gamma)$ and $\gamma_{\mathbf{D}}\mathbf{y} \in \mathbf{H}_{\perp}^{-\frac{1}{2}}(\operatorname{curl}_\Gamma, \Gamma)$ fulfilling (2.22), the following estimate is valid:*

$$
-\langle \gamma_{\mathbf{N}}\mathbf{y}, \gamma_{\mathbf{D}}\mathbf{y} \rangle_\tau \geq 0.
$$

Proof. Using the weak Calderon mapping (2.22) and choosing special test functions $\boldsymbol{\mu} = \gamma_{\mathbf{N}}\mathbf{y}$ and $\boldsymbol{\lambda} = \gamma_{\mathbf{D}}\mathbf{y}$ we obtain from the first equation and the symmetry property (Lemma 2.15)

$$
\langle \gamma_{\mathbf{N}}\mathbf{y}, \mathbf{A}(\gamma_{\mathbf{N}}\mathbf{y}) \rangle_\tau = \langle \gamma_{\mathbf{N}}\mathbf{y}, (\mathbf{C} - \mathbf{Id})(\gamma_{\mathbf{D}}\mathbf{y}) \rangle_\tau = \langle \mathbf{B}(\gamma_{\mathbf{N}}\mathbf{y}), \gamma_{\mathbf{D}}\mathbf{y} \rangle_\tau.
$$

Consequently from the second equation we obtain

$$
\begin{aligned}
-\langle \gamma_{\mathbf{N}}\mathbf{y}, \gamma_{\mathbf{D}}\mathbf{y} \rangle_\tau &= -\langle \mathbf{N}(\gamma_{\mathbf{D}}\mathbf{y}), \gamma_{\mathbf{D}}\mathbf{y} \rangle_\tau + \langle \mathbf{B}(\gamma_{\mathbf{N}}\mathbf{y}), \gamma_{\mathbf{D}}\mathbf{y} \rangle_\tau \\
&= -\langle \mathbf{N}(\gamma_{\mathbf{D}}\mathbf{y}), \gamma_{\mathbf{D}}\mathbf{y} \rangle_\tau + \langle \gamma_{\mathbf{N}}\mathbf{y}, \mathbf{A}(\gamma_{\mathbf{N}}\mathbf{y}) \rangle_\tau \geq 0.
\end{aligned}
$$

Now the result follows from the negative semi-definiteness of $\mathbf{N}$ and the positive definiteness of $\mathbf{A}$. $\quad\square$

For a comprehensive study of the boundary integral equations and the underlying boundary integral operators for the eddy current problem, we refer to [80, 81] and the references therein.

2.4 Discretization techniques

2.4.1 Triangulation

Without loss of generality, let $\Omega_1 \subset \mathbb{R}^3$ be a bounded polyhedral domain with Lipschitz boundary $\Gamma := \partial\Omega_1$. On the domain Ω_1 we define a triangulation $\mathcal{T}_h$ with tetrahedral elements. Since Ω_1 is a polyhedron, it can always be resolved by the discretization exactly. Furthermore, we assume that $\mathcal{T}_h$ is quasi-uniform with *mesh size $h > 0$* and shape regular. The triangulation $\mathcal{T}_h$ induces a *shape-regular* and *quasi-uniform* triangulation $\mathcal{K}_h$ of Γ into triangles.

2.4.2 Finite element method

As a discretization technique we use the *finite element method*, a Galerkin method with local basis functions. We use the space of continuous piecewise, linear functions $\mathcal{S}^1(\mathcal{T}_h)$ as the conforming finite element subspace of $H^1(\Omega_1)$. Furthermore, for $\mathbf{H}(\mathbf{curl}, \Omega_1)$, we use Nédélec basis functions of lowest order $\mathcal{N}\mathcal{D}^0(\mathcal{T}_h)$, see [120, 121]. We also need $\mathcal{S}_0^1(\mathcal{T}_h) = \mathcal{S}^1(\mathcal{T}_h) \cap H_0^1(\Omega_1)$ and $\mathcal{N}\mathcal{D}_0^0(\mathcal{T}_h) = \mathcal{N}\mathcal{D}^0(\mathcal{T}_h) \cap \mathbf{H_0}(\mathbf{curl}, \Omega_1)$.
The Friedrichs' inequality, cf. Lemma 2.8, is also valid in the finite element subspace.

Lemma 2.18 (Weighted Friedrichs' inequality for $\mathcal{N}\mathcal{D}^0(\mathcal{T}_h)$)**.** *Let Ω_1 be a simply-connected and bounded Lipschitz domain, $\mathcal{T}_h$ a quasi-uniform and shape regular triangulation with mesh size h, and $\sigma \in L^\infty(\Omega_1)$ with $\sigma \geq \underline{\sigma} > 0$. Suppose, that $\mathbf{y_h} \in \mathcal{N}\mathcal{D}^0(\mathcal{T}_h)$ is orthogonal to gradient functions in the sense*

$$(\sigma\mathbf{y_h}, \nabla q_h)_{\mathbf{0},\Omega_1} = 0, \quad \forall q_h \in \mathcal{S}^1(\mathcal{T}_h),$$

then there exists a constant $C_2^F > 0$ depending only on Ω and independent of h and σ, such that

$$\|\sqrt{\sigma}\mathbf{y_h}\|_{\mathbf{0},\Omega_1} \leq C_2^F \|\sqrt{\sigma}\,\mathbf{curl}\,\mathbf{y_h}\|_{\mathbf{0},\Omega_1}.$$

Proof. See [87, Lemma 4.2]. $\qquad\square$

Lemma 2.18 also holds for $\mathcal{N}\mathcal{D}^0(\mathcal{T}_h)$ and $\mathcal{S}^1(\mathcal{T}_h)$ replaced by $\mathcal{N}\mathcal{D}_0^0(\mathcal{T}_h)$ and $\mathcal{S}_0^1(\mathcal{T}_h)$, respectively. Furthermore, we collect the approximation properties of the finite element spaces $\mathcal{N}\mathcal{D}^0(\mathcal{T}_h)$. Let $\mathbf{\Pi}$ be the canonical interpolation operator for the finite element space $\mathcal{N}\mathcal{D}^0(\mathcal{T}_h)$. Then the following interpolation error estimate is valid:

Lemma 2.19. *For $\mathbf{y} \in \mathbf{H^s}(\mathbf{curl}, \Omega_1)$, $s > \frac{1}{2}$, the interpolation error can be estimated by*

$$\|\mathbf{y} - \mathbf{\Pi}\mathbf{y}\|_{\mathbf{curl},\Omega_1} \leq Ch^{\min(1,s)}\left(\|\mathbf{y}\|_{\mathbf{s},\Omega_1} + \|\mathbf{curl}\,\mathbf{y}\|_{\mathbf{s},\Omega_1}\right),$$

where the constant C is independent of the mesh size h.

Proof. See [39]. $\qquad\square$

2.4.3 Boundary element method

The Galerkin boundary element method is a special Galerkin finite element method applied to boundary integral equations. We use the Raviart-Thomas basis functions of lowest order $\mathcal{R}\mathcal{T}^0(\mathcal{K}_h)$, cf. [77], a conforming finite element subspace of $\mathbf{H}_{\|}^{-\frac{1}{2}}(\mathrm{div}_\Gamma, \Gamma)$. Furthermore, we use the finite element space $\mathcal{R}\mathcal{T}_0^0(\mathcal{K}_h) = \mathcal{R}\mathcal{T}^0(\mathcal{K}_h) \cap \mathbf{H}_{\|}^{-\frac{1}{2}}(\mathrm{div}_\Gamma\, 0, \Gamma)$. In order to construct a basis for $\mathcal{R}\mathcal{T}_0^0(\mathcal{K}_h)$, the identity

$$\mathcal{R}\mathcal{T}_0^0(\mathcal{K}_h) = \mathbf{curl}_\Gamma\, \mathcal{S}^1(\mathcal{K}_h),$$

where $\mathcal{S}^1(\mathcal{K}_h)$ is the space of continuous, piecewise linear functions on $\mathcal{K}_h$, can be used, cf. [80].
In order to give a bound for the approximation error on the boundary, we use the fact, that we are estimating Neumann traces of the interior functions.

Lemma 2.20. *Let* $\mathbf{y} \in \mathbf{H}(\mathbf{curl}^2, \Omega_1)$ *and* $\boldsymbol{\lambda} = \boldsymbol{\gamma_N}\mathbf{y} \in \mathbf{H}_{\parallel}^{-\frac{1}{2}}(\mathrm{div}_\Gamma\, 0, \Gamma)$, *the approximation error can be estimated by*

$$\inf_{\boldsymbol{\lambda_h} \in \mathcal{RT}_0^0(\mathcal{K}_h)} \|\boldsymbol{\lambda} - \boldsymbol{\lambda_h}\|_{\mathbf{H}_{\parallel}^{-\frac{1}{2}}(\mathrm{div}_\Gamma, \Gamma)} \leq C \|\mathbf{curl}\,\mathbf{y} - \boldsymbol{\Pi}\,\mathbf{curl}\,\mathbf{y}\|_{\mathbf{curl}, \Omega_1},$$

where the constant C *is independent of the mesh size* h.

Proof. See [80, Theorem 8.1]. □

2.5   Abstract results for time-dependent problems

In the following we want to analyze (possible nonlinear) initial value problems and (possible nonlinear) time-periodic problems. Therefore we introduce appropriate spaces that allow to state existence and uniqueness results. Let X be a Banach space, then we define the space

$$L_2((0,T), X) := \{v : (0,T) \to X : \|v\|_{L_2((0,T),X)} < \infty\}$$

with the norm

$$\|v\|_{L_2((0,T),X)}^2 := \int_0^T \|v(\cdot, t)\|_X^2 \mathrm{dt}.$$

Next we introduce the concept of *generalized weak derivatives*. For $v \in L_2((0,T), X)$, we denote by $\frac{\partial}{\partial t}v \in L_2((0,T), V^*)$ the *generalized weak derivative*, if there holds

$$\int_0^T v(t)\frac{\partial}{\partial t}\varphi(t)\,\mathrm{dt} = -\int_0^T \frac{\partial}{\partial t}v(t)\varphi(t)\,\mathrm{dt}, \quad \forall \varphi \in C_0^\infty(0,T).$$

Furthermore, we need the concept of *evolution triples*.

Definition 2.21. *An evolution triple* $V \subset H \subset V^*$ *is characterized by:*

    1. V is a real, separable and reflexive Banach space.

    2. H is a real, separable Hilbert space.

    3. The embedding $V \subset H$ is continuous and V is dense in H.

In the following let $V \subset H \subset V^*$ be an evolution triple. Using the generalized weak derivative, we can define the Sobolev space

$$W_2^1((0,T), V, H) := \left\{ v \in L_2((0,T), V) : \frac{\partial}{\partial t}v \in L_2((0,T), V^*) \right\},$$

with the associated norm

$$\|v\|_{W_2^1((0,T),V,H)}^2 := \|v\|_{L_2((0,T),V)}^2 + \left\|\frac{\partial}{\partial t}v\right\|_{L_2((0,T),V^*)}^2.$$

We mention, that the definition of $\frac{\partial}{\partial t}v$, the generalized derivative of v, is made so, that

$$\langle \frac{\partial}{\partial t}v, u\rangle_{V^* \times V} = \frac{\mathrm{d}}{\mathrm{dt}}(v(t), u)_H, \quad \forall\, v \in V.$$

Furthermore, we need the concepts of *monotone*, *coercive*, *bounded*, and *hemicontinuous* operators. An operator $\mathcal{A} : V^* \to V$ is called *monotone*, if and only if

$$\langle \mathcal{A}(y) - \mathcal{A}(v), y - v\rangle_{V^* \times V} \geq 0, \quad \forall\, y, v \in V,$$

coercive, if and only if

$$\lim_{\|y\|_V \to \infty} \frac{\langle \mathcal{A}(y), y \rangle_{V^* \times V}}{\|y\|_V^2} = \infty, \quad \forall\, y \in V,$$

bounded, if and only if

$$\langle \mathcal{A}(y), v \rangle_{V^* \times V} \leq c \|y\|_V \|v\|_V, \quad \forall\, y, v \in V,$$

for some constant c, and *hemicontinuous*, if and only if the real function

$$s \mapsto \langle \mathcal{A}(u + s\,v), w \rangle_{V^* \times V}$$

is continuous on $[0, s]$ for all $u, v, w \in V$. The main theorem on existence and uniqueness of nonlinear initial value problems is stated in the next theorem.

Theorem 2.22. *Let $V \subset H \subset V^*$ be an evolution triple. Let $\mathcal{A} : V \to V^*$ be a hemicontinuous, monotone, coercive and bounded operator. Suppose furthermore that $U \in L_2((0, T), V^*)$ and $y_0 \in H$ are given. Then the initial value problem*

$$\begin{cases} \dfrac{\partial}{\partial t} y(t) + \mathcal{A}(y(t)) = U(t), & \text{in } L_2((0, T), V^*), \\ y(0) = y_0, & \text{in } H, \end{cases}$$

has a unique solution $y \in W_2^1((0, T), V, H)$, that fulfills the a priori estimate

$$\|y\|_{W_2^1((0,T),V,H)} \leq c \left(\|U\|_{L_2((0,T),V^*)} + \|y_0\|_H \right),$$

with some constant $c > 0$.

Proof. See [162, Theorem 32.D]. □

A variant of Theorem 2.22 for time-periodic problems is also available.

Theorem 2.23. *Let $V \subset H \subset V^*$ be an evolution triple. Let $\mathcal{A} : V \to V^*$ be a hemicontinuous, monotone, coercive and bounded operator. Suppose furthermore that $U \in L_2((0, T), V^*)$ is given. Then the time-periodic problem*

$$\begin{cases} \dfrac{\partial}{\partial t} y(t) + \mathcal{A}(y(t)) = U(t), & \text{in } L_2((0, T), V^*), \\ y(0) = y(T), & \text{in } H, \end{cases}$$

has a unique solution $y \in W_2^1((0, T), V, H)$.

Proof. See [162, Theorem 32.D]. □

For a comprehensive study of the appropriate spaces for time-dependent problems, we refer to [161, 162].

2.6 Optimal control problems

The following theorem provides existence and uniqueness results for reduced optimal control problems.

Theorem 2.24. *Let U and H denote real Hilbert spaces, and let a nonempty, closed and convex $U_{ad} \subset U$, as well as some $y_d \in H$ and constant $\lambda > 0$ be given. Moreover, let $\mathcal{S} : U \to H$ be a continuous linear operator. Then the quadratic Hilbert space optimization problem*

$$\min_{u \in U_{ad}} \left[\frac{1}{2} \|\mathcal{S}\,u - y_d\|_H^2 + \frac{\lambda}{2} \|u\|_U^2 \right] \tag{2.23}$$

admits an optimal solution $\bar{u} \in U_{ad}$.

Proof. See [151, Theorem 2.14, Theorem 2.16]. □

The following result provides the first-order optimality conditions.

Theorem 2.25. *Let U and H denote real Hilbert spaces, and let a nonempty, closed and convex $U_{ad} \subset U$, as well as some $y_d \in H$ and constant $\lambda > 0$ be given. Moreover, let $\mathcal{S} : U \to H$ be a continuous linear operator. Then $\bar{u} \in U_{ad}$ is a solution to the minimization problem (2.23), if and only if $\bar{u}$ solves the variational inequality*

$$(\lambda \bar{u}, u - \bar{u})_U - (y_d - \mathcal{S}\bar{u}, \mathcal{S}(u - \bar{u}))_H \geq 0, \quad \forall\, u \in U_{ad}. \tag{2.24}$$

Proof. See [151, Theorem 2.22]. □

For the special case $U = U_{ad}$, (2.24) simplifies to

$$(\lambda \bar{u}, u)_U - (y_d - \mathcal{S}\bar{u}, \mathcal{S}u)_H = 0, \quad \forall\, u \in U.$$

For more details about the analysis of optimal control problems, we refer to the monograph [151].

Chapter 3

Modelling and analysis

Eddy current problems are fundamental different for conducting and non-conducting regions. While in conducting regions the problems are of *parabolic* type, in non-conducting regions the problems reduce to *elliptic* ones. Due to these fundamental different behaviors, the analysis is a delicate issue. In this chapter we investigate both, the eddy current problem and the eddy current optimal control problem, concerning existence and uniqueness of solutions for the parabolic-elliptic type of equations. Since the reluctivity appears as a diffusion coefficient in the vector potential formulation, the formulation fits into the framework of monotone operators. Therefore, the analysis for the eddy current problem is done for general nonlinear settings. In order to provide existence and uniqueness results for a general eddy current problem, consisting of both, conducting and (possible unbounded) non-conducting domains, the main tool is the reduction of the full (unbounded) computational domain to the (bounded) conducting domain only. This can be achieved by either using the framework of PDE-harmonic extensions, or by the framework of boundary integral operators.

Eddy current problems in bounded domains have already been analyzed in [17]. Therein PDE-harmonic extensions are used to reduce the full computational domain to the conducting domains only and existence and uniqueness results are provided in special gauged spaces. For other works we mention [3, 10, 97].

In order to extend the existence and uniqueness theory also to the case of unbounded domains, in principle the same approach of PDE-harmonic extensions can be used. The drawback of the latter mentioned approach is the need for introducing weighted Sobolev spaces [10], since we are dealing with an unbounded domain. In order to avoid this, we prefer to use the theoretical framework of boundary integral operators. Additionally this approach directly offers a starting point for a domain decomposition method in the terms of a FEM-BEM coupling.

Furthermore, we consider both, initial value and time-periodic problems. While for simple parabolic problems, existence and uniqueness results for the time-periodic problems can be deduced by existence and uniqueness results for initial value problems in a straightforward manner, in the case of eddy current problems, the deduction is a delicate issue due to the large kernel of $\mathbf{H}(\mathbf{curl}, \Omega_1)$, and therefore calls for a careful study.

In the optimal control case, we restrict our analysis to the case of distributed control, where the minimization is done with respect to the linear eddy current problem. Again, we provide existence and uniqueness results, where special attention is drawn to fulfilling the charge conservation law in the state equation. Also for the optimal control problem, the analysis is done for initial value and time-periodic eddy current problems.

For simplicity, we provide our analysis for the simple model problem consisting of one conductor Ω_1, surrounded by an unbounded air region Ω_2, see Figure 3.1. Indeed, Ω_1 is assumed to be a simply connected Lipschitz polyhedron, whereas Ω_2 is the complement of Ω_1 in $\mathbb{R}^3$, i.e., $\mathbb{R}^3 \backslash \overline{\Omega}_1$. Furthermore, we denote by Γ the interface of the two subdomains; i.e., $\Gamma = \overline{\Omega}_1 \cap \overline{\Omega}_2$. The exterior unit normal vector of Ω_1 on Γ is denoted by $\mathbf{n}$, i.e., $\mathbf{n}$ points from Ω_1 to Ω_2.

We assume, that the compact support of the current density $\mathbf{j}$ is located in the conductor Ω_1 and
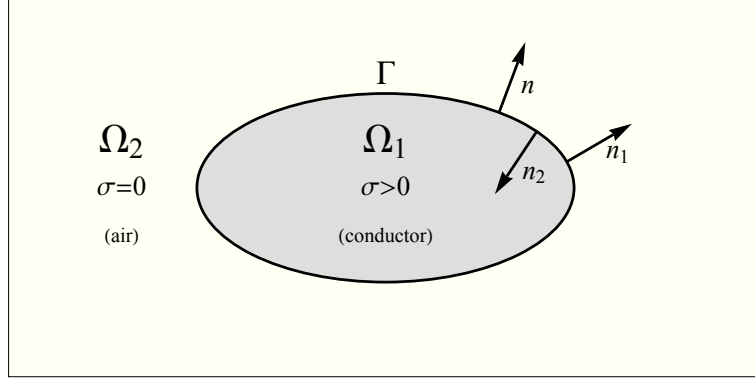
Figure 3.1: Simple model domain.

fulfills the conservation of charges law (cf. (1.2)), i.e.,

$$\operatorname{div}\mathbf{j} = 0, \quad \text{in } \Omega_1, \qquad \mathbf{j}\cdot\mathbf{n} = 0, \quad \text{on } \Gamma.$$

In the following, the contribution of the current density to the given right hand side is denoted by $\mathbf{u}$. Furthermore, the initial condition $\mathbf{y}(0)$ is only meaningful to be described in the conductor Ω_1.

Remark 3.1. *We mention, that the analysis can be generalized to the case of a domain consisting of multiple conductors or even to the case of multiply connected domains, cf. [5].*

3.1 Existence and uniqueness for the eddy current (EC) problem

This section provides existence and uniqueness results for the eddy current problem in the full computational domain $\Omega = \mathbb{R}^3$. In this section, we consider the general case of nonlinear reluctivity.

$$
\begin{cases}
\sigma\dfrac{\partial \mathbf{y}}{\partial t} + \mathbf{curl}(\nu\,\mathbf{curl}\,\mathbf{y}) = \mathbf{u}, & \text{in } \Omega_1 \times (0,T), \\[2mm]
\mathbf{curl}(\mathbf{curl}\,\mathbf{y}) = \mathbf{0}, & \text{in } \Omega_2 \times (0,T), \\[2mm]
\operatorname{div}\mathbf{y} = 0, & \text{in } \Omega_2 \times (0,T), \\[2mm]
\mathbf{y} = \mathcal{O}(|\mathbf{x}|^{-1}), & \text{for } |\mathbf{x}| \to \infty, \\[2mm]
\mathbf{curl}\,\mathbf{y} = \mathcal{O}(|\mathbf{x}|^{-1}), & \text{for } |\mathbf{x}| \to \infty, \\[2mm]
\mathbf{y}(0) = \mathbf{y_0}, & \text{in } \Omega_1, \\[2mm]
\mathbf{y}|_{\Omega_1} \times \mathbf{n} = \mathbf{y}|_{\Omega_2} \times \mathbf{n}, & \text{on } \Gamma \times (0,T), \\[2mm]
\nu\,\mathbf{curl}\,\mathbf{y}|_{\Omega_1} \times \mathbf{n} = \mathbf{curl}\,\mathbf{y}|_{\Omega_2} \times \mathbf{n}, & \text{on } \Gamma \times (0,T).
\end{cases}
\tag{3.1}
$$

In this section, the reluctivity ν is assumed to depend on $\mathbf{B} = \mathbf{curl}\,\mathbf{y}$, i.e., $\nu = \nu(|\mathbf{B}|) = \nu(|\,\mathbf{curl}\,\mathbf{y}|)$. Indeed, this setting renders the eddy current problem (3.1) nonlinear. Since ν is constant in the non-conducting region Ω_2, due to scaling arguments, it can always be achieved that $\nu = 1$ in Ω_2. The conductivity σ is zero in the non-conducting domain Ω_2 and piecewise constant and uniformly positive in the conductor Ω_1, i.e.,

$$
\begin{aligned}
\overline{\sigma} \geq \sigma \geq \underline{\sigma} > 0 \text{ a.e. in } \Omega_1 \quad &\text{and} \quad \sigma = 0 \text{ a.e. in } \Omega_2, \\
\overline{\nu} \geq \nu \geq \underline{\nu} > 0 \text{ a.e. in } \Omega_1 \quad &\text{and} \quad \nu = 1 \text{ a.e. in } \Omega_2.
\end{aligned}
\tag{3.2}
$$

Furthermore, the mapping $s \mapsto \nu(s)$ is assumed to be continuous and the mapping $s \mapsto \nu(s)s$ is assumed to be strictly monotone and Lipschitz continuous, which is an immediate consequence of the physical background.

Space-time variational formulation We start by deriving an appropriate space-time variational formulation. Therefore, we denote the underlying Hilbert space by $V = \mathbf{H}(\mathbf{curl}, \Omega_1)$ with the corresponding duality product $\langle \cdot, \cdot \rangle$. Furthermore, we recall the definitions of the abstract spaces $L_2((0, T), V)$ and $W_2^1((0, T), V, \mathbf{L_2}(\Omega_1))$ for functions in the space time cylinder $\Omega_1 \times (0, T)$, cf. Section 2.5. By multiplying the sum of the first two equations in (3.1) with a test function $\mathbf{v} \in L_2((0, T), \mathbf{H}(\mathbf{curl}, \Omega))$, integrating over the space-time cylinder and incorporating the interface conditions, we obtain

$$\int_0^T \int_{\Omega_1} \left[\sigma \frac{\partial \mathbf{y}}{\partial t} \cdot \mathbf{v} + \nu \, \mathbf{curl}\, \mathbf{y} \cdot \mathbf{curl}\, \mathbf{v} \right] \mathrm{dx}\, \mathrm{dt} + \int_0^T \int_{\Omega_2} \mathbf{curl}\, \mathbf{y} \cdot \mathbf{curl}\, \mathbf{v} \, \mathrm{dx}\, \mathrm{dt} = \int_0^T \int_{\Omega_1} \mathbf{u} \cdot \mathbf{v} \, \mathrm{dx}\, \mathrm{dt}.$$

We mention, that the reluctivity ν is nonlinear and depends on the spatial variable $\mathbf{x}$ as well as the time variable t, i.e., $\nu(\mathbf{x}, t) = \nu(\mathbf{x}, |\mathbf{curl}\, \mathbf{y}(\mathbf{x}, t)|)$. Applying the integration by parts formula in the exterior domain Ω_2, cf. (2.13), and using the fact, that there is no prescribed source in Ω_2, i.e., $\mathbf{curl}\, \mathbf{curl}\, \mathbf{y} = \mathbf{0}$, allows to reduce the variational problem to one just living in $\overline{\Omega}_1$, i.e.,

$$\int_0^T \int_{\Omega_1} \left[\sigma \frac{\partial \mathbf{y}}{\partial t} \cdot \mathbf{v} + \nu \, \mathbf{curl}\, \mathbf{y} \cdot \mathbf{curl}\, \mathbf{v} \right] \mathrm{dx}\, \mathrm{dt} - \int_0^T \langle \boldsymbol{\gamma_N} \mathbf{y}, \boldsymbol{\gamma_D} \mathbf{v} \rangle_\tau \, \mathrm{dt} = \int_0^T \int_{\Omega_1} \mathbf{u} \cdot \mathbf{v} \, \mathrm{dx}\, \mathrm{dt}. \quad (3.3)$$

For $t \in (0, T)$, we define the operator $\mathcal{A}_1 : V \to V^*$ by

$$\langle \mathcal{A}_1(\mathbf{y}(\cdot, t)), \mathbf{v}(\cdot, t) \rangle := \int_{\Omega_1} \nu(\cdot, |\mathbf{curl}\, \mathbf{y}(\cdot, t)|) \, \mathbf{curl}\, \mathbf{y}(\cdot, t) \cdot \mathbf{curl}\, \mathbf{v}(\cdot, t) \, \mathrm{dx},$$

and the operator $\mathcal{A}_2 : V \to V^*$ by

$$\langle \mathcal{A}_2(\mathbf{y}(\cdot, t)), \mathbf{v}(\cdot, t) \rangle := -\langle \boldsymbol{\gamma_N} \mathbf{y}(\cdot, t), \boldsymbol{\gamma_D} \mathbf{v}(\cdot, t) \rangle_\tau,$$

for all $\mathbf{y}(\cdot, t), \mathbf{v}(\cdot, t) \in V$. Furthermore, the right hand side can be regarded as a linear functional, i.e.,

$$\langle \mathbf{U}(t), \mathbf{v}(\cdot, t) \rangle := \int_{\Omega_1} \mathbf{u}(\mathbf{x}, t) \cdot \mathbf{v}(\mathbf{x}, t) \, \mathrm{dx},$$

with $\mathbf{U}(t) \in V^*$. Consequently, we can rewrite (3.3) in the equivalent form

$$\int_0^T \langle \sigma \frac{\partial}{\partial t} \mathbf{y}(\cdot, t), \mathbf{v}(\cdot, t) \rangle + \langle \mathcal{A}_1(\mathbf{y}(\cdot, t)), \mathbf{v}(\cdot, t) \rangle \mathrm{dt} + \int_0^T \langle \mathcal{A}_2(\mathbf{y}(\cdot, t)), \mathbf{v}(\cdot, t) \rangle \mathrm{dt} = \int_0^T \langle \mathbf{U}(t), \mathbf{v}(\cdot, t) \rangle \mathrm{dt},$$

where the derivative $\sigma \frac{\partial}{\partial t} \mathbf{y}(t)$ is considered as an abstract functional in V^*. By defining the operator $\mathcal{A} : V \to V^*$ by $\mathcal{A}(\mathbf{y}) := \mathcal{A}_1(\mathbf{y}) + \mathcal{A}_2(\mathbf{y})$, we can state (3.3) on the level of operator equations. Find $\mathbf{y} \in W_2^1((0, T), V, \mathbf{L_2}(\Omega_1))$, such that

$$\begin{cases} \sigma \dfrac{\partial \mathbf{y}}{\partial t} + \mathcal{A}(\mathbf{y}) = \mathbf{U}, & \text{in } L_2((0, T), V^*), \\ \mathbf{y}(0) = \mathbf{y_0}, & \text{in } \mathbf{L_2}(\Omega_1). \end{cases} \quad (3.4)$$

Now we provide the necessary tools for showing existence and uniqueness for the variational problem. We introduce the space of gradient functions

$$W := \{ \mathbf{v} \in V : \exists q \in H^1(\Omega_1) : \mathbf{v} = \nabla q, \int_{\Omega_1} q = 0, q|_\Gamma = c, c \in \mathbb{R} \},$$

and the factor space of divergence-free functions $\hat{V} := V|_W$ by

$$\hat{V} := \{\mathbf{y} \in V : (\sigma\mathbf{y}, \mathbf{v})_{\mathbf{0},\Omega_1} = 0, \forall\, \mathbf{v} \in W\}.$$

Furthermore, we also use

$$\hat{H}_1 := \{\mathbf{y} \in \mathbf{L_2}(\Omega_1) : (\mathbf{y}, \mathbf{v})_{\mathbf{0},\Omega_1} = 0, \forall\, \mathbf{v} \in W\}.$$

The main properties of $\mathcal{A}_1$ are summarized in the following lemma.

Lemma 3.2. *Let $s \mapsto \nu(s)s$ be strictly monotone and Lipschitz continuous and $s \mapsto \nu(s)$ uniformly positive and bounded, then the operator $\mathcal{A}_1$ is*

1. *monotone, i.e.,*

$$\langle \mathcal{A}_1(\mathbf{y}) - \mathcal{A}_1(\mathbf{v}), \mathbf{y} - \mathbf{v} \rangle \geq 0, \quad \forall\, \mathbf{v}, \mathbf{y} \in V,$$

2. *semi-coercive on V, i.e.,*

$$\langle \mathcal{A}_1(\mathbf{y}), \mathbf{y} \rangle \geq c\, \|\operatorname{\mathbf{curl}} \mathbf{y}\|_{\mathbf{0},\Omega_1}^2, \quad \forall\, \mathbf{y} \in V,$$

3. *bounded on V, i.e.,*

$$\langle \mathcal{A}_1(\mathbf{y}), \mathbf{v} \rangle \leq \overline{\nu}\, \|\mathbf{y}\|_{\mathbf{curl},\Omega_1} \|\mathbf{v}\|_{\mathbf{curl},\Omega_1}, \quad \forall\, \mathbf{y}, \mathbf{v} \in V,$$

4. *hemicontinuous,*

5. *coercive on $\hat{V}$, i.e.,*

$$\langle \mathcal{A}_1(\mathbf{y}), \mathbf{y} \rangle \geq c\, \|\mathbf{y}\|_{\mathbf{curl},\Omega_1}^2, \quad \forall\, \mathbf{y} \in \hat{V},$$

6. *and identically zero on W, i.e.,*

$$\langle \mathcal{A}_1(\mathbf{y}), \mathbf{w} \rangle = 0, \quad \forall\, \mathbf{y} \in V, \forall\, \mathbf{w} \in W,$$

with some constant $c > 0$.

Proof. Monotonicity, semi-coercivity and boundedness of $\mathcal{A}_1$ directly follow from (3.2) and $s \mapsto \nu(s)s$ being monotone. Hemicontinuity follows from the continuity of ν. Coercivity on $\hat{V}$ is an immediate consequence of the semi-coercivity and Friedrichs' inequality, cf. Lemma 2.8. Indeed, we have

$$\langle \mathcal{A}_1(\mathbf{y}), \mathbf{y} \rangle \geq c\, \|\operatorname{\mathbf{curl}} \mathbf{y}\|_{\mathbf{0},\Omega_1}^2 \geq c\left(\|\operatorname{\mathbf{curl}} \mathbf{y}\|_{\mathbf{0},\Omega_1}^2 + (C_2^F)^{-2}\|\mathbf{y}\|_{\mathbf{0},\Omega_1}^2\right) \geq c\|\mathbf{y}\|_{\mathbf{curl},\Omega_1}^2.$$

Finally, the last property is due to the non-trivial kernel of the **curl** operator,

$$\mathcal{A}_1(\mathbf{y}, \mathbf{w}) = \int_{\Omega_1} \nu \operatorname{\mathbf{curl}} \mathbf{y} \cdot \operatorname{\mathbf{curl}} \nabla q \, d\mathbf{x} = 0, \quad \forall\, \mathbf{w} = \nabla q \in W.$$

$\square$

The main properties of $\mathcal{A}_2$ are summarized in the following lemma.

Lemma 3.3. *The operator $\mathcal{A}_2$ is*

1. *linear, i.e.,*

$$\mathcal{A}_2(\alpha\mathbf{y}) = \alpha\mathcal{A}_2(\mathbf{y}), \quad \forall\, \mathbf{y} \in V, \alpha \in \mathbb{R},$$
$$\mathcal{A}_2(\mathbf{y} + \mathbf{v}) = \mathcal{A}_2(\mathbf{y}) + \mathcal{A}_2(\mathbf{v}), \quad \forall\, \mathbf{y}, \mathbf{v} \in V,$$

2. *semi-coercive on V, i.e.,*

$$\langle \mathcal{A}_2(\mathbf{y}), \mathbf{y} \rangle \geq 0, \quad \forall\, \mathbf{y} \in V,$$

3. *bounded, i.e.,*

$$\langle \mathcal{A}_2(\mathbf{y}), \mathbf{v} \rangle \leq c \, \|\mathbf{y}\|_{\mathbf{curl},\Omega_1} \|\mathbf{v}\|_{\mathbf{curl},\Omega_1}, \quad \forall \mathbf{y}, \mathbf{v} \in V,$$

4. *and identically zero on* W, *i.e.,*

$$\langle \mathcal{A}_2(\mathbf{y}), \mathbf{w} \rangle = 0, \quad \forall \mathbf{y} \in V, \forall \mathbf{w} \in W,$$

with some constant $c > 0$.

Proof. It is easy to see, that $\mathcal{A}_2$ is linear. The semi-coercivity is a direct consequence of Lemma 2.17. Boundedness follows from Lemma 2.11, and the fact that $\mathbf{curl}\,\mathbf{curl}\,\mathbf{y} = 0$ in Ω_2. Indeed, we have

$$\mathcal{A}_2(\mathbf{y}, \mathbf{v}) = -\langle \gamma_{\mathbf{N}}\mathbf{y}, \gamma_{\mathbf{D}}\mathbf{v} \rangle_\tau \leq \|\gamma_{\mathbf{N}}\mathbf{y}\|_{\mathbf{H}_\parallel^{-\frac{1}{2}}(\mathrm{div}_\Gamma,\Gamma)} \|\gamma_{\mathbf{D}}\mathbf{v}\|_{\mathbf{H}_\perp^{-\frac{1}{2}}(\mathrm{curl}_\Gamma,\Gamma)} \leq c\|\mathbf{y}\|_{\mathbf{curl}^2,\Omega_2} \|\mathbf{v}\|_{\mathbf{curl},\Omega_2}$$

$$= c\|\mathbf{y}\|_{\mathbf{curl},\Omega_2} \|\mathbf{v}\|_{\mathbf{curl},\Omega_2} \leq c\|\gamma_\times \mathbf{y}\|_{\mathbf{H}_\perp^{-\frac{1}{2}}(\mathrm{curl}_\Gamma,\Gamma)} \|\gamma_\times \mathbf{v}\|_{\mathbf{H}_\perp^{-\frac{1}{2}}(\mathrm{curl}_\Gamma,\Gamma)} \leq c\|\mathbf{y}\|_{\mathbf{curl},\Omega_1} \|\mathbf{v}\|_{\mathbf{curl},\Omega_1},$$

for some constant $c > 0$. The last property follows from Lemma 2.13, since

$$\mathcal{A}_2(\mathbf{y}, \mathbf{w}) = -\langle \gamma_{\mathbf{N}}\mathbf{y}, \gamma_{\mathbf{D}}(\nabla q) \rangle_\tau = -\langle \gamma_{\mathbf{N}}\mathbf{y}, \mathbf{grad}_\Gamma q \rangle_\tau = 0, \quad \forall \mathbf{w} = \nabla q \in W.$$

$\square$

Now, we are in the position to state and proof the main theorem concerning existence and uniqueness of a solution.

Theorem 3.4. *Let the source* $\mathbf{u} \in L_2((0,T), \mathbf{L_2}(\Omega_1))$ *be weakly divergence-free for all* $t \in (0,T)$, *i.e.,*

$$(\mathbf{u}(t), \mathbf{w})_{\mathbf{0},\Omega_1} = 0, \quad \forall \mathbf{w} \in W,$$

and the initial condition $\mathbf{y_0}$ *be weakly divergence-free, i.e.,*

$$(\sigma \mathbf{y_0}, \mathbf{w})_{\mathbf{0},\Omega_1} = 0, \quad \forall \mathbf{w} \in W.$$

There exists a unique solution $\mathbf{y} \in W_2^1((0,T), V, \mathbf{L_2}(\Omega_1))$, *such that*

$$\begin{cases} \sigma \dfrac{\partial \mathbf{y}}{\partial t} + \mathcal{A}(\mathbf{y}) = \mathbf{U}, & \text{in } L_2((0,T), V^*), \\ \mathbf{y}(0) = \mathbf{y_0}, & \text{in } \mathbf{L_2}(\Omega_1). \end{cases}$$

Furthermore, the following a priori estimate is valid

$$\|\mathbf{y}\|_{W_2^1((0,T),V,\mathbf{L_2}(\Omega_1))} \leq c \left(\|\mathbf{u}\|_{L_2((0,T),\mathbf{L_2}(\Omega_1))} + \|\mathbf{y_0}\|_{\mathbf{0},\Omega_1} \right),$$

for some constant $c > 0$.

Proof. We start by showing existence and uniqueness of (3.4) in the factor space of divergence-free functions $\hat{V}$. Due to Lemma 3.2 and Lemma 3.3, the operator $\mathcal{A}$ is hemicontinuous, monotone, coercive and bounded on $\hat{V}$. Therefore, existence and uniqueness of the solution $\mathbf{y} \in W_2^1((0,T), \hat{V}, \mathbf{L_2}(\Omega_1))$ follows from Theorem 2.22.

Let us consider a solution $\mathbf{y} \in W_2^1((0,T), V, \mathbf{L_2}(\Omega_1))$ of (3.4). By taking into account, that the source $\mathbf{u}(t)$ is weakly divergence-free, we can conclude from Lemma 3.2 and Lemma 3.3, that for all $t \in (0,T)$ the following identity is valid:

$$\langle \sigma \frac{\partial}{\partial t} \mathbf{y}(t), \mathbf{w} \rangle = \langle \mathbf{U}(t), \mathbf{w} \rangle - \langle \mathcal{A}(\mathbf{y}(t)), \mathbf{w} \rangle = 0, \quad \forall \mathbf{w} \in W. \tag{3.5}$$

Since the initial condition $\mathbf{y_0}$ is assumed to be divergence-free, we can conclude, that for all $t \in (0,T)$

$$(\sigma \mathbf{y}(t), \mathbf{w})_{\mathbf{0},\Omega_1} = (\sigma \mathbf{y}(0), \mathbf{w})_{\mathbf{0},\Omega_1} + \int_0^t \langle \sigma \frac{\partial}{\partial \tau} \mathbf{y}(t), \mathbf{w} \rangle \mathrm{d}\tau = 0, \quad \forall \mathbf{w} \in W.$$

Therefore we conclude $\mathbf{y}(t) \in \hat{V}$. Consequently $\mathbf{y} \in W_2^1((0,T), \hat{V}, \mathbf{L_2}(\Omega_1)) \subset W_2^1((0,T), V, \mathbf{L_2}(\Omega_1))$, where we have already shown existence and uniqueness of the solution. $\square$

3.1.1   Existence and uniqueness for time-periodic eddy current problems

We analyze the time-periodic eddy current problem, i.e., (3.1) with the initial condition $\mathbf{y}(0) = \mathbf{y_0}$ replaced by the periodicity condition $\mathbf{y}(0) = \mathbf{y}(T)$. The analysis of the periodic setting is more involving. Due to the absence of an initial condition, we can only show uniqueness of the solution in the gauged subspace $\hat{V}$. The main result concerning existence and uniqueness of a periodic solution is summarized in the following theorem.

Theorem 3.5. *Let the source* $\mathbf{u} \in L_2((0,T), \mathbf{L_2}(\Omega_1))$ *be weakly divergence-free for all* $t \in (0,T)$, *i.e.,*

$$(\mathbf{u}(t), \mathbf{w})_{\mathbf{0}, \Omega_1} = 0, \quad \forall \, \mathbf{w} \in W.$$

There exists a unique solution $\mathbf{y} \in W_2^1((0,T), \hat{V}, \mathbf{L_2}(\Omega_1))$, *such that*

$$\begin{cases} \sigma \dfrac{\partial \mathbf{y}}{\partial t} + \mathcal{A}(\mathbf{y}) = \mathbf{U}, & \text{in } L_2((0,T), \hat{V}^*), \\ \mathbf{y}(0) = \mathbf{y}(T), & \text{in } \mathbf{L_2}(\Omega_1). \end{cases}$$

Proof. The proof immediately follows from Theorem 3.4 and Theorem 2.23. □

Indeed, this result cannot be generalized to the full space $W_2^1((0,T), V, \mathbf{L_2}(\Omega_1))$. This can be seen in the following way. Again, the identity (3.5) is still valid. Anyhow, we have

$$(\sigma \mathbf{y}(t), \mathbf{w})_{\mathbf{0}, \Omega_1} = (\sigma \mathbf{y}(0), \mathbf{w})_{\mathbf{0}, \Omega_1} + \int_0^t \langle \sigma \frac{\partial}{\partial \tau} \mathbf{y}(t), \mathbf{w} \rangle \mathrm{d}\tau = (\sigma \mathbf{y}(0), \mathbf{w})_{\mathbf{0}, \Omega_1}, \quad \forall \, \mathbf{w} \in W.$$

Consequently, the solution $\mathbf{y}$ is only unique up to gradient functions $\mathbf{w} \in W$, that are constant in time. Hence, in the time-periodic setting it is essential to keep the divergence constraint imposed on $\mathbf{y}$.

3.1.2   Symmetric coupling in the time domain

Introducing the Neumann data $\boldsymbol{\gamma_N y}$ as an additional unknown, i.e., $\boldsymbol{\lambda} = \boldsymbol{\gamma_N y}$, and using the Calderon projection (2.22), allow to state the eddy current problem in a symmetric coupled framework: Find $(\mathbf{y}, \boldsymbol{\lambda}) \in W_2^1((0,T), V, \mathbf{L_2}(\Omega_1)) \times L_2((0,T), \mathbf{H}_{\parallel}^{-\frac{1}{2}}(\mathrm{div}_\Gamma \, 0, \Gamma))$ with $\mathbf{y}(\cdot, 0) = \mathbf{y_0}(\cdot)$ and $\boldsymbol{\lambda}(\cdot, 0) = \boldsymbol{\gamma_N}(\mathbf{y_0})$, such that

$$\begin{cases} \displaystyle\int_0^T \langle \sigma \frac{\partial \mathbf{y}}{\partial t}, \mathbf{v} \rangle + \langle \mathcal{A}_1(\mathbf{y}), \mathbf{v} \rangle - \langle \mathbf{N}(\boldsymbol{\gamma_D y}), \boldsymbol{\gamma_D v} \rangle_\tau + \langle \mathbf{B}(\boldsymbol{\lambda}), \boldsymbol{\gamma_D v} \rangle_\tau \, \mathrm{dt} = \int_0^T \langle \mathbf{U}, \mathbf{v} \rangle \mathrm{dt}, \\ \displaystyle\int_0^T \langle \boldsymbol{\zeta}, (\mathbf{Id} - \mathbf{C})(\boldsymbol{\gamma_D y}) \rangle_\tau - \langle \boldsymbol{\zeta}, \mathbf{A}(\boldsymbol{\lambda}) \rangle_\tau \, \mathrm{dt} = 0, \end{cases} \tag{3.6}$$

for all $(\mathbf{v}, \boldsymbol{\zeta}) \in L_2((0,T), V) \times L_2((0,T), \mathbf{H}_{\parallel}^{-\frac{1}{2}}(\mathrm{div}_\Gamma \, 0, \Gamma))$. In the case of the time-periodic eddy current problem, the initial conditions have to be replaced by the periodicity conditions $\mathbf{y}(\cdot, 0) = \mathbf{y}(\cdot, T)$ and $\boldsymbol{\lambda}(\cdot, 0) = \boldsymbol{\lambda}(\cdot, T)$. In Chapter 6, (3.6) is the starting point of a discretization in space and time.

3.2   Existence and uniqueness for the EC optimal control problem

This section provides existence and uniqueness results for eddy current optimal control problems in the case of distributed control and a linear state equation. Therefore, we assume, that the reluctivity ν is independent of the magnetic flux $\mathbf{B} = \mathbf{curl}\,\mathbf{y}$, which makes the state equation (3.1) linear. Typically, existence and uniqueness results for optimal control problems are deduced from existence

and uniqueness results for the state equation and assumptions imposed on the minimization functional by using standard arguments. Indeed, this approach can also be used in the setting of eddy current optimal control problem. Anyhow, in this special case, due to the *conservation of charges law* in the state equation, the control-to-solution map is only defined for weakly divergence-free sources $\mathbf{u}$, cf. Theorem 3.4. Therefore, the set of admissible controls $\mathbf{u}$ has to be restricted to the set of weakly divergence-free functions $\hat{H}_1$. Indeed, this restriction makes the resulting optimality very inconvenient to deal with. Therefore, we propose an alternative approach of dealing with the conservation of charges law in Subsection 3.2.2.

In this section we consider the functional

$$\mathcal{J}(\mathbf{y}, \mathbf{u}) := \frac{1}{2} \|\mathbf{y} - \mathbf{y_d}\|^2_{L_2((0,T),\mathbf{L_2}(\Omega_1))} + \frac{\lambda}{2} \|\mathbf{u}\|^2_{L_2((0,T),\mathbf{L_2}(\Omega_1))},$$

with given desired state $\mathbf{y_d} \in L_2((0,T),\mathbf{L_2}(\Omega_1))$ and given regularization parameter $\lambda > 0$. The corresponding minimization problem reads as: Find $(\hat{\mathbf{y}}, \hat{\mathbf{u}}) \in W_2^1((0,T),V,\mathbf{L_2}(\Omega_1)) \times L_2((0,T),\mathbf{L_2}(\Omega_1))$, such that

$$\mathcal{J}(\hat{\mathbf{y}}, \hat{\mathbf{u}}) = \min_{(\mathbf{y},\mathbf{u}) \in W_2^1((0,T),V,\mathbf{L_2}(\Omega_1)) \times L_2((0,T),\hat{H}_1)} \mathcal{J}(\mathbf{y}, \mathbf{u}), \tag{3.7}$$

where $(\mathbf{y}, \mathbf{u})$ fulfills the eddy current problem (3.1) in a weak sense. Due to the unique solvability of (3.1), cf. Theorem 3.4, we can define a (linear) solution operator

$$\mathcal{S} : L_2((0,T),\hat{H}_1) \times \mathbf{L_2}(\Omega_1) \to W_2^1((0,T),V,\mathbf{L_2}(\Omega_1)) : (\mathbf{u}, \mathbf{y_0}) \to \mathbf{y}. \tag{3.8}$$

Indeed, the operator $\mathcal{S}$ is well-defined and bounded, i.e.,

$$\|\mathcal{S}(\mathbf{u}, \mathbf{y_0})\|_{W_2^1((0,T),V,\mathbf{L_2}(\Omega_1))} \leq c \left(\|\mathbf{u}\|_{L_2((0,T),\mathbf{L_2}(\Omega_1))} + \|\mathbf{y_0}\|_{0,\Omega_1} \right).$$

Since the state equation (3.1) is linear, we have the following splitting (*superpositions principle*)

$$\mathcal{S}(\mathbf{u}, \mathbf{y_0}) = \mathcal{S}_1(\mathbf{u}) + \mathcal{S}_2(\mathbf{y_0}),$$

with the linear and bounded operators

$$\mathcal{S}_1 : L_2((0,T),\hat{V}) \to W_2^1((0,T),V,\mathbf{L_2}(\Omega_1)),$$
$$\mathcal{S}_2 : \mathbf{L_2}(\Omega_1) \to W_2^1((0,T),V,\mathbf{L_2}(\Omega_1)).$$

By defining $\tilde{\mathbf{y}}_{\mathbf{d}} := \mathbf{y_d} - \mathcal{S}_2(\mathbf{y_0}) \in L_2((0,T),\mathbf{L_2}(\Omega_1))$, we can state the reduced minimization problem as follows. Find $\hat{\mathbf{u}} \in L_2((0,T),\mathbf{L_2}(\Omega_1))$, such that

$$\begin{aligned}
\tilde{\mathcal{J}}(\hat{\mathbf{u}}) &= \min_{\mathbf{u} \in L_2((0,T),\hat{H}_1)} \tilde{\mathcal{J}}(\mathbf{u}) \\
&= \min_{\mathbf{u} \in L_2((0,T),\hat{H}_1)} \left[\frac{1}{2} \|\mathcal{S}_1(\mathbf{u}) - \tilde{\mathbf{y}}_{\mathbf{d}}\|^2_{L_2((0,T),\mathbf{L_2}(\Omega_1))} + \frac{\lambda}{2} \|\mathbf{u}\|^2_{L_2((0,T),\mathbf{L_2}(\Omega_1))} \right].
\end{aligned} \tag{3.9}$$

The main result of this section is summarized in the next theorem, that states, that the reduced minimization problem (3.9) has a unique solution.

Theorem 3.6. *The minimization problem (3.9), and therefore (3.7), has a unique solution.*

Proof. Since $\mathcal{S}_1$ is a linear and bounded operator, and $L_2((0,T),\hat{H}_1)$ is a nonempty, closed and convex subset of $L_2((0,T),\mathbf{L_2}(\Omega_1))$, existence and uniqueness follows with Theorem 2.24. □

3.2.1   Necessary and sufficient optimality conditions

A solution of the minimization problem (3.7) is characterized by the solution of the optimality system. Due to Theorem 2.25, the optimality system is given by the *state equation*

$$\begin{cases} \sigma \dfrac{\partial \mathbf{y}}{\partial t} + \mathcal{A}(\mathbf{y}) = \mathbf{U}, & \text{in } L_2((0,T), V^*), \\[2mm] \mathbf{y}(0) = \mathbf{y_0}, & \text{in } \mathbf{L_2}(\Omega_1), \end{cases} \tag{3.10a}$$

the *co-state equation*

$$\begin{cases} -\sigma \dfrac{\partial \mathbf{p}}{\partial t} + \mathcal{A}(\mathbf{p}) + \mathcal{I}(\mathbf{y}) = \mathbf{Y_d}, & \text{in } L_2((0,T), V^*), \\[2mm] \mathbf{p}(T) = \mathbf{0}, & \text{in } \mathbf{L_2}(\Omega_1), \end{cases} \tag{3.10b}$$

and the *variational inequality*

$$\int_0^T (\lambda \mathbf{u} - \mathbf{p}, \mathbf{v} - \mathbf{u})_{\mathbf{0},\Omega_1} \mathrm{d}t \geq 0, \quad \forall \mathbf{v} \in L_2((0,T), \hat{H}_1). \tag{3.10c}$$

Here $\mathcal{I} : V \to V^* : \mathbf{y} \mapsto \mathcal{I}(\mathbf{y})$ is the identity operator defined by

$$\langle \mathcal{I}(\mathbf{y}), \mathbf{v} \rangle := (\mathbf{y}, \mathbf{v})_H, \quad \forall \mathbf{v} \in V.$$

Furthermore, $\mathbf{Y_d}(t) \in V^*$ is given by

$$\langle \mathbf{Y_d}(t), \mathbf{v}(\cdot, t) \rangle := \int_{\Omega_1} \mathbf{y_d}(\mathbf{x}, t) \cdot \mathbf{v}(\mathbf{x}, t) \, \mathrm{d}\mathbf{x}, \quad \forall \mathbf{v}(\cdot, t) \in V.$$

Therefore, the solution of the optimal control problem can be determined by the solution of the following problem: Find $(\mathbf{y}, \mathbf{p}, \mathbf{u}) \in W_2^1((0,T), V, \mathbf{L_2}(\Omega_1)) \times W_2^1((0,T), V, \mathbf{L_2}(\Omega_1)) \times L_2((0,T), \mathbf{L_2}(\Omega_1))$, that fulfills (3.10). In this context the Lagrange multiplier $\mathbf{p}$ is referred as *co-state*.

3.2.2   Enforcing the charge conservation law in EC optimal control problems

In the last subsections, we have seen, that the charge conservation law

$$\operatorname{div} \mathbf{u} = 0, \quad \text{in } \Omega_1, \qquad \mathbf{u} \cdot \mathbf{n} = 0, \quad \text{on } \Gamma,$$

is essential for providing existence and uniqueness results for the state equation (cf. Theorem 3.4) and therefore for the optimal control problem (3.7). Indeed, the variational inequality (3.10c) is difficult to deal with.

In order to overcome this drawback, we employ a different approach and consider the minimization problem. Find $(\hat{\mathbf{y}}, \hat{\mathbf{u}}) \in W_2^1((0,T), V, \mathbf{L_2}(\Omega_1)) \times L_2((0,T), \mathbf{L_2}(\Omega_1))$, such that

$$\mathcal{J}(\hat{\mathbf{y}}, \hat{\mathbf{u}}) = \min_{(\mathbf{y}, \mathbf{u}) \in W_2^1((0,T), V, \mathbf{L_2}(\Omega_1)) \times L_2((0,T), \mathbf{L_2}(\Omega_1))} \mathcal{J}(\mathbf{y}, \mathbf{u}), \tag{3.11}$$

where $(\mathbf{y}, \mathbf{u})$ fulfills the eddy current problem (3.1) in a weak sense.

We show, that under mild assumptions, the minimum of the minimization problem indeed is attained by a divergence-free function $\mathbf{u}$, and therefore $\mathbf{y}$ is divergence-free as well. Therefore, the optimal control problem (3.11) obtains automatically the same solution as (3.7).

We start, by providing existence and uniqueness result for the eddy current problem without the divergence-free constraint imposed on the source $\mathbf{u}$.

Theorem 3.7. *Let the source* $\mathbf{u} \in L_2((0,T), \mathbf{L_2}(\Omega_1))$ *be given. Furthermore, let the initial condition* $\mathbf{y_0}$ *be weakly divergence-free, i.e.,*

$$(\sigma \mathbf{y_0}, \mathbf{w})_{\mathbf{0},\Omega_1} = 0, \quad \forall \, \mathbf{w} \in W.$$

Then there exists a unique solution $\mathbf{y} \in W_2^1((0,T), V, \mathbf{L_2}(\Omega_1))$, *such that*

$$\begin{cases} \sigma \dfrac{\partial \mathbf{y}}{\partial t} + \mathcal{A}(\mathbf{y}) = \mathbf{U}, & in \; L_2((0,T), V^*), \\[2mm] \mathbf{y}(0) = \mathbf{y_0}, & in \; \mathbf{L_2}(\Omega_1). \end{cases}$$

Proof. In order to find the solution $\mathbf{y}$, we use the orthogonal splitting of $W_2^1((0,T), V, \mathbf{L_2}(\Omega_1))$ with respect to $\int_0^1 (\sigma \cdot, \cdot)_{\mathbf{0},\Omega_1} \, dt$, given as follows

$$W_2^1((0,T), V, \mathbf{L_2}(\Omega_1)) = W_2^1((0,T), \hat{V}, \mathbf{L_2}(\Omega_1)) \oplus W_2^1((0,T), W, \mathbf{L_2}(\Omega_1)).$$

Due to Lemma 2.6, we have the Helmholtz decomposition of $\mathbf{y} \in W_2^1((0,T), V, \mathbf{L_2}(\Omega_1))$ in terms of

$$\mathbf{y} = \tilde{\mathbf{y}} + \nabla p, \quad \tilde{\mathbf{y}} \in W_2^1((0,T), \hat{V}, \mathbf{L_2}(\Omega_1)), \; \nabla p \in W_2^1((0,T), W, \mathbf{L_2}(\Omega_1)),$$

that is orthogonal with respect to $\int_0^T (\sigma \cdot, \cdot)_{\mathbf{0},\Omega_1} dt$, and of $\mathbf{u} \in L_2((0,T), \mathbf{L_2}(\Omega_1))$ in terms of

$$\mathbf{u} = \tilde{\mathbf{u}} + \nabla q, \quad \tilde{\mathbf{u}} \in L_2((0,T), \hat{H}_1), \; \nabla q \in L_2((0,T), W),$$

that is orthogonal with respect to $\int_0^T (\cdot, \cdot)_{\mathbf{0},\Omega_1} dt$. Therefore, we take advantage of the orthogonality of the gradient and divergence-free functions and compute the two components $\tilde{\mathbf{y}}$ and p individually. We start by investigating the divergence-free part. Find $\tilde{\mathbf{y}} \in W_2^1((0,T), \hat{V}, \mathbf{L_2}(\Omega_1))$ with $\mathbf{y}(\cdot, 0) = \mathbf{y_0}(\cdot)$, such that

$$\int_0^T \left[\langle \sigma \frac{\partial \tilde{\mathbf{y}}}{\partial t}, \mathbf{v} \rangle + \langle \mathcal{A}(\tilde{\mathbf{y}}), \mathbf{v} \rangle \right] dt = \int_0^T (\tilde{\mathbf{u}}, \mathbf{v})_{\mathbf{0},\Omega_1} \, dt,$$

for all $\mathbf{v} \in L_2((0,T), \hat{V})$. The existence and uniqueness of $\tilde{\mathbf{y}} \in W_2^1((0,T), \hat{V}, \mathbf{L_2}(\Omega_1))$ follows from Theorem 3.4. Furthermore, the gradient part is characterized as follows:
Find $\nabla p \in W_2^1((0,T), W, L_2(\Omega_1))$ with $\nabla p(\cdot, 0) = \mathbf{0}$, such that

$$\int_0^T \langle \sigma \frac{\partial \nabla p}{\partial t}, \nabla g \rangle \, dt = \int_0^T (\nabla q, \nabla g)_{\mathbf{0},\Omega_1} \, dt,$$

for all $\nabla g \in L_2((0,T), W)$. The unique solution $\nabla p(t) \in W$ is given by $\sigma \nabla p(t) = \int_0^t \nabla q(\tau) \, d\tau$. Therefore, we obtain the unique solution $\mathbf{y} = \tilde{\mathbf{y}} + \nabla p$. $\qquad \square$

Due to Theorem 3.7, there exists a unique solution $\mathbf{y}$, and therefore we can define a (linear) solution operator

$$\tilde{\mathcal{S}} : L_2((0,T), \mathbf{L_2}(\Omega_1)) \times \mathbf{L_2}(\Omega_1) \to W_2^1((0,T), V, \mathbf{L_2}(\Omega_1)). \tag{3.12}$$

Indeed, the operator $\mathcal{S}$ is well-defined and bounded.

Theorem 3.8. *(3.11) has a unique solution* $(\mathbf{y}, \mathbf{u}) \in W_2^1((0,T), V, \mathbf{L_2}(\Omega_1)) \times L_2((0,T), \mathbf{L_2}(\Omega_1))$. *Furthermore, under the assumption that* $\mathbf{y_d}$ *is divergence-free, i.e.,*

$$(\sigma \mathbf{y_d}(t), \mathbf{w})_{\mathbf{0},\Omega_1} = 0, \quad \forall \, \mathbf{w} \in W,$$

for all $t \in (0,T)$, *and* $\sigma \in \mathbb{R}^+$, $\mathbf{u}$ *and* $\mathbf{y}$ *are divergence-free as well, i.e.,*

$$(\mathbf{u}(t), \mathbf{w})_{\mathbf{0},\Omega_1} = 0, \quad \forall \, \mathbf{w} \in W,$$

and

$$(\sigma \mathbf{y}(t), \mathbf{w})_{\mathbf{0},\Omega_1} = 0, \quad \forall \, \mathbf{w} \in W,$$

for all $t \in (0,T)$.

Proof. Since the solution operator $\tilde{\mathcal{S}}$ is linear and bounded, existence and uniqueness of a solution pair $(\mathbf{y}, \mathbf{u})$ follows with Theorem 2.24, cf. proof of Theorem 3.6.

By definition $\tilde{\mathcal{S}}(\mathbf{u}, \mathbf{y_0}) = \mathbf{y}$. Furthermore, due to Lemma 2.6, we have the Helmholtz decomposition of $\mathbf{y} \in W_2^1((0,T), V, \mathbf{L_2}(\Omega_1))$ in terms of

$$\mathbf{y} = \tilde{\mathbf{y}} + \nabla p, \quad \tilde{\mathbf{y}} \in W_2^1((0,T), \hat{V}, \mathbf{L_2}(\Omega_1)), \ \nabla p \in W_2^1((0,T), W, \mathbf{L_2}(\Omega_1)),$$

that is orthogonal with respect to $\int_0^T (\sigma \cdot, \cdot)_{\mathbf{0}, \Omega_1} \mathrm{d}t$, and of $\mathbf{u} \in L_2((0,T), \mathbf{L_2}(\Omega_1))$ in terms of

$$\mathbf{u} = \tilde{\mathbf{u}} + \nabla q, \quad \tilde{\mathbf{u}} \in L_2((0,T), \hat{H}_1), \ \nabla q \in L_2((0,T), W),$$

that is orthogonal with respect to $\int_0^T (\cdot, \cdot)_{\mathbf{0}, \Omega_1} \mathrm{d}t$. Since the initial condition $\mathbf{y_0}$ is divergence-free, we have $\tilde{\mathcal{S}}(\tilde{\mathbf{u}}, \mathbf{y_0}) = \tilde{\mathbf{y}}$ and $\tilde{\mathcal{S}}(\nabla q, \mathbf{0}) = \nabla p$. Therefore, the pair $(\tilde{\mathbf{y}}, \tilde{\mathbf{u}})$ also satisfies the eddy current problem. Let us assume, that $\mathbf{y}$ and $\mathbf{u}$ are not divergence-free, i.e., $p \neq 0$ and $q \neq 0$. We have

$$\begin{aligned}
\tilde{\mathcal{J}}(\mathbf{u}) &= \frac{1}{2} \|\tilde{\mathcal{S}}(\mathbf{u}, \mathbf{y_0}) - \mathbf{y_d}\|_{L_2((0,T), \mathbf{L_2}(\Omega_1))}^2 + \frac{\lambda}{2} \|\mathbf{u}\|_{L_2((0,T), \mathbf{L_2}(\Omega_1))}^2 \\
&= \frac{1}{2} \left[\|\tilde{\mathcal{S}}(\tilde{\mathbf{u}}, \mathbf{y_0}) - \mathbf{y_d}\|_{L_2((0,T), \mathbf{L_2}(\Omega_1))}^2 + \|\nabla p\|_{L_2((0,T), \mathbf{L_2}(\Omega_1))}^2 \right] \\
&\quad + \frac{\lambda}{2} \left[\|\tilde{\mathbf{u}}\|_{L_2((0,T), \mathbf{L_2}(\Omega_1))}^2 + \|\nabla q\|_{L_2((0,T), \mathbf{L_2}(\Omega_1))}^2 \right] \\
&\geq \frac{1}{2} \|\tilde{\mathcal{S}}(\tilde{\mathbf{u}}, \mathbf{y_0}) - \mathbf{y_d}\|_{L_2((0,T), \mathbf{L_2}(\Omega_1))}^2 + \frac{\lambda}{2} \|\tilde{\mathbf{u}}\|_{L_2((0,T), \mathbf{L_2}(\Omega_1))}^2,
\end{aligned}$$

and therefore the pair $(\mathbf{y}, \mathbf{u})$ does not minimize the cost functional, which is a contradiction to the fact, that the pair $(\mathbf{y}, \mathbf{u})$ is the unique solution. Consequently, we conclude that $p = 0$ and $q = 0$, which means, that $\mathbf{y}$ and $\mathbf{u}$ are divergence-free, i.e., $\mathbf{y} = \tilde{\mathbf{y}}$ and $\mathbf{u} = \tilde{\mathbf{u}}$. $\qquad\square$

Due to Theorem 2.25, the optimality system of (3.11) is given by the *state equation*

$$\begin{cases} \sigma \dfrac{\partial \mathbf{y}}{\partial t} + \mathcal{A}(\mathbf{y}) = \mathbf{U}, & \text{in } L_2((0,T), V^*), \\[2mm] \mathbf{y}(0) = \mathbf{y_0}, & \text{in } \mathbf{L_2}(\Omega_1), \end{cases} \tag{3.13a}$$

the *co-state equation*

$$\begin{cases} -\sigma \dfrac{\partial \mathbf{p}}{\partial t} + \mathcal{A}(\mathbf{p}) + \mathcal{I}(\mathbf{y}) = \mathbf{Y_d}, & \text{in } L_2((0,T), V^*), \\[2mm] \mathbf{p}(T) = \mathbf{0}, & \text{in } \mathbf{L_2}(\Omega_1), \end{cases} \tag{3.13b}$$

and the *variational equality*

$$\int_0^T (\lambda \mathbf{u} - \mathbf{p}, \mathbf{v})_{\mathbf{0}, \Omega_1} \mathrm{d}t = 0, \quad \forall \mathbf{v} \in L_2((0,T), \mathbf{L_2}(\Omega_1)). \tag{3.13c}$$

From (3.13c) we learn that $\mathbf{u} = \lambda^{-1} \mathbf{p}$, and therefore the control $\mathbf{u}$ can be eliminated from the system (3.13). The resulting reduced optimality system is given by the *state equation*

$$\begin{cases} \sigma \dfrac{\partial \mathbf{y}}{\partial t} + \mathcal{A}(\mathbf{y}) - \dfrac{1}{\lambda} \mathcal{I}(\mathbf{p}) = \mathbf{0}, & \text{in } L_2((0,T), V^*), \\[2mm] \mathbf{y}(0) = \mathbf{y_0}, & \text{in } \mathbf{L_2}(\Omega_1), \end{cases} \tag{3.14a}$$

and the *co-state equation*

$$\begin{cases} -\sigma \dfrac{\partial \mathbf{p}}{\partial t} + \mathcal{A}(\mathbf{p}) + \mathcal{I}(\mathbf{y}) = \mathbf{Y_d}, & \text{in } L_2((0,T), V^*), \\[2mm] \mathbf{p}(T) = \mathbf{0}, & \text{in } \mathbf{L_2}(\Omega_1). \end{cases} \tag{3.14b}$$

Remark 3.9. *For the case of a general* $\sigma \in L^\infty(\Omega_1)$, $\sigma > 0$, *the same result as in Theorem 3.8 can be shown for the modified cost functional*

$$\mathcal{J}_\sigma(\mathbf{y}, \mathbf{u}) := \frac{1}{2}\|\sigma^{\frac{1}{2}}(\mathbf{y} - \mathbf{y_d})\|^2_{L_2((0,T),\mathbf{L_2}(\Omega_1))} + \frac{\lambda}{2}\|\mathbf{u}\|^2_{L_2((0,T),\mathbf{L_2}(\Omega_1))}.$$

Remark 3.10. *Theorem 3.8 is also valid in the case of general cost functionals of the form (1.9).*

Remark 3.11. *Another possibility to cope with the divergence-free constraint is to consider a vector potential ansatz* $\mathbf{u} = \mathbf{curl}\,\mathbf{w}$, *that automatically fulfills* $\operatorname{div}\mathbf{u} = 0$, $\mathbf{u} \cdot \mathbf{n} = 0$, *and to use the vector potential* $\mathbf{w} \in \mathbf{H_0}(\mathbf{curl}, \Omega_1)$ *as the control, cf. [159]. The corresponding minimization problem is given by*

$$\min_{\mathbf{y},\mathbf{w}} \mathcal{J}_\mathbf{w}(\mathbf{y}, \mathbf{w}) := \frac{1}{2}\|\mathbf{y} - \mathbf{y_d}\|^2_{L_2((0,T),\mathbf{L_2}(\Omega_1))} + \frac{\lambda}{2}\|\mathbf{w}\|^2_{L_2((0,T),V)}.$$

subject to

$$\begin{cases} \sigma\dfrac{\partial \mathbf{y}}{\partial t} + \mathcal{A}(\mathbf{y}) = \mathbf{W}\mathbf{w}, & \text{in } L_2((0,T), V^*), \\ \quad\quad\quad\;\, \mathbf{y}(0) = \mathbf{y_0}, & \text{in } \mathbf{L_2}(\Omega_1), \end{cases}$$

where $\mathbf{W}(t) : V \to V^*$ *is given by*

$$\langle \mathbf{W}(t)\mathbf{w}(\cdot, t), \mathbf{v}(\cdot, t)\rangle := \int_{\Omega_1} \mathbf{curl}\,\mathbf{w}(\mathbf{x}, t) \cdot \mathbf{v}(\mathbf{x}, t)\,\mathrm{d}\mathbf{x}, \quad \forall\,\mathbf{v}(\cdot, t) \in V.$$

Again, existence and uniqueness of a minimizer $(\mathbf{y}, \mathbf{w}) \in W_2^1((0,T), V, \mathbf{L_2}(\Omega_1)) \times L_2((0,T), V)$ *can be shown. The corresponding optimality system is given by the* state equation

$$\begin{cases} \sigma\dfrac{\partial \mathbf{y}}{\partial t} + \mathcal{A}(\mathbf{y}) = \mathbf{W}\mathbf{w}, & \text{in } L_2((0,T), V^*), \\ \quad\quad\quad\;\, \mathbf{y}(0) = \mathbf{y_0}, & \text{in } \mathbf{L_2}(\Omega_1), \end{cases} \tag{3.15a}$$

the co-state *equation*

$$\begin{cases} -\sigma\dfrac{\partial \mathbf{p}}{\partial t} + \mathcal{A}(\mathbf{p}) + \mathcal{I}(\mathbf{y}) = \mathbf{Y_d}, & \text{in } L_2((0,T), V^*), \\ \quad\quad\quad\quad\quad\; \mathbf{p}(T) = \mathbf{0}, & \text{in } \mathbf{L_2}(\Omega_1), \end{cases} \tag{3.15b}$$

and the variational equality

$$\lambda\,\mathcal{J}(\mathbf{w}) = \mathbf{W}^*\mathbf{p}, \quad \text{in } L_2((0,T), V^*). \tag{3.15c}$$

Here $\mathcal{J} : V \to V^*$ *denotes the Riesz isomorphism, and* $\mathbf{W}^* : V \to V^*$ *is the adjoint operator of* $\mathbf{W}$, *i.e.,*

$$\langle \mathbf{W}\mathbf{w}, \mathbf{v}\rangle = \langle \mathbf{W}^*\mathbf{v}, \mathbf{w}\rangle, \quad \forall\,\mathbf{w}, \mathbf{v} \in V.$$

3.2.3 Existence and uniqueness for time-periodic EC optimal control problems

In this subsection, we consider the time-periodic eddy current optimal control problem. As we have seen for the time-periodic eddy current problem in Subsection 3.1.1, we lose the unique solvability due to the periodicity conditions. Anyhow, in the time-periodic optimal control setting, the minimum of the minimization problem is automatically attained by the divergence-free pair $(\mathbf{y}, \mathbf{u})$ and therefore, the time-periodic optimal control problem is uniquely solvable.
Find $(\hat{\mathbf{y}}, \hat{\mathbf{u}}) \in W_2^1((0,T), V, \mathbf{L_2}(\Omega_1)) \times L_2((0,T), \mathbf{L_2}(\Omega_1))$, such that

$$\mathcal{J}(\hat{\mathbf{y}}, \hat{\mathbf{u}}) = \min_{(\mathbf{y},\mathbf{u})\in W_2^1((0,T),V,\mathbf{L_2}(\Omega_1))\times L_2((0,T),\mathbf{L_2}(\Omega_1))} \mathcal{J}(\mathbf{y}, \mathbf{u}), \tag{3.16}$$

where $(\mathbf{y}, \mathbf{u})$ fulfills the eddy current problem (3.1) with the initial condition replaced by a periodicity condition in a weak sense.

Theorem 3.12. *(3.16) has a unique solution* $(\mathbf{y}, \mathbf{u}) \in W_2^1((0,T), V, \mathbf{L_2}(\Omega_1)) \times L_2((0,T), \mathbf{L_2}(\Omega_1))$. *Furthermore, under the assumption that* $\mathbf{y_d}$ *is divergence-free, i.e.,*

$$(\sigma \mathbf{y_d}(t), \mathbf{w})_{\mathbf{0}, \Omega_1} = 0, \quad \forall \mathbf{w} \in W,$$

for all $t \in (0,T)$, *and* $\sigma \in \mathbb{R}^+$, $\mathbf{u}$ *and* $\mathbf{y}$ *are divergence-free as well, i.e.,*

$$(\mathbf{u}(t), \mathbf{w})_{\mathbf{0}, \Omega_1} = 0, \quad \forall \mathbf{w} \in W,$$

and

$$(\sigma \mathbf{y}(t), \mathbf{w})_{\mathbf{0}, \Omega_1} = 0, \quad \forall \mathbf{w} \in W,$$

for all $t \in (0,T)$.

Proof. The result can be deduced by using similar arguments as in the proof of Theorem 3.8 in order to show, that the minimum is automatically attained by in the space of divergence-free functions, where the control-to-state map is well defined and unique. □

The optimality system of (3.16) is given by the *state equation*

$$\begin{cases} \sigma \dfrac{\partial \mathbf{y}}{\partial t} + \mathcal{A}(\mathbf{y}) = \mathbf{U}, & \text{in } L_2((0,T), V^*), \\ \quad\quad\quad\; \mathbf{y}(0) = \mathbf{y}(T), & \text{in } \mathbf{L_2}(\Omega_1), \end{cases} \tag{3.17a}$$

the *co-state equation*

$$\begin{cases} -\sigma \dfrac{\partial \mathbf{p}}{\partial t} + \mathcal{A}(\mathbf{p}) + \mathcal{I}(\mathbf{y}) = \mathbf{Y_d}, & \text{in } L_2((0,T), V^*), \\ \quad\quad\quad\quad\quad\; \mathbf{p}(0) = \mathbf{p}(T), & \text{in } \mathbf{L_2}(\Omega_1), \end{cases} \tag{3.17b}$$

and the *variational equality*

$$\int_0^T (\lambda \mathbf{u} - \mathbf{p}, \mathbf{v})_{\mathbf{0}, \Omega_1} \mathrm{dt} = 0, \quad \forall \mathbf{v} \in L_2((0,T), \mathbf{L_2}(\Omega_1)). \tag{3.17c}$$

From (3.17c) we learn that $\mathbf{u} = \lambda^{-1}\mathbf{p}$, and therefore the control $\mathbf{u}$ can be eliminated from the system (3.17). The resulting reduced optimality system is given by the *state equation*

$$\begin{cases} \sigma \dfrac{\partial \mathbf{y}}{\partial t} + \mathcal{A}(\mathbf{y}) - \dfrac{1}{\lambda}\mathcal{I}(\mathbf{p}) = \mathbf{0}, & \text{in } L_2((0,T), V^*), \\ \quad\quad\quad\quad\quad\; \mathbf{y}(0) = \mathbf{y}(T), & \text{in } \mathbf{L_2}(\Omega_1), \end{cases} \tag{3.18a}$$

and the *co-state equation*

$$\begin{cases} -\sigma \dfrac{\partial \mathbf{p}}{\partial t} + \mathcal{A}(\mathbf{p}) + \mathcal{I}(\mathbf{y}) = \mathbf{Y_d}, & \text{in } L_2((0,T), V^*), \\ \quad\quad\quad\quad\quad\; \mathbf{p}(0) = \mathbf{p}(T), & \text{in } \mathbf{L_2}(\Omega_1). \end{cases} \tag{3.18b}$$

In Chapter 7, we investigate the efficient numerical solution of (3.18).

Remark 3.13. *As we have seen in (3.10), when dealing with initial value problems, the adjoint state has to vanish at the end time. This makes these kind of problems difficult to deal with, since at the same time an initial value problem and an end time problem have to be solved. In the periodic case, the optimality system (3.18) consists of two periodic problems. This simplifies the situation, because here both, the state and the co-state, are in the same space, and consequently, the problem obtains a symmetric structure.*

Chapter 4

Multiharmonic discretization techniques

This chapter is devoted to the discretization of time-periodic evolution equations in terms of a multiharmonic approach. Therefore, we introduce the concept of *periodic steady state* solutions. Indeed, this concept is used by engineers in different applications, where the main interest is not on the particular behavior of the solution in the initial phase, but the asymptotic and periodic behavior after some start-up period. Due to the periodic structure of the solution, an approximation in terms of a *Fourier series* or *multiharmonic approach* in time pops up naturally, e.g. [18, 66, 155]. We demonstrate, that the multiharmonic approach applied to linear evolution equations leads to a decoupling of the frequency domain equations with respect to the involved modes. For numerical treatment, only a finite number of modes is considered. It is shown, that this truncation of the Fourier series leads to a convergent discretization scheme in time and additionally an error estimate is provided.

Finally, we demonstrate the application of the multiharmonic approach to time-periodic optimal control problems. We derive the optimality system, where again a time-periodic structure is observed. The discretization in terms of the multiharmonic approach leads to a decoupling of the optimality system in the frequency domain with respect to the involved modes.

4.1 Periodic steady state solutions

Let us assume, that we have a variational triple $V \subset H \subset V^*$. The duality product in $V^* \times V$ is denoted by $\langle \cdot, \cdot \rangle$. Let us consider the abstract problem: For given $u \in L_2((0,T), V^*)$ and $y_0 \in H$, find $y \in W_2^1((0,T), V, H)$, such that

$$\frac{\partial}{\partial t} y + A\, y = u, \qquad\qquad \text{in } L_2((0,T), V^*), \qquad\qquad (4.1\text{a})$$

$$y(0) = y_0, \qquad\qquad \text{in } H. \qquad\qquad (4.1\text{b})$$

Here $A : V \to V^*$ is assumed to be a hemicontinuous, monotone, coercive and bounded operator. Therefore, (4.1) has a unique solution, cf. Theorem 2.22. Problem (4.1) can be stated in a variational framework as follows: Find $y \in W_2^1((0,T), V, H)$ with $y(0) = y_0$ in H, such that

$$\int_0^T \left\langle \frac{\partial}{\partial t} y(\cdot, t) + A\, y(\cdot, t), v(\cdot, t) \right\rangle \mathrm{dt} = \int_0^T \langle u(\cdot, t), v(\cdot, t) \rangle \, \mathrm{dt},$$

for all test functions $v \in L_2((0,T), V)$.

We start by introducing the concept of steady state solutions, that is a commonly used concept in the context of periodic computations.

Definition 4.1 (Steady state solution)**.** *The function $y(t)$ is called a* periodic steady state solution *of equation (4.1a)-(4.1b), if*

1. *y satisfies (4.1a), but not necessarily the initial condition (4.1b),*

2. *y is periodic, i.e., $y(0) = y(T)$.*

Using this alternative classification of a solution, problem (4.1) can be stated as follows: Find $y \in W_2^1((0,T), V, H)$, such that

$$\begin{cases} \dfrac{\partial}{\partial t} y + A\, y = u, & \text{in } L_2((0,T), V^*), \\ \quad\ y(0) = y(T), & \text{in } H. \end{cases} \tag{4.2}$$

Due to the assumptions imposed on A, the periodic problem (4.2) is uniquely solvable, cf. Theorem 2.23. Furthermore, we introduce the following spaces, that incorporate the periodicity conditions

$$W_{2,per}^1((0,T), V, H) := \{ y \in W_2^1((0,T), V, H) : y(0) = y(T) \text{ in } H \},$$
$$L_{2,per}((0,T), V) := \{ y \in L_2((0,T), V) : y(0) = y(T) \text{ in } H \}.$$

Using these spaces of abstract periodic functions, the variational formulation of (4.2) reads as: Find $y \in W_{2,per}^1((0,T), V, H)$, such that

$$\int_0^T \left\langle \frac{\partial}{\partial t} y(\cdot, t) + A\, y(\cdot, t), v(\cdot, t) \right\rangle \mathrm{dt} = \int_0^T \langle u(\cdot, t), v(\cdot, t) \rangle \, \mathrm{dt}, \quad \forall v \in L_{2,per}((0,T), V).$$

This variational formulation is the starting point of some discretization in time. We start by having a closer look at $L_{2,per}((0,T), V)$. Since with $\omega = 2\pi/T$, the set $\{\sin(k\omega t), \cos(k\omega t)\}_{k \in \mathbb{N}}$ is a basis for $L_2(0,T)$ and every function $v \in L_{2,per}((0,T), V)$ can be expanded into a Fourier series, i.e.,

$$v(t) = v_0^c + \sum_{k=1}^{\infty} v_k^c \cos(k\omega t) + v_k^s \sin(k\omega t),$$

with the Fourier coefficients $v_k^c, v_k^s \in V$, given by

$$v_0^c = T \int_0^T v \, \mathrm{dt}, \quad v_k^c = \frac{T}{2} \int_0^T v \cos(k\omega t) \, \mathrm{dt}, \quad v_k^s = \frac{T}{2} \int_0^T v \sin(k\omega t) \, \mathrm{dt}.$$

Indeed, this motivates to use Fourier series expansions as a discretization technique in time. Before we analyze the full time-periodic setting, i.e., infinite Fourier series, we consider the case of a multiharmonic approach, i.e., finite Fourier series.

4.2   Multiharmonic discretization

Before we consider the general time-periodic setting, we concentrate on those time-periodic functions, that have a representation in terms of a *finite* Fourier series. Therefore, we start by investigating multiharmonic excitations $u(t)$. Let us mention, that this approach is very reasonable in many practical applications. Indeed, for the multiharmonic setting, the essential tools of the harmonic balance method can already be derived. Let us consider $u \in L_{2,per}((0,T), V^*)$, of the form

$$u(t) = \sum_{k=0}^{N} u_k^c \cos(k\omega t) + u_k^s \sin(k\omega t), \tag{4.3}$$

with the Fourier coefficients $u_k^c, u_k^s \in V^*$, the base frequency $\omega = 2\pi/T > 0$ and some finite number $N \in \mathbb{N}$. Due to the linearity of (4.2), the solution $y \in W_{2,per}^1((0,T), V, H)$, has the same structure

$$y(t) = \sum_{k=0}^{N} y_k^c \cos(k\omega t) + y_k^s \sin(k\omega t), \tag{4.4}$$

with the Fourier coefficients $y_k^c, y_k^s \in V$ and the same base frequency ω, cf. Remark 4.3. Furthermore, we can compute the generalized derivative

$$\frac{\partial}{\partial t} y(t) = \sum_{k=1}^{N} k\omega \left(-\mathcal{I}(y_k^c) \sin(k\omega t) + \mathcal{I}(y_k^s) \cos(k\omega t) \right),$$

where $\mathcal{I} : V \to V^*$ is the identity operator, i.e., for $y \in V : \mathcal{I}(y) = y$, defined by

$$\langle \mathcal{I}(y), v \rangle := (y, v)_H, \quad \forall v \in V.$$

Clearly, the operator $\mathcal{I}$ is symmetric, positive and bounded, i.e., $\|\mathcal{I}(y)\|_{V^*} \le c\|y\|_V$. Indeed, using the continuous embedding of V into H, we have

$$\|\mathcal{I}(y)\|_{V^*} = \sup_{v \in V} \frac{\langle \mathcal{I}(y), v \rangle}{\|v\|_V} = \sup_{v \in V} \frac{(y, v)_H}{\|v\|_V} \le \sup_{v \in V} \frac{\|y\|_H \|v\|_H}{\|v\|_V} \le c \sup_{v \in V} \frac{\|y\|_V \|v\|_V}{\|v\|_V} \le c\|y\|_V.$$

Using these representations as a multiharmonic function in time, and exploiting the orthogonality of the sine and cosine functions in $(\cdot, \cdot)_{L_2(0,T)}$, we can state (4.2) as a problem for determining the Fourier coefficients in the frequency domain as follows. Find $(y_0^c, y_1^c, y_1^s, \ldots, y_N^c, y_N^s) \in V^{2N+1}$, such that

$$\langle A y_0^c, v_0^c \rangle + \sum_{k=1}^{N} \left[k\omega \left(-\langle \mathcal{I} y_k^c, v_k^s \rangle + \langle \mathcal{I} y_k^s, v_k^c \rangle \right) + \sum_{j \in \{c,s\}} \langle A y_k^j, v_k^j \rangle \right] = \langle u_0^c, v_0^c \rangle + \sum_{j \in \{c,s\}} \sum_{k=1}^{N} \langle u_k^j, v_k^j \rangle,$$

for all test functions $(v_0^c, v_1^c, v_1^s, \ldots, v_N^c, v_N^s) \in V^{2N+1}$. Due to the linearity of A, the problem decouples with respect to the modes k. Consequently, switching back to operator notation, we are dealing with the following problem: Find $y_0^c \in V$, such that

$$A y_0^c = u_0^c, \quad \text{in } V^*, \tag{4.5a}$$

and, for $k = 1, \ldots, N$, find $(y_k^c, y_k^s) \in V^2$, such that

$$\begin{cases} A y_k^c + k\omega \, \mathcal{I}(y_k^s) = u_k^c, & \text{in } V^*, \\ -k\omega \, \mathcal{I}(y_k^c) + A y_k^s = u_k^s, & \text{in } V^*. \end{cases} \tag{4.5b}$$

Theorem 4.2. *Problem (4.5) has a unique solution.*

Proof. Since A is a coercive and bounded operator, existence and uniqueness of a solution y_0^c of (4.5a), follows with Theorem 2.1. Similarly, since A is a coercive and bounded operator, and $\mathcal{I}$ is a positive and bounded operator, existence and uniqueness of a solution (y_k^c, y_k^s) of (4.5b) for a fixed mode k, follows with Theorem 2.1. $\square$

Remark 4.3. *The fact, that multiharmonicity of* **u** *implies multiharmonicity of* **y** *with the same number of modes N can be seen as follows. Problem (4.2) has a unique time-periodic solution. For a given multiharmonic right hand side* **u**, *it is shown in Theorem 4.2, that there exists a uniquely determined solution of the form (4.4), that obviously is time-periodic. Therefore, the unique time-periodic solution has to obtain the multiharmonic structure.*

4.3   Time-periodic discretization

In this section we extend the analysis of the previous one to the case of infinite Fourier series. Let us assume, that the right hand side is given by $\tilde{u}$ in terms of a Fourier series, i.e.,

$$\tilde{u}(t) = \sum_{k=0}^{\infty} u_k^c \cos(k\omega t) + u_k^s \sin(k\omega t), \tag{4.6}$$

with $u_k^c, u_k^s \in V^*$, and suppose, that we have a periodic solution $\tilde{y}$ with the same period $T = 2\pi/\omega$. Then $\tilde{y}$ has a representation as Fourier series, i.e.,

$$\tilde{y}(t) = \sum_{k=0}^{\infty} y_k^c \cos(k\omega t) + y_k^s \sin(k\omega t), \tag{4.7}$$

with $y_k^c, y_k^s \in V$. We start by investigating the right spaces for the Fourier expansions $\tilde{y}$ and $\tilde{u}$ with respect to the Fourier coefficients $\underline{y} = (y_0^c, y_1^c, y_1^s, \ldots)$ and $\underline{u} = (u_0^c, u_1^c, u_1^s, \ldots)$, respectively.
Clearly, $\tilde{y} \in L_{2,per}((0,T),V)$ and therefore, $\|\tilde{y}\|_{L_2((0,T),V)} < \infty$. Furthermore, for functions of the form (4.7), we introduce a norm based on the Fourier coefficients, given by

$$\|\underline{y}\|_{l_2^r(V)}^2 = \|y_0^c\|_V^2 + \sum_{k=1}^{\infty} \sum_{j \in \{c,s\}} \left[k^{2r} \langle \mathcal{I}(y_k^j), y_k^j \rangle + k^{2r-1} \|y_k^j\|_V^2 \right],$$

for $r \in \{1/2, 1\}$. Using this norm, we can define the space of Fourier coefficients, abbreviated by $\underline{y} = (y_0^c, y_1^c, y_1^s, \ldots)$, in terms of

$$l_2^r(V) := \left\{ \underline{y} \in V^{\mathbb{N}} : \|\underline{y}\|_{l_2^r(V)} < \infty \right\}.$$

Indeed, the space $l_2^r(V)$ is a Hilbert space. We continue by defining the operators $\mathcal{A} : l_2^{\frac{1}{2}}(V) \to l_2^{\frac{1}{2}}(V)^*$, by

$$\langle \mathcal{A}\,\underline{y}, \underline{v} \rangle_{l_2^{\frac{1}{2}}(V)^* \times l_2^{\frac{1}{2}}(V)} := \int_0^T \left\langle \frac{\partial}{\partial t} \tilde{y}(\cdot, t) + A\,\tilde{y}(\cdot, t), \tilde{v}(\cdot, t) \right\rangle \mathrm{dt},$$

and $\mathcal{U} \in l_2^{\frac{1}{2}}(V)^*$, by

$$\langle \mathcal{U}, \underline{v} \rangle_{l_2^{\frac{1}{2}}(V)^* \times l_2^{\frac{1}{2}}(V)} := \int_0^T \langle \tilde{u}(\cdot, t), \tilde{v}(\cdot, t) \rangle.$$

Now we are in the position to state the variational problem in the Fourier space. Find $\underline{y} \in l_2^{\frac{1}{2}}(V)$, such that

$$\langle \mathcal{A}\,\underline{y}, \underline{v} \rangle_{l_2^{\frac{1}{2}}(V)^* \times l_2^{\frac{1}{2}}(V)} = \langle \mathcal{U}, \underline{v} \rangle_{l_2^{\frac{1}{2}}(V)^* \times l_2^{\frac{1}{2}}(V)}, \tag{4.8}$$

for all $\underline{v} \in l_2^{\frac{1}{2}}(V)$. The unique solvability of the variational problem (4.8) is addressed in the following theorem.

Theorem 4.4. *Suppose, that the source u is given by a Fourier series*

$$u(t) = \sum_{k=0}^{\infty} u_k^c \cos(k\omega t) + u_k^s \sin(k\omega t),$$

with Fourier coefficients $u_k^j \in V^*$, for all $k \in \mathbb{N}$ and $j \in \{c, s\}$. Then the variational problem (4.8) has a unique periodic steady state solution. If moreover $\sum_{k=0}^{\infty} y_k^c = y_0$, the periodic steady state solution also satisfies the initial condition and hence solves the initial value problem (4.1).

Proof. We want to apply Theorem 2.1 and therefore we have to verify the inf-sup and sup-sup conditions. Firstly, the upper bound follows by reapplication of Cauchy's inequality and boundedness of the operator A. Indeed, we have

$$
\begin{aligned}
\langle \mathcal{A}\underline{y}, \underline{v}\rangle_{l_2^{\frac{1}{2}}(V)^* \times l_2^{\frac{1}{2}}(V)} &= \int_0^T \left\langle \frac{\partial}{\partial t}\tilde{y}(\cdot, t) + A\,\tilde{y}(\cdot, t), \tilde{v}(\cdot, t)\right\rangle \mathrm{dt} \\
&\leq c\sum_{k=1}^\infty k\left[\langle \mathcal{I}(y_k^s), v_k^c\rangle - \langle \mathcal{I}(y_k^c), v_k^s\rangle\right] + \langle A\,y_0^c, v_0^c\rangle + \sum_{j\in\{c,s\}}\sum_{k=1}^\infty \langle A\,y_k^j, v_k^j\rangle \\
&\leq c\,\|\underline{y}\|_{l_2^{\frac{1}{2}}(V)}\|\underline{v}\|_{l_2^{\frac{1}{2}}(V)},
\end{aligned}
$$

with a constant c, that only depends on the boundedness constant of the operator A and the frequency ω. In order to prove the inf-sup condition, we first use the special test function $\underline{y}^\dagger \in l_2^{\frac{1}{2}}(V)$ defined via

$$
\tilde{y}^\dagger(t) := y_0^c + \sum_{k=1}^\infty y_k^s\cos(k\omega t) - y_k^c\sin(k\omega t).
$$

Using this special test function, we obtain

$$
\langle \mathcal{A}\underline{y}, \underline{y}^\dagger\rangle_{l_2^{\frac{1}{2}}(V)^* \times l_2^{\frac{1}{2}}(V)} = \int_0^T \left\langle \frac{\partial}{\partial t}\tilde{y}(\cdot, t) + A\,\tilde{y}(\cdot, t), \tilde{y}^\dagger(\cdot, t)\right\rangle \mathrm{dt} \geq c\sum_{k=1}^\infty \sum_{j\in\{c,s\}} k\langle \mathcal{I}(y_k^j), y_k^j\rangle,
$$

with some constant c, only depending on the frequency ω. Secondly, due to the coercivity of A, we have

$$
\langle \mathcal{A}\underline{y}, \underline{y}\rangle_{l_2^{\frac{1}{2}}(V)^* \times l_2^{\frac{1}{2}}(V)} = \int_0^T \left\langle \frac{\partial}{\partial t}\tilde{y}(\cdot, t) + A\,\tilde{y}(\cdot, t), \tilde{y}(\cdot, t)\right\rangle \mathrm{dt} \geq c\left(\|y_0^c\|_V^2 + \sum_{k=1}^\infty \sum_{j\in\{c,s\}} \|y_k^j\|_V^2\right),
$$

with some constant c, only depending on the coercivity constant of A. Combining the last two equations, we obtain

$$
\langle \mathcal{A}\underline{y}, \underline{y}^\dagger + \underline{y}\rangle_{l_2^{\frac{1}{2}}(V)^* \times l_2^{\frac{1}{2}}(V)} \geq c\,\|\underline{y}\|_{l_2^{\frac{1}{2}}(V)}^2.
$$

Using the fact, that $\|\underline{y}^\dagger + \underline{y}\|_{l_2^{\frac{1}{2}}(V)}^2 = \sqrt{2}\|\underline{y}\|_{l_2^{\frac{1}{2}}(V)}^2$, the inf-sup constant follows. $\qquad\square$

4.4 Galerkin approximation

In this section we use the multiharmonic approach of Section 4.2 as a Galerkin approximation for time-periodic problems, and provide a discretization error analysis.

Let us introduce the family of subspaces $l_{2,N}^{\frac{1}{2}}(V) \subset l_2^{\frac{1}{2}}(V)$ by

$$
l_{2,N}^{\frac{1}{2}}(V) := \left\{\underline{y} \in l_2^{\frac{1}{2}}(V) : y_k^j = 0, j \in \{c, s\}, \forall k > N\right\}.
$$

Using $l_{2,N}^{\frac{1}{2}}(V)$, we can state the Galerkin system: Find $\underline{y}_N \in l_{2,N}^{\frac{1}{2}}(V)$, such that

$$
\langle \mathcal{A}\underline{y}_N, \underline{v}_N\rangle_{l_2^{\frac{1}{2}}(V)^* \times l_2^{\frac{1}{2}}(V)} = \langle \mathcal{U}, \underline{v}_N\rangle_{l_2^{\frac{1}{2}}(V)^* \times l_2^{\frac{1}{2}}(V)}, \tag{4.9}
$$

for all $\underline{v}_N \in l_{2,N}^{\frac{1}{2}}(V)$. The variational problem (4.9) has a unique solution $\underline{y}_N \in l_{2,N}^{\frac{1}{2}}(V)$, since the proof of Theorem 4.4 can be repeated step by step.

Due to Lemma 2.5, we can estimate the discretization error in terms of the best approximation error, i.e.,

$$\|\underline{y} - \underline{y}_N\|_{l_2^{\frac{1}{2}}(V)} \leq c \inf_{\underline{v}_N \in l_{2,N}^{\frac{1}{2}}(V)} \|\underline{y} - \underline{v}_N\|_{l_2^{\frac{1}{2}}(V)}.$$

Obviously, the approximation error to some function $\tilde{y}$, cf. (4.7), can be estimated by $\mathcal{S}_N \tilde{y}$, given by

$$\mathcal{S}_N \tilde{y} := \sum_{k=0}^{N} y_k^c \cos(k\omega t) + y_k^s \sin(k\omega t),$$

associated with the vector of the Fourier coefficients $\underline{\tilde{y}}_N \in l_2^{\frac{1}{2}}(V)$. Therefore, we obtain

$$\inf_{\underline{v}_N \in l_{2,N}^{\frac{1}{2}}(V)} \|\underline{y} - \underline{v}_N\|_{l_2^{\frac{1}{2}}(V)}^2 \leq \|\underline{y} - \underline{\tilde{y}}_N\|_{l_2^{\frac{1}{2}}(V)}^2 = \sum_{k=N+1}^{\infty} \sum_{j \in \{c,s\}} \left[k \langle \mathcal{I}(y_k^j), y_k^j \rangle + \|y_k^j\|_V^2 \right]$$

$$\leq cN^{-1} \sum_{k=N+1}^{\infty} \sum_{j \in \{c,s\}} \left[k^2 \langle \mathcal{I}(y_k^j), y_k^j \rangle + k \|y_k^j\|_V^2 \right] \leq c\, N^{-1} \|\underline{y}\|_{l_2^1(V)}^2,$$

with some constant c independent of N. Therefore the discretization error is fully determined by the approximation properties of Fourier series approximations. The main result is summarized in the following theorem.

Theorem 4.5. *Suppose, that the source u is given by a Fourier series*

$$u(t) = \sum_{k=0}^{\infty} u_k^c \cos(k\omega t) + u_k^s \sin(k\omega t), \tag{4.10}$$

with Fourier coefficients $u_k^j \in V^*$, for all $k \in \mathbb{N}$ and $j \in \{c,s\}$. Let $\underline{y}$ be the solution of (4.8), and $\underline{y}_N$ be the solution of (4.9). Suppose, that $\underline{y} \in l_2^1(V)$, then the following a priori error estimate is valid

$$\|\underline{y} - \underline{y}_N\|_{l_2^{\frac{1}{2}}(V)} \leq c\, N^{-\frac{1}{2}} \|\underline{y}\|_{l_2^1(V)}, \tag{4.11}$$

where the constant c is independent of N.

Remark 4.6. *The assumption (4.10) is not very restrictive, since every function $v \in L_2(0,T)$ possesses a convergent Fourier series representation.*

Remark 4.7. *For the solution $\tilde{y} \in W_2^1((0,T), V, H)$ of (4.2), the error estimate (4.11) immediately implies the weaker estimate*

$$\|\tilde{y} - \mathcal{S}_N \tilde{y}\|_{L_2((0,T),V)} \leq c\, N^{-\frac{1}{2}} \|\tilde{y}\|_{W_2^1((0,T),V,H)},$$

with some constant c independent of N.

Remark 4.8. *By introducing a Galerkin discretization of the full time-periodic case, we end up with the same kind of systems as in (4.5). Therefore, for numerical treatment, it is sufficient to investigate the properties of the system (4.5).*

4.5   Optimal control problems

In time-periodic optimization, the goal of optimization is to find the optimal control, which minimizes the objective functional $\mathcal{J}$ over a set of admissible controls, and in addition induces a prescribed

cyclic state with a fixed period, e.g. [1, 65, 86]. Therefore, let us consider the abstract minimization functional

$$\mathcal{J}(y, u) := \frac{1}{2}\|y - y_d\|^2_{L_2((0,T),H)} + \frac{\lambda}{2}\|u\|^2_{L_2((0,T),H)},$$

with given desired state $y_d \in L_2((0,T), H)$ and given regularization parameter $\lambda > 0$. The corresponding minimization problem reads as: Find $(\hat{y}, \hat{u}) \in V \times H$, such that

$$\mathcal{J}(\hat{y}, \hat{u}) = \min_{(y,u) \in V \times H} \mathcal{J}(y, u), \tag{4.12}$$

where (y, u) fulfills (4.2). The minimization problem (4.12) obtains a unique solution. The solution can be determined via the optimality system, that is given as follows: Find $(y, u, p) \in V \times H \times V$, such that

$$\begin{cases} -\dfrac{\partial}{\partial t}p + A\,p + \mathcal{I}(y) = \mathcal{I}(y_d), & \text{in } L_2((0,T), V^*), \\[2mm] \lambda u - p = 0, & \text{in } L_2((0,T), H), \\[2mm] \dfrac{\partial}{\partial t}y + A\,y = u, & \text{in } L_2((0,T), V^*), \\[2mm] y(0) = y(T),\ p(0) = p(T), & \text{in } H. \end{cases} \tag{4.13}$$

One important property of the system (4.13) is, that a periodicity condition is obtained for both, the state y and the co-state p. This is in stark contrast to the case of optimal control problems for initial value problems, where a forward and a backward problem have to be solved for the state and the co-state, respectively. Therefore, we obtain a symmetry of the state and the co-state concerning the initial condition.

In the usual manner, the control u can be eliminated. This gives rise to the reduced optimality system: Find $(y, p) \in V^2$, such that

$$\begin{cases} -\dfrac{\partial}{\partial t}p + A\,p + \mathcal{I}(y) = \mathcal{I}(y_d), & \text{in } L_2((0,T), V^*), \\[2mm] \dfrac{\partial}{\partial t}y + A\,y - \dfrac{1}{\lambda}\mathcal{I}(p) = 0, & \text{in } L_2((0,T), V^*), \\[2mm] y(0) = y(T),\ p(0) = p(T), & \text{in } H. \end{cases}$$

The reduced optimality system is the starting point of a discretization in time. Due to the periodic structure of the optimality system, a discretization in terms of a Fourier series approximation pops up naturally.

Let us assume, that the desired state $y_d(t)$ is given by a multiharmonic excitation, i.e.,

$$y_d(t) = \sum_{k=0}^{N} y^c_{d,k}\cos(k\omega t) + y^s_{d,k}\sin(k\omega t),$$

with the Fourier coefficients $y^c_{d,k}, y^s_{d,k} \in H$, the base frequency $\omega = 2\pi/T > 0$ and some finite number $N \in \mathbb{N}$. Due to the linearity of the minimization problem, the state y and the control u can be represented in the same form as the desired state y_d, cf. (4.4), (4.3) and Remark 4.3.

Again, the minimization problem decouples with respect to the modes k. Consequently, we are dealing with the following reduced optimality system in the frequency domain: Find $(y^c_0, p^c_0) \in V^2$, such that

$$\begin{cases} \mathcal{I}(y^c_0) + A\,p^c_0 = \mathcal{I}(y^c_{d,0}), & \text{in } V^*, \\[2mm] A\,y^c_0 - \dfrac{1}{\lambda}\mathcal{I}(p^c_0) = 0, & \text{in } V^*, \end{cases} \tag{4.14a}$$

and, for $k = 1, \ldots, N$, find $(y_k^c, y_k^s, p_k^c, p_k^s) \in V^4$, such that

$$
\begin{cases}
\mathcal{I}(y_k^c) + A\, p_k^c - k\omega\, \mathcal{I}(p_k^s) = \mathcal{I}(y_{d,k}^c), & \text{in } V^*, \\[2mm]
\mathcal{I}(y_k^s) + k\omega\, \mathcal{I}(p_k^c) + A\, p_k^s = \mathcal{I}(y_{d,k}^s), & \text{in } V^*, \\[2mm]
A\, y_k^c + k\omega\, \mathcal{I}(y_k^s) - \dfrac{1}{\lambda}\mathcal{I}(p_k^c) = 0, & \text{in } V^*, \\[2mm]
-k\omega\, \mathcal{I}(y_k^c) + A\, y_k^s - \dfrac{1}{\lambda}\mathcal{I}(p_k^s) = 0, & \text{in } V^*.
\end{cases}
\qquad (4.14b)
$$

Theorem 4.9. *The variational problem (4.14) has a unique solution.*

Proof. Since A is a coercive and bounded operator, and $\mathcal{I}$ is a positive and bounded operator, existence and uniqueness of a solution of (4.14a) and (4.14b) for a fixed mode k follows with Theorem 2.1. $\quad\square$

Chapter 5

Iterative solvers and preconditioning

As we have seen in Chapter 3 and Chapter 4, the system of linear equations stemming from harmonic balance approximations, FEM-BEM coupling methods or optimal control problems typically obtain saddle point structures. This chapter deals with the iterative solution of saddle point problems: For given $\mathbf{f} \in \mathbb{R}^n$, find $\mathbf{x} \in \mathbb{R}^n$, such that

$$\mathcal{A}\,\mathbf{x} = \mathbf{f}, \tag{5.1}$$

with the regular system matrix $\mathcal{A} \in \mathbb{R}^{n \times n}$ of the form

$$\mathcal{A} = \begin{pmatrix} A & B^T \\ B & -C \end{pmatrix}. \tag{5.2}$$

Here A and C are symmetric and positive semi-definite matrices, by which $\mathcal{A}$ becomes symmetric and indefinite, i.e., it has both positive and negative eigenvalues. One of the most famous iterative methods is the *conjugate gradient* (CG) method, but due to the indefiniteness of the system matrix $\mathcal{A}$ it may fail if applied to (5.1). One way out is to apply the Bramble Pasciak CG, cf. [30], or Zulehner CG, cf. [143], that require the construction of appropriate inner products, such that (5.2) becomes positive definite and self-adjoint with respect to this inner product. Alternative methods are the minimal residual method, that is designed as a Krylov subspace method for symmetric and indefinite problems, or the generalized minimal residual method, that is designed to deal with general non-symmetric problems. Due to the symmetry of (5.2) the minimal residual method is the method of choice in our framework.

5.1 The preconditioned MinRes method

The *minimal residual* (MinRes) method was introduced in [128] as a robust iterative method if applied to symmetric – but not necessary positive definite – linear systems of equations. MinRes belongs to the large class of Krylov subspace methods, that are known to be among the most effective methods for linear systems arising from the discretization of partial differential equations. Krylov subspace methods are composed of simple iterations that produce a sequence of approximations $\mathbf{x}^{(k)}$, that converges to the exact solution, as k increases.

Indeed, in the preconditioned MinRes method, the iterates $\mathbf{x}^{(k)}$ are determined by seeking to minimize the $\mathcal{P}^{-1}$-norm of the residual $\mathbf{r}^{(k)} = \mathbf{f} - \mathcal{A}\,\mathbf{x}^{(k)}$ over the Krylov subspace $\mathcal{K}_k(\mathcal{P}^{-1}\mathcal{A}; \mathcal{P}^{-1}\mathbf{r}^{(0)})$. Here, the symmetric and positive definite matrix $\mathcal{P}$ of the same size as $\mathcal{A}$ is called preconditioner (cf. Section 5.2) and the Krylov subspace is given by

$$\mathcal{K}_k(\mathcal{P}^{-1}\mathcal{A}; \mathcal{P}^{-1}\mathbf{r}^{(0)}) := \text{span}\{\mathcal{P}^{-1}\mathbf{r}^{(0)}, (\mathcal{P}^{-1}\mathcal{A})\mathcal{P}^{-1}\mathbf{r}^{(0)}, \dots, (\mathcal{P}^{-1}\mathcal{A})^k \mathcal{P}^{-1}\mathbf{r}^{(0)}\}.$$

Hence, the approximation at the step k is given as the solution of the minimization problem

$$\mathbf{x}^{(k)} = \underset{\mathbf{x} \in \mathbf{x}^{(0)} + \mathcal{K}_k(\mathcal{P}^{-1}\mathcal{A}; \mathcal{P}^{-1}\mathbf{r}^{(0)})}{\text{argmin}} \|\mathbf{r}^{(k)}\|_{\mathcal{P}^{-1}}.$$

This minimization problem is solved by building an orthonormal basis of the Krylov subspace, using the Lanczos algorithm. The solution of the minimization problem is based on a three-term recurrence in the Krylov subspace. For more details, we refer to [53]. Finally, this procedure gives rise to the preconditioned MinRes method as stated in Algorithm 1, see e.g., [53, Algorithm 6.1].

> **Input**: $\mathcal{A} \in \mathbb{R}^{n \times n}$ symmetric and regular, $\mathcal{P} \in \mathbb{R}^{n \times n}$ symmetric and positive definite, right hand-side $\mathbf{f} \in \mathbb{R}^n$, initial guess $\mathbf{x}^{(0)} \in \mathbb{R}^n$.
> **Output**: approximate solution $\mathbf{x}^{(k)}$.
> Set $\mathbf{v}^{(0)} := \mathbf{0}$, $\mathbf{w}^{(0)} := \mathbf{0}$, $\mathbf{w}^{(1)} := \mathbf{0}$;
> Set $\mathbf{v}^{(1)} := \mathbf{f} - \mathcal{A}\mathbf{x}^{(0)}$;
> Solve $\mathcal{P}\mathbf{z}^{(1)} = \mathbf{v}^{(1)}$;
> Set $\gamma_1 := \sqrt{\langle \mathbf{z}^{(1)}, \mathbf{v}^{(1)} \rangle}$;
> Set $\mathbf{z}^{(1)} := \mathbf{z}^{(1)}/\gamma_1$ and $\mathbf{v}^{(1)} := \mathbf{v}^{(1)}/\gamma_1$;
> Set $\eta_0 := \gamma_1$, $s_0 := s_1 := 0$, $c_0 := c_1 := 1$;
> Set $k := 1$;
> **while** *not converged* **do**
> > Set $\delta_k := \langle \mathbf{z}^{(k)}, \mathbf{z}^{(k)} \rangle$;
> > Set $\mathbf{v}^{(k+1)} := \mathcal{A}\mathbf{z}^{(k)} - \delta_k\mathbf{v}^{(k)} - \gamma_k\mathbf{v}^{(k-1)}$;
> > Solve $\mathcal{P}\mathbf{z}^{(k+1)} = \mathbf{v}^{(k+1)}$;
> > Set $\gamma_{k+1} := \sqrt{\langle \mathbf{z}^{(k+1)}, \mathbf{v}^{(k+1)} \rangle}$;
> > Set $\mathbf{z}^{(k+1)} := \mathbf{z}^{(k+1)}/\gamma_{k+1}$ and $\mathbf{v}^{(k+1)} := \mathbf{v}^{(k+1)}/\gamma_{k+1}$;
> > Set $\alpha_0 := c_k\delta_k - c_{k-1}s_k\gamma_k$ and $\alpha_1 := \sqrt{\alpha_0^2 + \gamma_{k+1}^2}$;
> > Set $\alpha_2 := s_k\delta_k + c_{k-1}c_k\gamma_k$ and $\alpha_3 := s_{k-1}\gamma_k$;
> > Set $c_{k+1} := \alpha_0/\alpha_1$ and $s_{k+1} := \gamma_{k+1}/\alpha_1$;
> > Set $\mathbf{w}^{(k+1)} := (\mathbf{z}^{(k)} - \alpha_3\mathbf{w}^{(k-1)} - \alpha_2\mathbf{w}^{(k)})/\alpha_1$;
> > Set $\mathbf{x}^{(k)} := \mathbf{x}^{(k-1)} + c_{k+1}\eta_{k-1}\mathbf{w}^{(k+1)}$;
> > Set $\eta_k := -s_{k+1}\eta_{k-1}$;
> > Set $k := k + 1$;
> **end**

Algorithm 1: The preconditioned MinRes method.

As a convergence criteria, e.g. the exceed of the relative norm of the unpreconditioned residual $\mathbf{r}^{(k)}$ in the $\mathcal{P}^{-1}$ norm below a certain tolerance can be used. This quantity can be accessed via the parameter η_k/η_0, since $\eta_k = \|\mathbf{r}^{(k)}\|_{\mathcal{P}^{-1}}$. Using this criteria, the convergence result of the MinRes method is summarized in the following theorem.

Theorem 5.1. *Let $\mathcal{A}$ be a regular and symmetric matrix. The preconditioned MinRes method applied to the system $\mathcal{A}\mathbf{x} = \mathbf{f}$ with some symmetric and positive definite preconditioner $\mathcal{P}$ converges to the solution of this system for an arbitrary initial guess $\mathbf{x}^{(0)}$. More precisely, the residual $\mathbf{r}^{(2m)} = \mathbf{f} - \mathcal{A}\mathbf{x}^{(2m)}$ after $2m$ iterations can be estimated in terms of the initial residual $\mathbf{r}^{(0)}$ as follows:*

$$\|\mathbf{r}^{(2m)}\|_{\mathcal{P}^{-1}} \leq \frac{2q^m}{1 + q^{2m}}\|\mathbf{r}^{(0)}\|_{\mathcal{P}^{-1}} \qquad with \quad q = \frac{\kappa_{\mathcal{P}}(\mathcal{P}^{-1}\mathcal{A}) - 1}{\kappa_{\mathcal{P}}(\mathcal{P}^{-1}\mathcal{A}) + 1}, \tag{5.3}$$

where $\kappa_{\mathcal{P}}(\mathcal{P}^{-1}\mathcal{A}) := \|\mathcal{P}^{-1}\mathcal{A}\|_{\mathcal{P}} \|\mathcal{A}^{-1}\mathcal{P}\|_{\mathcal{P}}$ is the condition number of the preconditioned system matrix and, depending on the context, $\|\cdot\|_{\mathcal{P}}$ is the $\mathcal{P}$-energy norm or the corresponding matrix norm, i.e.,

$$\|\mathbf{x}\|_{\mathcal{P}} = (\mathcal{P}\mathbf{x}, \mathbf{x})^{1/2} \quad or \quad \|\mathcal{A}\|_{\mathcal{P}} = \sup_{\mathbf{x} \in \mathbb{R}^n} \frac{\|\mathcal{A}\mathbf{x}\|_{\mathcal{P}}}{\|\mathbf{x}\|_{\mathcal{P}}}.$$

Proof. See Greenbaum [61]. $\square$

Theorem 5.1 states, that the convergence of the MinRes method is fully determined by the condition number $\kappa_{\mathcal{P}}(\mathcal{P}^{-1}\mathcal{A})$ of the preconditioned system matrix. Therefore, one of the key goals is to construct preconditioners, so that the condition number is small, i.e., as close as possible to one.

Remark 5.2. *We mention, that the convergence analysis of the GmRes method [139] applied to (5.4) is different. Especially, the rate of convergence of the GmRes method cannot be determined just from the knowledge of the condition number. Therefore, designing and analyzing preconditioners in a GmRes setting is a much harder topic, cf. [112].*

For more details about the preconditioned MinRes method as well as other iterative methods, we refer to the monographs [53, 61].

5.2   Preconditioners for saddle point problems

Beside the choice of a suitable Krylov subspace method, preconditioning is an important issue. By multiplying (5.1) by the inverse of a symmetric and positive definite matrix $\mathcal{P}$, called preconditioner, one tries to improve the convergence rate of any iterative method applied to the resulting system

$$\mathcal{P}^{-1}\mathcal{A}\mathbf{x} = \mathcal{P}^{-1}\mathbf{f}. \tag{5.4}$$

Here the application of the preconditioner $\mathcal{P}$ does not destroy the symmetry property of (5.4), since $\mathcal{P}^{-1}\mathcal{A}$ is still symmetric in the $\mathcal{P}$ inner product, i.e.,

$$(\mathcal{P}^{-1}\mathcal{A}\,u, v)_{\mathcal{P}} = (u, \mathcal{P}^{-1}\mathcal{A}\,v)_{\mathcal{P}}.$$

Furthermore, a preconditioner $\mathcal{P}$ should

- provide good condition numbers for the preconditioned system matrix and

- be realizable in an optimal way, i.e., the application of the inverse of the preconditioner should require not more than $\mathcal{O}(n)$ operations.

Indeed, these two properties are in stark contrast to each other. While on the one hand the choice $\mathcal{P} = \mathcal{A}$ yields the best condition number 1, but the realization of $\mathcal{P}^{-1}$ is as costly as $\mathcal{A}^{-1}$, on the other hand the choice $\mathcal{P} = Id$ does not improve the condition number, but the realization is very easy. Hence the Holy Grail of preconditioning is to find the right balance between these two issues. In the survey article [23] a wide range of preconditioners for saddle point problems of the form (5.1) are discussed. One of the key ideas of constructing preconditioners is, that once a proper preconditioner for the continuous problem is identified and a stable discretization of the problem is used, then one obtains the basic structure for the preconditioner of the corresponding discrete problem, see e.g. [117]. This motivates to study preconditioners in the continuous setting and leads to the problem setting of well-posedness in non-standard norms. Consequently, the choice of block-diagonal preconditioners is equivalent to choosing the right scalar product in the underlying Hilbert space. Based on this observation, for a wide range of problems, block-diagonal preconditioners have been developed already, see the survey article [117].
One key issue in this thesis is the construction of preconditioners for parameter-dependent problems, i.e., problems of the form

$$\mathcal{A}(\mathcal{Q})\,\mathbf{x} = \mathbf{f}, \tag{5.5}$$

where the system matrix $\mathcal{A}(\mathcal{Q})$ depends on a set of discretization, model or regularization parameters $\mathcal{Q}^1$. In typical applications, the condition number $\kappa(\mathcal{A}(\mathcal{Q}))$ is very large for a huge range of practical relevant parameter settings $\mathcal{Q}$. Indeed, the ultimate goal is to construct preconditioners $\mathcal{P}(\mathcal{Q})$, such that a condition number bound, uniformly in all feasible parameter sets $\mathcal{Q}$, can be obtained, i.e., $\kappa(\mathcal{P}^{-1}(\mathcal{Q})\mathcal{A}(\mathcal{Q})) \leq c$ with c independent of $\mathcal{Q}$ and possibly small. Indeed, this property is referred as *robust preconditioning* and can be achieved by using appropriate block-diagonal preconditioners. The approach of this work follows the article [164], that provides a more systematic search for the appropriate inner products and therefore for robust block-diagonal preconditioners. Indeed, the

---

[1]In this thesis, the set Q is typically a subset of $\{h, \omega, N, \sigma, \nu, \lambda, \varepsilon\}$, cf. Chapter 6 and Chapter 7.

latter mentioned approach extends the classical saddle point analysis of Brezzi, and a road map of this approach is given in Subsection 5.2.1. Even more striking, this systematic approach also leads to the theory of constructing the appropriate inner products by a matrix interpolation technique and is discussed in Subsection 5.2.2. Moreover, we discuss the relevance and practical realization of block-diagonal preconditioners in Subsection 5.2.4.

This subsection is heavily based on the work in [117, 164].

5.2.1 Well-posedness in non-standard norms and preconditioning

In this subsection we briefly outline the importance of the choice of the appropriate inner product and the corresponding norm in the underlying Hilbert space in the context of block-diagonal and parameter-robust preconditioning. First of all we regard the following relation:

$$\underline{c}\,\|z\|_X \le \|\mathcal{A}\,z\|_{X^*} \le \overline{c}\,\|z\|_X, \quad \forall\, z \in X. \tag{5.6}$$

Starting from (5.6), an immediate consequence is an estimate of the condition number $\kappa(\mathcal{A})$ in terms of $\underline{c}$ and $\overline{c}$, i.e.,

$$\kappa(\mathcal{A}) := \|\mathcal{A}\|_{L(X,X^*)}\|\mathcal{A}^{-1}\|_{L(X^*,X)} \le \frac{\overline{c}}{\underline{c}}.$$

Indeed, the estimate follows from

$$\|\mathcal{A}\|_{L(X,X^*)} = \sup_{z \in X} \frac{\|\mathcal{A}\,z\|_{X^*}}{\|z\|_X} \le \sup_{z \in X} \frac{\overline{c}\|z\|_X}{\|z\|_X} = \overline{c},$$

and by the substitution $\mathcal{A}^{-1}z = y \in X$ in

$$\|\mathcal{A}^{-1}\|_{L(X^*,X)} = \sup_{z \in X^*} \frac{\|\mathcal{A}^{-1}z\|_X}{\|z\|_{X^*}} = \sup_{y \in X^*} \frac{\|y\|_X}{\|\mathcal{A}\,y\|_{X^*}} \le \frac{1}{\underline{c}}.$$

Furthermore, the relation (5.6) provides the link between the proper choice of the block-diagonal preconditioner and the classical variational theory of Babuška-Aziz, since (5.6) is nothing else than the inf-sup and the sup-sup condition that appear in the Theorem of Babuška-Aziz [14], cf. Theorem 2.1. Consequently, robust estimates of the form (5.6) imply robust estimates for the condition number. More precisely, in the latter case (5.6) means, that solving the discrete variational problem connected with the inner product in X supplies a robust preconditioner for $\mathcal{A}$. This can be seen as follows: By introducing the Riesz map $\mathcal{P} : X \to X^*$, the inner product $(\cdot,\cdot)_X$ can be expressed as a duality product

$$(\cdot,\cdot)_X = \langle \mathcal{P}\cdot,\cdot\rangle_{X^* \times X}.$$

Using the Riesz map $\mathcal{P}$, a closed expression of the dual norm can be given in terms of

$$\|y\|_{X^*} = \sup_{x \in X} \frac{\langle y,x\rangle}{\|x\|_X} = \sup_{x \in X} \frac{\langle y,x\rangle}{\sqrt{\langle \mathcal{P}\,x,x\rangle}} = \sqrt{\langle y,\mathcal{P}^{-1}y\rangle}.$$

Consequently, (5.6) obtains the form

$$\underline{c}\sqrt{\langle \mathcal{P}\,z,z\rangle} \le \sqrt{\langle \mathcal{A}\,z,\mathcal{P}^{-1}\mathcal{A}\,z\rangle} \le \overline{c}\sqrt{\langle \mathcal{P}\,z,z\rangle}, \tag{5.7}$$

meaning, that the inverse of the Riesz map in the Hilbert space X is the right preconditioner to be used in a MinRes setting.

The main question is, how to find the right inner product in X, and therefore the appropriate preconditioner $\mathcal{P}$. Beside many intuitive approaches (see, e.g., [117]), a constructive way based on matrix interpolation is presented in the next subsection. Therefore, we revisit the equivalence relation (5.7) in the simpler case of finite dimensional vector spaces.

5.2.2 The interpolation method

This subsection follows [164], that provides the theory of constructing robust block-diagonal preconditioners for parameter-dependent saddle point problems. Although the theoretical framework is quite involving, the idea of constructing parameter-robust preconditioners is very intuitively:

1. Start from at least two parameter-robust preconditioners, that may have no easy realization.

2. Interpolate between these two preconditioners and obtain a family of new preconditioners, where one of those might come up with an easier realization.

For simplicity, in this subsection we work on the finite dimensional vector space $\mathbb{R}^n$, i.e., all operators have a representation as matrices and therefore the inner products are well defined via this matrix representation.

As a starting point, we recall the well-known parameter-robust Schur complement preconditioners for saddle point problems of the form (5.2).

Theorem 5.3. *Let A and C according to (5.2) be symmetric and positive definite matrices and let*

$$S = C + BA^{-1}B^T \qquad and \qquad R = A + B^TC^{-1}B$$

be the negative Schur complements of (5.2). If $\mathcal{A}$ is preconditioned by

$$\mathcal{P}_0 = \begin{pmatrix} A & 0 \\ 0 & S \end{pmatrix} \qquad or \qquad \mathcal{P}_1 = \begin{pmatrix} R & 0 \\ 0 & C \end{pmatrix}, \tag{5.8}$$

then the eigenvalues of the preconditioned matrices $\mathcal{P}_0^{-1}\mathcal{A}$ and $\mathcal{P}_1^{-1}\mathcal{A}$ are located in the set $(-1, \frac{1-\sqrt{5}}{2}] \cup \{1\} \cup (1, \frac{1+\sqrt{5}}{2}]$.

Proof. See [109] and [119]. $\qquad\square$

Theorem 5.3 immediately yields the following norm estimates.

Corollary 5.4. *The inequalities*

$$\underline{c}\,\|\mathbf{x}\|_{\mathcal{P}_0} \leq \|\mathcal{A}\,\mathbf{x}\|_{\mathcal{P}_0^{-1}} \leq \bar{c}\,\|\mathbf{x}\|_{\mathcal{P}_0} \quad and \quad \underline{c}\,\|\mathbf{x}\|_{\mathcal{P}_1} \leq \|\mathcal{A}\,x\|_{\mathcal{P}_1^{-1}} \leq \bar{c}\,\|\mathbf{x}\|_{\mathcal{P}_1} \tag{5.9}$$

are valid for all $\mathbf{x} \in \mathbb{R}^n$, with $\underline{c} = (\sqrt{5}-1)/2$ and $\bar{c} = (\sqrt{5}+1)/2$.

Although, both block-diagonal preconditioners $\mathcal{P}_0$ and $\mathcal{P}_1$ provide a good condition number, they are only of theoretical importance, since the application of the inverse of the Schur complements R and S is hard to realize in general. The idea is to apply the following operator interpolation theorem, which is based on the construction of intermediate spaces via the so called real method, which includes the J- and the K-method. The idea of these methods is due to Lions and Peetre and the theory of the real method is developed e.g. in [24], see also [4].

Theorem 5.5. *Let $\mathcal{A} : \mathbb{R}^n \longrightarrow \mathbb{R}^n$ be regular with*

$$\|\mathcal{A}\,\mathbf{x}\|_{Y_0} \leq c_0\|\mathbf{x}\|_{X_0} \qquad and \qquad \|\mathcal{A}\,\mathbf{x}\|_{Y_1} \leq c_1\|\mathbf{x}\|_{X_1},$$
$$\|\mathcal{A}^{-1}\mathbf{y}\|_{X_0} \leq c_2\|\mathbf{y}\|_{Y_0} \qquad and \qquad \|\mathcal{A}^{-1}\mathbf{y}\|_{X_1} \leq c_3\|\mathbf{y}\|_{Y_1},$$

where the norms $\|\cdot\|_{X_i}$ and $\|\cdot\|_{Y_i}$ are the interpolation norms associated to the inner products

$$(\mathbf{x}, \mathbf{y})_{X_i} = \langle M_i\,\mathbf{x}, \mathbf{y}\rangle \qquad and \qquad (\mathbf{x}, \mathbf{y})_{Y_i} = \langle N_i\,\mathbf{x}, \mathbf{y}\rangle,$$

with symmetric positive definite matrices $M_0, M_1, N_0, N_1 \in \mathbb{R}^{n \times n}$. Then, for $X_\theta = [X_0, X_1]_\theta$ and $Y_\theta = [Y_0, Y_1]_\theta$ with $\theta \in [0, 1]$, we have

$$c_2^{\theta-1}c_3^{-\theta}\|\mathbf{x}\|_{X_\theta} \leq \|\mathcal{A}\,\mathbf{x}\|_{Y_\theta} \leq c_0^{1-\theta}c_1^\theta\|\mathbf{x}\|_{X_\theta}. \tag{5.10}$$

The norms $\| \cdot \|_{X_\theta}$ and $\| \cdot \|_{Y_\theta}$ are the norms associated to the inner products

$$(\mathbf{x}, \mathbf{y})_{X_\theta} = \langle M_\theta \, \mathbf{x}, \mathbf{y} \rangle \quad with \quad M_\theta = [M_0, M_1]_\theta := M_0^{1/2} \left(M_0^{-1/2} M_1 M_0^{-1/2} \right)^\theta M_0^{1/2},$$

$$(\mathbf{x}, \mathbf{y})_{Y_\theta} = \langle N_\theta \, \mathbf{x}, \mathbf{y} \rangle \quad with \quad N_\theta = [N_0, N_1]_\theta := N_0^{1/2} \left(N_0^{-1/2} N_1 N_0^{-1/2} \right)^\theta N_0^{1/2}.$$

Here, the square root of a symmetric and positive definite matrix M is defined by $M = M^{\frac{1}{2}} M^{\frac{1}{2}}$.

Proof. See Adams and Fournier [4]. □

Hence, from interpolating between the block-diagonal preconditioners $\mathcal{P}_0$ and $\mathcal{P}_1$, we can obtain again parameter-independent condition number estimates for all $\theta \in [0,1]$. Indeed, choosing $M_0 = \mathcal{P}_0$, $M_1 = \mathcal{P}_1$, $N_0 = \mathcal{P}_0^{-1}$ and $N_1 = \mathcal{P}_1^{-1}$ in Theorem 5.5, one obtains the family of preconditioners

$$\mathcal{P}_\theta = [\mathcal{P}_0, \mathcal{P}_1]_\theta = \begin{pmatrix} [A, R]_\theta & 0 \\ 0 & [S, C]_\theta \end{pmatrix}. \tag{5.11}$$

Due to Theorems 5.3 and 5.5, we obtain the estimates

$$\underline{c} \, \|\mathbf{x}\|_{\mathcal{P}_\theta} \le \|\mathcal{A} \, \mathbf{x}\|_{\mathcal{P}_\theta^{-1}} \le \overline{c} \, \|\mathbf{x}\|_{\mathcal{P}_\theta},$$

which yield a robust estimate of the condition number

$$\kappa_{\mathcal{P}_\theta}(\mathcal{P}_\theta^{-1}\mathcal{A}) = \|\mathcal{P}_\theta^{-1}\mathcal{A}\|_{\mathcal{P}_\theta} \|(\mathcal{P}_\theta^{-1}\mathcal{A})^{-1}\|_{\mathcal{P}_\theta} \le \frac{\overline{c}}{\underline{c}}, \tag{5.12}$$

with positive constants $\underline{c} = (\sqrt{5} - 1)/2$ and $\overline{c} = (\sqrt{5} + 1)/2$. Indeed, the estimates follow from

$$\|\mathcal{P}_\theta^{-1}\mathcal{A}\|_{\mathcal{P}_\theta} = \sup_{\mathbf{x} \in \mathbb{R}^n} \frac{\|\mathcal{P}_\theta^{-1}\mathcal{A} \, \mathbf{x}\|_{\mathcal{P}_\theta}}{\|\mathbf{x}\|_{\mathcal{P}_\theta}} = \sup_{\mathbf{x} \in \mathbb{R}^n} \frac{\|\mathcal{A} \, \mathbf{x}\|_{\mathcal{P}_\theta^{-1}}}{\|\mathbf{x}\|_{\mathcal{P}_\theta}} \le \overline{c},$$

and by the substitution $(\mathcal{P}_\theta^{-1}\mathcal{A})^{-1}\mathbf{y} = \mathbf{x} \in \mathbb{R}^n$

$$\|(\mathcal{P}_\theta^{-1}\mathcal{A})^{-1}\|_{\mathcal{P}_\theta} = \sup_{\mathbf{x} \in \mathbb{R}^n} \frac{\|\mathcal{P}_\theta^{-1}\mathcal{A} \, \mathbf{x}\|_{\mathcal{P}_\theta}}{\|\mathbf{x}\|_{\mathcal{P}_\theta}} = \sup_{\mathbf{y} \in \mathbb{R}^n} \frac{\|\mathbf{y}\|_{\mathcal{P}_\theta}}{\|\mathcal{P}_\theta^{-1}\mathcal{A} \, \mathbf{y}\|_{\mathcal{P}_\theta}} = \sup_{\mathbf{y} \in \mathbb{R}^n} \frac{\|\mathbf{y}\|_{\mathcal{P}_\theta}}{\|\mathcal{A} \, \mathbf{y}\|_{\mathcal{P}_\theta^{-1}}} \le \frac{1}{\underline{c}}.$$

Up to now, the condition number bound (5.12) is only a result of theoretical importance, since neither it is clear if $\mathcal{P}_\theta$ can be computed in an explicit way, nor if the application of $\mathcal{P}_\theta$ can be realized in a robust and optimal way. It turns out, that in specific regimes, including our applications, the interpolation in (5.11) leads to nice expressions for certain choices of θ. Especially, the choice $\theta = 1/2$ plays an important role in many applications, cf. Subsection 6.1.4 and Subsection 7.1.4. In these cases, $\mathcal{P}_\theta$ can be replaced again by spectral equivalent preconditioners, cf. Subsection 5.2.4.

We mention, that the same approach can also be realized in a general Hilbert space setting. For more details about the construction of preconditioners by interpolation, we refer to the article [164].

5.2.3 Inexact Schur complement preconditioners

Let us consider the saddle point equation

$$\mathcal{A} = \begin{pmatrix} A & B^T \\ B & -C \end{pmatrix}.$$

Furthermore, let us assume that we have a preconditioner P for A, i.e., there exist constants $\underline{c}$ and $\overline{c}$, such that

$$\underline{c} \, \|\mathbf{x}\|_P \le \|A \, \mathbf{x}\|_{P^{-1}} \le \overline{c} \, \|\mathbf{x}\|_P, \quad \forall \mathbf{x} \in \mathbb{R}^m. \tag{5.13}$$

Then candidates for robust preconditioners are the Schur complement preconditioners

$$\mathcal{P}_1 = \begin{pmatrix} P & 0 \\ 0 & C + BP^{-1}B^T \end{pmatrix} \quad \text{and} \quad \mathcal{P}_2 = \begin{pmatrix} P + B^T A^{-1} B & 0 \\ 0 & C \end{pmatrix}.$$

The preconditioners $\mathcal{P}_1$ and $\mathcal{P}_2$ are referred as *inexact Schur complement* preconditioners. In general, the spectral equivalence (5.13) does not imply a spectral equivalence of the form

$$\underline{c}_{IS} \|\mathbf{x}\|_{\mathcal{P}_i} \le \|\mathcal{A}\mathbf{x}\|_{\mathcal{P}_i^{-1}} \le \overline{c}_{IS} \|\mathbf{x}\|_{\mathcal{P}_i}, \quad \forall \mathbf{x} \in \mathbb{R}^n, \ i = 1, 2, \tag{5.14}$$

for the preconditioned saddle point matrix $\mathcal{P}_i^{-1}\mathcal{A}$. Anyhow, in many cases the spectral equivalence (5.14) can be deduced separately. Therefore, beside of the *interpolation method* presented in the previous subsection, the method of *inexact Schur complement preconditioning* also offers another possibility to derive candidates for parameter-robust preconditioners.

5.2.4 Robust and optimal preconditioners

For the construction of preconditioners, it is important, that we are allowed to replace one preconditioner by another spectral equivalent preconditioner. This is precisely the case, that allows to replace computationally costly preconditioners by more effective ones. Of course, changing the preconditioner also effects the bound of the condition number of the new preconditioned systems. Hence the effect of changing preconditioners is topic of this subsection.

Spectral equivalent preconditioners Let us consider, that we have a preconditioner $\mathcal{P} \in \mathbb{R}^{n \times n}$ for the system matrix $\mathcal{A} \in \mathbb{R}^{n \times n}$, that fulfills the following condition number estimate:

$$\kappa_{\mathcal{P}}(\mathcal{P}^{-1}\mathcal{A}) = \|\mathcal{P}^{-1}\mathcal{A}\|_{\mathcal{P}} \|\mathcal{A}^{-1}\mathcal{P}\|_{\mathcal{P}} \le \frac{\overline{c}}{\underline{c}}. \tag{5.15}$$

Let us take another preconditioner $\tilde{\mathcal{P}} \in \mathbb{R}^{n \times n}$, that is spectral equivalent to the preconditioner $\mathcal{P}$, i.e.,

$$\underline{c}\,\mathbf{x}^T \tilde{\mathcal{P}}\mathbf{x} \le \mathbf{x}^T \mathcal{P}\mathbf{x} \le \tilde{c}\,\mathbf{x}^T \tilde{\mathcal{P}}\mathbf{x}, \quad \forall \mathbf{x} \in \mathbb{R}^n, \tag{5.16}$$

with the spectral equivalence constants $\underline{c}$ and $\tilde{c}$. The spectral equivalence inequalities (5.16) together with the condition number estimate (5.15) yield the estimate

$$\kappa_{\tilde{\mathcal{P}}}(\tilde{\mathcal{P}}^{-1}\mathcal{A}) = \|\tilde{\mathcal{P}}^{-1}\mathcal{A}\|_{\tilde{\mathcal{P}}} \|\mathcal{A}^{-1}\tilde{\mathcal{P}}\|_{\tilde{\mathcal{P}}} \le \frac{\overline{c}\,\tilde{c}}{\underline{c}\,\underline{c}} = \kappa_{\mathcal{P}}(\mathcal{P}^{-1}\mathcal{A})\kappa_{\tilde{\mathcal{P}}}(\tilde{\mathcal{P}}^{-1}\mathcal{P}) \tag{5.17}$$

for the condition number of $\tilde{\mathcal{P}}^{-1}\mathcal{A}$ with respect to the $\tilde{\mathcal{P}}$ energy norm. Indeed, on the one hand we have

$$\|\tilde{\mathcal{P}}^{-1}\mathcal{A}\|_{\tilde{\mathcal{P}}}^2 = \sup_{\mathbf{x}\in\mathbb{R}^n} \frac{(\tilde{\mathcal{P}}^{-1}\mathcal{A}\mathbf{x}, \mathcal{A}\mathbf{x})}{(\tilde{\mathcal{P}}\mathbf{x}, \mathbf{x})} \le \tilde{c}^2 \sup_{\mathbf{x}\in\mathbb{R}^n} \frac{(\mathcal{P}^{-1}\mathcal{A}\mathbf{x}, \mathcal{A}\mathbf{x})}{(\mathcal{P}\mathbf{x}, \mathbf{x})} = \tilde{c}^2 \|\mathcal{P}^{-1}\mathcal{A}\|_{\mathcal{P}}^2.$$

On the other hand, using the substitution $\mathbf{x} = \tilde{\mathcal{P}}^{-1}\mathbf{y}$, we get the estimate

$$\|\mathcal{A}^{-1}\tilde{\mathcal{P}}\|_{\tilde{\mathcal{P}}}^2 = \sup_{\mathbf{x}\in\mathbb{R}^n} \frac{(\tilde{\mathcal{P}}\mathcal{A}^{-1}\tilde{\mathcal{P}}\mathbf{x}, \mathcal{A}^{-1}\tilde{\mathcal{P}}\mathbf{x})}{(\tilde{\mathcal{P}}\mathbf{x}, \mathbf{x})} = \sup_{\mathbf{y}\in\mathbb{R}^n} \frac{(\tilde{\mathcal{P}}\mathcal{A}^{-1}\mathbf{y}, \mathcal{A}^{-1}\mathbf{y})}{(\tilde{\mathcal{P}}^{-1}\mathbf{y}, \mathbf{y})} \le \underline{c}^{-2} \|\mathcal{A}^{-1}\mathcal{P}\|_{\mathcal{P}}^2.$$

Hence (5.17) follows.

Spectral equivalent preconditioners in the case of block-diagonal preconditioners   Let us
consider a preconditioner $\mathcal{P}$ of a block-diagonal form, i.e.,

$$
\mathcal{P} = \begin{pmatrix} \mathcal{P}^{(1)} & & \\ & \ddots & \\ & & \mathcal{P}^{(d)} \end{pmatrix},
\tag{5.18}
$$

with $\mathcal{P}^{(i)} \in \mathbb{R}^{n^{(i)} \times n^{(i)}}$, $n^{(1)} + \ldots + n^{(d)} = n$. Suppose, that for the individual blocks $\mathcal{P}^{(i)}, i = 1, \ldots, n$
spectral equivalent matrices $\tilde{\mathcal{P}}^{(i)}$ are available, i.e.,

$$
\underset{\sim}{c}^{(i)} \, \mathbf{x}^T \tilde{\mathcal{P}}^{(i)} \mathbf{x} \le \mathbf{x}^T \mathcal{P}^{(i)} \mathbf{x} \le \tilde{c}^{(i)} \, \mathbf{x}^T \tilde{\mathcal{P}}^{(i)} \mathbf{x}, \quad \forall \, \mathbf{x} \in \mathbb{R}^{n^{(i)}}.
$$

Then for another block-diagonal preconditioner $\tilde{\mathcal{P}}$, given by

$$
\tilde{\mathcal{P}} = \begin{pmatrix} \tilde{\mathcal{P}}^{(1)} & & \\ & \ddots & \\ & & \tilde{\mathcal{P}}^{(d)} \end{pmatrix},
\tag{5.19}
$$

the following spectral equivalence is valid

$$
\left(\min_{i=1,\ldots,d} \underset{\sim}{c}^{(i)} \right) \mathbf{x}^T \tilde{\mathcal{P}} \mathbf{x} \le \mathbf{x}^T \mathcal{P} \mathbf{x} \le \left(\max_{i=1,\ldots,d} \tilde{c}^{(i)} \right) \mathbf{x}^T \tilde{\mathcal{P}} \mathbf{x}, \quad \forall \, \mathbf{x} \in \mathbb{R}^n.
\tag{5.20}
$$

A direct consequence of (5.19) and (5.20) is the condition number estimate

$$
\kappa_{\tilde{\mathcal{P}}}(\tilde{\mathcal{P}}^{-1}\mathcal{A}) = \|\tilde{\mathcal{P}}^{-1}\mathcal{A}\|_{\tilde{\mathcal{P}}} \|\mathcal{A}^{-1}\tilde{\mathcal{P}}\|_{\tilde{\mathcal{P}}} \le \frac{\overline{c} \, \max_{i=1,\ldots,d} \tilde{c}^{(i)}}{\underline{c} \, \min_{i=1,\ldots,d} \underset{\sim}{c}^{(i)}}.
$$

This result teaches us, that the individual blocks $\mathcal{P}^{(i)}$ of the block-diagonal preconditioner $\mathcal{P}$ can be
replaced by spectral equivalent preconditioners $\tilde{\mathcal{P}}^{(i)}$ again. Hence, in order to construct a fully robust
preconditioner for $\mathcal{A}$, the following step-by-step strategy can be pursued:

1. Design a robust block-diagonal preconditioner, e.g., by using the interpolation method presented
   in Subsection 5.2.2 or the method of inexact Schur complement preconditioning presented in
   Subsection 5.2.3.

2. Construct or use already existing robust preconditioners for the individual diagonal blocks.

We mention, that this approach is strongly linked to the method of *operator preconditioning*, see e.g.,
[82], where the common ingredients are the use of mapping properties of the underlying continuous
operators and numerical stability to derive the basic structure of the preconditioners for the finite-
dimensional systems derived from the discretization procedure.

The approach of block-diagonal preconditioning combined with the MinRes method as the Krylov
subspace method of our choice results in Algorithm 2.

Input: $\mathcal{A} \in \mathbb{R}^{n \times n}$, $\mathcal{P} \in \mathbb{R}^{n \times n}$ as given in (5.18), right hand-side $\mathbf{f} \in \mathbb{R}^n$, initial guess
$\quad\quad \mathbf{x}^{(0)} = (\mathbf{x_1}^{(0)}, \dots, \mathbf{x_d}^{(0)}) \in \mathbb{R}^n$.
Output: approximate solution $\mathbf{x}^{(k)} = (\mathbf{x_1}^{(k)}, \dots, \mathbf{x_d}^{(k)}) \in \mathbb{R}^n$.
Set $\mathbf{v}^{(0)} := \mathbf{0}$, $\mathbf{w}^{(0)} := \mathbf{0}$, $\mathbf{w}^{(1)} := \mathbf{0}$;
Set $\mathbf{v}^{(1)} := \mathbf{f} - \mathcal{A}\mathbf{x}^{(0)}$;
for $i = 1$ **to** d **do**
$\quad |\quad$ Solve $\mathcal{P}^{(i)}\mathbf{z_i}^{(1)} = \mathbf{v_i}^{(1)}$;
end
Set $\gamma_1 := \sqrt{\langle \mathbf{z}^{(1)}, \mathbf{v}^{(1)} \rangle}$;
Set $\mathbf{z}^{(1)} := \mathbf{z}^{(1)}/\gamma_1$ and $\mathbf{v}^{(1)} := \mathbf{v}^{(1)}/\gamma_1$;
Set $\eta_0 := \gamma_1$, $s_0 := s_1 := 0$, $c_0 := c_1 := 1$;
Set $k := 1$;
while *not converged* **do**
$\quad$ Set $\delta_k := \langle \mathbf{z}^{(k)}, \mathbf{z}^{(k)} \rangle$;
$\quad$ Set $\mathbf{v}^{(k+1)} := \mathcal{A}\mathbf{z}^{(k)} - \delta_k \mathbf{v}^{(k)} - \gamma_k \mathbf{v}^{(k-1)}$;
$\quad$ **for** $i = 1$ **to** d **do**
$\quad\quad |\quad$ Solve $\mathcal{P}^{(i)}\mathbf{z_i}^{(k+1)} = \mathbf{v_i}^{(k+1)}$;
$\quad$ **end**
$\quad$ Set $\gamma_{k+1} := \sqrt{\langle \mathbf{z}^{(k+1)}, \mathbf{v}^{(k+1)} \rangle}$;
$\quad$ Set $\mathbf{z}^{(k+1)} := \mathbf{z}^{(k+1)}/\gamma_{k+1}$ and $\mathbf{v}^{(k+1)} := \mathbf{v}^{(k+1)}/\gamma_{k+1}$;
$\quad$ Set $\alpha_0 := c_k \delta_k - c_{k-1} s_k \gamma_k$ and $\alpha_1 := \sqrt{\alpha_0^2 + \gamma_{k+1}^2}$;
$\quad$ Set $\alpha_2 := s_k \delta_k + c_{k-1} c_k \gamma_k$ and $\alpha_3 := s_{k-1}\gamma_k$;
$\quad$ Set $c_{k+1} := \alpha_0/\alpha_1$ and $s_{k+1} := \gamma_{k+1}/\alpha_1$;
$\quad$ Set $\mathbf{w}^{(k+1)} := (\mathbf{z}^{(k)} - \alpha_3 \mathbf{w}^{(k-1)} - \alpha_2 \mathbf{w}^{(k)})/\alpha_1$;
$\quad$ Set $\mathbf{x}^{(k)} := \mathbf{x}^{(k-1)} + c_{k+1}\eta_{k-1}\mathbf{w}^{(k+1)}$;
$\quad$ Set $\eta_k := -s_{k+1}\eta_{k-1}$;
$\quad$ Set $k := k + 1$;
end

Algorithm 2: The block-diagonal preconditioned MinRes method.

Chapter 6

Time-periodic eddy current problems

In eddy current computations with some time-periodic excitation of the right hand side, the steady state solution is often sufficient to describe the asymptotic electromagnetic processes after some initial or warm-up phase. One of the most challenging problems in computational electromagnetics is the efficient computation of solutions of time-periodic problems. Due to the periodic structure, an approximation in time in terms of Fourier series pops up naturally.

Therefore, this chapter is devoted to the simulation of linear and time-periodic eddy current problems by the MH-FEM-BEM method. Using the results of Chapter 4, we switch from the time domain to the frequency domain. The resulting frequency domain equations are discretized in terms of a finite element method or in terms of a finite element - boundary element coupling method, i.e., each Fourier coefficient is approximated by a FEM or FEM-BEM coupling method, respectively. Due to the linearity of our model problem, we observe a decoupling with respect to the Fourier modes $k = 0, \ldots, N$. For each mode k, we derive appropriate variational formulations for the frequency domain equations and show well-posedness in some non-standard norms. In order to obtain these non-standard norms, we heavily stress the theory developed in Chapter 5. Therefore, in this chapter, the main emphasize is on deriving candidates for these non-standard norms in a *constructive* fashion. Based on these well-posedness results, we propose block-diagonal preconditioners for the resulting systems of linear equations and provide rigorous condition number estimates for the preconditioned systems, that are uniform in all involved discretization and model parameters.

This chapter is divided into two main parts:

- We start by analyzing the eddy current problem on the bounded domain Ω_1, discretized in terms of the MH-FEM method. For the frequency domain equations, various commonly used variational formulations in primal and mixed forms are derived and discretized in terms of the finite element method. These different variational formulations are important for the analysis of different settings in the subsequent chapters, e.g. Chapter 7.

- In the second part, we extend the results obtained in the first one, by treating the exterior domain with a FEM-BEM coupling method leading to the full MH-FEM-BEM method. Again, we state appropriate variational formulations and analyze them.

The different primal and mixed variational formulations, that are derived for the frequency domain equations of the periodic eddy current problem, rely on already existing primal and mixed variational formulations for magnetostatic problems, see, e.g., [107]. Indeed, parameter-robust block-diagonal preconditioners have already been developed for a full range of variational formulations, see, e.g., the review article [117]. In our setting, the construction of block-diagonal preconditioners is even more involving, since we are dealing with a full range of model (ν, σ) and discretization parameters (h, ω, N), and additionally our systems obtain two-, three-, or four-fold saddle point structures.

Another important issue is, that in view of the charge conservation law, the applied current $\mathbf{u}$ needs

to satisfy the following consistency conditions

$$\operatorname{div} \mathbf{u} = 0 \quad \text{in } \Omega_1, \qquad \mathbf{u} \cdot \mathbf{n} = 0 \quad \text{on } \Gamma, \tag{6.1}$$

cf. Section 1.1. Throughout this work, this condition is claimed in a weak sense, i.e., we assume that the given right hand side $\mathbf{u}(t)$ is weakly divergence-free, i.e., for all t,

$$(\mathbf{u}(t), \nabla p)_{\mathbf{0},\Omega_1} = 0, \quad \forall\, p \in H^1(\Omega_1). \tag{6.2}$$

The chapter is completed by a full space- and time-discretization error analysis and the discussion of the application of the developed preconditioned solvers to nonlinear eddy current problems.

6.1   Symmetric FEM formulations

In this section, we restrict ourselves to the case of the conducting domain Ω_1, i.e., a bounded domain. Therefore, we are dealing with the following system of partial differential equations

$$
\begin{cases}
\sigma \dfrac{\partial \mathbf{y}}{\partial t} + \mathbf{curl}(\nu\, \mathbf{curl}\, \mathbf{y}) = \mathbf{u}, & \text{in } \Omega_1 \times (0, T), \\[4pt]
\operatorname{div}(\sigma \mathbf{y}) = 0, & \text{in } \Omega_1 \times (0, T), \\[4pt]
\mathbf{y}(0) = \mathbf{y}(T), & \text{in } \Omega_1, \\[4pt]
\mathbf{y} \times \mathbf{n} = \mathbf{0}, & \text{on } \Gamma \times (0, T),
\end{cases}
\tag{6.3}
$$

where we have added homogeneous Dirichlet boundary conditions on Γ.

The theory presented in this section is restricted to the case of strictly positive conductivity σ. However, the finite element analysis can also be extended to the case of a bounded domain consisting of both, conducting and non-conducting domains. In these cases, we have $\sigma \geq 0$, and therefore the non-conducting domains have to be treated by a parabolic or an elliptic regularization. In the case of parabolic regularization the conductivity σ is replaced by $\sigma_\varepsilon := \max(\sigma, \varepsilon)$ with some $\varepsilon > 0$. In the case of elliptic regularization, an additional lower order term $\varepsilon \mathbf{y}$ is added to the first equation in (6.3). For both regularization methods, an additional error of order $\mathcal{O}(\varepsilon)$ is introduced, cf. [136, 160].

6.1.1   Multiharmonic discretization

Following Chapter 4, we assume that the time-periodic right hand side $\mathbf{u}$ is given by a multiharmonic excitation in terms of a truncated Fourier series, i.e.,

$$\mathbf{u}(\mathbf{x}, t) = \sum_{k=0}^{N} \mathbf{u}_{\mathbf{k}}^{\mathbf{c}}(\mathbf{x}) \cos(k\omega t) + \mathbf{u}_{\mathbf{k}}^{\mathbf{s}}(\mathbf{x}) \sin(k\omega t). \tag{6.4}$$

The divergence constraint imposed on $\mathbf{u}$, cf. (6.2), is also valid in the frequency domain, i.e., for all modes $k = 0, \ldots, N$ and for $j \in \{c, s\}$. Indeed, we have

$$0 = (\mathbf{u}(t), \nabla p)_{\mathbf{0},\Omega_1} = \sum_{k=0}^{N} (\mathbf{u}_{\mathbf{k}}^{\mathbf{c}}, \nabla p)_{\mathbf{0},\Omega_1} \cos(k\omega t) + (\mathbf{u}_{\mathbf{k}}^{\mathbf{s}}, \nabla p)_{\mathbf{0},\Omega_1} \sin(k\omega t), \quad \forall t \in (0, T).$$

Due to the linear independence of the sine and cosine functions, we immediately obtain, that the amplitudes $\mathbf{u}_{\mathbf{k}}^{\mathbf{j}}$ are weakly divergence-free as well, i.e.,

$$(\mathbf{u}_{\mathbf{k}}^{\mathbf{j}}, \nabla p)_{\mathbf{0},\Omega_1} = 0, \quad \forall\, p \in H_0^1(\Omega_1), k = 0, \ldots, N, j \in \{c, s\}. \tag{6.5}$$

Consequently, we have, that the time-periodic solution $\mathbf{y}$, can also be expressed in terms of the same frequency ω and the amplitudes $\mathbf{y}_{\mathbf{k}}^{\mathbf{c}}$ and $\mathbf{y}_{\mathbf{k}}^{\mathbf{s}}$, i.e.,

$$\mathbf{y}(\mathbf{x}, t) = \sum_{k=0}^{N} \mathbf{y}_{\mathbf{k}}^{\mathbf{c}}(\mathbf{x}) \cos(k\omega t) + \mathbf{y}_{\mathbf{k}}^{\mathbf{s}}(\mathbf{x}) \sin(k\omega t). \tag{6.6}$$

Furthermore, analogous to (6.5), $\text{div}(\sigma \mathbf{y}) = 0$ is also imposed in the frequency domain. Using the multiharmonic representation of the solution (6.6), we can rewrite the eddy current problem (6.3) in the frequency domain as follows:

$$\text{For } k = 1, \ldots, N, \text{ find } (\mathbf{y_k^c}, \mathbf{y_k^s}): \begin{cases} k\omega\sigma \, \mathbf{y_k^s} + \mathbf{curl}(\nu \, \mathbf{curl} \, \mathbf{y_k^c}) = \mathbf{u_k^c}, & \text{in } \Omega_1, \\ -k\omega\sigma \, \mathbf{y_k^c} + \mathbf{curl}(\nu \, \mathbf{curl} \, \mathbf{y_k^s}) = \mathbf{u_k^s}, & \text{in } \Omega_1, \\ k\omega \, \text{div}(\sigma \mathbf{y_k^c}) = 0, & \text{in } \Omega_1, \\ k\omega \, \text{div}(\sigma \mathbf{y_k^s}) = 0, & \text{in } \Omega_1, \\ \mathbf{y_k^c} \times \mathbf{n} = \mathbf{0}, & \text{on } \partial\Omega_1, \\ \mathbf{y_k^s} \times \mathbf{n} = \mathbf{0}, & \text{on } \partial\Omega_1, \end{cases} \tag{6.7}$$

where we have multiplied the gauging equations $\text{div}(\sigma \mathbf{y_k^j}) = 0$, $j \in \{c, s\}$, by the base frequency $k\omega$. A first observation clarifies, that the divergence constraint on $\mathbf{y_k^j}$ is redundant in certain settings. Applying the divergence operator to the first two equations in (6.7) yields

$$k\omega \, \text{div}(\sigma \mathbf{y_k^s}) = \text{div} \, \mathbf{u_k^c} \quad \text{and} \quad -k\omega \, \text{div}(\sigma \mathbf{y_k^c}) = \text{div} \, \mathbf{u_k^s}.$$

Therefore, the demand on the right hand side $\mathbf{u}$ to be divergence-free is sufficient to guarantee that the solution $\mathbf{y}$ is divergence-free as well. Of course, the application of the div operator has to be thought in the *weak sense*. This property is exploited in certain variational formulations to drop the divergence constraints on the amplitudes of $\mathbf{y}$. Indeed this approach leads to a reduction of degrees of freedom. Nevertheless in many applications it is essential to keep the divergence constraint. Furthermore, for the mode $k = 0$, we are dealing with the following problem.

$$\text{Find } \mathbf{y_0^c}: \begin{cases} \mathbf{curl}(\nu \, \mathbf{curl} \, \mathbf{y_0^c}) = \mathbf{u_0^c}, & \text{in } \Omega_1, \\ \text{div}(\sigma \mathbf{y_0^c}) = 0, & \text{in } \Omega_1, \\ \mathbf{y_0^c} \times \mathbf{n} = \mathbf{0}, & \text{on } \partial\Omega_1. \end{cases} \tag{6.8}$$

In Subsection 3.1.1 we have seen, that the solution of the time-periodic eddy current problem is only unique up to gradient functions, that are *constant* in time. Indeed, this property is recovered by the multiharmonic discretization technique. While for the modes $k = 1, \ldots, N$, that represent the *non-constant* parts of the solution, the divergence constraint is not needed, for the mode $k = 0$, the divergence constraint is essential to recover the non-unique contribution $\mathbf{y_0^c}$ to the solution $\mathbf{y}$.

These systems of partial differential equations are the starting point for the derivation of variational formulations and the discretization in space by means of the finite element method.

Since the part corresponding to the time derivative vanishes for the case $k = 0$, this one is fundamentally different to the cases $k = 1, \ldots N$. Therefore, the analysis of this case has to be done in a separate fashion.

6.1.2 Symmetric variational formulation for FEM

In this subsection, we present different variational formulations for the frequency domain equations (6.7). We investigate both, primal and mixed variational formulations, wherein the Coulomb gauging condition is incorporated implicitly or explicitly, respectively. All the presented formulations are equivalent in the sense, that they obtain the same unique solution for the amplitudes $\mathbf{y_k^c}$ and $\mathbf{y_k^s}$. Since, for all modes $k = 1, \ldots, N$ the systems (6.7) have the same structure, we concentrate on the time-harmonic case, i.e., $k = 1$. The analysis for the remaining modes can be deduced by formally setting $\omega = k\omega$.

Furthermore, we also derive variational formulations for (6.8). The main important difference is, that in this case the Coulomb gauging condition has to be incorporated explicitly in all settings.

6.1.2.1 Symmetric formulations ($k = 1$)

We start by deriving the variational formulations for (6.7).

Formulation FEM 1 If we assume, that the source $\mathbf{u}$ is weakly divergence-free, cf. (6.5), we observe that the gauging condition $\mathrm{div}(\sigma\mathbf{y}^{\mathbf{j}}) = 0$, for $j \in \{c, s\}$ in (6.7) is fulfilled naturally. Therefore, it is not necessary to incorporated the gauging condition into the system (6.7) explicitly. Consequently, the corresponding variational problem can be stated as follows.

Problem 6.1 (Primal formulation). *Find* $(\mathbf{y^s}, \mathbf{y^c}) \in \mathbf{H_0}(\mathbf{curl}, \Omega_1)^2$, *such that*

$$\mathcal{A}_{F1}\left((\mathbf{y^s}, \mathbf{y^c}), (\mathbf{v^c}, \mathbf{v^s})\right) = \int_{\Omega_1} \left[\mathbf{u^c} \cdot \mathbf{v^c} + \mathbf{u^s} \cdot \mathbf{v^s}\right] \mathrm{d}\mathbf{x}, \tag{6.9}$$

for all test functions $(\mathbf{v^c}, \mathbf{v^s}) \in \mathbf{H_0}(\mathbf{curl}, \Omega_1)^2$. *Here the symmetric and indefinite bilinear form* $\mathcal{A}_{F1}$ *is given by*

$$\begin{aligned}
\mathcal{A}_{F1}\left((\mathbf{y^s}, \mathbf{y^c}), (\mathbf{v^c}, \mathbf{v^s})\right) :={}& (\nu\,\mathbf{curl}\,\mathbf{y^c}, \mathbf{curl}\,\mathbf{v^c})_{\mathbf{0},\Omega_1} + \omega(\sigma\mathbf{y^s}, \mathbf{v^c})_{\mathbf{0},\Omega_1} \\
& - \omega(\sigma\mathbf{y^c}, \mathbf{v^s})_{\mathbf{0},\Omega_1} + (\nu\,\mathbf{curl}\,\mathbf{y^s}, \mathbf{curl}\,\mathbf{v^s})_{\mathbf{0},\Omega_1}.
\end{aligned} \tag{6.10}$$

Problem 6.1 has a unique solution $(\mathbf{y^s}, \mathbf{y^c}) \in \mathbf{H_0}(\mathbf{curl}, \Omega_1)^2$, cf. Lemma 6.10. Additionally, for a weakly divergence-free source $\mathbf{u}$, cf. (6.5), the solution $(\mathbf{y^s}, \mathbf{y^c}) \in \mathbf{H_0}(\mathbf{curl}, \Omega_1)^2$ is weakly divergence-free as well, i.e., for $j \in \{c, s\}$ we have

$$(\sigma\mathbf{y^j}, \nabla p)_{\mathbf{0},\Omega_1} = 0, \quad \forall\, p \in H_0^1(\Omega_1). \tag{6.11}$$

Formulation FEM 2 Problem 6.2 is nothing than a rescaled version of Problem 6.1.

Problem 6.2 (Primal formulation). *Find* $(\mathbf{y^c}, \mathbf{y^s}) \in \mathbf{H_0}(\mathbf{curl}, \Omega_1)^2$, *such that*

$$\mathcal{A}_{F2}\left((\mathbf{y^c}, \mathbf{y^s}), (\mathbf{v^c}, \mathbf{v^s})\right) = \int_{\Omega_1} \left[\mathbf{u^c} \cdot \mathbf{v^c} - \mathbf{u^s} \cdot \mathbf{v^s}\right] \mathrm{d}\mathbf{x}, \tag{6.12}$$

for all test functions $(\mathbf{v^c}, \mathbf{v^s}) \in \mathbf{H_0}(\mathbf{curl}, \Omega_1)^2$. *Here the symmetric and indefinite bilinear form* $\mathcal{A}_{F2}$ *is given by*

$$\begin{aligned}
\mathcal{A}_{F2}\left((\mathbf{y^c}, \mathbf{y^s}), (\mathbf{v^c}, \mathbf{v^s})\right) :={}& (\nu\,\mathbf{curl}\,\mathbf{y^c}, \mathbf{curl}\,\mathbf{v^c})_{\mathbf{0},\Omega_1} + \omega(\sigma\mathbf{y^s}, \mathbf{v^c})_{\mathbf{0},\Omega_1} \\
& + \omega(\sigma\mathbf{y^c}, \mathbf{v^s})_{\mathbf{0},\Omega_1} - (\nu\,\mathbf{curl}\,\mathbf{y^s}, \mathbf{curl}\,\mathbf{v^s})_{\mathbf{0},\Omega_1}.
\end{aligned} \tag{6.13}$$

Problem 6.2 has a unique solution $(\mathbf{y^c}, \mathbf{y^s}) \in \mathbf{H_0}(\mathbf{curl}, \Omega_1)^2$, cf. Lemma 6.11. Additionally, for a weakly divergence-free source $\mathbf{u}$, cf. (6.5), the solution $(\mathbf{y^c}, \mathbf{y^s}) \in \mathbf{H_0}(\mathbf{curl}, \Omega_1)^2$ is weakly divergence-free as well, cf. (6.11).

Formulation FEM 3 In many cases it is very convenient to incorporate the gauging conditions $\mathrm{div}(\sigma\mathbf{y^j}) = 0$ $(j \in \{c, s\})$ in a mixed variational framework. Consequently, the corresponding variational problem can be stated as follows.

Problem 6.3 (Mixed formulation). *Find* $(\mathbf{y^c}, \mathbf{y^s}, p^c, p^s) \in \mathbf{H_0}(\mathbf{curl}, \Omega_1)^2 \times H_0^1(\Omega_1)^2$, *such that*

$$\mathcal{A}_{M1}\left((\mathbf{y^c}, \mathbf{y^s}, p^c, p^s), (\mathbf{v^c}, \mathbf{v^s}, q^c, q^s)\right) = \int_{\Omega_1} \left[\mathbf{u^c} \cdot \mathbf{v^c} - \mathbf{u^s} \cdot \mathbf{v^s}\right] \mathrm{d}\mathbf{x}, \tag{6.14}$$

for all test functions $(\mathbf{v^c}, \mathbf{v^s}, q^c, q^s) \in \mathbf{H_0}(\mathbf{curl}, \Omega_1)^2 \times H_0^1(\Omega_1)^2$. *Here the symmetric and indefinite bilinear form* $\mathcal{A}_{M1}$ *is given by*

$$\begin{aligned}
\mathcal{A}_{M1}&\left((\mathbf{y^c}, \mathbf{y^s}, p^c, p^s), (\mathbf{v^c}, \mathbf{v^s}, q^c, q^s)\right) := \\
&(\nu\,\mathbf{curl}\,\mathbf{y^c}, \mathbf{curl}\,\mathbf{v^c})_{\mathbf{0},\Omega_1} + \omega(\sigma\mathbf{y^s}, \mathbf{v^c})_{\mathbf{0},\Omega_1} + \omega(\sigma\mathbf{v^c}, \nabla p^c)_{\mathbf{0},\Omega_1} - \omega(\sigma\mathbf{v^s}, \nabla p^s)_{\mathbf{0},\Omega_1} \\
&- (\nu\,\mathbf{curl}\,\mathbf{y^s}, \mathbf{curl}\,\mathbf{v^s})_{\mathbf{0},\Omega_1} + \omega(\sigma\mathbf{y^c}, \mathbf{v^s})_{\mathbf{0},\Omega_1} + \omega(\sigma\mathbf{y^c}, \nabla q^c)_{\mathbf{0},\Omega_1} - \omega(\sigma\mathbf{y^s}, \nabla q^s)_{\mathbf{0},\Omega_1}.
\end{aligned} \tag{6.15}$$

Problem 6.3 has a unique solution $(\mathbf{y^c}, \mathbf{y^s}, p^c, p^s)$, cf. Lemma 6.12. Additionally, for a weakly divergence-free source $\mathbf{u}$, cf. (6.5), the solution $(\mathbf{y^s}, \mathbf{y^c}) \in \mathbf{H_0}(\mathbf{curl}, \Omega_1)^2$ is weakly divergence-free as well, cf. (6.11), and the Lagrange parameters p^c and p^s vanish at the solution, i.e., $p^c = 0$ and $p^s = 0$. Indeed, for the choice of the test functions $(\mathbf{v^c}, \mathbf{v^s}, q^c, q^s) = (\nabla g, \mathbf{0}, 0, g)$, with $g \in H_0^1(\Omega_1)$, equation (6.14) obtains the form: Find $p_c \in H_0^1(\Omega_1)$, such that

$$\omega(\sigma \nabla g, \nabla p^c)_0 = \int_{\Omega_1} \mathbf{f^c} \cdot \nabla g \, \mathrm{d}\mathbf{x} = 0, \quad \forall g \in H_0^1(\Omega_1).$$

Therefore, we can conclude, that $p^c = 0$. In the same manner, using the special choice $(\mathbf{v^c}, \mathbf{v^s}, q^c, q^s) = (\mathbf{0}, -\nabla g, g, 0)$, the same result can be deduced for p^s.

Formulation FEM 4 Since at the solution $(\mathbf{y^c}, \mathbf{y^s}, p^c, p^s)$ of Problem 6.3 the Lagrange parameters vanish, i.e., $p^c = 0$ and $p^s = 0$, we can add a suitable symmetric bilinear form to $\mathcal{A}_{M1}(\cdot, \cdot)$. Indeed, we choose

$$c((p^c, p^s), (q^c, q^s)) := -\omega(\sigma \nabla p^c, \nabla q^c)_{\mathbf{0},\Omega_1} + \omega(\sigma \nabla p^s, \nabla q^s)_{\mathbf{0},\Omega_1}. \tag{6.16}$$

Later on, we will see, that this choice is justified by the properties of the underlying Hilbert spaces.

Problem 6.4 (Mixed formulation with exact modification). *Find* $(\mathbf{y^c}, \mathbf{y^s}, p^c, p^s) \in \mathbf{H_0}(\mathbf{curl}, \Omega_1)^2 \times H_0^1(\Omega_1)^2$, *such that*

$$\mathcal{A}_{M2}\left((\mathbf{y^c}, \mathbf{y^s}, p^c, p^s), (\mathbf{v^c}, \mathbf{v^s}, q^c, q^s)\right) = \int_{\Omega_1} \left[\mathbf{u^c} \cdot \mathbf{v^c} - \mathbf{u^s} \cdot \mathbf{v^s}\right] \mathrm{d}\mathbf{x}, \tag{6.17}$$

for all test functions $(\mathbf{v^c}, \mathbf{v^s}, q^c, q^s) \in \mathbf{H_0}(\mathbf{curl}, \Omega_1)^2 \times H_0^1(\Omega_1)^2$. *Here the symmetric and indefinite bilinear form* $\mathcal{A}_{M2}$ *is given by*

$$\begin{aligned} \mathcal{A}_{M2}((\mathbf{y^c}, \mathbf{y^s}, p^c, p^s), (\mathbf{v^c}, \mathbf{v^s}, q^c, q^s)) &:= \mathcal{A}_{M1}((\mathbf{y^c}, \mathbf{y^s}, p^c, p^s), (\mathbf{v^c}, \mathbf{v^s}, q^c, q^s)) \\ &\quad - \omega(\sigma \nabla p^c, \nabla q^c)_{\mathbf{0},\Omega_1} + \omega(\sigma \nabla p^s, \nabla q^s)_{\mathbf{0},\Omega_1}. \end{aligned} \tag{6.18}$$

Problem 6.4 has a unique solution $(\mathbf{y^c}, \mathbf{y^s}, p^c, p^s)$, cf. Lemma 6.13. Additionally, the solution of Problem 6.4 also solves Problem 6.3, and vice versa.

Formulation FEM 5 Finally, we give a primal version of Problem 6.4, which is heavily based on the Helmholtz decomposition..

Problem 6.5 (Primal formulation with exact modification). *Find* $(\mathbf{y^c}, \mathbf{y^s}) \in \mathbf{H_0}(\mathbf{curl}, \Omega_1)^2$, *such that*

$$\mathcal{A}_{F3}\left((\mathbf{y^c}, \mathbf{y^s}), (\mathbf{v^c}, \mathbf{v^s})\right) = \int_{\Omega_1} \left[\mathbf{u^c} \cdot \mathbf{v^c} - \mathbf{u^s} \cdot \mathbf{v^s}\right] \mathrm{d}\mathbf{x}, \tag{6.19}$$

for all test functions $(\mathbf{v^c}, \mathbf{v^s}) \in \mathbf{H_0}(\mathbf{curl}, \Omega_1)^2$. *Here the symmetric and indefinite bilinear form* $\mathcal{A}_{F3}$ *is given by*

$$\begin{aligned} \mathcal{A}_{F3}\left((\mathbf{y^c}, \mathbf{y^s}), (\mathbf{v^c}, \mathbf{v^s})\right) &:= \\ (\nu \, \mathbf{curl}\, \mathbf{y^c}, \mathbf{curl}\, \mathbf{v^c})_{\mathbf{0},\Omega_1} &+ \omega(\sigma \nabla P_\sigma(\mathbf{y^c}), \nabla P_\sigma(\mathbf{v^c}))_{\mathbf{0},\Omega_1} + \omega(\sigma \mathbf{y^s}, \mathbf{v^c})_{\mathbf{0},\Omega_1} \\ -(\nu \, \mathbf{curl}\, \mathbf{y^s}, \mathbf{curl}\, \mathbf{v^s})_{\mathbf{0},\Omega_1} &- \omega(\sigma \nabla P_\sigma(\mathbf{y^s}), \nabla P_\sigma(\mathbf{v^s}))_{\mathbf{0},\Omega_1} + \omega(\sigma \mathbf{y^c}, \mathbf{v^s})_{\mathbf{0},\Omega_1}. \end{aligned} \tag{6.20}$$

Therein we use the weighted Helmholtz projection $P_\sigma : \mathbf{H_0}(\mathbf{curl}, \Omega_1) \to H_0^1(\Omega_1)$, where for given $\mathbf{y} \in \mathbf{H_0}(\mathbf{curl}, \Omega_1)$, $p := P_\sigma(\mathbf{y}) \in H_0^1(\Omega_1)$ is the unique solution of the variational problem. Find $p \in H_0^1(\Omega_1)$, such that

$$\int_{\Omega_1} \sigma \nabla p \cdot \nabla q \, \mathrm{d}\mathbf{x} = \int_{\Omega_1} \sigma \mathbf{y} \cdot \nabla q \, \mathrm{d}\mathbf{x}, \quad \forall q \in H_0^1(\Omega_1). \tag{6.21}$$

Indeed, P_σ projects on the divergence-free part of the Helmholtz decomposition, cf. Lemma 2.6. Furthermore, the operator P_σ is linear and bounded, i.e.,

$$\|\sqrt{\sigma}\nabla P_\sigma(\mathbf{y})\|_{\mathbf{0},\Omega_1} \leq \|\sqrt{\sigma}\mathbf{y}\|_{\mathbf{0},\Omega_1}. \tag{6.22}$$

The additional expression is chosen in such a way, that it does not vanish on the kernel of the **curl** operator, and on the other hand $P_\sigma(\mathbf{y^c})$ and $P_\sigma(\mathbf{y^s})$ vanish at the solution, i.e., $P_\sigma(\mathbf{y^c}) = 0$ and $P_\sigma(\mathbf{y^s}) = 0$. Problem 6.5 has a unique solution $(\mathbf{y^c}, \mathbf{y^s})$, cf. Lemma 6.14.

Furthermore, Problem 6.5 is nothing else than an equivalent primal formulation of Problem 6.4. Indeed, from Problem 6.5, we obtain for $j \in \{c, s\}$ by setting the test functions equal to zero, i.e., $\mathbf{v^j} = \mathbf{0}$:

$$\omega(\sigma\nabla p^j, \nabla q^j)_{\mathbf{0},\Omega_1} = \omega(\sigma\mathbf{y^j}, \nabla q^j)_{\mathbf{0},\Omega_1}, \quad \forall q^j \in H_0^1(\Omega_1),$$

and therefore by (6.21) $p^j = P(\mathbf{y^j})$. Furthermore, for $q^j = 0$, we obtain

$$\begin{aligned}
\mathcal{B}_{M2}((\mathbf{y^c},\mathbf{y^s},p^c,p^s),(\mathbf{v^c},\mathbf{v^s},0,0)) &= \mathcal{A}_{F2}\left((\mathbf{y^c},\mathbf{y^s}),(\mathbf{v^c},\mathbf{v^s})\right) + \omega(\sigma\mathbf{v^c},\nabla p^c)_{\mathbf{0},\Omega_1} - \omega(\sigma\mathbf{v^s},\nabla p^s)_{\mathbf{0},\Omega_1} \\
&= \mathcal{A}_{F2}\left((\mathbf{y^c},\mathbf{y^s}),(\mathbf{v^c},\mathbf{v^s})\right) + \omega(\sigma\nabla P_\sigma(\mathbf{v^c}),\nabla p^c)_{\mathbf{0},\Omega_1} - \omega(\sigma\nabla P_\sigma(\mathbf{v^s}),\nabla p^s)_{\mathbf{0},\Omega_1} \\
&= \mathcal{A}_{F2}\left((\mathbf{y^c},\mathbf{y^s}),(\mathbf{v^c},\mathbf{v^s})\right) + \omega(\sigma\nabla P_\sigma(\mathbf{v^c}),\nabla P_\sigma(\mathbf{y^c}))_{\mathbf{0},\Omega_1} - \omega(\sigma\nabla P_\sigma(\mathbf{v^s}),\nabla P_\sigma(\mathbf{y^s}))_{\mathbf{0},\Omega_1} \\
&= \mathcal{A}_{F3}\left((\mathbf{y^c},\mathbf{y^s}),(\mathbf{v^c},\mathbf{v^s})\right).
\end{aligned}$$

The first part $(\mathbf{y^c}, \mathbf{y^s})$ of the solution $(\mathbf{y^c}, \mathbf{y^s}, p^c, p^s)$ of Problem 6.4 solves Problem 6.5, and vice versa. The relation $p^j = P_\sigma(\mathbf{y^j}) = 0$ is nothing else than the weakly divergence-free property of the solution $(\mathbf{y^c}, \mathbf{y^s})$, cf. (6.11).

Formulation FEM 6   In some applications (cf. [100]), it is convenient to work with a scaled version of Problem 6.1. Hence, we introduce the scaled functions $\tilde{\mathbf{y}}^{\mathbf{c}} := (\omega\underline{\sigma})^{-1}\mathbf{y^c}$ and $\tilde{\mathbf{v}}^{\mathbf{c}} := \omega\underline{\sigma}\mathbf{y^c}$.

Problem 6.6 (Scaled primal formulation). *Find $(\mathbf{y^s}, \tilde{\mathbf{y}}^{\mathbf{c}}) \in \mathbf{H_0}(\mathbf{curl}, \Omega_1)^2$, such that*

$$\mathcal{A}_{F4}\left((\mathbf{y^s}, \tilde{\mathbf{y}}^{\mathbf{c}}), (\tilde{\mathbf{v}}^{\mathbf{c}}, \mathbf{v^s})\right) = \int_{\Omega_1} \left[(\omega\underline{\sigma})^{-1}\mathbf{u^c}\cdot\tilde{\mathbf{v}}^{\mathbf{c}} + \mathbf{u^s}\cdot\mathbf{v^s}\right]\mathrm{d}\mathbf{x}, \tag{6.23}$$

for all test functions $(\tilde{\mathbf{v}}^{\mathbf{c}}, \mathbf{v^s}) \in \mathbf{H_0}(\mathbf{curl}, \Omega_1)^2$. Here the symmetric and indefinite bilinear form $\mathcal{A}_{F4}$ is given by

$$\begin{aligned}
\mathcal{A}_{F4}\left((\mathbf{y^s}, \tilde{\mathbf{y}}^{\mathbf{c}}), (\tilde{\mathbf{v}}^{\mathbf{c}}, \mathbf{v^s})\right) := &\ (\nu\,\mathbf{curl}\,\tilde{\mathbf{y}}^{\mathbf{c}}, \mathbf{curl}\,\tilde{\mathbf{v}}^{\mathbf{c}})_{\mathbf{0},\Omega_1} + \underline{\sigma}^{-1}(\sigma\mathbf{y^s}, \tilde{\mathbf{v}}^{\mathbf{c}})_{\mathbf{0},\Omega_1} \\
&- (\omega^2\underline{\sigma})^2\underline{\sigma}^{-1}(\sigma\tilde{\mathbf{y}}^{\mathbf{c}}, \mathbf{v^s})_{\mathbf{0},\Omega_1} + (\nu\,\mathbf{curl}\,\mathbf{y^s}, \mathbf{curl}\,\mathbf{v^s})_{\mathbf{0},\Omega_1}.
\end{aligned} \tag{6.24}$$

Problem 6.6 has a unique solution $(\mathbf{y^s}, \tilde{\mathbf{y}}^{\mathbf{c}}) \in \mathbf{H_0}(\mathbf{curl}, \Omega_1)^2$, cf. Lemma 6.15. Additionally, for a weakly divergence-free source $\mathbf{u}$, cf. (6.5), the solution $(\mathbf{y^s}, \tilde{\mathbf{y}}^{\mathbf{c}}) \in \mathbf{H_0}(\mathbf{curl}, \Omega_1)^2$ is weakly divergence-free as well.

All the six presented variational formulations are equivalent in the sense, that they obtain the same unique solution for the amplitudes $\mathbf{y^c}$ and $\mathbf{y^s}$.

6.1.2.2   Symmetric formulations $(k = 0)$

We continue by deriving variational formulations for (6.8). As we have seen at the beginning of this chapter, it is essential, to incorporate the gauging conditions $\operatorname{div}(\sigma\mathbf{y_0^c}) = 0$ in order to recover the uniqueness of the solution corresponding to the mode $k = 0$. Due to the absence of a lower order term, the variational formulations for the mode $k = 0$ are heavily related to the variational formulations for the magneto static case, cf. [107].

Formulation FEM 3 $(k = 0)$ In this setting, the gauging condition is incorporated in a mixed variational framework.

Problem 6.7 (Mixed formulation). *Find* $(\mathbf{y_0^c}, p_0^c) \in \mathbf{H_0}(\mathbf{curl}, \Omega_1) \times H_0^1(\Omega_1)$, *such that*

$$\mathcal{A}_{M1,0}\left((\mathbf{y_0^c}, p_0^c), (\mathbf{v^c}, q^c)\right) = \int_{\Omega_1} \mathbf{u_0^c} \cdot \mathbf{v^c} \mathrm{d}\mathbf{x}, \tag{6.25}$$

for all test functions $(\mathbf{v^c}, q^c) \in \mathbf{H_0}(\mathbf{curl}, \Omega_1) \times H_0^1(\Omega_1)$. *Here the symmetric and indefinite bilinear form* $\mathcal{A}_{M1,0}$ *is given by*

$$\mathcal{A}_{M1,0}\left((\mathbf{y_0^c}, p_0^c), (\mathbf{v^c}, q^c)\right) := (\nu \, \mathbf{curl}\, \mathbf{y_0^c}, \mathbf{curl}\, \mathbf{v^c})_{\mathbf{0},\Omega_1} + (\sigma \mathbf{v^c}, \nabla p_0^c)_{\mathbf{0},\Omega_1} + (\sigma \mathbf{y_0^c}, \nabla q^c)_{\mathbf{0},\Omega_1}. \tag{6.26}$$

Problem 6.7 has a unique solution $(\mathbf{y_0^c}, p_0^c)$, cf. Lemma 6.17. Additionally, for a weakly divergence-free source $\mathbf{u}$, cf. (6.5), the solution $\mathbf{y_0^c} \in \mathbf{H_0}(\mathbf{curl}, \Omega_1)$ is weakly divergence-free as well, cf. (6.11), and the Lagrange parameter p_0^c vanishes at the solution, i.e., $p_0^c = 0$.

Formulation FEM 4 $(k = 0)$ Since at the solution $(\mathbf{y_0^c}, p_0^c)$ of Problem 6.7 the Lagrange parameter vanishes, i.e., $p_0^c = 0$, we can add a suitable symmetric bilinear form to $\mathcal{A}_{M1,0}(\cdot, \cdot)$. Indeed, we choose

$$c(p_0^c, q^c) := -(\sigma \nabla p_0^c, \nabla q^c)_{\mathbf{0},\Omega_1}. \tag{6.27}$$

Problem 6.8 (Mixed formulation with exact modification). *Find* $(\mathbf{y_0^c}, p_0^c) \in \mathbf{H_0}(\mathbf{curl}, \Omega_1)^2 \times H_0^1(\Omega_1)^2$, *such that*

$$\mathcal{A}_{M2,0}\left((\mathbf{y_0^c}, p_0^c), (\mathbf{v^c}, q^c)\right) = \int_{\Omega_1} \mathbf{u_0^c} \cdot \mathbf{v^c} \mathrm{d}\mathbf{x}, \tag{6.28}$$

for all test functions $(\mathbf{v^c}, q^c) \in \mathbf{H_0}(\mathbf{curl}, \Omega_1) \times H_0^1(\Omega_1)$. *Here the symmetric and indefinite bilinear form* $\mathcal{A}_{M2,0}$ *is given by*

$$\begin{aligned}
\mathcal{A}_{M2}((\mathbf{y_0^c}, p_0^c), (\mathbf{v^c}, q^c)) := {}&(\nu \, \mathbf{curl}\, \mathbf{y_0^c}, \mathbf{curl}\, \mathbf{v_0^c})_{\mathbf{0},\Omega_1} + (\sigma \mathbf{v^c}, \nabla p_0^c)_{\mathbf{0},\Omega_1} \\
&+ (\sigma \mathbf{y_0^c}, \nabla q^c)_{\mathbf{0},\Omega_1} - (\sigma \nabla p_0^c, \nabla q^c)_{\mathbf{0},\Omega_1}.
\end{aligned} \tag{6.29}$$

Problem 6.8 has a unique solution $(\mathbf{y_0^c}, p_0^c)$, cf. Lemma 6.16. Additionally, the solution of Problem 6.8 also solves Problem 6.7, and vice versa.

Formulation FEM 5 $(k = 0)$ Finally, we give a primal version of Problem 6.8.

Problem 6.9 (Primal formulation with exact modification). *Find* $\mathbf{y_0^c} \in \mathbf{H_0}(\mathbf{curl}, \Omega_1)$, *such that*

$$\mathcal{A}_{F3,0}\left(\mathbf{y_0^c}, \mathbf{v^c}\right) = \int_{\Omega_1} \mathbf{u_0^c} \cdot \mathbf{v^c} \mathrm{d}\mathbf{x}, \tag{6.30}$$

for all test functions $\mathbf{v_0^c} \in \mathbf{H_0}(\mathbf{curl}, \Omega_1)$. *Here the symmetric and positive definite bilinear form* $\mathcal{A}_{F3,0}$ *is given by*

$$\mathcal{A}_{F3,0}\left(\mathbf{y_0^c}, \mathbf{v^c}\right) := (\nu \, \mathbf{curl}\, \mathbf{y_0^c}, \mathbf{curl}\, \mathbf{v^c})_{\mathbf{0},\Omega_1} + (\sigma \nabla P_\sigma(\mathbf{y_0^c}), \nabla P_\sigma(\mathbf{v^c}))_{\mathbf{0},\Omega_1}. \tag{6.31}$$

Problem 6.9 has a unique solution $\mathbf{y_0^c}$. Furthermore, Problem 6.9 is nothing else than an equivalent primal formulation of Problem 6.8.

All the three presented variational formulations are equivalent in the sense, that they obtain the same unique solution for the amplitude $\mathbf{y_0^c}$.

6.1.3   Discretization

The variational forms $\mathcal{A}_{F1}$, $\mathcal{A}_{F2}$, $\mathcal{A}_{M1}$, $\mathcal{A}_{M2}$, $\mathcal{A}_{F3}$, $\mathcal{A}_{F4}$, $\mathcal{A}_{M1,0}$, $\mathcal{A}_{M2,0}$ and $\mathcal{A}_{F3,0}$ are the starting points of a discretization in space. Therefore, we use a regular triangulation $\mathcal{T}_h$, with mesh size $h > 0$, of the computational domain Ω_1 with tetrahedral elements.

On this mesh we consider Nédélec basis functions of lowest order $\mathcal{ND}_0^0(\mathcal{T}_h)$, a conforming finite element subspace of $\mathbf{H_0}(\mathbf{curl}, \Omega_1)$, and $\mathcal{S}_0^1(\mathcal{T}_h)$, a conforming finite element subspace of $H_0^1(\Omega_1)$, cf. Section 2.4. Indeed, the pair $(\mathcal{ND}_0^0(\mathcal{T}_h), \mathcal{S}_0^1(\mathcal{T}_h))$ yields a stable discretization of the mixed variational problems. Let $\{\boldsymbol{\varphi_i}\}_{i=1,N_h}$ denote the usual edge basis of $\mathcal{ND}_0^0(\mathcal{T}_h)$, and let $\{\psi_i\}_{i=1,M_h}$ denote the usual nodal basis of $\mathcal{S}_0^1(\mathcal{T}_h)$, respectively. We define the following FEM matrices:

$$
\begin{aligned}
(\mathbf{K}_{\boldsymbol{\nu}})_{ij} &= (\nu\,\mathbf{curl}\,\boldsymbol{\varphi_i}, \mathbf{curl}\,\boldsymbol{\varphi_j})_{\mathbf{0},\Omega_1}, \\
(\mathbf{K}_{\mathbf{r},\boldsymbol{\nu}})_{ij} &= (\nu\,\mathbf{curl}\,\boldsymbol{\varphi_i}, \mathbf{curl}\,\boldsymbol{\varphi_j})_{\mathbf{0},\Omega_1} + \omega(\sigma\nabla P_{\sigma,h}(\boldsymbol{\varphi_i}), \nabla P_{\sigma,h}(\boldsymbol{\varphi_j}))_{\mathbf{0},\Omega_1}, \\
(\mathbf{M}_{\boldsymbol{\sigma},\boldsymbol{\omega}})_{ij} &= \omega(\sigma\boldsymbol{\varphi_i}, \boldsymbol{\varphi_j})_{\mathbf{0},\Omega_1}, \\
(\tilde{\mathbf{M}}_{\boldsymbol{\sigma}})_{ij} &= \underline{\sigma}^{-1}(\sigma\boldsymbol{\varphi_i}, \boldsymbol{\varphi_j})_{\mathbf{0},\Omega_1}, \\
(\mathbf{D}_{\boldsymbol{\sigma},\boldsymbol{\omega}})_{ij} &= \omega(\sigma\boldsymbol{\varphi_i}, \nabla\psi_j)_{\mathbf{0},\Omega_1}, \\
(\mathbf{L}_{\boldsymbol{\sigma},\boldsymbol{\omega}})_{ij} &= \omega(\sigma\nabla\psi_i, \nabla\psi_j)_{\mathbf{0},\Omega_1}.
\end{aligned}
$$

Here, for given $\mathbf{y_h} \in \mathcal{ND}_0^0(\mathcal{T}_h)$, $p_h := P_{\sigma,h}(\mathbf{y_h}) \in S_0^1(\mathcal{T}_h)$ is the unique solution of the variational form:

$$
\int_{\Omega_1} \sigma\nabla p_h \cdot \nabla q_h \, \mathrm{d}\mathbf{x} = \int_{\Omega_1} \sigma\mathbf{y_h} \cdot \nabla q_h \, \mathrm{d}\mathbf{x}, \quad \forall q_h \in \mathcal{S}_0^1(\mathcal{T}_h).
$$

Due to the properties of the underlying operators, the matrix $\mathbf{K}_{\boldsymbol{\nu}}$ is symmetric and positive semi-definite, the matrices $\mathbf{K}_{\mathbf{r},\boldsymbol{\nu}}$, $\mathbf{M}_{\boldsymbol{\sigma},\boldsymbol{\omega}}$, $\tilde{\mathbf{M}}_{\boldsymbol{\sigma}}$, $\mathbf{L}_{\boldsymbol{\sigma},\boldsymbol{\omega}}$ are symmetric and positive definite, and the matrix $\mathbf{D}_{\boldsymbol{\sigma},\boldsymbol{\omega}}$ has full rank.

The entries of the right hand side vectors are given by the formulas $(\mathbf{u_h^c})_i = (\mathbf{u^c}, \boldsymbol{\varphi_i})_{\mathbf{0},\Omega_1}$ and $(\mathbf{u_h^s})_i = (\mathbf{u^s}, \boldsymbol{\varphi_i})_{\mathbf{0},\Omega_1}$. The resulting systems of the finite element equations have the following structure:

6.1.3.1   Symmetric formulations $(k = 1)$

Formulation FEM 1:

$$
\text{Find } (\mathbf{y_h^s}, \mathbf{y_h^c})^T \in \mathbb{R}^{2N_h} : \quad \underbrace{\begin{pmatrix} \mathbf{M}_{\boldsymbol{\sigma},\boldsymbol{\omega}} & \mathbf{K}_{\boldsymbol{\nu}} \\ \mathbf{K}_{\boldsymbol{\nu}} & -\mathbf{M}_{\boldsymbol{\sigma},\boldsymbol{\omega}} \end{pmatrix}}_{=:\mathcal{A}_{F1}} \begin{pmatrix} \mathbf{y_h^s} \\ \mathbf{y_h^c} \end{pmatrix} = \begin{pmatrix} \mathbf{u_h^c} \\ \mathbf{u_h^s} \end{pmatrix}.
$$

Formulation FEM 2:

$$
\text{Find } (\mathbf{y_h^c}, \mathbf{y_h^s})^T \in \mathbb{R}^{2N_h} : \quad \underbrace{\begin{pmatrix} \mathbf{K}_{\boldsymbol{\nu}} & \mathbf{M}_{\boldsymbol{\sigma},\boldsymbol{\omega}} \\ \mathbf{M}_{\boldsymbol{\sigma},\boldsymbol{\omega}} & -\mathbf{K}_{\boldsymbol{\nu}} \end{pmatrix}}_{=:\mathcal{A}_{F2}} \begin{pmatrix} \mathbf{y_h^c} \\ \mathbf{y_h^s} \end{pmatrix} = \begin{pmatrix} \mathbf{u_h^c} \\ -\mathbf{u_h^s} \end{pmatrix}.
$$

Formulation FEM 3:

$$
\text{Find } (\mathbf{y_h^c}, \mathbf{y_h^s}, \mathbf{p_h^c}, \mathbf{p_h^s})^T \in \mathbb{R}^{2(N_h+M_h)} : \quad \underbrace{\begin{pmatrix} \mathbf{K}_{\boldsymbol{\nu}} & \mathbf{M}_{\boldsymbol{\sigma},\boldsymbol{\omega}} & \mathbf{D}_{\boldsymbol{\sigma},\boldsymbol{\omega}}^T & \mathbf{0} \\ \mathbf{M}_{\boldsymbol{\sigma},\boldsymbol{\omega}} & -\mathbf{K}_{\boldsymbol{\nu}} & \mathbf{0} & -\mathbf{D}_{\boldsymbol{\sigma},\boldsymbol{\omega}}^T \\ \mathbf{D}_{\boldsymbol{\sigma},\boldsymbol{\omega}} & \mathbf{0} & \mathbf{0} & \mathbf{0} \\ \mathbf{0} & -\mathbf{D}_{\boldsymbol{\sigma},\boldsymbol{\omega}} & \mathbf{0} & \mathbf{0} \end{pmatrix}}_{=:\mathcal{A}_{M1}} \begin{pmatrix} \mathbf{y_h^c} \\ \mathbf{y_h^s} \\ \mathbf{p_h^c} \\ \mathbf{p_h^s} \end{pmatrix} = \begin{pmatrix} \mathbf{u_h^c} \\ -\mathbf{u_h^s} \\ \mathbf{0} \\ \mathbf{0} \end{pmatrix}.
$$

Formulation FEM 4:

$$\text{Find } (\mathbf{y_h^c}, \mathbf{y_h^s}, \mathbf{p_h^c}, \mathbf{p_h^s})^T \in \mathbb{R}^{2(N_h+M_h)} \; : \quad \underbrace{\begin{pmatrix} \mathbf{K}_\nu & \mathbf{M}_{\sigma,\omega} & \mathbf{D}_{\sigma,\omega}{}^T & \mathbf{0} \\ \mathbf{M}_{\sigma,\omega} & -\mathbf{K}_\nu & \mathbf{0} & -\mathbf{D}_{\sigma,\omega}{}^T \\ \mathbf{D}_{\sigma,\omega} & \mathbf{0} & -\mathbf{L}_{\sigma,\omega} & \mathbf{0} \\ \mathbf{0} & -\mathbf{D}_{\sigma,\omega} & \mathbf{0} & \mathbf{L}_{\sigma,\omega} \end{pmatrix}}_{=:\mathcal{A}_{M2}} \begin{pmatrix} \mathbf{y_h^c} \\ \mathbf{y_h^s} \\ \mathbf{p_h^c} \\ \mathbf{p_h^s} \end{pmatrix} = \begin{pmatrix} \mathbf{u_h^c} \\ -\mathbf{u_h^s} \\ \mathbf{0} \\ \mathbf{0} \end{pmatrix}.$$

Formulation FEM 5:

$$\text{Find } (\mathbf{y_h^c}, \mathbf{y_h^s})^T \in \mathbb{R}^{2N_h} \; : \quad \underbrace{\begin{pmatrix} \mathbf{K_{r,\nu}} & \mathbf{M}_{\sigma,\omega} \\ \mathbf{M}_{\sigma,\omega} & -\mathbf{K_{r,\nu}} \end{pmatrix}}_{=:\mathcal{A}_{F3}} \begin{pmatrix} \mathbf{y_h^c} \\ \mathbf{y_h^s} \end{pmatrix} = \begin{pmatrix} \mathbf{u_h^c} \\ -\mathbf{u_h^s} \end{pmatrix}.$$

Formulation FEM 6:

$$\text{Find } (\mathbf{y_h^s}, \tilde{\mathbf{y}}_\mathbf{h}^\mathbf{c})^T \in \mathbb{R}^{2N_h} \; : \quad \underbrace{\begin{pmatrix} \tilde{\mathbf{M}}_\sigma & \mathbf{K}_\nu \\ \mathbf{K}_\nu & -(\omega\underline{\sigma})^2\tilde{\mathbf{M}}_\sigma \end{pmatrix}}_{=:\mathcal{A}_{F4}} \begin{pmatrix} \mathbf{y_h^s} \\ \tilde{\mathbf{y}}_\mathbf{h}^\mathbf{c} \end{pmatrix} = \begin{pmatrix} \frac{1}{\sigma\omega}\mathbf{u_h^c} \\ \mathbf{u_h^s} \end{pmatrix}.$$

Here we use the scaled variable $\tilde{\mathbf{y}}_\mathbf{h}^\mathbf{c} := (\omega\underline{\sigma})^{-1}\mathbf{y_h^c}$.

In fact, the system matrices $\mathcal{A}_{F1}$, $\mathcal{A}_{F2}$, $\mathcal{A}_{M1}$, $\mathcal{A}_{M2}$, $\mathcal{A}_{F3}$ and $\mathcal{A}_{F4}$ are symmetric and indefinite, and have a saddle point or double saddle point structure. Typically small mesh sizes h, large or small ω and large jumps in the material coefficients ν and σ across interfaces lead to a dramatic growth in the condition number of these matrices. Therefore, we expect a very bad convergence rate if any Krylov subspace method, like the MinRes method, is applied to the unpreconditioned systems of equations. Hence appropriate preconditioning is an important issue.

6.1.3.2 Symmetric formulations $(k = 0)$

With the new matrices $\mathbf{D}_{\boldsymbol{\sigma}} = \mathbf{D}_{\boldsymbol{\sigma},1}$, $\mathbf{L}_{\boldsymbol{\sigma}} = \mathbf{L}_{\boldsymbol{\sigma},1}$, and $\mathbf{K}_{\mathbf{r},0,\nu} = \mathbf{K}_{\mathbf{r},\nu}|_{\omega=1}$, the resulting linear systems for the mode $k = 0$ have the following forms:

Formulation FEM 3 $(k = 0)$:

$$\text{Find } (\mathbf{y_h^c}, \mathbf{p_h^c})^T \in \mathbb{R}^{N_h+M_h} \; : \quad \underbrace{\begin{pmatrix} \mathbf{K}_\nu & \mathbf{D}_{\boldsymbol{\sigma}}{}^T \\ \mathbf{D}_{\boldsymbol{\sigma}} & \mathbf{0} \end{pmatrix}}_{=:\mathcal{A}_{M1,0}} \begin{pmatrix} \mathbf{y_h^c} \\ \mathbf{p_h^c} \end{pmatrix} = \begin{pmatrix} \mathbf{u_h^c} \\ \mathbf{0} \end{pmatrix}.$$

Formulation FEM 4 $(k = 0)$:

$$\text{Find } (\mathbf{y_h^c}, \mathbf{p_h^c})^T \in \mathbb{R}^{N_h+M_h} \; : \quad \underbrace{\begin{pmatrix} \mathbf{K}_\nu & \mathbf{D}_{\boldsymbol{\sigma}}{}^T \\ \mathbf{D}_{\boldsymbol{\sigma}} & -\mathbf{L}_{\boldsymbol{\sigma}} \end{pmatrix}}_{=:\mathcal{A}_{M2,0}} \begin{pmatrix} \mathbf{y_h^c} \\ \mathbf{p_h^c} \end{pmatrix} = \begin{pmatrix} \mathbf{u_h^c} \\ \mathbf{0} \end{pmatrix}.$$

Formulation FEM 5 $(k = 0)$:

$$\text{Find } \mathbf{y_h^c} \in \mathbb{R}^{N_h} \; : \quad \underbrace{\mathbf{K}_{\mathbf{r},0,\nu}}_{=:\mathcal{A}_{F3,0}} \mathbf{y_h^c} = \mathbf{u_h^c}.$$

In fact, the system matrices $\mathcal{A}_{M1,0}$ and $\mathcal{A}_{M2,0}$ are symmetric and indefinite, and have a saddle point structure. The system matrix $\mathcal{A}_{F3,0}$ is symmetric and positive definite. Also in these cases, the condition numbers of the system matrices suffer from small mesh sizes h and large jumps in the material coefficients ν and σ across interfaces.

6.1.4   Block-diagonal preconditioners

This subsection is devoted to the construction of parameter-robust preconditioners for the systems of linear equations of the last subsection. For each proposed formulation, we investigate its structure to construct a preconditioner either by the matrix interpolation technique, cf. Subsection 5.2.2, or the technique of inexact Schur complement preconditioning, cf. Subsection 5.2.3. Furthermore, we provide condition number bounds for the resulting preconditioned systems of linear equations, by showing well-posedness of the underlying systems of partial differential equations in non-standard norms.

6.1.4.1   Symmetric formulations ($k = 1$)

Formulation FEM 1   We explore the 2×2 block-structure of our system matrix $\mathcal{A}_{F1}$. In order to construct parameter-robust and block-diagonal preconditioners, we use the matrix interpolation theory presented in Subsection 5.2.2. Since $\mathbf{M}_{\boldsymbol{\sigma},\boldsymbol{\omega}}$ is symmetric and positive definite, we can build both Schur complements $\mathbf{R}$ and $\mathbf{S}$, given by $\mathbf{S} = \mathbf{R} = \mathbf{M}_{\boldsymbol{\sigma},\boldsymbol{\omega}} + \mathbf{K}_{\boldsymbol{\nu}}\mathbf{M}_{\boldsymbol{\sigma},\boldsymbol{\omega}}^{-1}\mathbf{K}_{\boldsymbol{\nu}}$, and therefore the Schur complement preconditioners (cf. Theorem 5.3). Due to Theorem 5.5 a candidate for a parameter-robust and block-diagonal preconditioner is an interpolant of the standard Schur complement preconditioners. Therefore we choose $\theta = 1/2$ and interpolate to obtain a new preconditioner

$$\tilde{\mathcal{P}} = \begin{pmatrix} [\mathbf{M}_{\boldsymbol{\sigma},\boldsymbol{\omega}}, \mathbf{S}]_{\frac{1}{2}} & \mathbf{0} \\ \mathbf{0} & [\mathbf{S}, \mathbf{M}_{\boldsymbol{\sigma},\boldsymbol{\omega}}]_{\frac{1}{2}} \end{pmatrix}.$$

The following computations are straightforward, using the simple spectral inequality

$$\frac{1}{\sqrt{2}}\mathbf{x}^T(\mathbf{I} + \mathbf{A}^{\frac{1}{2}})\mathbf{x} \leq \mathbf{x}^T(\mathbf{I} + \mathbf{A})^{\frac{1}{2}}\mathbf{x} \leq \mathbf{x}^T(\mathbf{I} + \mathbf{A}^{\frac{1}{2}})\mathbf{x}, \quad \forall \mathbf{x} \in \mathbb{R}^{N_h}, \tag{6.32}$$

where $\mathbf{I} \in \mathbb{R}^{n \times n}$ denotes the identity matrix and $\mathbf{A} \in \mathbb{R}^{n \times n}$ is an arbitrary symmetric and positive definite matrix. Consequently, we can derive another new preconditioner $\mathcal{P}$, that is spectral equivalent to the interpolated preconditioner $\tilde{\mathcal{P}}$:

$$\mathbf{x}^T[\mathbf{M}_{\boldsymbol{\sigma},\boldsymbol{\omega}}, \mathbf{S}]_{\frac{1}{2}}\mathbf{x} = \mathbf{x}^T[\mathbf{S}, \mathbf{M}_{\boldsymbol{\sigma},\boldsymbol{\omega}}]_{\frac{1}{2}}\mathbf{x} = \mathbf{x}^T\mathbf{M}_{\boldsymbol{\sigma},\boldsymbol{\omega}}^{\frac{1}{2}}\left(\mathbf{M}_{\boldsymbol{\sigma},\boldsymbol{\omega}}^{-\frac{1}{2}}(\mathbf{M}_{\boldsymbol{\sigma},\boldsymbol{\omega}} + \mathbf{K}_{\boldsymbol{\nu}}\mathbf{M}_{\boldsymbol{\sigma},\boldsymbol{\omega}}^{-1}\mathbf{K}_{\boldsymbol{\nu}})\mathbf{M}_{\boldsymbol{\sigma},\boldsymbol{\omega}}^{-\frac{1}{2}}\right)^{\frac{1}{2}}\mathbf{M}_{\boldsymbol{\sigma},\boldsymbol{\omega}}^{\frac{1}{2}}\mathbf{x}$$

$$\leq \mathbf{x}^T\left(\mathbf{M}_{\boldsymbol{\sigma},\boldsymbol{\omega}} + \mathbf{M}_{\boldsymbol{\sigma},\boldsymbol{\omega}}^{\frac{1}{2}}\left(\mathbf{M}_{\boldsymbol{\sigma},\boldsymbol{\omega}}^{-\frac{1}{2}}\mathbf{K}_{\boldsymbol{\nu}}\mathbf{M}_{\boldsymbol{\sigma},\boldsymbol{\omega}}^{-1}\mathbf{K}_{\boldsymbol{\nu}}\mathbf{M}_{\boldsymbol{\sigma},\boldsymbol{\omega}}^{-\frac{1}{2}}\right)^{\frac{1}{2}}\mathbf{M}_{\boldsymbol{\sigma},\boldsymbol{\omega}}^{\frac{1}{2}}\right)\mathbf{x}$$

$$= \mathbf{x}^T\left(\mathbf{M}_{\boldsymbol{\sigma},\boldsymbol{\omega}} + \mathbf{M}_{\boldsymbol{\sigma},\boldsymbol{\omega}}^{\frac{1}{2}}\left(\mathbf{M}_{\boldsymbol{\sigma},\boldsymbol{\omega}}^{-\frac{1}{2}}\mathbf{K}_{\boldsymbol{\nu}}\mathbf{M}_{\boldsymbol{\sigma},\boldsymbol{\omega}}^{-\frac{1}{2}}\right)\mathbf{M}_{\boldsymbol{\sigma},\boldsymbol{\omega}}^{\frac{1}{2}}\right)\mathbf{x}$$

$$= \mathbf{x}^T\left(\mathbf{M}_{\boldsymbol{\sigma},\boldsymbol{\omega}} + \mathbf{K}_{\boldsymbol{\nu}}\right)\mathbf{x}, \quad \forall \mathbf{x} \in (\ker \mathbf{K}_{\boldsymbol{\nu}})^{\perp},$$

and

$$\mathbf{x}^T[\mathbf{M}_{\boldsymbol{\sigma},\boldsymbol{\omega}}, \mathbf{S}]_{\frac{1}{2}}\mathbf{x} = \mathbf{x}^T[\mathbf{S}, \mathbf{M}_{\boldsymbol{\sigma},\boldsymbol{\omega}}]_{\frac{1}{2}}\mathbf{x} = \mathbf{x}^T\mathbf{M}_{\boldsymbol{\sigma},\boldsymbol{\omega}}^{\frac{1}{2}}\left(\mathbf{M}_{\boldsymbol{\sigma},\boldsymbol{\omega}}^{-\frac{1}{2}}(\mathbf{M}_{\boldsymbol{\sigma},\boldsymbol{\omega}} + \mathbf{K}_{\boldsymbol{\nu}}\mathbf{M}_{\boldsymbol{\sigma},\boldsymbol{\omega}}^{-1}\mathbf{K}_{\boldsymbol{\nu}})\mathbf{M}_{\boldsymbol{\sigma},\boldsymbol{\omega}}^{-\frac{1}{2}}\right)^{\frac{1}{2}}\mathbf{M}_{\boldsymbol{\sigma},\boldsymbol{\omega}}^{\frac{1}{2}}\mathbf{x}$$

$$\geq \frac{1}{\sqrt{2}}\mathbf{x}^T\left(\mathbf{M}_{\boldsymbol{\sigma},\boldsymbol{\omega}} + \mathbf{M}_{\boldsymbol{\sigma},\boldsymbol{\omega}}^{\frac{1}{2}}\left(\mathbf{M}_{\boldsymbol{\sigma},\boldsymbol{\omega}}^{-\frac{1}{2}}\mathbf{K}_{\boldsymbol{\nu}}\mathbf{M}_{\boldsymbol{\sigma},\boldsymbol{\omega}}^{-1}\mathbf{K}_{\boldsymbol{\nu}}\mathbf{M}_{\boldsymbol{\sigma},\boldsymbol{\omega}}^{-\frac{1}{2}}\right)^{\frac{1}{2}}\mathbf{M}_{\boldsymbol{\sigma},\boldsymbol{\omega}}^{\frac{1}{2}}\right)\mathbf{x}$$

$$= \frac{1}{\sqrt{2}}\mathbf{x}^T\left(\mathbf{M}_{\boldsymbol{\sigma},\boldsymbol{\omega}} + \mathbf{M}_{\boldsymbol{\sigma},\boldsymbol{\omega}}^{\frac{1}{2}}\left(\mathbf{M}_{\boldsymbol{\sigma},\boldsymbol{\omega}}^{-\frac{1}{2}}\mathbf{K}_{\boldsymbol{\nu}}\mathbf{M}_{\boldsymbol{\sigma},\boldsymbol{\omega}}^{-\frac{1}{2}}\right)\mathbf{M}_{\boldsymbol{\sigma},\boldsymbol{\omega}}^{\frac{1}{2}}\right)\mathbf{x}$$

$$= \frac{1}{\sqrt{2}}\mathbf{x}^T\left(\mathbf{M}_{\boldsymbol{\sigma},\boldsymbol{\omega}} + \mathbf{K}_{\boldsymbol{\nu}}\right)\mathbf{x}, \quad \forall \mathbf{x} \in (\ker \mathbf{K}_{\boldsymbol{\nu}})^{\perp}.$$

Hence, from Subsection 5.2.2 and Subsection 5.2.4, we have, that the preconditioner $\mathcal{P}$, given by the block-diagonal matrix

$$\mathcal{P} = \begin{pmatrix} \mathbf{M}_{\boldsymbol{\sigma},\boldsymbol{\omega}} + \mathbf{K}_{\boldsymbol{\nu}} & \mathbf{0} \\ \mathbf{0} & \mathbf{M}_{\boldsymbol{\sigma},\boldsymbol{\omega}} + \mathbf{K}_{\boldsymbol{\nu}} \end{pmatrix}, \tag{6.33}$$

is a candidate for a parameter-robust preconditioner. In the subspace $\left[(\ker \mathbf{K}_{\boldsymbol{\nu}})^{\perp}\right]^2 \subset \mathbb{R}^{2N_h}$, we immediately obtain the condition number estimate

$$\kappa_{\mathcal{P}}(\mathcal{P}^{-1}\mathcal{A}_{F1}) := \|\mathcal{P}^{-1}\mathcal{A}_{F1}\|_{\mathcal{P}}\|\mathcal{A}_{F1}^{-1}\mathcal{P}\|_{\mathcal{P}} \leq \frac{\sqrt{2}(\sqrt{5}+1)}{\sqrt{5}-1} \approx 3.702.$$

In the next step, we extend the estimate of the condition number to the full vector space $\mathbb{R}^{2N_h}$ and even improve the quantitative condition number bound. Inspired by the structure of the preconditioner (6.33), we introduce the non-standard norm $\|\cdot\|_{\mathcal{P}}$ in $\mathbf{H_0}(\mathbf{curl}, \Omega_1)^2$ by

$$\|(\mathbf{y^s}, \mathbf{y^c})\|_{\mathcal{P}}^2 = \sum_{j \in \{c,s\}} (\nu \, \mathbf{curl}\, \mathbf{y^j}, \mathbf{curl}\, \mathbf{y^j})_{\mathbf{0},\Omega_1} + \omega(\sigma\mathbf{y^j}, \mathbf{y^j})_{\mathbf{0},\Omega_1}.$$

The main result is summarized in the following lemma, that claims that an inf-sup and a sup-sup condition are fulfilled with parameter-independent constants, namely $1/\sqrt{2}$ and 1.

Lemma 6.10. *We have*

$$\frac{1}{\sqrt{2}}\|(\mathbf{y^s}, \mathbf{y^c})\|_{\mathcal{P}} \leq \sup_{(\mathbf{v^c}, \mathbf{v^s}) \in \mathbf{H_0}(\mathbf{curl},\Omega_1)^2} \frac{\mathcal{A}_{F1}((\mathbf{y^s}, \mathbf{y^c}), (\mathbf{v^c}, \mathbf{v^s}))}{\|(\mathbf{v^c}, \mathbf{v^s})\|_{\mathcal{P}}} \leq \|(\mathbf{y^s}, \mathbf{y^c})\|_{\mathcal{P}}, \qquad (6.34)$$

for all $(\mathbf{y^s}, \mathbf{y^c}) \in \mathbf{H_0}(\mathbf{curl}, \Omega_1).$

Proof. Boundedness follows from reapplication of Cauchy's inequality. The lower estimate can be attained by choosing $\mathbf{v^c} = \mathbf{y^c} + \mathbf{y^s}$ and $\mathbf{v^s} = \mathbf{y^s} - \mathbf{y^c}$. Note that, for this special choice of the test functions, we have $\|(\mathbf{v^c}, \mathbf{v^s})\|_{\mathcal{P}} = \sqrt{2}\|(\mathbf{y^s}, \mathbf{y^c})\|_{\mathcal{P}}$. $\qquad\square$

In general, an inf-sup bound for $\mathbf{H_0}(\mathbf{curl}, \Omega_1)^2$ does not imply such a lower bound on the finite element subspace $\mathcal{ND}_0^0(\mathcal{T}_h)^2$. However, in this case the inequalities (6.34) remain also valid for the Nédélec finite element subspace $\mathcal{ND}_0^0(\mathcal{T}_h)^2$, since the proof can be repeated for the finite element functions step by step. Therefore, we obtain the improved condition number estimate

$$\kappa_{\mathcal{P}}(\mathcal{P}^{-1}\mathcal{A}_{F1}) := \|\mathcal{P}^{-1}\mathcal{A}_{F1}\|_{\mathcal{P}}\|\mathcal{A}_{F1}^{-1}\mathcal{P}\|_{\mathcal{P}} \leq \sqrt{2} \approx 1.414.$$

A similar block-diagonal preconditioner, yielding a condition number of $\sqrt{2}$ has also been derived in [38, 82].

Formulation FEM 2 Due to the non-trivial kernel of the **curl** operator the matrix $\mathbf{K}_{\boldsymbol{\nu}}$ is only positive semi-definite. Therefore, we cannot form the Schur complements and, consequently, the interpolation theory presented in Subsection 5.2.2 is not applicable. Nevertheless, using the non-standard $\mathcal{P}$-norm, we can verify an inf-sup and sup-sup condition with parameter-independent constants, namely $1/\sqrt{2}$ and 1.

Lemma 6.11. *We have*

$$\frac{1}{\sqrt{2}}\|(\mathbf{y^c}, \mathbf{y^s})\|_{\mathcal{P}} \leq \sup_{(\mathbf{v^c}, \mathbf{v^s}) \in \mathbf{H_0}(\mathbf{curl},\Omega_1)^2} \frac{\mathcal{A}_{F2}((\mathbf{y^c}, \mathbf{y^s}), (\mathbf{v^c}, \mathbf{v^s}))}{\|(\mathbf{v^c}, \mathbf{v^s})\|_{\mathcal{P}}} \leq \|(\mathbf{y^s}, \mathbf{y^c})\|_{\mathcal{P}}, \qquad (6.35)$$

for all $(\mathbf{y^c}, \mathbf{y^s}) \in \mathbf{H_0}(\mathbf{curl}, \Omega_1).$

Proof. Boundedness follows from reapplication of Cauchy's inequality. The lower estimate can be attained by choosing $\mathbf{v^c} = \mathbf{y^s} + \mathbf{y^c}$ and $\mathbf{v^s} = \mathbf{y^c} - \mathbf{y^s}$. Note that, for this special choice of the test functions, we have $\|(\mathbf{v^c}, \mathbf{v^s})\|_{\mathcal{P}} = \sqrt{2}\|(\mathbf{y^c}, \mathbf{y^s})\|_{\mathcal{P}}$. $\qquad\square$

Furthermore, the inequalities (6.35) remain valid for the finite element subspace $\mathcal{ND}_0^0(\mathcal{T}_h)^2$, since the proof can be repeated for the finite element functions step by step. Therefore, we obtain the condition number estimate

$$\kappa_{\mathcal{P}}(\mathcal{P}^{-1}\mathcal{A}_{F2}) := \|\mathcal{P}^{-1}\mathcal{A}_{F2}\|_{\mathcal{P}}\|\mathcal{A}_{F2}^{-1}\mathcal{P}\|_{\mathcal{P}} \leq \sqrt{2} \approx 1.414.$$

Formulation FEM 3   Since we already have a robust preconditioner for $\mathcal{A}_{F2}$, we pursue the strategy of inexact Schur complement preconditioning, cf. Subsection 5.2.3. Therefore, we propose the following block-diagonal inexact Schur complement preconditioner

$$\mathcal{P}_M = \operatorname{diag}\left(\mathbf{M}_{\boldsymbol{\sigma},\boldsymbol{\omega}} + \mathbf{K}_{\boldsymbol{\nu}}, \mathbf{M}_{\boldsymbol{\sigma},\boldsymbol{\omega}} + \mathbf{K}_{\boldsymbol{\nu}}, \mathbf{S}_I, \mathbf{S}_I\right), \tag{6.36}$$

where $\mathbf{S}_I = \mathbf{D}_{\boldsymbol{\sigma},\boldsymbol{\omega}}(\mathbf{M}_{\boldsymbol{\sigma},\boldsymbol{\omega}} + \mathbf{K}_{\boldsymbol{\nu}})^{-1}\mathbf{D}_{\boldsymbol{\sigma},\boldsymbol{\omega}}{}^T$. Since the matrix $\mathbf{D}_{\boldsymbol{\sigma},\boldsymbol{\omega}}$ has full rank, the block $\mathbf{S}_I$ is positive definite and therefore the whole preconditioner $\mathcal{P}_M$ is positive definite. According to the choice of the block-diagonal preconditioner (6.36), we introduce the non-standard norm $\|\cdot\|_{\mathcal{P}_M}$ in the product space $\mathbf{H_0}(\mathbf{curl}, \Omega_1)^2 \times H_0^1(\Omega_1)^2$:

$$\|(\mathbf{y^c}, \mathbf{y^s}, p^c, p^s)\|_{\mathcal{P}_M}^2 := \sum_{j \in \{c,s\}} (\nu\,\mathbf{curl}\,\mathbf{y^j}, \mathbf{curl}\,\mathbf{y^j})_{\mathbf{0},\Omega_1} + \omega(\sigma\mathbf{y^j}, \mathbf{y^j})_{\mathbf{0},\Omega_1}$$
$$+ \sup_{\mathbf{v^j} \in \mathbf{H_0}(\mathbf{curl},\Omega_1)} \frac{\omega^2(\sigma\mathbf{v^j}, \nabla p^j)_{\mathbf{0},\Omega_1}^2}{(\nu\,\mathbf{curl}\,\mathbf{v^j}, \mathbf{curl}\,\mathbf{v^j})_{\mathbf{0},\Omega_1} + \omega(\sigma\mathbf{v^j}, \mathbf{v^j})_{\mathbf{0},\Omega_1}}.$$

Therein, the sup-expression is nothing else than the continuous representation of the Schur complement in (6.36). Before we consider an inf-sup and a sup-sup condition for $\mathcal{A}_{M1}(\cdot, \cdot)$, we have a closer look at the $H_0^1(\Omega_1)$ contribution to $\|\cdot\|_{\mathcal{P}_M}$. Indeed, we can verify the following norm equivalence

$$\omega(\sigma\nabla p^j, \nabla p^j)_{\mathbf{0},\Omega_1} \leq \sup_{\mathbf{v^j} \in \mathbf{H_0}(\mathbf{curl},\Omega_1)} \frac{\omega(\sigma\mathbf{v^j}, \nabla p^j)_{\mathbf{0},\Omega_1}^2}{(\nu\,\mathbf{curl}\,\mathbf{v^j}, \mathbf{curl}\,\mathbf{v^j})_{\mathbf{0},\Omega_1} + \omega(\sigma\mathbf{v^j}, \mathbf{v^j})_{\mathbf{0},\Omega_1}} \leq \omega(\sigma\nabla p^j, \nabla p^j)_{\mathbf{0},\Omega_1}.$$

The lower bound follows with the choice $\mathbf{v^j} = \nabla p^j \in \mathbf{H_0}(\mathbf{curl}, \Omega_1)$, and the upper bound by Cauchy's inequality. Therefore, we obtain the identity

$$\sup_{\mathbf{v^j} \in \mathbf{H_0}(\mathbf{curl},\Omega_1)} \frac{\omega(\sigma\mathbf{v^j}, \nabla p^j)_{\mathbf{0},\Omega_1}^2}{(\nu\,\mathbf{curl}\,\mathbf{v^j}, \mathbf{curl}\,\mathbf{v^j})_{\mathbf{0},\Omega_1} + \omega(\sigma\mathbf{v^j}, \mathbf{v^j})_{\mathbf{0},\Omega_1}} = \omega(\sigma\nabla p^j, \nabla p^j)_{\mathbf{0},\Omega_1}, \quad \forall p^j \in H_0^1(\Omega). \tag{6.37}$$

Consequently, we have the simpler representation of the $\mathcal{P}_M$-norm in terms of

$$\|(\mathbf{y^c}, \mathbf{y^s}, p^c, p^s)\|_{\mathcal{P}_M}^2 = \sum_{j \in \{c,s\}} (\nu\,\mathbf{curl}\,\mathbf{y^j}, \mathbf{curl}\,\mathbf{y^j})_{\mathbf{0},\Omega_1} + \omega(\sigma\mathbf{y^j}, \mathbf{y^j})_{\mathbf{0},\Omega_1} + \omega(\sigma\nabla p^j, \nabla p^j)_{\mathbf{0},\Omega_1}.$$

Furthermore, the identity (6.37) can also be verified for the finite element subspaces $\mathcal{S}_0^1(\mathcal{T}_h)$, where the supremum is taken over $\mathcal{N}_0^0(\mathcal{T}_h)$, yielding the new block-diagonal preconditioner

$$\mathcal{P}_M = \operatorname{diag}\left(\mathbf{M}_{\boldsymbol{\sigma},\boldsymbol{\omega}} + \mathbf{K}_{\boldsymbol{\nu}}, \mathbf{M}_{\boldsymbol{\sigma},\boldsymbol{\omega}} + \mathbf{K}_{\boldsymbol{\nu}}, \mathbf{L}_{\boldsymbol{\sigma},\boldsymbol{\omega}}, \mathbf{L}_{\boldsymbol{\sigma},\boldsymbol{\omega}}\right).$$

The main result is summarized in the following lemma, that claims that an inf-sup condition and a sup-sup condition are fulfilled with parameter-independent constants, namely $\frac{1}{3\sqrt{2}}$ and $\frac{1+\sqrt{5}}{2}$.

Lemma 6.12. *We have*

$$\frac{1}{3\sqrt{2}}\|(\mathbf{y^c}, \mathbf{y^s}, p^c, p^s)\|_{\mathcal{P}_M} \leq \sup_{0 \neq (\mathbf{v^c}, \mathbf{v^s}, q^c, q^s)} \frac{\mathcal{A}_{M1}((\mathbf{y^c}, \mathbf{y^s}, p^c, p^s), (\mathbf{v^c}, \mathbf{v^s}, q^c, q^s))}{\|(\mathbf{v^c}, \mathbf{v^s}, q^c, q^s)\|_{\mathcal{P}_M}},$$
$$\frac{1+\sqrt{5}}{2}\|(\mathbf{y^c}, \mathbf{y^s}, p^c, p^s)\|_{\mathcal{P}_M} \geq \sup_{0 \neq (\mathbf{v^c}, \mathbf{v^s}, q^c, q^s)} \frac{\mathcal{A}_{M1}((\mathbf{y^c}, \mathbf{y^s}, p^c, p^s), (\mathbf{v^c}, \mathbf{v^s}, q^c, q^s))}{\|(\mathbf{v^c}, \mathbf{v^s}, q^c, q^s)\|_{\mathcal{P}_M}}, \tag{6.38}$$

for all $(\mathbf{y^c}, \mathbf{y^s}, p^c, p^s) \in \mathbf{H_0}(\mathbf{curl}, \Omega_1)^2 \times H_0^1(\Omega_1)^2$.

Proof. For the proof, we split the bilinear form $\mathcal{A}_{M1}$ as follows:

$$\mathcal{A}_{M1}((\mathbf{y^c}, \mathbf{y^s}, p^c, p^s), (\mathbf{v^c}, \mathbf{v^s}, q^c, q^s)) = a((\mathbf{y^c}, \mathbf{y^s}), (\mathbf{v^c}, \mathbf{v^s})) + b((\mathbf{v^c}, \mathbf{v^s}), (p^c, p^s)) + b((\mathbf{y^c}, \mathbf{y^s}), (q^c, q^s)),$$

with

$$a((\mathbf{y^c}, \mathbf{y^s}), (\mathbf{v^c}, \mathbf{v^s})) := \mathcal{A}_{F2}((\mathbf{y^c}, \mathbf{y^s}), (\mathbf{v^c}, \mathbf{v^s})),$$
$$b((\mathbf{v^c}, \mathbf{v^s}), (p^c, p^s)) := \omega(\sigma \mathbf{v^c}, \nabla p^c)_{\mathbf{0}, \Omega_1} - \omega(\sigma \mathbf{v^s}, \nabla p^s)_{\mathbf{0}, \Omega_1},$$

and verify the conditions in the theorem of Brezzi, cf. Theorem 2.3. The bilinear form $a(\cdot, \cdot)$ is bounded with constant 1 and fulfills an inf-sup condition with constant $1/\sqrt{2}$, cf. Lemma 6.11. Boundedness of $b(\cdot, \cdot)$ follows by Cauchy's inequality, i.e.,

$$\omega(\sigma \mathbf{y^j}, \nabla p^j)_{\mathbf{0}, \Omega_1} \leq \|\sqrt{\omega \sigma} \mathbf{y^j}\|_{\mathbf{0}, \Omega_1} \|\sqrt{\omega \sigma} \nabla p^j\|_{\mathbf{0}, \Omega_1}.$$

Therefore, boundedness of $b(\cdot, \cdot)$ follows with constant 1. Finally, the bilinear form $b(\cdot, \cdot)$, satisfies an inf-sup condition with constant $1/2$. Indeed, for the choices $(\mathbf{v^c}, \mathbf{v^s}) = (\nabla p^c, \mathbf{0})$ and $(\mathbf{v^c}, \mathbf{v^s}) = (\mathbf{0}, \nabla p^s)$, we obtain

$$\sup_{(\mathbf{v^c}, \mathbf{v^s})} \frac{b((\mathbf{v^c}, \mathbf{v^s}), (p^c, p^s))}{\sqrt{\sum_{j \in \{c,s\}} (\nu \, \mathbf{curl} \, \mathbf{v^j}, \mathbf{curl} \, \mathbf{v^j})_{\mathbf{0}, \Omega_1} + \omega(\sigma \mathbf{v^j}, \mathbf{v^j})_{\mathbf{0}, \Omega_1}}} \geq \frac{1}{2} \sum_{j \in \{c,s\}} \omega(\sigma \nabla p^j, \nabla p^j)_{\mathbf{0}, \Omega_1}.$$

Consequently, the inf-sup and sup-sup condition for $\mathcal{A}_{M1}(\cdot, \cdot)$ can be derived by combining the estimates according to Theorem 2.3. $\qquad \square$

Furthermore, the inequalities (6.38) remain valid for the finite element subspace $\mathcal{ND}_0^0(\mathcal{T}_h)^2 \times \mathcal{S}_0^1(\mathcal{T}_h)^2$, since the proof can be repeated for the finite element functions step by step. Therefore, we obtain the condition number estimate

$$\kappa_{\mathcal{P}_M}(\mathcal{P}_M^{-1} \mathcal{A}_{M1}) := \|\mathcal{P}_M^{-1} \mathcal{A}_{M1}\|_{\mathcal{P}_M} \|\mathcal{A}_{M1}^{-1} \mathcal{P}_M\|_{\mathcal{P}_M} \leq \frac{3\sqrt{2}(1 + \sqrt{5})}{2} \approx 6.865.$$

Formulation FEM 4 Due to the special choice of $c(\cdot, \cdot)$ in (6.16), again the $\mathcal{P}_M$-norm can be used in this setting. The main result is summarized in the following lemma, that claims that an inf-sup and a sup-sup condition are fulfilled with parameter-independent constants, namely $\frac{1}{\sqrt{2}}$ and 2.

Lemma 6.13. *We have*

$$\frac{1}{\sqrt{2}} \|(\mathbf{y^c}, \mathbf{y^s}, p^c, p^s)\|_{\mathcal{P}_M} \leq \sup_{0 \neq (\mathbf{v^c}, \mathbf{v^s}, q^c, q^s)} \frac{\mathcal{A}_{M2}((\mathbf{y^c}, \mathbf{y^s}, p^c, p^s), (\mathbf{v^c}, \mathbf{v^s}, q^c, q^s))}{\|(\mathbf{v^c}, \mathbf{v^s}, q^c, q^s)\|_{\mathcal{P}_M}},$$
$$2 \|(\mathbf{y^c}, \mathbf{y^s}, p^c, p^s)\|_{\mathcal{P}_M} \geq \sup_{0 \neq (\mathbf{v^c}, \mathbf{v^s}, q^c, q^s)} \frac{\mathcal{A}_{M2}((\mathbf{y^c}, \mathbf{y^s}, p^c, p^s), (\mathbf{v^c}, \mathbf{v^s}, q^c, q^s))}{\|(\mathbf{v^c}, \mathbf{v^s}, q^c, q^s)\|_{\mathcal{P}_M}},$$

(6.39)

for all $(\mathbf{y^c}, \mathbf{y^s}, p^c, p^s) \in \mathbf{H_0}(\mathbf{curl}, \Omega_1)^2 \times H_0^1(\Omega_1)^2$.

Proof. Boundedness follows from reapplication of Cauchy's inequality. The lower estimate can be attained by choosing $\mathbf{v^c} = \mathbf{y^c} - \mathbf{y^s}$, $\mathbf{v^s} = \mathbf{y^s} + \mathbf{y^c}$, $q^c = p^s - p^c$ and $q^s = p^s + p^c$. Note that, for this special choice of the test functions, we have $\|(\mathbf{v^c}, \mathbf{v^s}, q^c, q^s)\|_{\mathcal{P}_M} = \sqrt{2} \|(\mathbf{y^c}, \mathbf{y^s}, p^c, p^s)\|_{\mathcal{P}_M}$. $\qquad \square$

Furthermore, the inequalities (6.39) remain valid for the finite element subspace $\mathcal{ND}_0^0(\mathcal{T}_h)^2 \times \mathcal{S}_0^1(\mathcal{T}_h)^2$, since the proof can be repeated for the finite element functions step by step. Therefore, we obtain the condition number estimate

$$\kappa_{\mathcal{P}_M}(\mathcal{P}_M^{-1} \mathcal{A}_{M2}) := \|\mathcal{P}_M^{-1} \mathcal{A}_{M2}\|_{\mathcal{P}_M} \|\mathcal{A}_{M2}^{-1} \mathcal{P}_M\|_{\mathcal{P}_M} \leq 2\sqrt{2} \approx 2.865.$$

Formulation FEM 5 Due to the exact modification, $\mathbf{K}_{r,\nu}$ is positive definite, and therefore, again the technique of operator interpolation can be used to derive a candidate for a parameter-robust preconditioner. Anyhow, we verify, that also in this case the $\mathcal{P}$-norm can be used. The main result is summarized in the following lemma, that claims that an inf-sup condition and a sup-sup condition are fulfilled with parameter-independent constants, namely $\frac{1}{\sqrt{2}}$ and 2.

Lemma 6.14. *We have*

$$\frac{1}{\sqrt{2}}\|(\mathbf{y^c},\mathbf{y^s})\|_{\mathcal{P}} \leq \sup_{0\neq(\mathbf{v^c},\mathbf{v^s})\in\mathbf{H_0}(\mathbf{curl},\Omega_1)^2} \frac{\mathcal{A}_{F3}((\mathbf{y^c},\mathbf{y^s}),(\mathbf{v^c},\mathbf{v^s}))}{\|(\mathbf{v^c},\mathbf{v^s})\|_{\mathcal{P}}} \leq 2\|(\mathbf{y^c},\mathbf{y^s})\|_{\mathcal{P}}, \qquad (6.40)$$

for all $(\mathbf{y^c},\mathbf{y^s}) \in \mathbf{H_0}(\mathbf{curl},\Omega_1)^2$.

Proof. Boundedness follows from reapplication of Cauchy's inequality and the estimate (6.22). The lower estimate can be attained by choosing $\mathbf{v^c} = \mathbf{y^s} + \mathbf{y^c}$ and $\mathbf{v^s} = \mathbf{y^c} - \mathbf{y^s}$. Note that, for this special choice of the test functions, we have $\|(\mathbf{v^c},\mathbf{v^s})\|_{\mathcal{P}} = \sqrt{2}\|(\mathbf{y^c},\mathbf{y^s})\|_{\mathcal{P}}$. $\qquad\square$

Furthermore, the inequalities (6.40) remain valid for the finite element subspace $\mathcal{ND}_0^0(\mathcal{T}_h)^2$, since the proof can be repeated for the finite element functions step by step. Therefore, we obtain the condition number estimate

$$\kappa_{\mathcal{P}}(\mathcal{P}^{-1}\mathcal{A}_{F3}) := \|\mathcal{P}^{-1}\mathcal{A}_{F3}\|_{\mathcal{P}}\|\mathcal{A}_{F3}^{-1}\mathcal{P}\|_{\mathcal{P}} \leq 2\sqrt{2} \approx 2.865.$$

Formulation FEM 6 We explore the 2×2 block-structure of our system matrix $\mathcal{A}_{F4}$. In order to construct parameter-robust and block-diagonal preconditioners, we use the matrix interpolation theory presented in Subsection 5.2.2. Since $\tilde{\mathbf{M}}_{\boldsymbol{\sigma}}$ and $(\omega\underline{\sigma})^2\tilde{\mathbf{M}}_{\boldsymbol{\sigma}}$ are both symmetric and positive definite, we can build both Schur complements $\mathbf{R} = \tilde{\mathbf{M}}_{\boldsymbol{\sigma}} + (\omega\underline{\sigma})^{-2}\mathbf{K}_{\nu}\tilde{\mathbf{M}}_{\boldsymbol{\sigma}}^{-1}\mathbf{K}_{\nu}$ and $\mathbf{S} = (\omega\underline{\sigma})^2\mathbf{R}$, and therefore the Schur complement preconditioners (cf. Theorem 5.3). Due to Theorem 5.5 a candidate for a parameter-robust and block-diagonal preconditioner is an interpolant of the previous standard Schur complement preconditioners. Therefore we choose $\theta = 1/2$ and interpolate to obtain a new preconditioner

$$\tilde{\mathcal{P}}_{S1} = \begin{pmatrix} [\tilde{\mathbf{M}}_{\boldsymbol{\sigma}},\mathbf{R}]_{\frac{1}{2}} & \mathbf{0} \\ \mathbf{0} & [\mathbf{S},(\omega\underline{\sigma})^2\tilde{\mathbf{M}}_{\boldsymbol{\sigma}}]_{\frac{1}{2}} \end{pmatrix} = \begin{pmatrix} [\tilde{\mathbf{M}}_{\boldsymbol{\sigma}},\mathbf{R}]_{\frac{1}{2}} & \mathbf{0} \\ \mathbf{0} & (\omega\underline{\sigma})^2[\tilde{\mathbf{M}}_{\boldsymbol{\sigma}},\mathbf{R}]_{\frac{1}{2}} \end{pmatrix}.$$

The following computations are straightforward, using the simple spectral inequality (6.32). Consequently, we can derive another new preconditioner $\mathcal{P}_{S1}$, that is spectral equivalent to the interpolation preconditioner $\tilde{\mathcal{P}}_{S1}$:

$$\mathbf{x}^T[\tilde{\mathbf{M}}_{\boldsymbol{\sigma}},\mathbf{R}]_{\frac{1}{2}}\mathbf{x} = \mathbf{x}^T[\mathbf{R},\tilde{\mathbf{M}}_{\boldsymbol{\sigma}}]_{\frac{1}{2}}\mathbf{x} = \mathbf{x}^T\mathbf{M}_{\boldsymbol{\sigma},\omega}^{\frac{1}{2}}\left(\mathbf{M}_{\boldsymbol{\sigma},\omega}^{-\frac{1}{2}}(\tilde{\mathbf{M}}_{\boldsymbol{\sigma}}+(\omega\underline{\sigma})^{-2}\mathbf{K}_{\nu}\mathbf{M}_{\boldsymbol{\sigma},\omega}^{-1}\mathbf{K}_{\nu})\mathbf{M}_{\boldsymbol{\sigma},\omega}^{-\frac{1}{2}}\right)^{\frac{1}{2}}\mathbf{M}_{\boldsymbol{\sigma},\omega}^{\frac{1}{2}}\mathbf{x}$$

$$\leq \mathbf{x}^T\left(\tilde{\mathbf{M}}_{\boldsymbol{\sigma}}+(\omega\underline{\sigma})^{-1}\mathbf{M}_{\boldsymbol{\sigma},\omega}^{\frac{1}{2}}\left(\mathbf{M}_{\boldsymbol{\sigma},\omega}^{-\frac{1}{2}}\mathbf{K}_{\nu}\mathbf{M}_{\boldsymbol{\sigma},\omega}^{-1}\mathbf{K}_{\nu}\mathbf{M}_{\boldsymbol{\sigma},\omega}^{-\frac{1}{2}}\right)^{\frac{1}{2}}\mathbf{M}_{\boldsymbol{\sigma},\omega}^{\frac{1}{2}}\right)\mathbf{x}$$

$$= \mathbf{x}^T\left(\tilde{\mathbf{M}}_{\boldsymbol{\sigma}}+(\omega\underline{\sigma})^{-1}\mathbf{M}_{\boldsymbol{\sigma},\omega}^{\frac{1}{2}}\left(\mathbf{M}_{\boldsymbol{\sigma},\omega}^{-\frac{1}{2}}\mathbf{K}_{\nu}\mathbf{M}_{\boldsymbol{\sigma},\omega}^{-\frac{1}{2}}\right)\mathbf{M}_{\boldsymbol{\sigma},\omega}^{\frac{1}{2}}\right)\mathbf{x}$$

$$= \mathbf{x}^T\left(\tilde{\mathbf{M}}_{\boldsymbol{\sigma}}+(\omega\underline{\sigma})^{-1}\mathbf{K}_{\nu}\right)\mathbf{x}, \quad \forall \mathbf{x} \in (\ker\mathbf{K}_{\nu})^{\perp},$$

and

$$\mathbf{x}^T[\tilde{\mathbf{M}}_{\boldsymbol{\sigma}},\mathbf{R}]_{\frac{1}{2}}\mathbf{x} = \mathbf{x}^T[\mathbf{R},\tilde{\mathbf{M}}_{\boldsymbol{\sigma}}]_{\frac{1}{2}}\mathbf{x} = \mathbf{x}^T\mathbf{M}_{\boldsymbol{\sigma},\omega}^{\frac{1}{2}}\left(\mathbf{M}_{\boldsymbol{\sigma},\omega}^{-\frac{1}{2}}(\tilde{\mathbf{M}}_{\boldsymbol{\sigma}}+(\omega\underline{\sigma})^{-2}\mathbf{K}_{\nu}\mathbf{M}_{\boldsymbol{\sigma},\omega}^{-1}\mathbf{K}_{\nu})\mathbf{M}_{\boldsymbol{\sigma},\omega}^{-\frac{1}{2}}\right)^{\frac{1}{2}}\mathbf{M}_{\boldsymbol{\sigma},\omega}^{\frac{1}{2}}\mathbf{x}$$

$$\geq \frac{1}{\sqrt{2}}\mathbf{x}^T\left(\tilde{\mathbf{M}}_{\boldsymbol{\sigma}}+(\omega\underline{\sigma})^{-1}\mathbf{M}_{\boldsymbol{\sigma},\omega}^{\frac{1}{2}}\left(\mathbf{M}_{\boldsymbol{\sigma},\omega}^{-\frac{1}{2}}\mathbf{K}_{\nu}\mathbf{M}_{\boldsymbol{\sigma},\omega}^{-1}\mathbf{K}_{\nu}\mathbf{M}_{\boldsymbol{\sigma},\omega}^{-\frac{1}{2}}\right)^{\frac{1}{2}}\mathbf{M}_{\boldsymbol{\sigma},\omega}^{\frac{1}{2}}\right)\mathbf{x}$$

$$= \frac{1}{\sqrt{2}}\mathbf{x}^T\left(\tilde{\mathbf{M}}_{\boldsymbol{\sigma}}+(\omega\underline{\sigma})^{-1}\mathbf{M}_{\boldsymbol{\sigma},\omega}^{\frac{1}{2}}\left(\mathbf{M}_{\boldsymbol{\sigma},\omega}^{-\frac{1}{2}}\mathbf{K}_{\nu}\mathbf{M}_{\boldsymbol{\sigma},\omega}^{-\frac{1}{2}}\right)\mathbf{M}_{\boldsymbol{\sigma},\omega}^{\frac{1}{2}}\right)\mathbf{x}$$

$$= \frac{1}{\sqrt{2}}\mathbf{x}^T\left(\tilde{\mathbf{M}}_{\boldsymbol{\sigma}}+(\omega\underline{\sigma})^{-1}\mathbf{K}_{\nu}\right)\mathbf{x}, \quad \forall \mathbf{x} \in (\ker\mathbf{K}_{\nu})^{\perp}.$$

Hence, from Subsection 5.2.4, we have, that the preconditioner $\mathcal{P}_{S1}$, given by the block-diagonal matrix

$$\mathcal{P}_{S1} = \begin{pmatrix} \tilde{\mathbf{M}}_{\boldsymbol{\sigma}} + (\omega\underline{\sigma})^{-1}\mathbf{K}_{\boldsymbol{\nu}} & \mathbf{0} \\ \mathbf{0} & (\omega\underline{\sigma})^2\left(\tilde{\mathbf{M}}_{\boldsymbol{\sigma}} + (\omega\underline{\sigma})^{-1}\mathbf{K}_{\boldsymbol{\nu}}\right) \end{pmatrix}, \tag{6.41}$$

is a candidate for a parameter-robust preconditioner. Inspired by the structure of the preconditioner (6.41), we introduce the non-standard norm $\|\cdot\|_{\mathcal{P}_{S1}}$ in $\mathbf{H_0}(\mathbf{curl}, \Omega_1)^2$ by

$$\|(\mathbf{y^s}, \tilde{\mathbf{y}}^{\mathbf{c}})\|^2_{\mathcal{P}_{S1}} = (\omega\underline{\sigma})^{-1}(\nu\,\mathbf{curl}\,\tilde{\mathbf{y}}^{\mathbf{s}}, \mathbf{curl}\,\tilde{\mathbf{y}}^{\mathbf{s}})_{\mathbf{0},\Omega_1} + \underline{\sigma}^{-1}(\sigma\mathbf{y^s}, \mathbf{y^s})_{\mathbf{0},\Omega_1}$$
$$+ (\omega\underline{\sigma})(\nu\,\mathbf{curl}\,\tilde{\mathbf{y}}^{\mathbf{c}}, \mathbf{curl}\,\tilde{\mathbf{y}}^{\mathbf{c}})_{\mathbf{0},\Omega_1} + (\omega\underline{\sigma})^2\underline{\sigma}^{-1}(\sigma\mathbf{y^c}, \mathbf{y^c})_{\mathbf{0},\Omega_1}.$$

The main result is summarized in the following lemma, that claims that an inf-sup and a sup-sup condition are fulfilled with parameter-independent constants, namely $1/\sqrt{2}$ and 1.

Lemma 6.15. *We have*

$$\frac{1}{\sqrt{2}}\|(\mathbf{y^s}, \tilde{\mathbf{y}}^{\mathbf{c}})\|_{\mathcal{P}_{S1}} \leq \sup_{0 \neq (\tilde{\mathbf{v}}^{\mathbf{c}}, \mathbf{v^s}) \in \mathbf{H_0}(\mathbf{curl},\Omega_1)^2} \frac{\mathcal{A}_{F4}((\mathbf{y^s}, \tilde{\mathbf{y}}^{\mathbf{c}}), (\tilde{\mathbf{v}}^{\mathbf{c}}, \mathbf{v^s}))}{\|(\tilde{\mathbf{v}}^{\mathbf{c}}, \mathbf{v^s})\|_{\mathcal{P}_{S1}}} \leq \|(\mathbf{y^c}, \mathbf{y^s})\|_{\mathcal{P}_{S1}}, \tag{6.42}$$

for all $(\mathbf{y^s}, \tilde{\mathbf{y}}^{\mathbf{c}}) \in \mathbf{H_0}(\mathbf{curl}, \Omega_1)^2$.

Proof. Boundedness follows from reapplication of Cauchy's inequality. The lower estimate can be attained by choosing $\tilde{\mathbf{v}}^{\mathbf{c}} = \omega\underline{\sigma}\tilde{\mathbf{y}}^{\mathbf{c}} + \mathbf{y^s}$ and $\mathbf{v^s} = (\omega\underline{\sigma})^{-1}\mathbf{y^s} - \tilde{\mathbf{y}}^{\mathbf{c}}$. Note that, for this special choice of the test functions, we have $\|(\tilde{\mathbf{v}}^{\mathbf{c}}, \mathbf{v^s})\|_{\mathcal{P}_{S1}} = \sqrt{2}\|(\mathbf{y^s}, \tilde{\mathbf{y}}^{\mathbf{c}})\|_{\mathcal{P}_{S1}}$. $\square$

Furthermore, the inequalities (6.42) remain valid for the finite element subspace $\mathcal{ND}_0^0(\mathcal{T}_h)^2$, since the proof can be repeated for the finite element functions step by step. Therefore, we obtain the improved condition number estimate

$$\kappa_{\mathcal{P}_{S1}}(\mathcal{P}_{S1}^{-1}\mathcal{A}_{F4}) := \|\mathcal{P}_{S1}^{-1}\mathcal{A}_{F4}\|_{\mathcal{P}_{S1}}\|\mathcal{A}_{F4}^{-1}\mathcal{P}_{S1}\|_{\mathcal{P}_{S1}} \leq \sqrt{2} \approx 1.414.$$

This result has also been derived in [100].

6.1.4.2 Symmetric formulations ($k = 0$)

In this setting, it is convenient to start the analysis for *Formulation FEM 4* ($k = 0$).

Formulation FEM 4 ($k = 0$) We explore the 2×2 block structure of our system matrix $\mathcal{A}_{M2,0}$. In order to construct a parameter-robust and block-diagonal preconditioner, we use a Schur complement preconditioner, cf. Theorem 5.3. Since $\mathbf{L}_{\boldsymbol{\sigma}}$ is symmetric and positive definite, we can build the Schur complement

$$\mathcal{P}_0 = \begin{pmatrix} \mathbf{K}_{\boldsymbol{\nu}} + \mathbf{D}_{\boldsymbol{\sigma}}{}^T\mathbf{L}_{\boldsymbol{\sigma}}^{-1}\mathbf{D}_{\boldsymbol{\sigma}} & \mathbf{0} \\ \mathbf{0} & \mathbf{L}_{\boldsymbol{\sigma}} \end{pmatrix}.$$

Immediately, we obtain the condition number estimate

$$\kappa_{\mathcal{P}_0}(\mathcal{P}_0^{-1}\mathcal{A}_{M2,0}) := \|\mathcal{P}_0^{-1}\mathcal{A}_{M2,0}\|_{\mathcal{P}_0}\|\mathcal{A}_{M2,0}^{-1}\mathcal{P}_0\|_{\mathcal{P}_0} \leq \frac{\sqrt{5}+1}{\sqrt{5}-1} \approx 2.618. \tag{6.43}$$

Inspired by the structure of the preconditioner (6.43), we introduce the non-standard norm $\|\cdot\|_{\mathcal{P}_0}$ in $\mathbf{H_0}(\mathbf{curl}, \Omega_1) \times H_0^1(\Omega_1)$ by

$$\|(\mathbf{y}, p)\|^2_{\mathcal{P}_0} = (\nu\,\mathbf{curl}\,\mathbf{y}, \mathbf{curl}\,\mathbf{y})_{\mathbf{0},\Omega_1} + \sup_{q \in H_0^1(\Omega_1)} \frac{(\sigma\mathbf{y}, \nabla q)_{\mathbf{0},\Omega_1}}{(\sigma\nabla q, \nabla q)_{\mathbf{0},\Omega_1}} + (\sigma\nabla p, \nabla p)_{\mathbf{0},\Omega_1}.$$

The main result is summarized in the following lemma, that claims that an inf-sup and a sup-sup condition are fulfilled with parameter-independent constants, namely $(\sqrt{5}-1)/2$ and $(\sqrt{5}+1)/2$.

Lemma 6.16. *We have*

$$\frac{\sqrt{5}-1}{2}\|(\mathbf{y_0^c}, p_0^c)\|_{\mathcal{P}_0} \leq \sup_{(\mathbf{v^c}, q^c) \in \mathbf{H_0}(\mathbf{curl}, \Omega_1) \times H_0^1(\Omega_1)} \frac{\mathcal{A}_{M2,0}((\mathbf{y_0^c}, p_0^c), (\mathbf{v^c}, q^c))}{\|(\mathbf{v^c}, q^c)\|_{\mathcal{P}_0}} \leq \frac{\sqrt{5}+1}{2}\|(\mathbf{y_0^c}, p_0^c)\|_{\mathcal{P}_0},$$

(6.44)

for all $(\mathbf{y_0^c}, p_0^c) \in \mathbf{H_0}(\mathbf{curl}, \Omega_1) \times H_0^1(\Omega_1)$.

Proof. Follows from Theorem 5.3. □

Formulation FEM 3 $(k = 0)$ In this setting, again we can use the $\mathcal{P}_0$-norm to show well-posedness. The main result is summarized in the following lemma, that claims that an inf-sup and a sup-sup condition are fulfilled with parameter-independent constants, namely $1/\sqrt{2}$ and $(1 + \sqrt{5})/2$.

Lemma 6.17. *We have*

$$\frac{1}{\sqrt{2}}\|(\mathbf{y_0^c}, p_0^c)\|_{\mathcal{P}_0} \leq \sup_{(\mathbf{v^c}, q^c) \in \mathbf{H_0}(\mathbf{curl}, \Omega_1) \times H_0^1(\Omega_1)} \frac{\mathcal{A}_{M1,0}((\mathbf{y_0^c}, p_0^c), (\mathbf{v^c}, q^c))}{\|(\mathbf{v^c}, q^c)\|_{\mathcal{P}_0}} \leq \frac{1+\sqrt{5}}{2}\|(\mathbf{y_0^c}, p_0^c)\|_{\mathcal{P}_0}, \quad (6.45)$$

for all $(\mathbf{y_0^c}, p_0^c) \in \mathbf{H_0}(\mathbf{curl}, \Omega_1) \times H_0^1(\Omega_1)$.

Proof. For the proof, we split the bilinear form $\mathcal{A}_{M1,0}$ as follows:

$$\mathcal{A}_{M1,0}((\mathbf{y_0^c}, p_0^c), (\mathbf{v^c}, q^c)) = a(\mathbf{y_0^c}, \mathbf{v^c}) + b(\mathbf{v^c}, p_0^c) + b(\mathbf{y_0^c}, q^c),$$

with

$$a(\mathbf{y_0^c}, \mathbf{v^c}) := (\nu\,\mathbf{curl}\,\mathbf{y_0^c}, \mathbf{curl}\,\mathbf{v^c})_{\mathbf{0},\Omega_1}, \qquad b(\mathbf{v^c}, p_0^c) := (\sigma\mathbf{v^c}, \nabla p_0^c)_{\mathbf{0},\Omega_1},$$

and verify the conditions in the theorem of Brezzi, cf. Theorem 2.3. The bilinear forms $a(\cdot, \cdot)$ and $b(\cdot, \cdot)$ are bounded with constant 1. Furthermore, $a(\cdot, \cdot)$ is coercive on the kernel of $b(\cdot, \cdot)$, with constant 1. Indeed,

$$a(\mathbf{y_0^c}, \mathbf{y_0^c}) = (\nu\,\mathbf{curl}\,\mathbf{y_0^c}, \mathbf{curl}\,\mathbf{y_0^c})_{\mathbf{0},\Omega_1} = (\nu\,\mathbf{curl}\,\mathbf{y_0^c}, \mathbf{curl}\,\mathbf{y_0^c})_{\mathbf{0},\Omega_1} + \sup_{q \in H_0^1(\Omega_1)} \frac{(\sigma\mathbf{y_0^c}, \nabla q)_{\mathbf{0},\Omega_1}}{(\sigma\nabla q, \nabla q)_{\mathbf{0},\Omega_1}},$$

since $b(\mathbf{y_0^c}, \nabla p) = 0$ for all $p \in H_0^1(\Omega_1)$. Finally, the bilinear form $b(\cdot, \cdot)$ satisfies an inf-sup condition with constant 1. By using the special test function $\mathbf{v^c} = \nabla p_0^c$ and applying Cauchy's inequality in the denominator, we obtain

$$\sup_{\mathbf{v^c} \in \mathbf{H_0}(\mathbf{curl}, \Omega_1)} \frac{b(\mathbf{v^c}, p_0^c)}{(\nu\,\mathbf{curl}\,\mathbf{v^c}, \mathbf{curl}\,\mathbf{v^c})_{\mathbf{0},\Omega_1} + \sup_{q \in H_0^1(\Omega_1)} \frac{(\sigma\mathbf{v^c}, \nabla q)_{\mathbf{0},\Omega_1}}{(\sigma\nabla q, \nabla q)_{\mathbf{0},\Omega_1}}}$$

$$\geq \frac{(\sigma\nabla p_0^c, \nabla p_0^c)_{\mathbf{0},\Omega_1}}{\sup_{q \in H_0^1(\Omega_1)} \frac{(\sigma\nabla p^c, \nabla q)_{\mathbf{0},\Omega_1}}{(\sigma\nabla q, \nabla q)_{\mathbf{0},\Omega_1}}} \geq (\sigma\nabla p_0^c, \nabla p_0^c)_{\mathbf{0},\Omega_1}.$$

Consequently, the inf-sup and sup-sup condition for $\mathcal{A}_{M1,0}(\cdot, \cdot)$ can be derived by combining the estimates according to Theorem 2.3. □

Furthermore, the inequalities (6.45) remain valid for the finite element subspace $\mathcal{ND}_0^0(\mathcal{T}_h) \times \mathcal{S}_0^1(\mathcal{T}_h)$, since the proof can be repeated for the finite element functions step by step. Therefore, we obtain the condition number estimate

$$\kappa_{\mathcal{P}_0}(\mathcal{P}_0^{-1}\mathcal{A}_{M1,0}) := \|\mathcal{P}_0^{-1}\mathcal{A}_{M1,0}\|_{\mathcal{P}_0}\|\mathcal{A}_{M1,0}^{-1}\mathcal{P}_0\|_{\mathcal{P}_0} \leq \frac{1+\sqrt{5}}{\sqrt{2}} \approx 2.288.$$

Formulation FEM 5 $(k = 0)$ Due to the primal reformulation, we are already dealing with a symmetric and positive definite problem consisting of only one block. Anyhow, in this setting, the area of investigation is the practical realization of the regularized matrix $\mathbf{K_{r,0,\nu}}$.

Lemma 6.18. *We have*

$$(\sigma \nabla P_\sigma(\mathbf{y}), \nabla P_\sigma(\mathbf{y}))_{\mathbf{0},\Omega_1} = \sup_{p \in H_0^1(\Omega_1)} \frac{(\sigma \mathbf{y}, \nabla p)^2_{\mathbf{0},\Omega_1}}{(\sigma \nabla p, \nabla p)_{\mathbf{0},\Omega_1}},$$

for all $\mathbf{y} \in \mathbf{H_0}(\mathbf{curl}, \Omega_1)$.

Proof. Using the definition of the Helmholtz projection P_σ, we have

$$(\sigma \nabla P_\sigma(\mathbf{y}), \nabla P_\sigma(\mathbf{y}))_{\mathbf{0},\Omega_1} = \frac{(\sigma \mathbf{y}, \nabla P_\sigma(\mathbf{y}))^2_{\mathbf{0},\Omega_1}}{(\sigma \nabla P_\sigma(\mathbf{y}), \nabla P_\sigma(\mathbf{y}))_{\mathbf{0},\Omega_1}} \leq \sup_{p \in H_0^1(\Omega_1)} \frac{(\sigma \mathbf{y}, \nabla p)^2_{\mathbf{0},\Omega_1}}{(\sigma \nabla p, \nabla p)_{\mathbf{0},\Omega_1}}.$$

On the other hand, exploiting again the definition of P_σ and using Cauchy's inequality, we have

$$\sup_{p \in H_0^1(\Omega_1)} \frac{(\sigma \mathbf{y}, \nabla p)^2_{\mathbf{0},\Omega_1}}{(\sigma \nabla p, \nabla p)_{\mathbf{0},\Omega_1}} = \sup_{p \in H_0^1(\Omega_1)} \frac{(\sigma \nabla P_\sigma(\mathbf{y}), \nabla p)^2_{\mathbf{0},\Omega_1}}{(\sigma \nabla p, \nabla p)_{\mathbf{0},\Omega_1}} \leq (\sigma \nabla P_\sigma(\mathbf{y}), \nabla P_\sigma(\mathbf{y}))_{\mathbf{0},\Omega_1}.$$

$\square$

Furthermore, the identity can also be verified in the finite element subspaces $\mathcal{ND}_0^0(\mathcal{T}_h)$, where the supremum is taken over $\mathcal{S}_0^1(\mathcal{T}_h)$. Consequently, the matrix identity $\mathbf{K_{r,0,\nu}} = \mathbf{K_\nu} + \mathbf{D_\sigma}^T \mathbf{L_\sigma}^{-1} \mathbf{D_\sigma}$ follows.

6.1.5 Summary

We table the condition number κ and the theoretical number of MinRes iterations *maxiter* needed, for reducing the initial error by a factor of 10^{-8}, if the proposed block-diagonal preconditioners are used. Furthermore, we collect the diagonal blocks, that are needed for the application of the block-diagonal preconditioner. For the modes $k = 1$, and therefore also for all modes $k = 1, \dots, N$, we obtain:

	κ	maxiter	diagonal blocks
Formulation FEM 1	1.414	22	$\mathbf{K_\nu} + \mathbf{M_{\sigma,\omega}}$
Formulation FEM 2	1.414	22	$\mathbf{K_\nu} + \mathbf{M_{\sigma,\omega}}$
Formulation FEM 3	6.864	132	$\mathbf{K_\nu} + \mathbf{M_{\sigma,\omega}}, \mathbf{L_{\sigma,\omega}}$
Formulation FEM 4	2.828	52	$\mathbf{K_\nu} + \mathbf{M_{\sigma,\omega}}, \mathbf{L_{\sigma,\omega}}$
Formulation FEM 5	2.828	52	$\mathbf{K_\nu} + \mathbf{M_{\sigma,\omega}}$
Formulation FEM 6	1.414	22	$\tilde{\mathbf{M}}_\sigma + (\omega\underline{\sigma})^{-1}\mathbf{K_\nu}$

For the modes $k = 0$, we obtain:

	κ	maxiter	diagonal blocks
Formulation FEM 3 $(k = 0)$	2.288	42	$\mathbf{K_\nu} + \mathbf{D_\sigma}^T \mathbf{L_\sigma}^{-1} \mathbf{D_\sigma}, \mathbf{L_\sigma}$
Formulation FEM 4 $(k = 0)$	2.618	48	$\mathbf{K_\nu} + \mathbf{D_\sigma}^T \mathbf{L_\sigma}^{-1} \mathbf{D_\sigma}, \mathbf{L_\sigma}$
Formulation FEM 5 $(k = 0)$	-	-	$\mathbf{K_\nu} + \mathbf{D_\sigma}^T \mathbf{L_\sigma}^{-1} \mathbf{D_\sigma}$

It is obvious, that all these estimates are uniform in the discretization parameters h, ω, N and the model parameters ν and σ. The realization of the diagonal blocks $\mathbf{K_\nu} + \mathbf{M_{\sigma,\omega}}$, $\mathbf{K_\nu} + \mathbf{D_\sigma}^T \mathbf{L_\sigma}^{-1} \mathbf{D_\sigma}$ and $\mathbf{L_{\sigma,\omega}}$ is discussed in Chapter 8.

6.1.6   Numerics

In order to confirm our theoretical results numerically, we report on our first numerical tests for an academic example. Therefore, we consider the solution of the system corresponding to the block of the mode $k = 1$. The numerical results presented in this section were attained using ParMax[1]. First, we demonstrate the robustness of the block-diagonal preconditioners with respect to the frequency ω and the conductivity σ. Therefore, for the solution of the preconditioning equations arising from the diagonal blocks, we use the sparse direct solver UMFPACK[2] that is very efficient for several thousand unknowns in the case of three dimensional problems [45, 46, 47].

In the following numerical experiments, we provide the number of MinRes iterations needed for reducing the initial residual by a factor of 10^{-8} for different ω, σ and h for Problem 6.1–6.6. These numerical experiments were performed for a three-dimensional linear problem on the unit cube $\Omega_1 = (0,1)^3$, discretized by tetrahedra. Furthermore the piecewise constant conductivity σ is given by

$$\sigma = \left\{ \begin{array}{ll} \sigma_1 & \text{in } \Omega_a = \{(x,y,z)^T \in [0,1]^3 : z > 0.5\} \\ \sigma_2 & \text{in } \Omega_b = \{(x,y,z)^T \in [0,1]^3 : z \leq 0.5\} \end{array} \right. . \tag{6.46}$$

Formulation FEM 2   Table 6.1 and Table 6.2 provide the number of MinRes iterations needed for reducing the initial residual by a factor 10^{-8}. These experiments demonstrate the independence of the MinRes convergence rate on the parameters ω and σ, and the mesh size h since the number of iterations is bounded by 22 for all computed constellations.

Formulation FEM 3   Table 6.3 and Table 6.4 provide the number of MinRes iterations needed for reducing the initial residual by a factor 10^{-8}. These experiments demonstrate the independence of the MinRes convergence rate on the parameters ω and σ, and the mesh size h since the number of iterations is bounded by 22 for all computed constellations.

Formulation FEM 4   Table 6.5 and Table 6.6 provide the same experiments for *Formulation FEM 4*. Again, the numerical results show robustness of our preconditioner, since the number of iterations is bounded by 23 for all computed constellations.

Formulation FEM 5   Table 6.7 and Table 6.8 provide the same experiments for *Formulation FEM 6*. The application of the Helmholtz projector P_h is realized via the Schur complement $\mathbf{D}_{\sigma,\omega}{}^T \mathbf{L}_{\sigma,\omega}{}^{-1} \mathbf{D}_{\sigma,\omega}$. Again, the numerical results show robustness of our preconditioner, since the number of iterations is bounded by 27 for all computed constellations.

The numerical experiments presented in this section clearly demonstrate the theoretical robustness of the proposed block-diagonal preconditioners. Especially, we want to point out, that not only the robustness with respect to the space discretization parameter h and the time discretization parameters ω and N, but also the robustness with respect to the model parameters σ and ν, are well confirmed by our numerical tests. In large-scale applications, the realization of the diagonal preconditioner by using a sparse direct solver like UMFPACK is illusive. The practical realization of our preconditioners is addressed in Chapter 8.

6.1.7   Error analysis

For an analysis of the full space and time discretization error of the MH-FEM method applied to the eddy current problem in the case of a bounded domain, we refer to [17], where, under certain regularity assumptions on the right hand side $\mathbf{u}$, an error estimate of the kind $\|\mathbf{y} - \mathbf{y_{Nh}}\| = \mathcal{O}(N^{-1} + h)$ is shown. Furthermore, we refer to Subsection 6.2.6, where a discretization error analysis for the MH-FEM-BEM method applied to the eddy current problem in an unbounded domain is given in detail.

---

[1] `http://www.numa.uni-linz.ac.at/P19255/software.shtml`
[2] `http://www.cise.ufl.edu/research/sparse/umfpack/`

DOF	ω										
	10^{-10}	10^{-8}	10^{-6}	10^{-4}	10^{-2}	1	10^2	10^4	10^6	10^8	10^{10}
38	4	4	2	3	3	9	16	8	4	4	2
196	6	4	2	3	3	9	16	10	6	4	4
1208	6	4	4	2	3	9	19	14	6	4	4
16736	6	4	4	2	3	9	20	20	8	4	4
62048	8	4	4	2	3	7	19	22	8	4	4

Table 6.1: Formulation FEM 2. Number of MinRes iterations for different values of ω and various DOF using the EXACT version of the preconditioner with UMFPACK for $\mathbf{K_\nu} + \mathbf{M_{\sigma,\omega}}$ ($\nu = \sigma = 1$).

DOF	σ_2										
	10^{-10}	10^{-8}	10^{-6}	10^{-4}	10^{-2}	1	10^2	10^4	10^6	10^8	10^{10}
38	7	7	7	7	7	9	18	14	6	4	4
196	4	5	5	7	7	9	17	9	9	9	9
1208	6	5	5	7	7	9	19	12	9	9	9
16736	6	5	5	5	7	9	18	17	9	9	9
62048	8	4	5	5	7	7	17	18	8	7	7

Table 6.2: Formulation FEM 2. Number of MinRes iterations for different values of σ_2 and various DOF using the EXACT version of the preconditioner with UMFPACK for $\mathbf{K_\nu} + \mathbf{M_{\sigma,\omega}}$ ($\nu = \omega = \sigma_1 = 1$).

DOF	ω										
	10^{-10}	10^{-8}	10^{-6}	10^{-4}	10^{-2}	1	10^2	10^4	10^6	10^8	10^{10}
54	2	2	2	2	2	2	2	2	2	2	1
250	6	6	4	6	6	12	17	9	5	5	4
1458	10	8	6	4	6	12	20	13	7	5	5
9826	14	8	6	4	6	12	22	19	7	5	5
71874	15	9	8	4	6	12	22	23	9	5	5

Table 6.3: Formulation FEM 3. Number of MinRes iterations for different values of ω and various DOF using the EXACT version of the preconditioner with UMFPACK for $\mathbf{K_\nu} + \mathbf{M_{\sigma,\omega}}$ and $\mathbf{L_{\sigma,\omega}}$ ($\nu = \sigma = 1$).

DOF	σ_2										
	10^{-10}	10^{-8}	10^{-6}	10^{-4}	10^{-2}	1	10^2	10^4	10^6	10^8	10^{10}
54	2	2	2	2	2	2	2	2	2	2	1
250	12	12	12	12	12	12	21	12	12	12	12
1458	12	10	10	8	10	12	22	14	12	12	12
9826	14	10	10	8	10	12	21	19	10	10	10
71874	15	12	10	10	10	12	20	19	10	10	10

Table 6.4: Formulation FEM 3. Number of MinRes iterations for different values of σ_2 and various DOF using the EXACT version of the preconditioner with UMFPACK for $\mathbf{K_\nu} + \mathbf{M_{\sigma,\omega}}$ and $\mathbf{L_{\sigma,\omega}}$ ($\nu = \omega = \sigma_1 = 1$).

DOF	ω										
	10^{-10}	10^{-8}	10^{-6}	10^{-4}	10^{-2}	1	10^2	10^4	10^6	10^8	10^{10}
54	2	2	2	2	2	2	2	2	2	2	1
250	10	8	6	8	8	14	18	11	7	7	5
1458	12	10	8	6	8	14	20	15	9	7	7
9826	15	10	10	6	8	14	22	19	9	7	7
71874	16	11	10	7	8	12	22	23	11	7	7

Table 6.5: Formulation FEM 4. Number of MinRes iterations for different values of ω and various DOF using the EXACT version of the preconditioner with UMFPACK for $\mathbf{K_\nu} + \mathbf{M_{\sigma,\omega}}$ and $\mathbf{L_{\sigma,\omega}}$ ($\nu = \sigma = 1$).

DOF	σ_2										
	10^{-10}	10^{-8}	10^{-6}	10^{-4}	10^{-2}	1	10^2	10^4	10^6	10^8	10^{10}
54	2	2	2	2	2	2	2	2	2	2	1
250	14	14	14	14	14	14	22	13	13	12	12
1458	12	12	12	10	12	14	22	15	14	14	14
9826	15	12	12	11	12	14	22	19	12	12	12
71874	16	14	12	12	10	12	21	19	12	12	12

Table 6.6: Formulation FEM 4. Number of MinRes iterations for different values of σ_2 and various DOF using the EXACT version of the preconditioner with UMFPACK for $\mathbf{K}_\nu + \mathbf{M}_{\sigma,\omega}$ and $\mathbf{L}_{\sigma,\omega}$ ($\nu = \omega = \sigma_1 = 1$).

DOF	ω										
	10^{-10}	10^{-8}	10^{-6}	10^{-4}	10^{-2}	1	10^2	10^4	10^6	10^8	10^{10}
38	5	5	5	5	6	10	17	8	6	6	6
196	9	8	8	8	8	12	22	13	10	10	10
1208	11	9	9	9	10	14	24	17	11	11	11
16736	12	10	10	10	10	14	27	25	13	13	13
62048	13	9	8	8	8	12	24	25	13	9	9

Table 6.7: Formulation FEM 5. Number of MinRes iterations for different values of ω and various DOF using the EXACT version of the preconditioner with UMFPACK for $\mathbf{K}_\nu + \mathbf{M}_{\sigma,\omega}$ ($\nu = \sigma = 1$).

DOF	σ_2										
	10^{-10}	10^{-8}	10^{-6}	10^{-4}	10^{-2}	1	10^2	10^4	10^6	10^8	10^{10}
38	22	20	16	14	10	10	20	14	9	8	8
196	6	7	8	10	10	12	21	14	13	12	12
1208	9	8	10	10	12	14	24	16	12	12	12
16736	11	8	10	12	12	14	24	22	12	12	12
62048	13	8	9	10	10	12	22	22	12	12	12

Table 6.8: Formulation FEM 5. Number of MinRes iterations for different values of σ_2 and various DOF using the EXACT version of the preconditioner with UMFPACK for $\mathbf{K}_\nu + \mathbf{M}_{\sigma,\omega}$ ($\nu = \omega = \sigma_1 = 1$).

6.2 Symmetric FEM-BEM couplings

In the previous section, we have presented several variational formulations which aim a FEM discretization. In all the cases, we restricted the analysis to the bounded domain Ω_1. Now we want the domain to be unbounded. Therefore, in this section, we consider the eddy current problem in the full computational domain $\mathbb{R}^3$. Hence, we are dealing with the following system of partial differential equations

$$
\begin{cases}
\sigma \dfrac{\partial \mathbf{y}}{\partial t} + \mathbf{curl}(\nu \, \mathbf{curl} \, \mathbf{y}) = \mathbf{u}, & \text{in } \Omega_1 \times (0, T), \\
\operatorname{div}(\sigma \mathbf{y}) = 0, & \text{in } \Omega_1 \times (0, T), \\
\mathbf{curl}(\mathbf{curl} \, \mathbf{y}) = \mathbf{0}, & \text{in } \Omega_2 \times (0, T), \\
\operatorname{div} \mathbf{y} = 0, & \text{in } \Omega_2 \times (0, T), \\
\mathbf{y} = \mathcal{O}(|\mathbf{x}|^{-1}), & \text{for } |\mathbf{x}| \to \infty, \\
\mathbf{curl} \, \mathbf{y} = \mathcal{O}(|\mathbf{x}|^{-1}), & \text{for } |\mathbf{x}| \to \infty, \\
\mathbf{y}(0) = \mathbf{y}(T), & \text{in } \Omega_1, \\
\mathbf{y}|_{\Omega_1} \times \mathbf{n} = \mathbf{y}|_{\Omega_2} \times \mathbf{n}, & \text{on } \Gamma \times (0, T), \\
\nu \, \mathbf{curl} \, \mathbf{y}|_{\Omega_1} \times \mathbf{n} = \mathbf{curl} \, \mathbf{y}|_{\Omega_2} \times \mathbf{n}, & \text{on } \Gamma \times (0, T).
\end{cases}
\tag{6.47}
$$

As already exposed in Chapter 3, the application of the BEM is restricted to the exterior domain Ω_2, with homogeneous properties of the underlying partial differential equations, i.e., $\nu|_{\Omega_2} = const$, $\sigma|_{\Omega_2} = 0$, and $\mathbf{u}|_{\Omega_2} = \mathbf{0}$.

6.2.1 Multiharmonic discretization

Following Chapter 4, we assume that the periodic right hand side $\mathbf{u}$ is given by a multiharmonic excitation in terms of a truncated Fourier series, cf. (6.4). Consequently, we have, that the time-periodic solution $\mathbf{y}$, also can be expressed in terms of the same frequency ω and the amplitudes $\mathbf{y_k^c}$ and $\mathbf{y_k^s}$, i.e.,

$$
\mathbf{y}(\mathbf{x}, t) = \sum_{k=0}^{N} \mathbf{y_k^c}(\mathbf{x}) \cos(k\omega t) + \mathbf{y_k^s}(\mathbf{x}) \sin(k\omega t).
\tag{6.48}
$$

Using multiharmonic representation of the solution, we can rewrite the eddy current problem (6.47) in the frequency domain as follows: For $k = 1, \ldots, N$, find $(\mathbf{y_k^c}, \mathbf{y_k^s})$, such that

$$
\begin{cases}
k\omega\sigma \, \mathbf{y_k^s} + \mathbf{curl}(\nu \, \mathbf{curl} \, \mathbf{y_k^c}) = \mathbf{u_k^c}, & \text{in } \Omega_1, \\
-k\omega\sigma \, \mathbf{y_k^c} + \mathbf{curl}(\nu \, \mathbf{curl} \, \mathbf{y_k^s}) = \mathbf{u_k^s}, & \text{in } \Omega_1, \\
\mathbf{curl}(\mathbf{curl} \, \mathbf{y_k^j}) = \mathbf{0}, & \text{in } \Omega_2, j \in \{c, s\}, \\
\operatorname{div} \mathbf{y_k^j} = 0, & \text{in } \Omega_2, j \in \{c, s\}, \\
\mathbf{y_k^j} = \mathcal{O}(|\mathbf{x}|^{-1}), & \text{for } |\mathbf{x}| \to \infty, j \in \{c, s\}, \\
\mathbf{curl} \, \mathbf{y_k^j} = \mathcal{O}(|\mathbf{x}|^{-1}), & \text{for } |\mathbf{x}| \to \infty, j \in \{c, s\}, \\
\mathbf{y_k^j}|_{\Omega_1} \times \mathbf{n} = \mathbf{y_k^j}|_{\Omega_2} \times \mathbf{n}, & \text{on } \Gamma, j \in \{c, s\}, \\
\nu \, \mathbf{curl} \, \mathbf{y_k^j}|_{\Omega_1} \times \mathbf{n} = \mathbf{curl} \, \mathbf{y_k^j}|_{\Omega_2} \times \mathbf{n}, & \text{on } \Gamma, j \in \{c, s\}.
\end{cases}
\tag{6.49}
$$

As already discussed in the previous section, we drop the divergence condition imposed on the solution in the interior domain Ω_1. Furthermore, for the mode $k = 0$, we are dealing with the following

problem:

$$
\begin{cases}
\mathbf{curl}(\nu\,\mathbf{curl}\,\mathbf{y_0^c}) = \mathbf{u_0^c}, & \text{in } \Omega_1, \\
\operatorname{div}(\sigma\mathbf{y^c}) = 0, & \text{in } \Omega_1, \\
\mathbf{curl}(\mathbf{curl}\,\mathbf{y_0^c}) = \mathbf{0}, & \text{in } \Omega_2, \\
\operatorname{div}\mathbf{y_0^c} = 0, & \text{in } \Omega_2, \\
\mathbf{y_0^c} = \mathcal{O}(|\mathbf{x}|^{-1}), & \text{for } |\mathbf{x}| \to \infty, \\
\mathbf{curl}\,\mathbf{y_0^c} = \mathcal{O}(|\mathbf{x}|^{-1}), & \text{for } |\mathbf{x}| \to \infty, \\
\mathbf{y_0^c}|_{\Omega_1} \times \mathbf{n} = \mathbf{y_0^c}|_{\Omega_2} \times \mathbf{n}, & \text{on } \Gamma, \\
\nu\,\mathbf{curl}\,\mathbf{y_0^c}|_{\Omega_1} \times \mathbf{n} = \mathbf{curl}\,\mathbf{y_0^c}|_{\Omega_2} \times \mathbf{n}, & \text{on } \Gamma.
\end{cases}
\tag{6.50}
$$

These systems of partial differential equations are the starting point for the derivation of a variational formulation and the discretization in space by means of the finite element - boundary element coupling method, i.e., each Fourier coefficient $\mathbf{y_k^j}$ is approximated in terms of a FEM-BEM coupling method. Since the part corresponding to the time derivative vanishes for the case $k = 0$, this one is fundamentally different to the cases $k = 1, \ldots N$. Therefore, the analysis of this case has to be done in a separate fashion.

6.2.2   Symmetric variational formulations for FEM-BEM

In this subsection, we present different variational formulations for the frequency domain equations (6.49). We perform a symmetric coupling method to reduce the unbounded exterior domain Ω_2 to the boundary Γ. Since, for all modes $k = 1, \ldots, N$ the systems (6.49) have the same structure, we concentrate on the time-harmonic case, i.e., $k = 1$. The analysis for the remaining modes can be deduced by formally setting $\omega = k\omega$.

Furthermore, we also derive a variational formulation for (6.50).

6.2.2.1   Symmetric formulations ($k = 1$)

We start by deriving the variational formulations for (6.49).

Formulation FEM-BEM 1   In Ω_1, we use the approach of *Formulation FEM 1*, and therefore, we do not have to incorporate the gauging condition explicitly. Deriving the variational formulation and integrating by parts once more in the exterior domain yields: Find $(\mathbf{y^c}, \mathbf{y^s}) \in \mathbf{H}(\mathbf{curl}, \Omega_1)^2$ such that

$$
\begin{cases}
\omega(\sigma\mathbf{y^s}, \mathbf{v^c})_{\mathbf{0},\Omega_1} + (\nu\,\mathbf{curl}\,\mathbf{y^c}, \mathbf{curl}\,\mathbf{v^c})_{\mathbf{0},\Omega_1} - \langle \boldsymbol{\gamma}_\mathbf{N}\mathbf{y^c}, \boldsymbol{\gamma}_\mathbf{D}\mathbf{v^c}\rangle_\tau = \langle \mathbf{u^c}, \mathbf{v^c}\rangle, \\
-\omega(\sigma\mathbf{y^c}, \mathbf{v^s})_{\mathbf{0},\Omega_1} + (\nu\,\mathbf{curl}\,\mathbf{y^s}, \mathbf{curl}\,\mathbf{v^s})_{\mathbf{0},\Omega_1} - \langle \boldsymbol{\gamma}_\mathbf{N}\mathbf{y^s}, \boldsymbol{\gamma}_\mathbf{D}\mathbf{v^s}\rangle_\tau = \langle \mathbf{u^s}, \mathbf{v^s}\rangle,
\end{cases}
$$

for all $(\mathbf{v^c}, \mathbf{v^s}) \in \mathbf{H}(\mathbf{curl}, \Omega_1)^2$. We are now in the position to state the symmetric coupled variational problem. Introducing the Neumann data of $\mathbf{y^c}$ and $\mathbf{y^s}$ as additional unknowns, i.e.,

$$
\boldsymbol{\lambda^c} := \boldsymbol{\gamma}_\mathbf{N}\mathbf{y^c} \quad \text{and} \quad \boldsymbol{\lambda^s} := \boldsymbol{\gamma}_\mathbf{N}\mathbf{y^s},
$$

and using the Calderon projection (2.22) for both, the cosine and the sine component, allow us to state the eddy current problem in a framework, that is suited for a FEM-BEM discretization. For simplicity, we introduce the abbreviation

$$
\Upsilon := (\mathbf{y^s}, \boldsymbol{\lambda^s}, \mathbf{y^c}, \boldsymbol{\lambda^c}) \quad \text{and} \quad \Theta := (\mathbf{v^c}, \boldsymbol{\mu^c}, \mathbf{v^s}, \boldsymbol{\mu^s}),
$$

and the corresponding product space

$$
\mathcal{W} := \mathbf{H}(\mathbf{curl}, \Omega_1) \times \mathbf{H}_\|^{-\frac{1}{2}}(\operatorname{div}_\Gamma 0, \Gamma) \times \mathbf{H}(\mathbf{curl}, \Omega_1) \times \mathbf{H}_\|^{-\frac{1}{2}}(\operatorname{div}_\Gamma 0, \Gamma).
$$

Therefore, we end up with the weak formulation of the coupled system: Find $\Upsilon \in \mathcal{W}$, such that

$$
\begin{cases}
\omega(\sigma \mathbf{y^s}, \mathbf{v^c})_{\mathbf{0},\Omega_1} + (\nu\,\mathbf{curl}\,\mathbf{y^c}, \mathbf{curl}\,\mathbf{v^c})_{\mathbf{0},\Omega_1} - \langle \mathbf{N}(\boldsymbol{\gamma_D}\mathbf{y^c}), \boldsymbol{\gamma_D}\mathbf{v^c}\rangle_\tau + \langle \mathbf{B}(\boldsymbol{\lambda^c}), \boldsymbol{\gamma_D}\mathbf{v^c}\rangle_\tau = \langle \mathbf{u^c}, \mathbf{v^c}\rangle, \\
\qquad\qquad \langle \boldsymbol{\mu^c}, (\mathbf{C}-\mathbf{Id})(\boldsymbol{\gamma_D}\mathbf{y^c})\rangle_\tau - \langle \boldsymbol{\mu^c}, \mathbf{A}(\boldsymbol{\lambda^c})\rangle_\tau = 0, \\
-\omega(\sigma \mathbf{y^c}, \mathbf{v^s})_{\mathbf{0},\Omega_1} + (\nu\,\mathbf{curl}\,\mathbf{y^s}, \mathbf{curl}\,\mathbf{v^s})_{\mathbf{0},\Omega_1} - \langle \mathbf{N}(\boldsymbol{\gamma_D}\mathbf{y^s}), \boldsymbol{\gamma_D}\mathbf{v^s}\rangle_\tau + \langle \mathbf{B}(\boldsymbol{\lambda^s}), \boldsymbol{\gamma_D}\mathbf{v^s}\rangle_\tau = \langle \mathbf{u^s}, \mathbf{v^s}\rangle, \\
\qquad\qquad \langle \boldsymbol{\mu^s}, (\mathbf{C}-\mathbf{Id})(\boldsymbol{\gamma_D}\mathbf{y^s})\rangle_\tau - \langle \boldsymbol{\mu^s}, \mathbf{A}(\boldsymbol{\lambda^s})\rangle_\tau = 0,
\end{cases}
\tag{6.51}
$$

for all $\Theta \in \mathcal{W}$. Consequently, the corresponding variational problem can be stated as follows.

Problem 6.19 (FEM-BEM formulation)**.** *Find $\Upsilon \in \mathcal{W}$, such that*

$$
\mathcal{A}_{B1}\left((\Upsilon, \Theta)\right) = \int_{\Omega_1} [\mathbf{u^c} \cdot \mathbf{v^c} + \mathbf{u^s} \cdot \mathbf{v^s}]\,\mathrm{d}\mathbf{x},
\tag{6.52}
$$

for all test functions $\Theta \in \mathcal{W}$. Here the symmetric and indefinite bilinear form $\mathcal{A}_{B1}$ is given by

$$
\begin{aligned}
\mathcal{A}_{B1}(\Upsilon, \Theta) := \mathcal{A}_{F1}((\mathbf{y^c}, \mathbf{y^s}), (\mathbf{v^c}, \mathbf{v^s})) + \sum_{j \in \{c,s\}} \Big[&- \langle \mathbf{N}(\boldsymbol{\gamma_D}\mathbf{y^j}), \boldsymbol{\gamma_D}\mathbf{v^j}\rangle_\tau + \langle \mathbf{B}(\boldsymbol{\lambda^j}), \boldsymbol{\gamma_D}\mathbf{v^j}\rangle_\tau \\
&+ \big\langle \boldsymbol{\mu^j}, (\mathbf{C}-\mathbf{Id})(\boldsymbol{\gamma_D}\mathbf{y^j})\big\rangle_\tau - \big\langle \boldsymbol{\mu^j}, \mathbf{A}(\boldsymbol{\lambda^j})\big\rangle_\tau \Big].
\end{aligned}
\tag{6.53}
$$

Problem 6.19 has a unique solution $\Upsilon \in \mathcal{W}$, cf. Lemma 6.24.

Remark 6.20. *It is clear, that, in order to incorporate the divergence constraint on $\mathbf{y}$ in an explicit way, the corresponding FEM-BEM formulations to the FEM formulations Formulation FEM 3, Formulation FEM 4, and Formulation FEM 5 can be derived and analyzed in an analogous way.*

6.2.2.2 Symmetric formulations ($k = 0$)

We continue by deriving variational formulations for (6.50).

Formulation FEM-BEM 3 ($k = 0$) As already mentioned, due to the lack of a lower order term, it is essential, to incorporate the gauging conditions $\mathrm{div}(\sigma \mathbf{y_0^c}) = 0$ in a mixed variational framework.

Problem 6.21 (Mixed formulation FEM-BEM)**.** *Find $(\mathbf{y_0^c}, \boldsymbol{\lambda_0^c}, p_0^c) \in \mathbf{H_0}(\mathbf{curl}, \Omega_1) \times \mathbf{H}_\|^{-\frac{1}{2}}(\mathrm{div}_\Gamma\, 0, \Gamma) \times \dot{H}^1(\Omega_1)$, such that*

$$
\mathcal{A}_{B3,0}\left((\mathbf{y_0^c}, \boldsymbol{\lambda_0^c}, p_0^c), (\mathbf{v^c}, \boldsymbol{\mu^c}, q^c)\right) = \int_{\Omega_1} \mathbf{u_0^c} \cdot \mathbf{v^c}\mathrm{d}\mathbf{x},
\tag{6.54}
$$

for all test functions $(\mathbf{v^c}, \boldsymbol{\mu^c}, q^c) \in \mathbf{H_0}(\mathbf{curl}, \Omega_1) \times \mathbf{H}_\|^{-\frac{1}{2}}(\mathrm{div}_\Gamma\, 0, \Gamma) \times \dot{H}^1(\Omega_1)$. Here the symmetric and indefinite bilinear form $\mathcal{A}_{B3,0}$ is given by

$$
\begin{aligned}
\mathcal{A}_{B3,0}\left((\mathbf{y_0^c}, \boldsymbol{\lambda_0^c}, p_0^c), (\mathbf{v^c}, \boldsymbol{\mu^c}, q^c)\right) := \mathcal{A}_{M1,0}&((\mathbf{y_0^c}, p_0^c), (\mathbf{v^c}, q^c)) \\
&- \langle \mathbf{N}(\boldsymbol{\gamma_D}\mathbf{y_0^c}), \boldsymbol{\gamma_D}\mathbf{v^c}\rangle_\tau + \langle \mathbf{B}(\boldsymbol{\lambda_0^c}), \boldsymbol{\gamma_D}\mathbf{v^c}\rangle_\tau \\
&+ \big\langle \boldsymbol{\mu^c}, (\mathbf{C}-\mathbf{Id})(\boldsymbol{\gamma_D}\mathbf{y_0^c})\big\rangle_\tau - \big\langle \boldsymbol{\mu^c}, \mathbf{A}(\boldsymbol{\lambda_0^c})\big\rangle_\tau.
\end{aligned}
\tag{6.55}
$$

Problem 6.21 has a unique solution $(\mathbf{y_0^c}, \boldsymbol{\lambda_0^c}, p_0^c)$, cf. Lemma 6.27. Additionally, for a weakly divergence-free source $\mathbf{u}$, cf. (6.5), the solution $\mathbf{y_0^c} \in \mathbf{H_0}(\mathbf{curl}, \Omega_1)$ is weakly divergence-free as well, cf. (6.11), and the Lagrange parameter p_0^c vanishes at the solution, i.e., $p_0^c = 0$.

Formulation FEM-BEM 4 $(k = 0)$ Since at the solution $(\mathbf{y_0^c}, p_0^c)$ of Problem 6.21, the Lagrange parameter vanishes, i.e., $p_0^c = 0$, we can add a suitable symmetric bilinear form to $\mathcal{A}_{B3,0}(\cdot, \cdot)$. Indeed, we choose $c(\cdot, \cdot)$ as given in (6.27).

Problem 6.22 (Mixed formulation FEM-BEM with exact modification).   *Find* $(\mathbf{y_0^c}, \boldsymbol{\lambda_0^c}, p_0^c) \in$
$\mathbf{H_0}(\mathbf{curl}, \Omega_1) \times \mathbf{H}_\|^{-\frac{1}{2}}(\mathrm{div}_\Gamma\, 0, \Gamma) \times \dot{H}^1(\Omega_1)$, *such that*

$$\mathcal{A}_{B4,0}\left((\mathbf{y_0^c}, \boldsymbol{\lambda_0^c}, p_0^c), (\mathbf{v^c}, \boldsymbol{\mu^c}, q^c)\right) = \int_{\Omega_1} \mathbf{u_0^c} \cdot \mathbf{v^c} \mathrm{d}\mathbf{x}, \tag{6.56}$$

for all test functions $(\mathbf{v^c}, \boldsymbol{\mu^c}, q^c) \in \mathbf{H_0}(\mathbf{curl}, \Omega_1) \times \mathbf{H}_\|^{-\frac{1}{2}}(\mathrm{div}_\Gamma\, 0, \Gamma) \times \dot{H}^1(\Omega_1)$. *Here the symmetric and indefinite bilinear form* $\mathcal{A}_{B4,0}$ *is given by*

$$\mathcal{A}_{B4,0}\left((\mathbf{y_0^c}, \boldsymbol{\lambda_0^c}, p_0^c), (\mathbf{v^c}, \boldsymbol{\mu^c}, q^c)\right) := \mathcal{A}_{B3,0}\left((\mathbf{y_0^c}, \boldsymbol{\lambda_0^c}, p_0^c), (\mathbf{v^c}, \boldsymbol{\mu^c}, q^c)\right) - (\sigma \nabla p_0^c, \nabla q^c)_{\mathbf{0}, \Omega_1}. \tag{6.57}$$

Problem 6.22 has a unique solution $(\mathbf{y_0^c}, p_0^c)$, cf. Lemma 6.26. Additionally, the solution of Problem 6.22 also solves Problem 6.21, and vice versa.

Formulation FEM-BEM 5 $(k = 0)$ Finally, we give a primal version of Problem 6.22.

Problem 6.23 (Primal formulation FEM-BEM with exact modification).   *Find* $(\mathbf{y_0^c}, \boldsymbol{\lambda_0^c}) \in$
$\mathbf{H_0}(\mathbf{curl}, \Omega_1) \times \mathbf{H}_\|^{-\frac{1}{2}}(\mathrm{div}_\Gamma\, 0, \Gamma)$, *such that*

$$\mathcal{A}_{B3,0}\left((\mathbf{y_0^c}, \boldsymbol{\lambda_0^c}), (\mathbf{v^c}, \boldsymbol{\mu^c})\right) = \int_{\Omega_1} \mathbf{u_0^c} \cdot \mathbf{v^c} \mathrm{d}\mathbf{x}, \tag{6.58}$$

for all test functions $\mathbf{v_0^c} \in \mathbf{H_0}(\mathbf{curl}, \Omega_1)$. *Here the symmetric and positive definite bilinear form* $\mathcal{A}_{BF3,0}$ *is given by*

$$\begin{aligned}
\mathcal{A}_{B3,0}\left((\mathbf{y_0^c}, \boldsymbol{\lambda_0^c}), (\mathbf{v^c}, \boldsymbol{\mu^c})\right) &:= (\nu \,\mathbf{curl}\, \mathbf{y_0^c}, \mathbf{curl}\, \mathbf{v^c})_{\mathbf{0}, \Omega_1} + (\sigma \nabla \dot{P}_\sigma(\mathbf{y_0^c}), \nabla \dot{P}_\sigma(\mathbf{v^c}))_{\mathbf{0}, \Omega_1} \\
&\quad - \langle \mathbf{N}(\gamma_\mathbf{D} \mathbf{y_0^c}), \gamma_\mathbf{D} \mathbf{v^c} \rangle_\tau + \langle \mathbf{B}(\boldsymbol{\lambda_0^c}), \gamma_\mathbf{D} \mathbf{v^c} \rangle_\tau + \langle \boldsymbol{\mu^c}, (\mathbf{C} - \mathbf{Id})(\gamma_\mathbf{D} \mathbf{y_0^c}) \rangle_\tau - \langle \boldsymbol{\mu^c}, \mathbf{A}(\boldsymbol{\lambda_0^c}) \rangle_\tau.
\end{aligned} \tag{6.59}$$

Therein we use the weighted Helmholtz projection $\dot{P}_\sigma : \mathbf{H}(\mathbf{curl}, \Omega_1) \to \dot{H}^1(\Omega_1)$, where for given $\mathbf{y} \in \mathbf{H}(\mathbf{curl}, \Omega_1)$, $p := \dot{P}_\sigma(\mathbf{y}) \in \dot{H}^1(\Omega_1)$ is the unique solution of the variational problem. Find $p \in \dot{H}^1(\Omega_1)$, such that

$$\int_{\Omega_1} \sigma \nabla p \cdot \nabla q \, \mathrm{d}\mathbf{x} = \int_{\Omega_1} \sigma \mathbf{y} \cdot \nabla q \, \mathrm{d}\mathbf{x}, \quad \forall q \in \dot{H}^1(\Omega_1). \tag{6.60}$$

The operator $\dot{P}_\sigma$ is linear and bounded, i.e.,

$$\|\sqrt{\sigma} \nabla \dot{P}_\sigma(\mathbf{y})\|_{\mathbf{0}, \Omega_1} \le \|\sqrt{\sigma} \mathbf{y}\|_{\mathbf{0}, \Omega_1}. \tag{6.61}$$

The additional expression is chosen in such a way, that it does not vanish on the kernel of the **curl** operator, and on the other hand $\dot{P}_\sigma(\mathbf{y_0^c})$ vanishes at the solution, i.e., $\dot{P}_\sigma(\mathbf{y_0^c}) = 0$. Problem 6.23 has a unique solution $\mathbf{y_0^c}$. Furthermore, Problem 6.23 is nothing else, than an equivalent primal formulation of Problem 6.22.

6.2.3   Discretization

In order to discretize the problems, we use $\mathcal{ND}^0(\mathcal{T}_h)$, a conforming finite element subspace of $\mathbf{H}(\mathbf{curl}, \Omega_1)$, and $\mathcal{RT}_0^0(\mathcal{K}_h)$, a conforming finite element subspace of $\mathbf{H}_\|^{-\frac{1}{2}}(\mathrm{div}_\Gamma\, 0, \Gamma)$, cf. Section 2.4. Furthermore, we define the product space $\mathcal{W}_h$, given by

$$\mathcal{W}_h := \mathcal{ND}^0(\mathcal{T}_h) \times \mathcal{RT}_0^0(\mathcal{K}_h) \times \mathcal{ND}^0(\mathcal{T}_h) \times \mathcal{RT}_0^0(\mathcal{K}_h).$$

Let $\{\varphi_i\}_{i=1,N_h}$ denote the usual edge basis of $\mathcal{ND}^0(\mathcal{T}_h)$, and let $\{\xi_i\}_{i=1,L_h}$ denote the usual cell basis of $\mathcal{RT}_0^0(\mathcal{K}_h)$. We define the following FEM and BEM matrices:

$$
\begin{aligned}
(\tilde{\mathbf{K}}_{\boldsymbol{\nu}})_{ij} &:= (\nu \,\mathbf{curl}\,\boldsymbol{\varphi_i}, \mathbf{curl}\,\boldsymbol{\varphi_j})_{\mathbf{0},\Omega_1} - \langle \mathbf{N}(\gamma_{\mathbf{D}}\boldsymbol{\varphi_i}), \gamma_{\mathbf{D}}\boldsymbol{\varphi_j}\rangle_\tau, \\
(\mathbf{M}_{\sigma,\omega})_{ij} &:= \omega(\sigma\boldsymbol{\varphi_i},\boldsymbol{\varphi_j})_{\mathbf{0},\Omega_1}, \\
(\mathbf{A})_{ij} &:= \langle \boldsymbol{\xi_i}, \mathbf{A}(\boldsymbol{\xi_j})\rangle_\tau, \\
(\mathbf{B})_{ij} &:= \langle \boldsymbol{\xi_i}, (\mathbf{C}-\mathbf{Id})(\gamma_{\mathbf{D}}\boldsymbol{\varphi_j})\rangle_\tau.
\end{aligned}
\tag{6.62}
$$

The resulting systems of the finite and boundary element equations have the following structure.

6.2.3.1 Symmetric formulations ($k = 1$)

Formulation FEM-BEM 1

Find $(\mathbf{y_h^s}, \boldsymbol{\lambda_h^s}, \mathbf{y_h^c}, \boldsymbol{\lambda_h^c})^T \in \mathbb{R}^{2(N_h+L_h)}$:
$$
\underbrace{\begin{pmatrix} \mathbf{M}_{\sigma,\omega} & \mathbf{0} & \tilde{\mathbf{K}}_{\boldsymbol{\nu}} & \mathbf{B}^T \\ \mathbf{0} & \mathbf{0} & \mathbf{B} & -\mathbf{A} \\ \tilde{\mathbf{K}}_{\boldsymbol{\nu}} & \mathbf{B}^T & -\mathbf{M}_{\sigma,\omega} & \mathbf{0} \\ \mathbf{B} & -\mathbf{A} & \mathbf{0} & \mathbf{0} \end{pmatrix}}_{=:\mathcal{A}_{B1}} \begin{pmatrix} \mathbf{y_h^s} \\ \boldsymbol{\lambda_h^s} \\ \mathbf{y_h^c} \\ \boldsymbol{\lambda_h^c} \end{pmatrix} = \begin{pmatrix} \mathbf{u_h^c} \\ \mathbf{0} \\ \mathbf{u_h^s} \\ \mathbf{0} \end{pmatrix}.
$$

In fact, the system matrix $\mathcal{A}_{B1}$ is symmetric and indefinite, and has a double saddle point structure. Typically small mesh sizes h, large or small ω and large jumps in the material coefficients ν and σ across interfaces lead to a dramatic growth in the condition number of these matrices. Therefore, we expect a very bad convergence rate if any Krylov subspace method, like the MinRes method, is applied to the unpreconditioned systems of equations. Hence appropriate preconditioning is an important issue.

6.2.3.2 Symmetric formulations ($k = 0$)

With the new matrices $\mathbf{D}_{\boldsymbol{\sigma}} = \mathbf{D}_{\boldsymbol{\sigma},\mathbf{1}}$, $\mathbf{L}_{\boldsymbol{\sigma}} = \mathbf{L}_{\boldsymbol{\sigma},\mathbf{1}}$, and $\tilde{\mathbf{K}}_{\mathbf{r},\mathbf{0},\boldsymbol{\nu}} = \tilde{\mathbf{K}}_{\mathbf{r},\boldsymbol{\nu}}|_{\omega=1}$, the resulting linear systems for the mode $k = 0$ have the following forms:

Formulation FEM-BEM 3 ($k = 0$)

Find $(\mathbf{y_h^c}, \boldsymbol{\lambda_h^c}, \mathbf{p_h^c})^T \in \mathbb{R}^{N_h+L_h+M_h}$:
$$
\underbrace{\begin{pmatrix} \tilde{\mathbf{K}}_{\boldsymbol{\nu}} & \mathbf{B}^T & \mathbf{D}_{\boldsymbol{\sigma}}^T \\ \mathbf{B} & -\mathbf{A} & \mathbf{0} \\ \mathbf{D}_{\boldsymbol{\sigma}} & \mathbf{0} & \mathbf{0} \end{pmatrix}}_{=:\mathcal{A}_{B3,0}} \begin{pmatrix} \mathbf{y_h^c} \\ \boldsymbol{\lambda_h^c} \\ \mathbf{p_h^c} \end{pmatrix} = \begin{pmatrix} \mathbf{u_h^c} \\ \mathbf{0} \\ \mathbf{0} \end{pmatrix}.
$$

Formulation FEM-BEM 4 ($k = 0$)

Find $(\mathbf{y_h^c}, \boldsymbol{\lambda_h^c}, \mathbf{p_h^c})^T \in \mathbb{R}^{N_h+L_h+M_h}$:
$$
\underbrace{\begin{pmatrix} \tilde{\mathbf{K}}_{\boldsymbol{\nu}} & \mathbf{B}^T & \mathbf{D}_{\boldsymbol{\sigma}}^T \\ \mathbf{B} & -\mathbf{A} & \mathbf{0} \\ \mathbf{D}_{\boldsymbol{\sigma}} & \mathbf{0} & -\mathbf{L}_{\boldsymbol{\sigma}} \end{pmatrix}}_{=:\mathcal{A}_{B4,0}} \begin{pmatrix} \mathbf{y_h^c} \\ \boldsymbol{\lambda_h^c} \\ \mathbf{p_h^c} \end{pmatrix} = \begin{pmatrix} \mathbf{u_h^c} \\ \mathbf{0} \\ \mathbf{0} \end{pmatrix}.
$$

Formulation FEM-BEM 5 ($k = 0$)

Find $(\mathbf{y_h^c}, \boldsymbol{\lambda_h^c})^T \in \mathbb{R}^{N_h+L_h}$:
$$
\underbrace{\begin{pmatrix} \tilde{\mathbf{K}}_{\mathbf{r},\mathbf{0},\boldsymbol{\nu}} & \mathbf{B}^T \\ \mathbf{B} & -\mathbf{A} \end{pmatrix}}_{=:\mathcal{A}_{B5,0}} \begin{pmatrix} \mathbf{y_h^c} \\ \boldsymbol{\lambda_h^c} \end{pmatrix} = \begin{pmatrix} \mathbf{u_h^c} \\ \mathbf{0} \end{pmatrix}.
$$

In fact, the system matrices $\mathcal{A}_{B3,0}$, $\mathcal{A}_{B4,0}$ and $\mathcal{A}_{B5,0}$ are symmetric and indefinite, and have a saddle point structure. Also in these cases, the condition numbers of the system matrices suffer from small mesh sizes h and large jumps in the material coefficients ν and σ across interfaces.

6.2.4   Block-diagonal preconditioners

This subsection is devoted to the construction of parameter-robust preconditioners for the systems of linear equations of the last subsection. For each proposed formulation, we investigate its structure to construct a preconditioner by the technique of inexact Schur complement preconditioning, cf. Subsection 5.2.3. Furthermore, we provide condition number bounds for the resulting preconditioned systems of linear equations, by showing well-posedness of the underlying systems of partial differential equations in non-standard norms.

6.2.4.1   Symmetric formulations ($k = 1$)

Formulation FEM-BEM 1   We explore the structure of the system matrix $\mathcal{A}_{B1}$. Since we already have a robust preconditioner for the part of $\mathcal{A}_{B1}$, corresponding to the interior, i.e., $\mathcal{A}_{F1}$, we pursue the strategy of inexact Schur complement preconditioning, cf. Subsection 5.2.3. The contribution from the boundary is taken into account by forming the Schur complements. Therefore, we propose the following two block-diagonal inexact Schur complement preconditioners

$$\mathcal{P}_{B1} = \text{diag} \left(\tilde{\mathbf{K}}_{\boldsymbol{\nu}} + \mathbf{M}_{\boldsymbol{\sigma},\boldsymbol{\omega}} + \mathbf{B}^T \mathbf{A}^{-1} \mathbf{B}, \mathbf{A}, \tilde{\mathbf{K}}_{\boldsymbol{\nu}} + \mathbf{M}_{\boldsymbol{\sigma},\boldsymbol{\omega}} + \mathbf{B}^T \mathbf{A}^{-1} \mathbf{B}, \mathbf{A} \right) \tag{6.63}$$

and

$$\mathcal{P}_{B2} = \text{diag} \left(\tilde{\mathbf{K}}_{\boldsymbol{\nu}} + \mathbf{M}_{\boldsymbol{\sigma},\boldsymbol{\omega}}, \mathbf{A} + \mathbf{B}(\tilde{\mathbf{K}}_{\boldsymbol{\nu}} + \mathbf{M}_{\boldsymbol{\sigma},\boldsymbol{\omega}})^{-1}\mathbf{B}^T, \tilde{\mathbf{K}}_{\boldsymbol{\nu}} + \mathbf{M}_{\boldsymbol{\sigma},\boldsymbol{\omega}}, \mathbf{A} + \mathbf{B}(\tilde{\mathbf{K}}_{\boldsymbol{\nu}} + \mathbf{M}_{\boldsymbol{\sigma},\boldsymbol{\omega}})^{-1}\mathbf{B}^T \right).$$

According to the choice of the block-diagonal preconditioners $\mathcal{P}_{B1}$ and $\mathcal{P}_{B2}$, we introduce the non-standard norms $\|\cdot\|_{\mathcal{P}_{B1}}$ and $\|\cdot\|_{\mathcal{P}_{B2}}$ in the product space $\mathcal{W}$:

$$\|\Upsilon\|_{\mathcal{P}_{B1}}^2 := \|(\mathbf{y^c}, \mathbf{y^s})\|_{\mathcal{P}}^2 + \sum_{j \in \{c,s\}} \left[-\langle \mathbf{N}(\gamma_{\mathbf{D}}\mathbf{y^j}), \gamma_{\mathbf{D}}\mathbf{y^j} \rangle_\tau + \sup_{\boldsymbol{\lambda} \in \mathbf{H}_{\|}^{-\frac{1}{2}}(\text{div}_\Gamma 0, \Gamma)} \frac{\langle \mathbf{B}(\boldsymbol{\lambda}), \gamma_{\mathbf{D}}\mathbf{y^j} \rangle_\tau^2}{\langle \mathbf{A}(\boldsymbol{\lambda}), \boldsymbol{\lambda} \rangle_\tau} \right]$$
$$+ \sum_{j \in \{c,s\}} \langle \boldsymbol{\lambda^j}, \mathbf{A}(\boldsymbol{\lambda^j}) \rangle_\tau.$$

and

$$\|\Upsilon\|_{\mathcal{P}_{B2}}^2 := \|(\mathbf{y^c}, \mathbf{y^s})\|_{\mathcal{P}}^2 - \sum_{j \in \{c,s\}} \langle \mathbf{N}(\gamma_{\mathbf{D}}\mathbf{y^j}), \gamma_{\mathbf{D}}\mathbf{y^j} \rangle_\tau$$
$$+ \sum_{j \in \{c,s\}} \left[\langle \boldsymbol{\lambda^j}, \mathbf{A}(\boldsymbol{\lambda^j}) \rangle_\tau + \sup_{\mathbf{v} \in \mathbf{H}(\mathbf{curl},\Omega_1)} \frac{\langle \mathbf{B}(\boldsymbol{\lambda^j}), \gamma_{\mathbf{D}}\mathbf{v} \rangle_\tau^2}{(\nu \, \mathbf{curl}\,\mathbf{v}, \mathbf{curl}\,\mathbf{v})_{\mathbf{0},\Omega_1} + \omega(\sigma\mathbf{v}, \mathbf{v})_{\mathbf{0},\Omega_1}} \right].$$

The first main result is summarized in the following lemma, that claims that an inf-sup condition and a sup-sup condition in the $\mathcal{P}_{B1}$-norm are fulfilled with parameter-independent constants, namely $\frac{1}{2\sqrt{3}}$ and 3.

Lemma 6.24. *We have*

$$\frac{1}{2\sqrt{3}}\|\Upsilon\|_{\mathcal{P}_{B1}} \le \sup_{\Theta \in \mathcal{W}} \frac{\mathcal{A}_{B1}(\Upsilon, \Theta)}{\|\Theta\|_{\mathcal{P}_{B1}}} \le 2\|\Upsilon\|_{\mathcal{P}_{B1}}, \tag{6.64}$$

for all $\Upsilon \in \mathcal{W}$.

Proof. Boundedness follows from reapplication of Cauchy's inequality with constant 2. For the special choices of the test function $\Theta_1 = (\mathbf{y^s}, \boldsymbol{\lambda^s}, -\mathbf{y^c}, -\boldsymbol{\lambda^c})$ and $\Theta_2 = (\mathbf{y^c}, -\boldsymbol{\lambda^c}, \mathbf{y^s}, -\boldsymbol{\lambda^s})$ we have

$$\mathcal{A}_{B1}(\Upsilon, \Theta_1) = \sum_{j \in \{c,s\}} \omega(\sigma\mathbf{y}^j, \mathbf{y}^j)_{\mathbf{0},\Omega_1},$$
$$\mathcal{A}_{B1}(\Upsilon, \Theta_2) = \sum_{j \in \{c,s\}} (\nu \, \mathbf{curl}\,\mathbf{y^j}, \mathbf{curl}\,\mathbf{y^j})_{\mathbf{0},\Omega_1} - \langle \mathbf{N}(\gamma_{\mathbf{D}}\mathbf{y^j}), \gamma_{\mathbf{D}}\mathbf{y^j} \rangle_\tau + \langle \boldsymbol{\lambda^j}, \mathbf{A}(\boldsymbol{\lambda^j}) \rangle_\tau,$$

and therefore

$$\sup_{\Theta \in \mathcal{W}} \frac{\mathcal{A}_{B1}(\Upsilon, \Theta)}{\|\Theta\|_{\mathcal{P}_{B1}}} \geq \frac{\mathcal{A}_{B1}(\Upsilon, \Theta_1 + 2\Theta_2)}{\|\Theta_1 + 2\Theta_2\|_{\mathcal{P}_{B1}}} = \frac{\mathcal{A}_{B1}(\Upsilon, \Theta_1 + 2\Theta_2)}{\sqrt{3}\|\Upsilon\|_{\mathcal{P}_{B1}}}$$

$$\geq \frac{\|(\mathbf{y^s}, \mathbf{y^c})\|_{\mathcal{P}^2}^2 + \sum_{j \in \{c,s\}} \left[-\langle \mathbf{N}(\gamma_{\mathbf{D}}\mathbf{y^j}), \gamma_{\mathbf{D}}\mathbf{y^j} \rangle_\tau + 2\langle \boldsymbol{\lambda}^{\mathbf{j}}, \mathbf{A}(\boldsymbol{\lambda}^{\mathbf{j}}) \rangle_\tau \right]}{\sqrt{3}\|\Upsilon\|_{\mathcal{P}_{B1}}}.$$

Furthermore, for the choice $\Theta_3 = (\mathbf{0}, \boldsymbol{\mu}^{\mathbf{c}}, \mathbf{0}, \boldsymbol{\mu}^{\mathbf{s}})$, we have

$$\sup_{\Theta \in \mathcal{W}} \frac{\mathcal{A}_{B1}(\Upsilon, \Theta)}{\|\Theta\|_{\mathcal{P}_{B1}}} \geq \sup_{(\boldsymbol{\mu}^{\mathbf{c}}, \boldsymbol{\mu}^{\mathbf{s}})} \frac{\mathcal{A}_{B1}(\Upsilon, \Theta_3)}{\|\Theta_3\|_{\mathcal{P}_{B1}}} = \sup_{(\boldsymbol{\mu}^{\mathbf{c}}, \boldsymbol{\mu}^{\mathbf{s}})} \frac{\sum_{j \in \{c,s\}} \left[\langle \mathbf{B}(\boldsymbol{\mu}^{\mathbf{j}}), \gamma_{\mathbf{D}}\mathbf{y^j} \rangle_\tau - \langle \boldsymbol{\mu}^{\mathbf{j}}, \mathbf{A}(\boldsymbol{\lambda}^{\mathbf{j}}) \rangle_\tau \right]}{\sqrt{\sum_{j \in \{c,s\}} \langle \boldsymbol{\mu}^{\mathbf{j}}, \mathbf{A}(\boldsymbol{\mu}^{\mathbf{j}}) \rangle_\tau}}$$

$$\geq \sum_{j \in \{c,s\}} \sup_{\boldsymbol{\mu}^{\mathbf{j}}} \frac{\langle \mathbf{B}(\boldsymbol{\mu}^{\mathbf{j}}), \gamma_{\mathbf{D}}\mathbf{y^j} \rangle_\tau - \sqrt{\langle \boldsymbol{\mu}^{\mathbf{j}}, \mathbf{A}(\boldsymbol{\mu}^{\mathbf{j}}) \rangle_\tau} \sqrt{\langle \boldsymbol{\lambda}^{\mathbf{j}}, \mathbf{A}(\boldsymbol{\lambda}^{\mathbf{j}}) \rangle_\tau}}{\sqrt{\langle \boldsymbol{\mu}^{\mathbf{j}}, \mathbf{A}(\boldsymbol{\mu}^{\mathbf{j}}) \rangle_\tau}}$$

$$= \sum_{j \in \{c,s\}} \sup_{\boldsymbol{\mu}^{\mathbf{j}}} \frac{\langle \mathbf{B}(\boldsymbol{\mu}^{\mathbf{j}}), \gamma_{\mathbf{D}}\mathbf{y^j} \rangle_\tau}{\sqrt{\langle \boldsymbol{\mu}^{\mathbf{j}}, \mathbf{A}(\boldsymbol{\mu}^{\mathbf{j}}) \rangle_\tau}} - \sqrt{\langle \boldsymbol{\lambda}^{\mathbf{j}}, \mathbf{A}(\boldsymbol{\lambda}^{\mathbf{j}}) \rangle_\tau}$$

$$\geq \sum_{j \in \{c,s\}} \frac{\sup_{\boldsymbol{\mu}^{\mathbf{j}}} \frac{\langle \mathbf{B}(\boldsymbol{\mu}^{\mathbf{j}}), \gamma_{\mathbf{D}}\mathbf{y^j} \rangle_\tau^2}{\langle \boldsymbol{\mu}^{\mathbf{j}}, \mathbf{A}(\boldsymbol{\mu}^{\mathbf{j}}) \rangle_\tau} - \langle \boldsymbol{\lambda}^{\mathbf{j}}, \mathbf{A}(\boldsymbol{\lambda}^{\mathbf{j}}) \rangle_\tau}{\sqrt{2}\sqrt{\sup_{\boldsymbol{\mu}^{\mathbf{j}}} \frac{\langle \mathbf{B}(\boldsymbol{\mu}^{\mathbf{j}}), \gamma_{\mathbf{D}}\mathbf{y^j} \rangle_\tau^2}{\langle \boldsymbol{\mu}^{\mathbf{j}}, \mathbf{A}(\boldsymbol{\mu}^{\mathbf{j}}) \rangle_\tau} + \langle \boldsymbol{\lambda}^{\mathbf{j}}, \mathbf{A}(\boldsymbol{\lambda}^{\mathbf{j}}) \rangle_\tau}} \qquad (6.65)$$

$$\geq \frac{\sum_{j \in \{c,s\}} \sup_{\boldsymbol{\mu}^{\mathbf{j}}} \frac{\langle \mathbf{B}(\boldsymbol{\mu}^{\mathbf{j}}), \gamma_{\mathbf{D}}\mathbf{y^j} \rangle_\tau^2}{\langle \boldsymbol{\mu}^{\mathbf{j}}, \mathbf{A}(\boldsymbol{\mu}^{\mathbf{j}}) \rangle_\tau} - \langle \boldsymbol{\lambda}^{\mathbf{j}}, \mathbf{A}(\boldsymbol{\lambda}^{\mathbf{j}}) \rangle_\tau}{\sqrt{2}\sqrt{\sum_{j \in \{c,s\}} \sup_{\boldsymbol{\mu}^{\mathbf{j}}} \frac{\langle \mathbf{B}(\boldsymbol{\mu}^{\mathbf{j}}), \gamma_{\mathbf{D}}\mathbf{y^j} \rangle_\tau^2}{\langle \boldsymbol{\mu}^{\mathbf{j}}, \mathbf{A}(\boldsymbol{\mu}^{\mathbf{j}}) \rangle_\tau} + \langle \boldsymbol{\lambda}^{\mathbf{j}}, \mathbf{A}(\boldsymbol{\lambda}^{\mathbf{j}}) \rangle_\tau}}$$

$$\geq \frac{\sum_{j \in \{c,s\}} \sup_{\boldsymbol{\mu}^{\mathbf{j}}} \frac{\langle \mathbf{B}(\boldsymbol{\mu}^{\mathbf{j}}), \gamma_{\mathbf{D}}\mathbf{y^j} \rangle_\tau^2}{\langle \boldsymbol{\mu}^{\mathbf{j}}, \mathbf{A}(\boldsymbol{\mu}^{\mathbf{j}}) \rangle_\tau} - \langle \boldsymbol{\lambda}^{\mathbf{j}}, \mathbf{A}(\boldsymbol{\lambda}^{\mathbf{j}}) \rangle_\tau}{\sqrt{2}\|\Upsilon\|_{\mathcal{P}_{B1}}}.$$

Combining these two estimates, we obtain

$$\sup_{\Theta \in \mathcal{W}} \frac{\mathcal{A}_{B1}(\Upsilon, \Theta)}{\|\Theta\|_{\mathcal{P}_{B1}}} \geq \frac{1}{2\max(\sqrt{3}, \sqrt{2})}\|\Upsilon\|_{\mathcal{P}_{B1}} = \frac{1}{2\sqrt{3}}\|\Upsilon\|_{\mathcal{P}_{B1}},$$

and therefore the inf-sup condition follows. $\square$

The second main result is summarized in the following lemma, that claims that an inf-sup condition and a sup-sup condition in the $\mathcal{P}_{B2}$-norm are fulfilled with parameter-independent constants, namely $\frac{1}{\sqrt{7}}$ and 2.

Lemma 6.25. *We have*

$$\frac{1}{\sqrt{7}}\|\Upsilon\|_{\mathcal{P}_{B2}} \leq \sup_{\Theta \in \mathcal{W}} \frac{\mathcal{A}_{B1}(\Upsilon, \Theta)}{\|\Theta\|_{\mathcal{P}_{B2}}} \leq 2\|\Upsilon\|_{\mathcal{P}_{B2}}, \qquad (6.66)$$

for all $\Upsilon \in \mathcal{W}$.

Proof. The proof basically follows the same line as the proof of Theorem 6.24. For details, see [102, Lemma 1]. $\square$

Furthermore, the inequalities (6.64) and (6.66) remain valid for the finite element subspace $\mathcal{W}_h$, since the proofs can be repeated for the finite element functions step by step. Therefore, we obtain the condition number estimates

$$\kappa_{\mathcal{P}_{B1}}(\mathcal{P}_{B1}^{-1}\mathcal{A}_{B1}) := \|\mathcal{P}_{B1}^{-1}\mathcal{A}_{B1}\|_{\mathcal{P}_{B1}}\|\mathcal{A}_{B1}^{-1}\mathcal{P}_{B1}\|_{\mathcal{P}_{B1}} \leq 4\sqrt{3} \approx 6.928,$$

$$\kappa_{\mathcal{P}_{B2}}(\mathcal{P}_{B2}^{-1}\mathcal{A}_{B1}) := \|\mathcal{P}_{B2}^{-1}\mathcal{A}_{B1}\|_{\mathcal{P}_{B2}}\|\mathcal{A}_{B1}^{-1}\mathcal{P}_{B2}\|_{\mathcal{P}_{B2}} \leq 2\sqrt{7} \approx 5.291.$$

6.2.4.2   Symmetric formulations ($k = 0$)

Formulation FEM-BEM 4 ($k = 0$)   We explore the 2×2 structure of our system matrix $\mathcal{A}_{B4,0}$. In order to construct a parameter-robust and block-diagonal preconditioner, we use a Schur complement preconditioner, cf. Theorem 5.3. Since $\operatorname{diag}(\mathbf{A}, \mathbf{L}_{\boldsymbol{\sigma}})$ is positive definite, we can build the Schur complement

$$\mathcal{P}_{B4,0} = \begin{pmatrix} \tilde{\mathbf{K}}_{\boldsymbol{\nu}} + \mathbf{D}_{\boldsymbol{\sigma}} \mathbf{L}_{\boldsymbol{\sigma}}^{-1} \mathbf{D}_{\boldsymbol{\sigma}} + \mathbf{B}^T \mathbf{A}^{-1} \mathbf{B} & \mathbf{0} & \mathbf{0} \\ \mathbf{0} & \mathbf{A} & \mathbf{0} \\ \mathbf{0} & \mathbf{0} & \mathbf{L}_{\boldsymbol{\sigma}} \end{pmatrix}. \tag{6.67}$$

Immediately, we obtain the condition number estimate

$$\kappa_{\mathcal{P}_{B4,0}}(\mathcal{P}_{B4,0}^{-1} \mathcal{A}_{B4,0}) := \|\mathcal{P}_{B4,0}^{-1} \mathcal{A}_{B4,0}\|_{\mathcal{P}_{B4,0}} \|\mathcal{A}_{B4,0}^{-1} \mathcal{P}_{B4,0}\|_{\mathcal{P}_{B4,0}} \leq \frac{\sqrt{5}+1}{\sqrt{5}-1} \approx 2.618. \tag{6.68}$$

Inspired by the structure of the preconditioner (6.68), we introduce the non-standard norm $\| \cdot \|_{\mathcal{P}_{B4,0}}$ in $\mathbf{H_0}(\mathbf{curl}, \Omega_1) \times \mathbf{H}_{\|}^{-\frac{1}{2}}(\operatorname{div}_\Gamma 0, \Gamma) \times \dot{H}^1(\Omega_1)$ by

$$\begin{aligned} \|(\mathbf{y}, \boldsymbol{\lambda}, p)\|_{\mathcal{P}_{P5,0}}^2 = (\nu \,\mathbf{curl}\, \mathbf{y}, \mathbf{curl}\, \mathbf{y})_{0,\Omega_1} &+ \sup_{q \in \dot{H}^1(\Omega_1)} \frac{(\sigma \mathbf{y} \nabla q)_{0,\Omega_1}^2}{(\sigma \nabla q, \nabla q)_{0,\Omega_1}} \\ &- \langle \mathbf{N}(\boldsymbol{\gamma}_{\mathbf{D}} \mathbf{y}), \boldsymbol{\gamma}_{\mathbf{D}} \mathbf{y} \rangle_\tau + \sup_{\boldsymbol{\lambda} \in \mathbf{H}_{\|}^{-\frac{1}{2}}(\operatorname{div}_\Gamma 0, \Gamma)} \frac{\langle \mathbf{B}(\boldsymbol{\lambda}), \boldsymbol{\gamma}_{\mathbf{D}} \mathbf{y} \rangle_\tau^2}{\langle \mathbf{A}(\boldsymbol{\lambda}), \boldsymbol{\lambda} \rangle_\tau} + \langle \mathbf{A}(\boldsymbol{\lambda}), \boldsymbol{\lambda} \rangle_\tau \\ &+ (\sigma \nabla p, \nabla p)_{0,\Omega_1}. \end{aligned}$$

The main result is summarized in the following lemma, that claims that an inf-sup and a sup-sup condition are fulfilled with parameter-independent constants, namely $(\sqrt{5} - 1)/2$ and $(\sqrt{5} + 1)/2$.

Lemma 6.26. *We have*

$$\begin{aligned} \frac{\sqrt{5}-1}{2} \|(\mathbf{y_0^c}, \boldsymbol{\lambda_0^c}, p_0^c)\|_{\mathcal{P}_{B4,0}} &\leq \sup_{(\mathbf{v^c}, \boldsymbol{\lambda^c}, q^c)} \frac{\mathcal{A}_{B4,0}((\mathbf{y_0^c}, \boldsymbol{\lambda_0^c}, p_0^c), (\mathbf{v^c}, \boldsymbol{\mu^c}, q^c))}{\|(\mathbf{v^c}, \boldsymbol{\mu^c}, q^c)\|_{\mathcal{P}_{B4,0}}} \\ \frac{\sqrt{5}+1}{2} \|(\mathbf{y_0^c}, \boldsymbol{\lambda_0^c}, p_0^c)\|_{\mathcal{P}_{B4,0}} &\geq \sup_{(\mathbf{v^c}, \boldsymbol{\lambda^c}, q^c)} \frac{\mathcal{A}_{B4,0}((\mathbf{y_0^c}, \boldsymbol{\lambda_0^c}, p_0^c), (\mathbf{v^c}, \boldsymbol{\mu^c}, q^c))}{\|(\mathbf{v^c}, \boldsymbol{\mu^c}, q^c)\|_{\mathcal{P}_{B4,0}}}, \end{aligned} \tag{6.69}$$

for all $(\mathbf{y_0^c}, \boldsymbol{\lambda_0^c}, p_0^c) \in \mathbf{H_0}(\mathbf{curl}, \Omega_1) \times \mathbf{H}_{\|}^{-\frac{1}{2}}(\operatorname{div}_\Gamma 0, \Gamma) \times \dot{H}^1(\Omega_1)$.

Proof. Follows from Theorem 5.3. □

Formulation FEM-BEM 3 ($k = 0$)   In this setting, again we can use the $\mathcal{P}_{B4,0}$-norm to show well-posedness. The main result is summarized in the following lemma, that claims, that an inf-sup and sup-sup condition are fulfilled with parameter-independent constants, namely $\frac{1}{2\sqrt{3}}$ and 2.

Lemma 6.27. *We have*

$$\begin{aligned} \frac{1}{2\sqrt{3}} \|(\mathbf{y_0^c}, \boldsymbol{\lambda_0^c}, p_0^c)\|_{\mathcal{P}_{B4,0}} &\leq \sup_{(\mathbf{v^c}, \boldsymbol{\lambda^c}, q^c)} \frac{\mathcal{A}_{B3,0}((\mathbf{y_0^c}, \boldsymbol{\lambda_0^c}, p_0^c), (\mathbf{v^c}, \boldsymbol{\mu^c}, q^c))}{\|(\mathbf{v^c}, \boldsymbol{\mu^c}, q^c)\|_{\mathcal{P}_{B4,0}}} \\ 2 \|(\mathbf{y_0^c}, \boldsymbol{\lambda_0^c}, p_0^c)\|_{\mathcal{P}_{B4,0}} &\geq \sup_{(\mathbf{v^c}, \boldsymbol{\lambda^c}, q^c)} \frac{\mathcal{A}_{B3,0}((\mathbf{y_0^c}, \boldsymbol{\lambda_0^c}, p_0^c), (\mathbf{v^c}, \boldsymbol{\mu^c}, q^c))}{\|(\mathbf{v^c}, \boldsymbol{\mu^c}, q^c)\|_{\mathcal{P}_{B4,0}}}, \end{aligned} \tag{6.70}$$

for all $(\mathbf{y_0^c}, \boldsymbol{\lambda_0^c}, p_0^c) \in \mathbf{H_0}(\mathbf{curl}, \Omega_1) \times \mathbf{H}_{\|}^{-\frac{1}{2}}(\operatorname{div}_\Gamma 0, \Gamma) \times \dot{H}^1(\Omega_1)$.

Proof. The proof can be done in the same fashion as the proof of Lemma 6.17 in combination with Lemma 6.24. □

Formulation FEM-BEM 5 ($k = 0$) We explore the 2×2 block structure of our system matrix $\mathcal{A}_{B5,0}$. In order to construct a parameter-robust and block-diagonal preconditioner, we use a Schur complement preconditioner, cf. Theorem 5.3. Since $\mathbf{A}$ is symmetric and positive definite, we can build the Schur complement

$$\mathcal{P}_{B5,0} = \begin{pmatrix} \mathbf{K_{r,0,\nu}} - \mathbf{N} + \mathbf{B}^T \mathbf{A}^{-1} \mathbf{B} & \mathbf{0} \\ \mathbf{0} & \mathbf{A} \end{pmatrix}. \tag{6.71}$$

Immediately, we obtain the condition number estimate

$$\kappa_{\mathcal{P}_{B5,0}}(\mathcal{P}_{B5,0}^{-1}\mathcal{A}_{B5,0}) := \|\mathcal{P}_{B5,0}^{-1}\mathcal{A}_{B5,0}\|_{\mathcal{P}_{B5,0}}\|\mathcal{A}_{B5,0}^{-1}\mathcal{P}_{B5,0}\|_{\mathcal{P}_{B5,0}} \le \frac{\sqrt{5}+1}{\sqrt{5}-1} \approx 2.618. \tag{6.72}$$

Inspired by the structure of the preconditioner (6.71), we introduce the non-standard norm $\|\cdot\|_{\mathcal{P}_{B5,0}}$ in $\mathbf{H_0}(\mathbf{curl}, \Omega_1) \times \mathbf{H}_\parallel^{-\frac{1}{2}}(\operatorname{div}_\Gamma 0, \Gamma)$ by

$$\|(\mathbf{y}, \boldsymbol{\lambda})\|_{\mathcal{P}_{P5,0}}^2 = (\nu\,\mathbf{curl\,y}, \mathbf{curl\,y})_{\mathbf{0},\Omega_1} + (\sigma\nabla\dot{P}\mathbf{y}, \nabla\dot{P}\mathbf{y})_{\mathbf{0},\Omega_1}$$

$$- \langle \mathbf{N}(\boldsymbol{\gamma_D y}), \boldsymbol{\gamma_D y}\rangle_\tau + \sup_{\boldsymbol{\lambda}\in\mathbf{H}_\parallel^{-\frac{1}{2}}(\operatorname{div}_\Gamma 0,\Gamma)} \frac{\langle \mathbf{B}(\boldsymbol{\lambda}), \boldsymbol{\gamma_D y}\rangle_\tau^2}{\langle \mathbf{A}(\boldsymbol{\lambda}), \boldsymbol{\lambda}\rangle_\tau} + \langle \mathbf{A}(\boldsymbol{\lambda}), \boldsymbol{\lambda}\rangle_\tau.$$

The main result is summarized in the following lemma, that claims that an inf-sup and sup-sup condition are fulfilled with parameter-independent constants, namely $(\sqrt{5}-1)/2$ and $(\sqrt{5}+1)/2$.

Lemma 6.28. *We have*

$$\frac{\sqrt{5}-1}{2}\|(\mathbf{y_0^c}, \boldsymbol{\lambda_0^c})\|_{\mathcal{P}_{B5,0}} \le \sup_{(\mathbf{v^c}, \boldsymbol{\lambda^c})} \frac{\mathcal{A}_{B5,0}((\mathbf{y_0^c}, \boldsymbol{\lambda_0^c}), (\mathbf{v^c}, \boldsymbol{\mu^c}))}{\|(\mathbf{v^c}, \boldsymbol{\mu^c})\|_{\mathcal{P}_{B5,0}}} \le \frac{\sqrt{5}+1}{2}\|(\mathbf{y_0^c}, \boldsymbol{\lambda_0^c})\|_{\mathcal{P}_{B5,0}}, \tag{6.73}$$

for all $(\mathbf{y_0^c}, \boldsymbol{\lambda_0^c}) \in \mathbf{H_0}(\mathbf{curl}, \Omega_1) \times \mathbf{H}_\parallel^{-\frac{1}{2}}(\operatorname{div}_\Gamma 0, \Gamma)$.

Proof. Follows from Theorem 5.3. $\qquad\square$

6.2.5 Summary

We table the condition number κ and the theoretical number of MinRes iterations *maxiter* needed, for reducing the initial error by a factor of 10^{-8}, if the proposed block-diagonal preconditioners are used. Furthermore, we collect the diagonal blocks, that are needed for the application of the block-diagonal preconditioner.

	κ	maxiter	diagonal blocks
Formulation FEM-BEM 1	6.928	132	$\tilde{\mathbf{K}}_{\boldsymbol{\nu}} + \mathbf{M}_{\boldsymbol{\sigma,\omega}} + \mathbf{B}^T\mathbf{A}^{-1}\mathbf{B}$, $\mathbf{A}$
Formulation FEM-BEM 1	5.291	100	$\tilde{\mathbf{K}}_{\boldsymbol{\nu}} + \mathbf{M}_{\boldsymbol{\sigma,\omega}}$, $\mathbf{A} + \mathbf{B}(\tilde{\mathbf{K}}_{\boldsymbol{\nu}} + \mathbf{M}_{\boldsymbol{\sigma,\omega}})^{-1}\mathbf{B}^T$

	κ	maxiter	diagonal blocks
Formulation FEM-BEM 3 ($k = 0$)	6.928	132	$\tilde{\mathbf{K}}_{\boldsymbol{\nu}} + \mathbf{D}_{\boldsymbol{\sigma}}^T\mathbf{L}_{\boldsymbol{\sigma}}^{-1}\mathbf{D}_{\boldsymbol{\sigma}} + \mathbf{B}^T\mathbf{A}^{-1}\mathbf{B}$, $\mathbf{A}$, $\mathbf{L}_{\boldsymbol{\sigma}}$
Formulation FEM-BEM 4 ($k = 0$)	2.618	48	$\tilde{\mathbf{K}}_{\boldsymbol{\nu}} + \mathbf{D}_{\boldsymbol{\sigma}}^T\mathbf{L}_{\boldsymbol{\sigma}}^{-1}\mathbf{D}_{\boldsymbol{\sigma}} + \mathbf{B}^T\mathbf{A}^{-1}\mathbf{B}$, $\mathbf{A}$, $\mathbf{L}_{\boldsymbol{\sigma}}$
Formulation FEM-BEM 5 ($k = 0$)	2.618	48	$\tilde{\mathbf{K}}_{\boldsymbol{\nu}} + \mathbf{D}_{\boldsymbol{\sigma}}^T\mathbf{L}_{\boldsymbol{\sigma}}^{-1}\mathbf{D}_{\boldsymbol{\sigma}} + \mathbf{B}^T\mathbf{A}^{-1}\mathbf{B}$, $\mathbf{A}$

Remark 6.29. *In order to realize the preconditioner $\mathcal{P}_{B1}$, the diagonal block $\tilde{\mathbf{K}}_{\boldsymbol{\nu}} + \mathbf{M}_{\boldsymbol{\sigma,\omega}} + \mathbf{B}^T\mathbf{A}^{-1}\mathbf{B}$ has to be realized. It would be convenient, to replace this Schur complement by the easier block $\mathbf{K}_{\boldsymbol{\nu}} + \mathbf{M}_{\boldsymbol{\sigma,\omega}}$, see e.g., [80]. This replacement yields a dependence of the condition number on the parameters ν, ω and σ. Therefore, heading for a parameter-robust preconditioning technique, it is*

essential to consider the contribution from the Schur complement, since this reflects the different parameter settings in the exterior and interior domain.
Anyhow, using the simpler diagonal block $\mathbf{K_{\nu}} + \mathbf{M_{\sigma,\omega}}$*, mesh independent bounds for the condition number can immediately be obtained, cf. [57]. The same statement holds, if* $\tilde{\mathbf{K}}_{\nu} + \mathbf{D}_{\sigma}{}^{T}\mathbf{L}_{\sigma}{}^{-1}\mathbf{D}_{\sigma} + \mathbf{B}^{T}\mathbf{A}^{-1}\mathbf{B}$ *is replaced by* $\mathbf{K_{\nu}} + \mathbf{M_{\sigma}}$*.*

It is obvious, that all these estimates are uniform in the discretization parameters h, ω, N and the model parameters ν and σ. The efficient realization of the diagonal blocks is discussed in Chapter 8.

6.2.6   Error analysis

In this subsection, we perform an error analysis for the MH-FEM-BEM method applied to the eddy current problem in unbounded domains. We provide error estimates in terms of the space discretization parameter h and the time discretization parameter N. Therefore, throughout this section, we use a generic constant c, that is independent of h and N.

Let us denote the underlying Hilbert spaces by $V = \mathbf{H}(\mathbf{curl}, \Omega_1)$ and $R = \mathbf{H}_{\|}^{-\frac{1}{2}}(\mathrm{div}_{\Gamma}, \Gamma)$, and the corresponding graph norms by $\|\cdot\|_V$ and $\|\cdot\|_R$, respectively. For the product space $\mathcal{W}$ we also use the standard graph norm $\|\cdot\|_{\mathcal{W}}$, given by

$$\|\Upsilon\|_{\mathcal{W}}^2 := \sum_{j \in \{c,s\}} \|\mathbf{y^j}\|_{\mathbf{curl}, \Omega_1}^2 + \|\boldsymbol{\lambda}^{\mathbf{j}}\|_R^2.$$

The full discretization error estimate is provided in the following norm

$$\|(\tilde{\mathbf{y}}, \tilde{\boldsymbol{\lambda}})\|_{L_2((0,T),V \times R)}^2 = \|\tilde{\mathbf{y}}\|_{L_2((0,T),V)}^2 + \|\tilde{\boldsymbol{\lambda}}\|_{L_2((0,T),R)}^2.$$

In order to estimate the discretization error, we need three levels of discretizations.

1. By $(\tilde{\mathbf{y}}, \tilde{\boldsymbol{\lambda}})$, we denote the exact steady state solution of the time-periodic eddy current problem (3.6) written as an infinite Fourier series, i.e.,

$$\tilde{\mathbf{y}} = \mathbf{y_0^c} + \sum_{k=1}^{\infty} \mathbf{y_k^c} \cos(k\omega t) + \mathbf{y_k^s} \sin(k\omega t), \quad \tilde{\boldsymbol{\lambda}} = \boldsymbol{\lambda_0^c} + \sum_{k=1}^{\infty} \boldsymbol{\lambda_k^c} \cos(k\omega t) + \boldsymbol{\lambda_k^s} \sin(k\omega t),$$

   with the associated vectors of Fourier coefficients denoted by $\underline{\mathbf{y}} = (\mathbf{y_0^c}, \mathbf{y_1^c}, \mathbf{y_1^s}, \ldots)$ and $\underline{\boldsymbol{\lambda}} = (\boldsymbol{\lambda_0^c}, \boldsymbol{\lambda_1^c}, \boldsymbol{\lambda_1^s}, \ldots)$.

2. By $(\mathbf{y_N}, \boldsymbol{\lambda_N})$ we denote the steady state solution of the time-periodic eddy current problem (3.6) in terms of a truncated Fourier series with exact Fourier coefficients, i.e.,

$$\mathbf{y_N} = \mathbf{y_0^c} + \sum_{k=1}^{N} \mathbf{y_k^c} \cos(k\omega t) + \mathbf{y_k^s} \sin(k\omega t), \quad \boldsymbol{\lambda_N} = \boldsymbol{\lambda_0^c} + \sum_{k=1}^{N} \boldsymbol{\lambda_k^c} \cos(k\omega t) + \boldsymbol{\lambda_k^s} \sin(k\omega t),$$

   with the associated vector of Fourier coefficients denoted by $\underline{\mathbf{y}}_{\mathbf{N}} = (\mathbf{y_0^c}, \ldots, \mathbf{y_N^c}, \mathbf{y_N^s}, \mathbf{0}, \mathbf{0}, \ldots)$, and $\underline{\boldsymbol{\lambda}}_{\mathbf{N}} = (\boldsymbol{\lambda_0^c}, \ldots, \boldsymbol{\lambda_N^c}, \boldsymbol{\lambda_N^s}, \mathbf{0}, \mathbf{0}, \ldots)$.

3. By $(\mathbf{y_{N,h}}, \boldsymbol{\lambda_{N,h}})$, we denote the truncated solution $(\mathbf{y_N}, \boldsymbol{\lambda_N})$ with FEM-BEM approximated Fourier coefficients of the eddy current problem (3.6), i.e.,

$$\mathbf{y_{N,h}} = \mathbf{y_{0,h}^c} + \sum_{k=1}^{N} \mathbf{y_{k,h}^c} \cos(k\omega t) + \mathbf{y_{k,h}^s} \sin(k\omega t),$$

$$\boldsymbol{\lambda_{N,h}} = \boldsymbol{\lambda_{0,h}^c} + \sum_{k=1}^{N} \boldsymbol{\lambda_{k,h}^c} \cos(k\omega t) + \boldsymbol{\lambda_{k,h}^s} \sin(k\omega t),$$

   with the FEM approximations of the amplitudes $\mathbf{y_{k,h}^j}$, $j \in \{c, s\}$, and the BEM approximations of the amplitudes $\boldsymbol{\lambda_{k,h}^j}$, $j \in \{c, s\}$.

Clearly, we can split the full discretization error into the parts corresponding to the time and space discretization error, i.e.,

$$\|(\tilde{\mathbf{y}}, \tilde{\boldsymbol{\lambda}}) - (\mathbf{y_{Nh}}, \boldsymbol{\lambda_{Nh}})\|_{L_2((0,T),V\times R)} \leq$$
$$\|(\tilde{\mathbf{y}}, \tilde{\boldsymbol{\lambda}}) - (\mathbf{y_N}, \boldsymbol{\lambda_N})\|_{L_2((0,T),V\times R)} + \|(\mathbf{y_N}, \boldsymbol{\lambda_N}) - (\mathbf{y_{Nh}}, \boldsymbol{\lambda_{Nh}})\|_{L_2((0,T),V\times R)}. \tag{6.74}$$

Therefore, it remains to estimate the time and space discretization errors individually.

Error due to the time discretization We start by estimating the error due to the time discretization, i.e., the truncation of the Fourier series. The main result is summarized in the following Lemma.

Lemma 6.30. *Let the steady state solution $\tilde{\mathbf{y}}$ of the eddy current problem (3.6) be as regular as*

$$\tilde{\mathbf{y}} \in W_2^1((0,T), \mathbf{H}(\mathbf{curl}^2, \Omega_1), \mathbf{L_2}(\Omega_1)).$$

Then the following estimate holds:

$$\|(\tilde{\mathbf{y}}, \tilde{\boldsymbol{\lambda}}) - (\mathbf{y_N}, \boldsymbol{\lambda_N})\|_{L_2((0,T),V\times R)} \leq c\, N^{-\frac{1}{2}} \|\tilde{\mathbf{y}}\|_{W_2^1((0,T),\mathbf{H}(\mathbf{curl}^2,\Omega_1),\mathbf{L_2}(\Omega_1))},$$

where the constant c is independent of the mesh size h and the number of modes N.

Proof. We start by exploring the theory developed in Chapter 4 to estimate the $L_2((0,T), V\times R)$ norm by the corresponding norm in the space of the Fourier coefficients, i.e.,

$$\|(\tilde{\mathbf{y}}, \tilde{\boldsymbol{\lambda}}) - (\mathbf{y_N}, \boldsymbol{\lambda_N})\|_{L_2((0,T),V\times R)} \leq c\, \|(\underline{\mathbf{y}}, \underline{\boldsymbol{\lambda}}) - (\underline{\mathbf{y}}_{\mathbf{N}}, \underline{\boldsymbol{\lambda}}_{\mathbf{N}})\|_{l_2^{\frac{1}{2}}(V\times R)}.$$

Using $\tilde{\boldsymbol{\lambda}} = \boldsymbol{\gamma_N}\tilde{\mathbf{y}}$, one obtains

$$\|(\underline{\mathbf{y}}, \underline{\boldsymbol{\lambda}})\|_{l_2^1(V\times R)} \leq c\left(\|\tilde{\mathbf{y}}\|_{W_2^1((0,T),V,\mathbf{L_2}(\Omega_1))} + \|\tilde{\boldsymbol{\lambda}}\|_{W_2^1((0,T),R,\mathbf{L_2}(\Omega_1))}\right)$$
$$\leq c\,\|\tilde{\mathbf{y}}\|_{W_2^1((0,T),\mathbf{H}(\mathbf{curl}^2,\Omega_1),\mathbf{L_2}(\Omega_1))},$$

and therefore $(\underline{\mathbf{y}}, \underline{\boldsymbol{\lambda}}) \in l_2^1(V\times R)$. Consequently, due to Theorem 4.5, we obtain the error estimate

$$\|(\underline{\mathbf{y}}, \underline{\boldsymbol{\lambda}}) - (\underline{\mathbf{y}}_{\mathbf{N}}, \underline{\boldsymbol{\lambda}}_{\mathbf{N}})\|_{l_2^{\frac{1}{2}}(V\times R)} \leq c\, N^{-\frac{1}{2}} \|(\underline{\mathbf{y}}, \underline{\boldsymbol{\lambda}})\|_{l_2^1(V\times R)}.$$

Furthermore, using $\boldsymbol{\lambda_k^c} = \boldsymbol{\gamma_N}\mathbf{y_k^j}$ and the trace theorem, we obtain

$$\|(\underline{\mathbf{y}}, \underline{\boldsymbol{\lambda}})\|_{l_2^1(V\times R)}^2 \leq c\left(\|\mathbf{y_0^c}\|_V^2 + \|\boldsymbol{\lambda_0^c}\|_R^2 + \sum_{j=1}^\infty \sum_{j\{c,s\}} k^2\left[\|\mathbf{y_k^j}\|_V^2 + \|\boldsymbol{\lambda_k^j}\|_R^2\right]\right)$$
$$\leq c\left(\|\mathbf{y_0^c}\|_{\mathbf{curl}^2,\Omega_1}^2 + \sum_{j=1}^\infty \sum_{j\{c,s\}} k^2\|\mathbf{y_k^j}\|_{\mathbf{curl}^2,\Omega_1}^2\right)$$
$$\leq c\,\|\tilde{\mathbf{y}}\|_{W_2^1((0,T),\mathbf{H}(\mathbf{curl}^2,\Omega_1),\mathbf{L_2}(\Omega_1))}^2.$$

This finishes the proof. $\qquad\square$

Error due to the space discretization Next we estimate the error due to the discretization in space in terms of a FEM-BEM coupling method. Again, we estimate the $L_2((0,T), V\times R)$ norm by the corresponding norm in the space of the Fourier coefficients, i.e.,

$$\|(\mathbf{y_N}, \boldsymbol{\lambda_N}) - (\mathbf{y_{Nh}}, \boldsymbol{\lambda_{Nh}})\|_{L_2((0,T),V\times R)}^2 \leq$$
$$c\left[\|\mathbf{y_0^c} - \mathbf{y_{0,h}^c}\|_{\mathbf{curl},\Omega_1}^2 + \|\boldsymbol{\lambda_0^c} - \boldsymbol{\lambda_{0,h}^c}\|_R^2 + \sum_{k=1}^N \|\Upsilon_k - \Upsilon_{k,h}\|_{\mathcal{W}}^2\right].$$

Due to the decoupling of the Fourier coefficients with respect to the modes k, the discretization error in space is analyzed for a fixed mode k. The full discretization error in space then follows by summing over all modes $k = 1, \ldots, N$.

Lemma 6.31. *Let the solution* $(\mathbf{y^c}, \mathbf{y^s})$ *of Problem 6.19 be as regular as*

$$\mathbf{y^j} \in \mathbf{H^s}(\mathbf{curl}^2, \Omega_1) := \{\mathbf{y} \in \mathbf{H^s}(\Omega_1) : \mathbf{curl\, y} \in \mathbf{H^s}(\Omega_1), \mathbf{curl\, curl\, y} \in \mathbf{H^s}(\Omega_1)\}, \quad j \in \{c, s\},$$

for some $s > \frac{1}{2}$. *Then the following estimate holds:*

$$\|\Upsilon - \Upsilon_h\|_{\mathcal{W}} \leq c\, N^{\frac{1}{2}}\, h^{\min(1,s)} \bigg(\sum_{j \in \{c,s\}} \|\mathbf{y^j}\|_{\mathbf{s},\Omega_1} + \|\,\mathbf{curl\, y^j}\|_{\mathbf{s},\Omega_1} + \|\,\mathbf{curl\, curl\, y^j}\|_{\mathbf{s},\Omega_1} \bigg),$$

where the constant c *is independent of the mesh size* h *and the number of modes* N.

Proof. The key tools of this proof are the Cea-type estimate

$$\|\Upsilon - \Upsilon_h\|_{\mathcal{P}_{B1}} \leq c \inf_{\theta_h \in \mathcal{W}_h} \|\Upsilon - \Theta_h\|_{\mathcal{P}_{B1}},$$

in combination with the approximation properties in Lemma 2.19 and Lemma 2.20. Indeed, switching back to standard norms, we have

$$\|\Upsilon - \Upsilon_h\|_{\mathcal{W}} \leq c\|\Upsilon - \Upsilon_h\|_{\mathcal{P}_{B1}} \leq c \inf_{\Theta_h \in \mathcal{W}_h} \|\Upsilon - \Theta_h\|_{\mathcal{P}_{B1}} \leq c N^{\frac{1}{2}} \inf_{\Theta_h} \|\Upsilon - \Theta_h\|_{\mathcal{W}}.$$

Furthermore, we use the approximation properties of the sine and cosine components of the product space $\mathcal{W}$:

$$\inf_{\lambda_h \in \mathcal{RT}_0^0(\mathcal{K}_h)} \|\boldsymbol{\lambda} - \boldsymbol{\lambda_h}\|_R \leq c\|\,\mathbf{curl\, y} - \mathbf{\Pi\, curl\, y}\|_{\mathbf{curl},\Omega_1}$$

$$\leq c\, h^{\min(1,s)}\, (\|\,\mathbf{curl\, y}\|_{\mathbf{s},\Omega_1} + \|\,\mathbf{curl\, curl\, y}\|_{\mathbf{s},\Omega_1})$$

and

$$\inf_{\mathbf{y_h} \in \mathcal{ND}^0(\mathcal{T}_h)} \|\mathbf{y} - \mathbf{y_h}\|_{\mathbf{curl},\Omega_1} \leq \|\mathbf{y} - \mathbf{\Pi y}\|_{\mathbf{curl},\Omega_1} \leq c\, h^{\min(1,s)}\, (\|\mathbf{y}\|_{\mathbf{s},\Omega_1} + \|\,\mathbf{curl\, y}\|_{\mathbf{s},\Omega_1}).$$

By applying the previous two estimates to the sine and cosine components of the product space $\mathcal{W}$, the desired result follows. □

Full error estimate   Now we are in the position to give a full error estimate in terms of the space discretization parameter h and the time discretization parameter N. The main result is summarized in the following theorem.

Theorem 6.32. *Let the steady state solution* $\tilde{\mathbf{y}}$ *of the eddy current problem (3.6) be as regular as*

$$\tilde{\mathbf{y}} \in W_2^1((0,T), \mathbf{H^s}(\mathbf{curl}^2, \Omega_1), \mathbf{L_2}(\Omega_1))$$

for some $s > \frac{1}{2}$. *Then the following estimate holds:*

$$\|(\tilde{\mathbf{y}}, \tilde{\boldsymbol{\lambda}}) - (\mathbf{y_{N,h}}, \boldsymbol{\lambda_{N,h}})\|_{L_2((0,T), V \times R)} \leq c \left(N^{-\frac{1}{2}} + N^{\frac{1}{2}} h^{\min(1,s)} \right) \|\tilde{\mathbf{y}}\|_{W_2^1((0,T), \mathbf{H^s}(\mathbf{curl}^2, \Omega_1), \mathbf{L_2}(\Omega_1))},$$

where the constant c *is independent of the mesh size* h *and the number of modes* N.

Proof. Using (6.74), Lemma 6.30 and Lemma 6.31, we obtain

$$\|(\tilde{\mathbf{y}}, \tilde{\boldsymbol{\lambda}}) - (\mathbf{y_{Nh}}, \boldsymbol{\lambda_{Nh}})\|_{L_2((0,T), V \times R)}$$

$$\leq c \left(N^{-\frac{1}{2}} \|\tilde{\mathbf{y}}\|_{W_2^1((0,T), \mathbf{H}(\mathbf{curl}^2, \Omega_1), \mathbf{L_2}(\Omega_1))} + h^{\min(1,s)} N^{\frac{1}{2}} \|\tilde{\mathbf{y}}\|_{L_2((0,T), \mathbf{H^s}(\mathbf{curl}^2, \Omega_1))} \right)$$

$$\leq c \left(N^{-\frac{1}{2}} + N^{\frac{1}{2}} h^{\min(1,s)} \right) \|\tilde{\mathbf{y}}\|_{W_2^1((0,T), \mathbf{H^s}(\mathbf{curl}^2, \Omega_1), \mathbf{L_2}(\Omega_1))}.$$

This finishes the proof.   □

Therefore, under the compatibility condition $N < h^{2\varepsilon - 2\min(1,s)}$, for $\varepsilon > 0$, we have convergence of the MH-FEM-BEM approximated solution to the exact periodic steady state solution.

Remark 6.33 (Regularity in time). *Sufficient regularity of the periodic steady state solution $\tilde{\mathbf{y}}$ (in time) can be deduced by the regularity of the source $\tilde{\mathbf{u}}$. Indeed, from $\tilde{\mathbf{u}} \in L_2((0,T), \mathbf{L_2}(\Omega_1))$, we can deduce $\tilde{\mathbf{y}} \in W_2^1((0,T), V, \mathbf{L_2}(\Omega_1))$, cf. [54, §7.1.3, Theorem 6].*

6.3 Nonlinear problems

This section is devoted to the discussion of efficient solution strategies for nonlinear eddy current problems. We present a candidate for an efficient solution procedure without providing theoretical results. The heuristic arguments used in this section are strongly related to the theory developed in the previous two sections.

So far we have assumed that the coefficient ν only depends on the spatial variable $\mathbf{x}$. However, for ferromagnetic materials the reluctivity ν depends on the absolute value of the magnetic induction $\mathbf{B}$ as well, i.e.,

$$\nu = \nu(|\mathbf{B}|) = \nu(|\operatorname{\mathbf{curl}} \mathbf{y}|), \quad \text{in } \Omega_1, \tag{6.75}$$

cf. Section 1.1. For the analysis of the multiharmonic FEM applied to nonlinear eddy current problems, we refer to [15, 17, 18], see also [41, 96]. It turns out, that, due to the nonlinearity, even for harmonic excitation of the form

$$\mathbf{u}(\mathbf{x}, t) = \mathbf{u^c} \cos(\omega t) + \mathbf{u^s} \sin(\omega t),$$

the full range of modes has to be taken into account. For numerical computations we only consider a finite number of Fourier modes, i.e.,

$$\mathbf{y}(t) = \sum_{k=0}^{N} \mathbf{y_k^c} \cos(k\omega t) + \mathbf{y_k^s} \sin(k\omega t).$$

Moreover the nonlinear reluctivity (6.75) causes a full coupling of the sine and cosine coefficients with respect to all modes $k = 0, \ldots, N$, and therefore we lose the advantageous block-diagonal structure.

FEM After a FEM discretization in the conducting domain Ω_1, we are dealing with the nonlinear system of equations:

$$\text{Find } \mathbf{y} \in \mathbb{R}^{(2N+1)N_h}: \ (\mathcal{K}[\mathbf{y}] + \mathcal{D}) \, \mathbf{y} = \mathbf{u}.$$

Since the Fréchet derivative of the nonlinear frequency domain equations is explicitly computable, the nonlinearity can be overcome by applying Newton's method. Anyhow, at each step of the Newton iteration, a huge and fully block-coupled Jacobi system with sparse blocks has to be solved. Indeed, the defect equation has the following structure:

$$\text{Find } \mathbf{w} \in \mathbb{R}^{(2N+1)N_h}: \ (\mathcal{K}'[\mathbf{y}] + \mathcal{D}) \, \mathbf{w} = \mathbf{d}.$$

Here the block-diagonal and block-skew symmetric matrix $\mathcal{D}$ is given by

$$\mathcal{D} = \operatorname{diag} \begin{pmatrix} \mathbf{0} & \mathbf{M_{\sigma, k\omega}} \\ -\mathbf{M_{\sigma, k\omega}} & \mathbf{0} \end{pmatrix}_{k=0,\ldots,N},$$

and the fully populated and symmetric block-matrix $\mathcal{K}'[\mathbf{y}]$ for a given approximation of the solution $\mathbf{y}$ is given by

$$\mathcal{K}'[\mathbf{y}] = \begin{pmatrix} \mathbf{K_{kl}^{cc}}[\mathbf{y}] & \mathbf{K_{kl}^{sc}}[\mathbf{y}] \\ \mathbf{K_{kl}^{cs}}[\mathbf{y}] & \mathbf{K_{kl}^{ss}}[\mathbf{y}] \end{pmatrix}_{k,l=0,\ldots,N}.$$

Here the matrices $\mathbf{K_{kl}^{cc}}[\mathbf{y}]$, $\mathbf{K_{kl}^{cs}}[\mathbf{y}]$, $\mathbf{K_{kl}^{sc}}[\mathbf{y}]$, and $\mathbf{K_{kl}^{ss}}[\mathbf{y}]$ are given by

$$(\mathbf{K_{kl}^{cc}})_{ij} = (\tilde{\nu}_{kl}^{cc}(|\operatorname{\mathbf{curl}}\mathbf{y}|)\operatorname{\mathbf{curl}}\boldsymbol{\varphi_i}, \operatorname{\mathbf{curl}}\boldsymbol{\varphi_j})_{\mathbf{0},\Omega_1},$$
$$(\mathbf{K_{kl}^{cs}})_{ij} = (\tilde{\nu}_{kl}^{cs}(|\operatorname{\mathbf{curl}}\mathbf{y}|)\operatorname{\mathbf{curl}}\boldsymbol{\varphi_i}, \operatorname{\mathbf{curl}}\boldsymbol{\varphi_j})_{\mathbf{0},\Omega_1},$$
$$(\mathbf{K_{kl}^{sc}})_{ij} = (\tilde{\nu}_{kl}^{sc}(|\operatorname{\mathbf{curl}}\mathbf{y}|)\operatorname{\mathbf{curl}}\boldsymbol{\varphi_i}, \operatorname{\mathbf{curl}}\boldsymbol{\varphi_j})_{\mathbf{0},\Omega_1},$$
$$(\mathbf{K_{kl}^{ss}})_{ij} = (\tilde{\nu}_{kl}^{ss}(|\operatorname{\mathbf{curl}}\mathbf{y}|)\operatorname{\mathbf{curl}}\boldsymbol{\varphi_i}, \operatorname{\mathbf{curl}}\boldsymbol{\varphi_j})_{\mathbf{0},\Omega_1},$$

with the coefficients $\tilde{\nu}^{cc}$, $\tilde{\nu}^{cs} = \tilde{\nu}^{sc}$, and $\tilde{\nu}^{ss}$, that can be computed in the following manner, cf. [17],

$$
\begin{aligned}
\tilde{\nu}_{kl}^{cc}(|\mathbf{B}|) &= \frac{2}{T}\int_0^T \left[\nu'(|\mathbf{B}(t)|)\frac{(\mathbf{B}(t))^T(\mathbf{B}(t))}{|(\mathbf{B}(t))|} + \nu(|(\mathbf{B}(t))|)\mathbf{I}\right]\cos(k\omega t)\cos(l\omega t)\,\mathrm{dt}, \\
\tilde{\nu}_{kl}^{cs}(|\mathbf{B}|) &= \frac{2}{T}\int_0^T \left[\nu'(|\mathbf{B}(t)|)\frac{(\mathbf{B}(t))^T(\mathbf{B}(t))}{|(\mathbf{B}(t))|} + \nu(|(\mathbf{B}(t))|)\mathbf{I}\right]\cos(k\omega t)\sin(l\omega t)\,\mathrm{dt}, \qquad (6.76)\\
\tilde{\nu}_{kl}^{ss}(|\mathbf{B}|) &= \frac{2}{T}\int_0^T \left[\nu'(|\mathbf{B}(t)|)\frac{(\mathbf{B}(t))^T(\mathbf{B}(t))}{|(\mathbf{B}(t))|} + \nu(|(\mathbf{B}(t))|)\mathbf{I}\right]\sin(k\omega t)\sin(l\omega t)\,\mathrm{dt}.
\end{aligned}
$$

One important issue is the fast evaluation of these kind of integrals. This can be done in an efficient way, e.g., by using the idea of forward-backward recurrence, that is based on the three-term recurrence for the sine and cosine functions, cf. Remark 6.35.

Furthermore, due to the block-skew symmetric contribution from $\mathcal{D}$, we are dealing with a non-symmetric problem. Hence the MinRes method is no longer applicable, but, for instance, the GmRes method [139] or QMR method [56] can be used. Anyhow, preconditioning is still an important issue, but the fact, that the system matrix is non-symmetric, complicates the issue of preconditioning and analyzing.

Inspired by the structure of the preconditioner (6.33), we propose to use the block-diagonal preconditioner

$$\mathcal{P} = \operatorname{diag}\ (\mathcal{P}_k)_{k=0,\dots,N}\,,$$

with

$$\mathcal{P}_k = \operatorname{diag}\ \left(\mathbf{K_{kk}^{cc}} + \mathbf{M_{\sigma,k\omega}}, -(\mathbf{K_{kk}^{ss}} + \mathbf{M_{\sigma,k\omega}})\right).$$

Unfortunately the convergence rate analysis for the preconditioned GmRes method is more involving, since an estimate of the condition number of the preconditioned system is not sufficient. Indeed, a field of value estimate, see e.g. [112], is needed.

Remark 6.34. *In order to investigate preconditioners for the Jacobi system, it is important to investigate the non-symmetric system*

$$\underbrace{\begin{pmatrix} \mathbf{K_\nu} & \mathbf{M_{\sigma,\omega}} \\ -\mathbf{M_{\sigma,\omega}} & \mathbf{K_\nu} \end{pmatrix}}_{=:\bar{\mathcal{A}}_{F1}} \begin{pmatrix} \mathbf{y_h^c} \\ \mathbf{y_h^s} \end{pmatrix} = \begin{pmatrix} \mathbf{u_h^c} \\ \mathbf{u_h^s} \end{pmatrix}, \qquad (6.77)$$

that reflects the structure of the Jacobi system in the nonlinear case. Indeed, such a kind of system has already been considered in [18], wherein a multigrid-preconditioned QMR solver is proposed. The main ingredient of this solver is a specific block preconditioner $\hat{\mathcal{P}}$, that only involves the inversion of standard $\mathbf{H}(\operatorname{\mathbf{curl}}, \Omega_1)$ problems

$$\hat{\mathcal{P}}^{-1} := \frac{1}{2}\begin{pmatrix} (\mathbf{K_\nu} + \mathbf{M_{\sigma,\omega}})^{-1} & \mathbf{0} \\ \mathbf{0} & (\mathbf{K_\nu} + \mathbf{M_{\sigma,\omega}})^{-1} \end{pmatrix}\begin{pmatrix} \mathbf{I} & \mathbf{I} \\ \mathbf{I} & -\mathbf{I} \end{pmatrix}.$$

This preconditioner leads to a parameter-robust bound for the condition number of the preconditioned system, i.e.,

$$\kappa_{\mathcal{P}}(\hat{\mathcal{P}}^{-1}\bar{\mathcal{A}}_{F1}) := \|\hat{\mathcal{P}}^{-1}\bar{\mathcal{A}}_{F1}\|_{\mathcal{P}}\|\bar{\mathcal{A}}_{F1}^{-1}\hat{\mathcal{P}}^{-1}\|_{\mathcal{P}} \le 2.$$

Following the approach of Section 6.1, we can even do better. Inspired by the parameter-robust preconditioner (6.33) we propose the following preconditioner for the non-symmetric case

$$\bar{\mathcal{P}} = \begin{pmatrix} \mathbf{K}_\nu + \mathbf{M}_{\sigma,\omega} & \mathbf{0} \\ \mathbf{0} & -(\mathbf{K}_\nu + \mathbf{M}_{\sigma,\omega}) \end{pmatrix}.$$

Again we can verify an inf-sup condition and a sup-sup condition in a non-standard norm, and analogous to the symmetric case we obtain the condition number estimate

$$\kappa_{\mathcal{P}}(\bar{\mathcal{P}}^{-1}\bar{\mathcal{A}}_{F1}) = \kappa_{\mathcal{P}}(\mathcal{P}^{-1}\mathcal{A}_{F2}) \leq \sqrt{2}.$$

FEM-BEM In the non-conducting (unbounded) domain Ω_2, we are still dealing with a linear problem. Anyhow, after a FEM-BEM discretization in the full computational domain Ω, a nonlinear system is obtained. Since the nonlinearity is just due to the FEM contribution, the defect equation can be derived as in the pure FEM case. Therefore, at each Newton step a defect equation of the form

$$\text{Find } \mathbf{w} \in \mathbb{R}^{(2N+1)(N_h+L_h)}: \ (\mathcal{K}'_B[\mathbf{w}] + \mathcal{D}_B)\,\mathbf{w} = \mathbf{d},$$

has to be solved. In this setting the block-diagonal matrix $\mathcal{D}_B$ is given by

$$\mathcal{D}_B = \text{diag} \begin{pmatrix} -\mathbf{N} & \mathbf{B}^T & \mathbf{M}_{\sigma,k\omega} & \mathbf{0} \\ \mathbf{B} & -\mathbf{A} & \mathbf{0} & \mathbf{0} \\ -\mathbf{M}_{\sigma,k\omega} & \mathbf{0} & -\mathbf{N} & \mathbf{B}^T \\ \mathbf{0} & \mathbf{0} & \mathbf{B} & -\mathbf{A} \end{pmatrix}_{k=0,\dots,N},$$

and the block-matrix $\mathcal{K}'_B[\mathbf{y}]$ is given by

$$\mathcal{K}'_B[\mathbf{y}] = \begin{pmatrix} \mathbf{K}^{cc}_{kl}[\mathbf{y}] & \mathbf{0} & \mathbf{K}^{sc}_{kl}[\mathbf{y}] & \mathbf{0} \\ \mathbf{0} & \mathbf{0} & \mathbf{0} & \mathbf{0} \\ \mathbf{K}^{cs}_{kl}[\mathbf{y}] & \mathbf{0} & \mathbf{K}^{ss}_{kl}[\mathbf{y}] & \mathbf{0} \\ \mathbf{0} & \mathbf{0} & \mathbf{0} & \mathbf{0} \end{pmatrix}_{k,l=0,\dots,N}.$$

Again, inspired by the structure of the preconditioner (6.63), we propose to use the block-diagonal preconditioner

$$\mathcal{C} = \text{diag}\ (\mathcal{C}_k)_{k=0,\dots,N}$$

with

$$\mathcal{C}_k = \text{diag}\ \left(\mathbf{K}^{cc}_{kk} + \mathbf{M}_{\sigma,k\omega} - \mathbf{N} + \mathbf{B}^T\mathbf{A}^{-1}\mathbf{B}, \mathbf{A}, -(\mathbf{K}^{ss}_{kk} + \mathbf{M}_{\sigma,k\omega} - \mathbf{N} + \mathbf{B}^T\mathbf{A}^{-1}\mathbf{B}), -\mathbf{A}\right).$$

Hence, the preconditioners developed in Section 6.1 and 6.2 are very promising to be usable also in the nonlinear case. Anyhow, any theoretical results concerning robustness with respect to the involved parameters are illusive at the moment.

Beside the efficient solution of the Jacobi system, also the assembling of the Jacobi matrix $\mathcal{K}'[\mathbf{y}]$ has to be done in an efficient way. Due to the time integral in the coefficients in (6.76), efficient time integration methods have to be developed. For example, exploring the orthogonality of the sine and cosine functions, three-term recurrences can be used to evaluate the integrals by a forward-backward recursion.

Remark 6.35. *In order to evaluate integrals of the following form*

$$J_{kl} = \frac{2}{T}\int_0^T f(t)\cos(l\omega t)\underbrace{\cos(k\omega t)}_{=:T_k(t)}\,\mathrm{dt},$$

a three-term recurrence for the cosine by means of $T_{k+1}(t) = 2\cos(\omega t)T_k(t) - T_{k-1}(t)$ can be used. Indeed, a three-term recurrence for J_{kl} can be deduced as follows

$$J_{k+1,l} = \frac{2}{T}\int_0^T f(t)T_{k+1}(t)T_l(t)\mathrm{dt} = \frac{2}{T}\int_0^T f(t)T_k(t)\left[2\cos(\omega t)T_l(t)\right]\mathrm{dt} - \frac{2}{T}\int_0^T f(t)T_{k-1}(t)T_l(t)\mathrm{dt}$$

$$= \frac{2}{T}\int_0^T f(t)T_k(t)\left[T_{l+1}(t) + T_{l-1}(t)\right]\mathrm{dt} - \frac{2}{T}\int_0^T f(t)T_{k-1}(t)T_l(t)\mathrm{dt} = J_{k,l+1} + J_{k,l-1} - J_{k-1,l}.$$

Therefore, after the initialization of $2N$ initial values $J_{0,l}$ ($l = 0, \dots 2N$), the remaining terms can be computed by using the recurrence for $J_{k,l}$. A similar approach can be used for the integrals that are stemming from the $\sin(l\omega t)\cos(k\omega t)$ and $\sin(l\omega t)\sin(k\omega t)$ terms in (6.76).

6.4   Summary

In order to keep the presentation clear, we summarize the results obtained for the time-periodic eddy current problem in this chapter.

We established the multiharmonic discretization technique as an adequate tool to discretize time-periodic eddy current problems. This approach allows to switch from the time-domain to the frequency domain, and therefore to replace the solution of a time-dependent problem by a system of time-independent problems in the Fourier coefficients. Due to the linear nature of the underlying problem, a total decoupling of the individual modes is observed. We have analyzed numerous FEM and FEM-BEM formulations for the frequency domain equations in the continuous and discrete setting.

In order to obtain parameter-robust preconditioners for appropriate iterative solution techniques, we heavily explored the operator preconditioning technique to construct and analyze block-diagonal preconditioners for a huge range of problem settings in the regime of eddy current computations. In all the considered settings, we were able to construct preconditioners, that yield condition number bounds for the preconditioned system matrices, that are independent of the discretization parameters h, ω, N, as well as the model parameters σ and ν.

One of the big advantages of our block-diagonal preconditioning technique is, that for the realization of the diagonal blocks, only solvers for *standard* problems, that for example also appear in the magnetostatic case are needed. Indeed, we are dealing with the following five fundamental kinds of problems:

FEM	$\mathbf{K}_\nu + \mathbf{M}_\sigma$	$\mathbf{H}(\mathbf{curl}, \Omega_1)$ inner product
FEM	$\mathbf{K}_\nu + \mathbf{D}_\sigma \mathbf{L}_\sigma{}^{-1}\mathbf{D}_\sigma{}^T$	$\mathbf{H}(\mathbf{curl}, \Omega_1)$ inner product
FEM	$\mathbf{L}_\sigma$	$H_0^1(\Omega_1)$ inner product
BEM	$\mathbf{A}$	$\mathbf{H}_{\parallel}^{-1/2}(\mathrm{div}_\Gamma, \Gamma)$ inner product
FEM-BEM	$\mathbf{K}_\nu + \mathbf{M}_\sigma - \mathbf{N} + \mathbf{B}^T\mathbf{A}^{-1}\mathbf{B}$	$\mathbf{H}(\mathbf{curl}, \Omega_1)$ inner product (FEM-BEM Schur complement)

The efficient realization of these diagonal blocks is discussed in Chapter 8.

Indeed, the combination of the multiharmonic FEM-BEM coupling discretization technique with the robust and efficient solution strategies for the resulting systems of linear equations, justifies this method as a very powerful tool in the framework of time-periodic eddy current computations, not only in the considered linear setting, but also in the general nonlinear setting.

Finally, we briefly summarize the most important benefits of the proposed method:

- The periodic structure of our problem is treated by a natural approach in terms of a Fourier approximation. Therefore, the computations can be done in the frequency domain, where we can benefit from the full decoupling with respect to the individual modes.

- Unbounded domains are treated in terms of a FEM-BEM method.

- Parameter-robust solvers for the resulting systems of linear equations in the frequency domain guarantee competitiveness of the proposed method not only in theory but also in practice.

- Due to the decoupling nature of the frequency domain equations with respect to the individual modes, a parallelization of the proposed method is straightforward.

- Since, our proposed solver just relies on solvers or preconditioners for *standard* problems, any further improvements of these solvers or preconditioners will lead to additional improvements of our solver as well.

In the next Chapter, we use the MH-FEM-BEM method in order to discretize periodic optimal control problems. Optimal control problems are typically solved by deriving the optimality system. Due to the saddle point structure of the optimality system on the one hand, and due to the fact, that we have already constructed parameter-robust solvers for the state equations on the other hand, a generalization of the theory developed in this chapter seems to be obvious.

Chapter 7

Time-periodic eddy current optimal control problems

One basic task in optimal control of electromagnetic processes is to control a magnetic field $\mathbf{B} = \mathbf{curl\,y}$ by an applied current $\mathbf{j_i} = \mathbf{u}$, e.g., [152]. Again, the key point of interest is the asymptotic behavior of the magnetic field, i.e., we want to obtain a *steady state solution*. This approach leads to the framework of time-periodic optimal control problems. As for time-periodic eddy current problems, an approximation in time in terms of a truncated Fourier series is an adequate tool to derive sufficient approximations to the time-periodic solution.

Therefore, this chapter is devoted to the numerical treatment of eddy current optimal control problems by the MH-FEM-BEM method. Using the results of Chapter 4, we switch from the time domain to the frequency domain. For the optimal control problem in the frequency domain, we state the reduced optimality system and discretize it by means of a finite element method or by means of a finite element - boundary element coupling method. We derive appropriate variational formulations and show well-posedness in non-standard norms. In order to obtain these norms, we heavily stress the theory developed in Chapter 5. Based on these well-posedness results, we propose block-diagonal preconditioners for the resulting systems of linear equations and provide rigorous condition number estimates for the preconditioned systems, that are uniform in all involved discretization, model and regularization parameters.

In this chapter the main emphasis is on the development of robust preconditioners for the resulting frequency domain equations. Therefore, we mostly consider the simple model problem

$$\mathcal{J}(\hat{\mathbf{y}}, \hat{\mathbf{u}}) = \min_{(\mathbf{y},\mathbf{u}) \in W_2^1((0,T),\mathbf{H}(\mathbf{curl},\Omega_1)) \times L_2((0,T),\mathbf{L_2}(\Omega_1))} \mathcal{J}(\mathbf{y}, \mathbf{u}), \tag{7.1}$$

subject to the state equation (6.47). Indeed, in Section 7.1 and Section 7.2, we consider the simple case of distributed control, i.e., the minimization functional under consideration is given by

$$\mathcal{J}(\mathbf{y}, \mathbf{u}) = \frac{1}{2} \int_{\Omega_1 \times (0,T)} |\mathbf{y} - \mathbf{y_d}|^2 \mathrm{d}\mathbf{x}\,\mathrm{dt} + \frac{\lambda}{2} \int_{\Omega_1 \times (0,T)} |\mathbf{u}|^2 \mathrm{d}\mathbf{x}\,\mathrm{dt}. \tag{7.2}$$

Here $\mathbf{y_d} \in L_2((0,T), \mathbf{L_2}(\Omega_1))$ is a given desired state and $\lambda > 0$ is a cost or regularization parameter. As we have seen in Section 3.2, under mild assumptions, both, the conservation of charges law imposed on the control $\mathbf{u}$, and the divergence condition imposed on the state $\mathbf{y}$, are fulfilled for (7.1)-(7.2) at the solution in a natural way, and therefore they can be omitted. Consequently, this model problem is well suited to demonstrate the construction and analysis of efficient and robust solution strategies. Following the spirit of the previous chapter, this chapter is divided into four main parts:

- In Section 7.1 we start by analyzing the eddy current optimal control problem on the bounded domain Ω_1, discretized in terms of the MH-FEM method. Therein we consider the different variational formulations of the state equation, that have been derived in Chapter 6.

- In Section 7.2, we extend the results obtained in Section 7.1, by taking the exterior domain into account in terms of a FEM-BEM coupling method, leading to a full MH-FEM-BEM discretization of the optimality system.

- Furthermore, we discuss the application of the solvers constructed in Section 7.1 to problems with various constraints. We include the cases of different control and observation domains, observation of the **B**-field and box constraints imposed on the Fourier coefficients of the state **y** and/or the control **u**. In all these cases, the decoupling of the resulting systems of linear equations with respect to the individual modes is retained.

- Finally, we also discuss the application of our solver to constrained optimization problems, where the advantageous decoupling structure is lost. As an example we consider the case of the observation at the final time.

In most of the cases, the optimality system obtains a linear structure, and therefore it is sufficient to analyze the efficient and robust solution of the resulting linear system of equations. Anyhow, box constraints imposed on the Fourier coefficients of the control and/or the state render the resulting optimality systems nonlinear. In these two cases, linear solvers for the Jacobi systems, that have to be solved at each step of a semi-smooth Newton iteration, are proposed and analysed.

7.1   Symmetric FEM formulations

In this section, we restrict ourselves to the case of a problem, that is located in the conducting domain Ω_1. Therefore, we consider equation (6.3) as a PDE constraint in (7.1). Indeed, in this setting we are dealing with a special regime in the framework of optimal control problems with distributed control, since all three domains, the computational domain of the state equation, the observation domain and the control domain coincide with Ω_1.

7.1.1   Multiharmonic discretization

Following Chapter 4, we assume that the desired state $\mathbf{y_d}$ is given by a multiharmonic excitation in terms of a truncated Fourier series, i.e.,

$$\mathbf{y_d}(\mathbf{x},t) = \sum_{k=0}^{N} \mathbf{y_{d,k}^c}(\mathbf{x}) \cos(k\omega t) + \mathbf{y_{d,k}^s}(\mathbf{x}) \sin(k\omega t). \tag{7.3}$$

Consequently, we have, that the time-periodic state $\mathbf{y}$ and the periodic control $\mathbf{u}$, can be expressed in terms of the same frequency ω, i.e.,

$$\mathbf{y}(\mathbf{x},t) = \sum_{k=0}^{N} \mathbf{y_k^c}(\mathbf{x}) \cos(k\omega t) + \mathbf{y_k^s}(\mathbf{x}) \sin(k\omega t),$$

$$\mathbf{u}(\mathbf{x},t) = \sum_{k=0}^{N} \mathbf{u_k^c}(\mathbf{x}) \cos(k\omega t) + \mathbf{u_k^s}(\mathbf{x}) \sin(k\omega t). \tag{7.4}$$

Using the multiharmonic representations (7.3) and (7.4), we can rewrite the eddy current optimal control problem in the frequency domain as follows: For all modes $k = 1, \ldots, N$, find $(\hat{\mathbf{y}}_k^c, \hat{\mathbf{y}}_k^s, \hat{\mathbf{u}}_k^c, \hat{\mathbf{u}}_k^s)$, such that

$$\tilde{\mathcal{J}}(\hat{\mathbf{y}}_k^c, \hat{\mathbf{y}}_k^s, \hat{\mathbf{u}}_k^c, \hat{\mathbf{u}}_k^s) = \min_{(\mathbf{y}_k^c, \mathbf{y}_k^s, \mathbf{u}_k^c, \mathbf{u}_k^s)} \sum_{j \in \{c,s\}} \left[\frac{1}{2} \int_{\Omega_1} |\mathbf{y}_k^j - \mathbf{y}_{d,k}^j|^2 d\mathbf{x} + \frac{\lambda}{2} \int_{\Omega_1} |\mathbf{u}_k^j|^2 d\mathbf{x} \right], \tag{7.5}$$

where $(\mathbf{y_k^c}, \mathbf{y_k^s}, \mathbf{u_k^c}, \mathbf{u_k^s})$ fulfills (6.7). Furthermore, for the mode $k = 0$, we are dealing with the minimization problem: Find $(\hat{\mathbf{y}}_0^c, \hat{\mathbf{u}}_0^c)$, such that

$$\tilde{\mathcal{J}}(\hat{\mathbf{y}}_0^c, \hat{\mathbf{u}}_0^c) = \min_{(\mathbf{y_0^c}, \mathbf{u_0^c})} \frac{1}{2} \int_{\Omega_1} |\mathbf{y_0^c} - \mathbf{y_{d,0}^c}|^2 \mathrm{d}\mathbf{x} + \frac{\lambda}{2} \int_{\Omega_1} |\mathbf{u_0^c}|^2 \mathrm{d}\mathbf{x}, \tag{7.6}$$

where $(\mathbf{y_0^c}, \mathbf{u_0^c})$ fulfills (6.8). Due to the linearity of the state equation, we obtain a decoupling of our minimization problem with respect to the modes $k = 0, \ldots, N$. For the minimization problems (7.5) and (7.6) for a fixed mode k a similar result as in Subsection 3.2.2 is valid. Under the assumptions of Theorem 3.8 the Fourier coefficients $\mathbf{u_k^j}, j \in \{c, s\}$, of the state $\mathbf{u}$, automatically fulfill (6.5) at the solution.

7.1.2 Symmetric variational formulation for FEM

In order to solve the minimization problem in the frequency domain, we compute the corresponding optimality system. Therefore, we use the different variational formulations for the state equation, derived in Subsection 6.1.2. Indeed, we concentrate on the two variational formulations *Formulation FEM 1* and *Formulation FEM 3*. Since for each mode $k = 0, \ldots, N$, the optimality systems have the same structure, we concentrate on the time-harmonic case, i.e., $k = 1$. The analysis for the remaining modes can be deduced by formally setting $\omega = k\omega$. In contrast to the forward problem, in the optimal control setting the analysis for the mode $k = 0$ can also be deduced from the analysis for the mode $k = 1$ by setting $k = 0$ and dropping the two equations, that correspond to the sine parts of the state and the co-state.

Formulation OC-FEM 1   We start by considering the state equation in the variational formulation *Formulation FEM 1*, cf. Problem 6.1. Following Subsection 3.2.2 and Section 4.5, the multiharmonic approach is applied to the optimal control problem and the optimality system is derived. In the usual manner we are using the identity $\mathbf{u} = \lambda^{-1}\mathbf{p}$ in order to remove the control $\mathbf{u}$ from the optimality system. Hence, we are dealing with the reduced optimality system in the frequency domain, given by: For each mode $k = 0, 1, \ldots, N$, find the Fourier coefficients $(\mathbf{y_k^c}, \mathbf{y_k^s}, \mathbf{p_k^c}, \mathbf{p_k^s}) \in \mathbf{H_0}(\mathbf{curl}, \Omega_1)^4$, such that

$$\begin{cases} -\omega k(\sigma\mathbf{p_k^s}, \mathbf{v_k^c})_{0,\Omega_1} + (\nu\,\mathbf{curl}\,\mathbf{p_k^c}, \mathbf{curl}\,\mathbf{v_k^c})_{0,\Omega_1} + (\mathbf{y_k^c}, \mathbf{v_k^c})_{0,\Omega_1} = (\mathbf{y_{d,k}^c}, \mathbf{v_k^c})_{0,\Omega_1}, \\[4pt] \omega k(\sigma\mathbf{p_k^c}, \mathbf{v_k^s})_{0,\Omega_1} + (\nu\,\mathbf{curl}\,\mathbf{p_k^s}, \mathbf{curl}\,\mathbf{v_k^s})_{0,\Omega_1} + (\mathbf{y_k^s}, \mathbf{v_k^s})_{0,\Omega_1} = (\mathbf{y_{d,k}^s}, \mathbf{v_k^s})_{0,\Omega_1}, \\[4pt] \omega k(\sigma\mathbf{y_k^s}, \mathbf{q_k^c})_{0,\Omega_1} + (\nu\,\mathbf{curl}\,\mathbf{y_k^c}, \mathbf{curl}\,\mathbf{q_k^c})_{0,\Omega_1} - \lambda^{-1}(\mathbf{p_k^c}, \mathbf{q_k^c})_{0,\Omega_1} = 0, \\[4pt] -\omega k(\sigma\mathbf{y_k^c}, \mathbf{q_k^s})_{0,\Omega_1} + (\nu\,\mathbf{curl}\,\mathbf{y_k^s}, \mathbf{curl}\,\mathbf{q_k^s})_{0,\Omega_1} - \lambda^{-1}(\mathbf{p_k^s}, \mathbf{q_k^s})_{0,\Omega_1} = 0, \end{cases} \tag{7.7}$$

for all test functions $(\mathbf{v_k^c}, \mathbf{v_k^s}, \mathbf{q_k^c}, \mathbf{q_k^s}) \in \mathbf{H_0}(\mathbf{curl}, \Omega_1)^4$. Indeed, this is the kind of equation under consideration in this section. Due to the decoupling nature, it is sufficient to investigate (7.7) for the fixed mode $k = 1$. Consequently, the corresponding variational problem can be stated as follows.

Problem 7.1 (Primal formulation). *Find* $(\mathbf{y^c}, \mathbf{y^s}, \mathbf{p^c}, \mathbf{p^s}) \in \mathbf{H_0}(\mathbf{curl}, \Omega_1)^4$, *such that*

$$\mathcal{B}\left((\mathbf{y^c}, \mathbf{y^s}, \mathbf{p^c}, \mathbf{p^s}), (\mathbf{v^c}, \mathbf{v^s}, \mathbf{q^c}, \mathbf{q^s})\right) = \int_{\Omega_1} \left[\mathbf{y_d^c} \cdot \mathbf{v^c} + \mathbf{y_d^s} \cdot \mathbf{v^s}\right] \mathrm{d}\mathbf{x}, \tag{7.8}$$

for all test functions $(\mathbf{v^c}, \mathbf{v^s}, \mathbf{q^c}, \mathbf{q^s}) \in \mathbf{H_0}(\mathbf{curl}, \Omega_1)^4$. *Here the symmetric and indefinite bilinear form* $\mathcal{B}$ *is given by*

$$\begin{aligned} \mathcal{B}\left((\mathbf{y^c}, \mathbf{y^s}, \mathbf{p^c}, \mathbf{p^s}), (\mathbf{v^c}, \mathbf{v^s}, \mathbf{q^c}, \mathbf{q^s})\right) := & \sum_{j \in \{c,s\}} (\mathbf{y^j}, \mathbf{v^j})_{0,\Omega_1} + \mathcal{A}_{F1}((\mathbf{v^s}, \mathbf{v^c}), (\mathbf{p^c}, \mathbf{p^s})) \\ & + \mathcal{A}_{F1}((\mathbf{y^s}, \mathbf{y^c}), (\mathbf{q^c}, \mathbf{q^s})) - \frac{1}{\lambda} \sum_{j \in \{c,s\}} (\mathbf{p^j}, \mathbf{q^j})_{0,\Omega_1}. \end{aligned} \tag{7.9}$$

Problem 6.1 has a unique solution $(\mathbf{y^c}, \mathbf{y^s}, \mathbf{p^c}, \mathbf{p^s}) \in \mathbf{H_0}(\mathbf{curl}, \Omega_1)^4$, cf. Lemma 7.3. Under the assumptions of Theorem 3.8, the solution $(\mathbf{y^c}, \mathbf{y^s}, \mathbf{p^c}, \mathbf{p^s})$ is weakly divergence-free, and therefore the charge conservation law is fulfilled automatically.

Formulation OC-FEM 2   Next we consider the state equation in the variational formulation *Formulation FEM 3*, cf. Problem 6.3, where the divergence constraint on the state $\mathbf{y}$ is incorporated in a mixed variational framework. Applying the multiharmonic approach and deriving the optimality system, we end up with the following system of partial differential equations in the frequency domain: For each mode $k = 0, 1, \ldots, N$, find the Fourier coefficients $(\mathbf{y_k^c}, \mathbf{y_k^s}, \mathbf{p_k^c}, \mathbf{p_k^s}, \mu_k^c, \mu_k^s, \rho_k^c, \rho_k^s) \in$
$\mathbf{H_0}(\mathbf{curl}, \Omega_1)^4 \times H_0^1(\Omega_1)^4$, such that

$$
\begin{cases}
-\omega k(\sigma \mathbf{p_k^s}, \mathbf{v_k^c})_{\mathbf{0},\Omega_1} + (\nu \, \mathbf{curl} \, \mathbf{p_k^c}, \mathbf{curl} \, \mathbf{v_k^c})_{\mathbf{0},\Omega_1} \\
\qquad\qquad + (\mathbf{y_k^c}, \mathbf{v_k^c})_{\mathbf{0},\Omega_1} + \omega k(\sigma \mathbf{v_k^c}, \nabla \rho_k^c)_{\mathbf{0},\Omega_1} = (\mathbf{y_{d,k}^c}, \mathbf{v_k^c})_{\mathbf{0},\Omega_1}, \\
\qquad\qquad\qquad\qquad \omega k(\sigma \mathbf{p_k^c}, \nabla \eta_k^c)_{\mathbf{0},\Omega_1} = 0, \\
\omega k(\sigma \mathbf{p_k^c}, \mathbf{v_k^s})_{\mathbf{0},\Omega_1} + (\nu \, \mathbf{curl} \, \mathbf{p_k^s}, \mathbf{curl} \, \mathbf{v_k^s})_{\mathbf{0},\Omega_1} \\
\qquad\qquad + (\mathbf{y_k^s}, \mathbf{v_k^s})_{\mathbf{0},\Omega_1} + \omega k(\sigma \mathbf{v_k^s}, \nabla \rho_k^s)_{\mathbf{0},\Omega_1} = (\mathbf{y_{d,k}^s}, \mathbf{v_k^s})_{\mathbf{0},\Omega_1}, \\
\qquad\qquad\qquad\qquad \omega k(\sigma \mathbf{p_k^s}, \nabla \eta_k^s)_{\mathbf{0},\Omega_1} = 0, \\
\omega k(\sigma \mathbf{y_k^s}, \mathbf{q_k^c})_{\mathbf{0},\Omega_1} + (\nu \, \mathbf{curl} \, \mathbf{y_k^c}, \mathbf{curl} \, \mathbf{q_k^c})_{\mathbf{0},\Omega_1} \\
\qquad\qquad - \lambda^{-1}(\mathbf{p_k^c}, \mathbf{q_k^c})_{\mathbf{0},\Omega_1} + \omega k(\sigma \mathbf{q_k^c}, \nabla \mu_k^c)_{\mathbf{0},\Omega_1} = 0, \\
\qquad\qquad\qquad\qquad \omega k(\sigma \mathbf{y_k^c}, \nabla \theta_k^c)_{\mathbf{0},\Omega_1} = 0, \\
-\omega k(\sigma \mathbf{y_k^c}, \mathbf{q_k^s})_{\mathbf{0},\Omega_1} + (\nu \, \mathbf{curl} \, \mathbf{y_k^s}, \mathbf{curl} \, \mathbf{q_k^s})_{\mathbf{0},\Omega_1} \\
\qquad\qquad - \lambda^{-1}(\mathbf{p_k^s}, \mathbf{q_k^s})_{\mathbf{0},\Omega_1} + \omega k(\sigma \mathbf{q_k^s}, \nabla \mu_k^s)_{\mathbf{0},\Omega_1} = 0, \\
\qquad\qquad\qquad\qquad \omega k(\sigma \mathbf{y_k^s}, \nabla \theta_k^s)_{\mathbf{0},\Omega_1} = 0,
\end{cases}
$$

for all test functions $(\mathbf{v_k^c}, \mathbf{v_k^s}, \mathbf{q_k^c}, \mathbf{q_k^s}, \eta_k^c, \eta_k^s, \theta_k^c, \theta_k^s) \in \mathbf{H_0}(\mathbf{curl}, \Omega_1)^4 \times H_0^1(\Omega_1)^4$. For convenience, we introduce the following abbreviation

$$
\begin{aligned}
\Upsilon &:= (\mathbf{y^c}, \mathbf{y^s}, \mathbf{p^c}, \mathbf{p^s}) \quad \text{and} \quad \Psi := (\mu^c, \mu^s, \rho^c, \rho^s), \\
\Phi &:= (\mathbf{v^c}, \mathbf{v^s}, \mathbf{q^c}, \mathbf{q^s}) \quad \text{and} \quad \Theta := (\eta^c, \eta^s, \theta^c, \theta^s).
\end{aligned}
$$

For a fixed mode $k = 1$, the corresponding variational formulation reads as follows.

Problem 7.2 (Mixed formulation). *Find* $(\Upsilon, \Psi) \in \mathbf{H_0}(\mathbf{curl}, \Omega_1)^4 \times H_0^1(\Omega_1)^4$, *such that*

$$
\mathcal{B}_M\left((\Upsilon, \Psi), (\Phi, \Theta)\right) = \int_{\Omega_1} \left[\mathbf{y_d^c} \cdot \mathbf{v^c} + \mathbf{y_d^s} \cdot \mathbf{v^s} \right] d\mathbf{x}, \tag{7.10}
$$

for all test functions $(\Phi, \Theta) \in \mathbf{H_0}(\mathbf{curl}, \Omega_1)^4 \times H_0^1(\Omega_1)$. *Here the symmetric and indefinite bilinear form* $\mathcal{B}_M$ *is given by*

$$
\mathcal{B}_M\left((\Upsilon, \Psi), (\Phi, \Theta)\right) := \mathcal{B}(\Upsilon, \Phi) + b(\Phi, \Psi) + b(\Upsilon, \Theta), \tag{7.11}
$$

where the bilinear form $b(\cdot, \cdot)$ *is given by*

$$
b(\Phi, \Psi) := \omega \sum_{j \in \{c,s\}} \left[(\sigma \mathbf{v^j}, \nabla \rho^j)_{\mathbf{0},\Omega_1} + (\sigma \mathbf{q^j}, \nabla \mu^j)_{\mathbf{0},\Omega_1} \right].
$$

Problem 7.2 has a unique solution $(\Upsilon, \Psi) \in \mathbf{H_0}(\mathbf{curl}, \Omega_1)^4 \times H_0^1(\Omega_1)^4$, cf. Lemma 7.4. Under the assumptions of Theorem 3.8, the solution Υ is weakly divergence-free.

7.1.3   Discretization

In order to discretize the problems, we use $\mathcal{ND}_0^0(\mathcal{T}_h)$, a conforming finite element subspace of $\mathbf{H_0}(\mathbf{curl}, \Omega_1)$, and $\mathcal{S}_0^1(\mathcal{T}_h)$, a conforming finite element subspace of $H_0^1(\Omega_1)$, cf. Section 2.4. Let $\{\varphi_\mathbf{i}\}_{i=1,N_h}$ denote the usual edge basis of $\mathcal{ND}_0^0(\mathcal{T}_h)$, and let $\{\psi_i\}_{i=1,M_h}$ denote the usual nodal basis of $\mathcal{S}_0^1(\mathcal{T}_h)$, respectively. We define the following FEM matrices:

$$
\begin{aligned}
(\mathbf{K_\nu})_{ij} &= (\nu \, \mathbf{curl} \, \varphi_\mathbf{i}, \mathbf{curl} \, \varphi_\mathbf{j})_{\mathbf{0}, \Omega_1}, \\
(\mathbf{M_{\sigma,\omega}})_{ij} &= \omega(\sigma\varphi_\mathbf{i}, \varphi_\mathbf{j})_{\mathbf{0}, \Omega_1}, \\
(\mathbf{M})_{ij} &= (\varphi_\mathbf{i}, \varphi_\mathbf{j})_{\mathbf{0}, \Omega_1}, \\
(\mathbf{D_{\sigma,\omega}})_{ij} &= \omega(\sigma\varphi_\mathbf{i}, \nabla\psi_j)_{\mathbf{0}, \Omega_1}, \\
(\mathbf{L_{\sigma,\omega}})_{ij} &= \omega(\sigma\nabla\psi_i, \nabla\psi_j)_{\mathbf{0}, \Omega_1}.
\end{aligned}
\tag{7.12}
$$

7.1.3.1   Symmetric formulations ($k = 1$)

Formulation OC-FEM 1   Find $(\mathbf{y_h^c}, \mathbf{y_h^s}, \mathbf{p_h^c}, \mathbf{p_h^s})^T \in \mathbb{R}^{4N_h}$:

$$
\underbrace{\begin{pmatrix}
\mathbf{M} & \mathbf{0} & \mathbf{K_\nu} & -\mathbf{M_{\sigma,\omega}} \\
\mathbf{0} & \mathbf{M} & \mathbf{M_{\sigma,\omega}} & \mathbf{K_\nu} \\
\mathbf{K_\nu} & \mathbf{M_{\sigma,\omega}} & -\lambda^{-1}\mathbf{M} & \mathbf{0} \\
-\mathbf{M_{\sigma,\omega}} & \mathbf{K_\nu} & \mathbf{0} & -\lambda^{-1}\mathbf{M}
\end{pmatrix}}_{=:\mathcal{B}}
\begin{pmatrix}
\mathbf{y_h^c} \\
\mathbf{y_h^s} \\
\mathbf{p_h^c} \\
\mathbf{p_h^s}
\end{pmatrix}
=
\begin{pmatrix}
\mathbf{y_{d,h}^c} \\
\mathbf{y_{d,h}^s} \\
\mathbf{0} \\
\mathbf{0}
\end{pmatrix}.
\tag{7.13}
$$

Formulation OC-FEM 2   Find $(\mathbf{y_h^c}, \mathbf{y_h^s}, \mathbf{p_h^c}, \mathbf{p_h^s}, \boldsymbol{\mu}_\mathbf{h}^\mathbf{c}, \boldsymbol{\mu}_\mathbf{h}^\mathbf{s}, \boldsymbol{\rho}_\mathbf{h}^\mathbf{c}, \boldsymbol{\rho}_\mathbf{h}^\mathbf{s})^T \in \mathbb{R}^{4(N_h+M_h)}$:

$$
\underbrace{\begin{pmatrix}
\mathbf{M} & \mathbf{0} & \mathbf{K_\nu} & -\mathbf{M_{\sigma,\omega}} & \mathbf{0} & \mathbf{0} & \mathbf{D_{\sigma,\omega}}^T & \mathbf{0} \\
\mathbf{0} & \mathbf{M} & \mathbf{M_{\sigma,\omega}} & \mathbf{K_\nu} & \mathbf{0} & \mathbf{0} & \mathbf{0} & \mathbf{D_{\sigma,\omega}}^T \\
\mathbf{K_\nu} & \mathbf{M_{\sigma,\omega}} & -\lambda^{-1}\mathbf{M} & \mathbf{0} & \mathbf{D_{\sigma,\omega}}^T & \mathbf{0} & \mathbf{0} & \mathbf{0} \\
-\mathbf{M_{\sigma,\omega}} & \mathbf{K_\nu} & \mathbf{0} & -\lambda^{-1}\mathbf{M} & \mathbf{0} & \mathbf{D_{\sigma,\omega}}^T & \mathbf{0} & \mathbf{0} \\
\mathbf{0} & \mathbf{0} & \mathbf{D_{\sigma,\omega}} & \mathbf{0} & \mathbf{0} & \mathbf{0} & \mathbf{0} & \mathbf{0} \\
\mathbf{0} & \mathbf{0} & \mathbf{0} & \mathbf{D_{\sigma,\omega}} & \mathbf{0} & \mathbf{0} & \mathbf{0} & \mathbf{0} \\
\mathbf{D_{\sigma,\omega}} & \mathbf{0} & \mathbf{0} & \mathbf{0} & \mathbf{0} & \mathbf{0} & \mathbf{0} & \mathbf{0} \\
\mathbf{0} & \mathbf{D_{\sigma,\omega}} & \mathbf{0} & \mathbf{0} & \mathbf{0} & \mathbf{0} & \mathbf{0} & \mathbf{0}
\end{pmatrix}}_{=:\mathcal{B}_M}
\begin{pmatrix}
\mathbf{y_h^c} \\
\mathbf{y_h^s} \\
\mathbf{p_h^c} \\
\mathbf{p_h^s} \\
\boldsymbol{\mu}_\mathbf{h}^\mathbf{c} \\
\boldsymbol{\mu}_\mathbf{h}^\mathbf{s} \\
\boldsymbol{\rho}_\mathbf{h}^\mathbf{c} \\
\boldsymbol{\rho}_\mathbf{h}^\mathbf{s}
\end{pmatrix}
=
\begin{pmatrix}
\mathbf{y_{d,h}^c} \\
\mathbf{y_{d,h}^s} \\
\mathbf{0} \\
\mathbf{0} \\
\mathbf{0} \\
\mathbf{0} \\
\mathbf{0} \\
\mathbf{0}
\end{pmatrix}.
$$

$$\tag{7.14}$$

In fact, the system matrices $\mathcal{B}$ and $\mathcal{B}_M$ are symmetric and indefinite, and have double or three-fold saddle point structure. Typically small mesh sizes h, large or small ω, small λ and large jumps in the material coefficients ν and σ across interfaces lead to a dramatic growth in the condition number of these matrices. Therefore, we expect a very bad convergence rate if any Krylov subspace method, like the MinRes method, is applied to the unpreconditioned systems of equations. Hence appropriate preconditioning is an important issue.

7.1.4   Block-diagonal preconditioners

This subsection is devoted to the construction of parameter-robust preconditioners for the systems of linear equations of the last subsection. For each proposed formulation, we investigate its structure to construct a preconditioner either by the matrix interpolation technique, cf. Subsection 5.2.2, or the technique of inexact Schur complement preconditioning, cf. Subsection 5.2.3. Furthermore, we provide condition number bounds for the resulting preconditioned systems of linear equations, by showing well-posedness of the underlying systems of partial differential equations in non-standard norms.

Formulation OC-FEM 1   In order to construct parameter-robust and block-diagonal precondi-
tioners, we want to use the matrix interpolation theory presented in Subsection 5.2.2. We start by
analyzing the special case of constant conductivity in Ω_1, i.e., $\sigma(\mathbf{x}) = \sigma \in \mathbb{R}^+$. In this special setting,
we have $\mathbf{M}_{\sigma,\omega} = \omega\sigma\mathbf{M}$ with the constant positive conductivity σ. Due to this special structure, this
case is much easier to handle. We explore the saddle point structure of our system matrix $\mathcal{B}$ that can
be rewritten as follows:

$$\mathcal{B} = \begin{pmatrix} \mathbf{A} & \mathbf{B^T} \\ \mathbf{B} & -\mathbf{C} \end{pmatrix},$$

where the blocks $\mathbf{A}$, $\mathbf{B}$, and $\mathbf{C}$ are defined by the relations

$$\mathbf{A} = \begin{pmatrix} \mathbf{M} & \mathbf{0} \\ \mathbf{0} & \mathbf{M} \end{pmatrix}, \quad \mathbf{B} = \begin{pmatrix} \mathbf{K}_{\boldsymbol{\nu}} & \mathbf{M}_{\sigma,\omega} \\ -\mathbf{M}_{\sigma,\omega} & \mathbf{K}_{\boldsymbol{\nu}} \end{pmatrix} \quad \text{and} \quad \mathbf{C} = \frac{1}{\lambda}\mathbf{A}.$$

Since $\mathbf{A}$ is symmetric and positive definite, we can build both Schur complements $\mathbf{S}$ and $\mathbf{R} = \lambda\mathbf{S}$,
given by

$$\mathbf{S} = \begin{pmatrix} (\lambda^{-1} + \omega^2\sigma^2)\mathbf{M} + \mathbf{K}_{\boldsymbol{\nu}}\mathbf{M}^{-1}\mathbf{K}_{\boldsymbol{\nu}} & \mathbf{0} \\ \mathbf{0} & (\lambda^{-1} + \omega^2\sigma^2)\mathbf{M} + \mathbf{K}_{\boldsymbol{\nu}}\mathbf{M}^{-1}\mathbf{K}_{\boldsymbol{\nu}} \end{pmatrix},$$

and therefore the Schur complement preconditioners (cf. Theorem 5.3). Due to Theorem 5.5, a
candidate for a parameter-robust and block-diagonal preconditioner is an interpolant of the previous
standard Schur complement preconditioners. Therefore we choose $\theta = 1/2$ and interpolate to obtain
a new preconditioner

$$\tilde{\mathcal{C}} = \begin{pmatrix} [\mathbf{A}, \mathbf{R}]_{\frac{1}{2}} & \mathbf{0} \\ \mathbf{0} & [\mathbf{S}, \mathbf{C}]_{\frac{1}{2}} \end{pmatrix} = \mathrm{diag}\ \left([\mathbf{M}, \lambda\mathbf{G}]_{\frac{1}{2}}, [\mathbf{M}, \lambda\mathbf{G}]_{\frac{1}{2}}, [\mathbf{G}, \lambda^{-1}\mathbf{M}]_{\frac{1}{2}}, [\mathbf{G}, \lambda^{-1}\mathbf{M}]_{\frac{1}{2}} \right)$$

$$= \mathrm{diag}\ \left(\sqrt{\lambda}[\mathbf{M}, \mathbf{G}]_{\frac{1}{2}}, \sqrt{\lambda}[\mathbf{M}, \mathbf{G}]_{\frac{1}{2}}, \frac{1}{\sqrt{\lambda}}[\mathbf{M}, \mathbf{G}]_{\frac{1}{2}}, \frac{1}{\sqrt{\lambda}}[\mathbf{M}, \mathbf{G}]_{\frac{1}{2}} \right),$$

where $\mathbf{G} := (\lambda^{-1} + \omega^2\sigma^2)\mathbf{M} + \mathbf{K}_{\boldsymbol{\nu}}\mathbf{M}^{-1}\mathbf{K}_{\boldsymbol{\nu}}$. Due to the restriction of the conductivity to be constant,
the interpolation of two by two block matrices reduces to the simpler interpolation $[\mathbf{M}, \mathbf{G}]_{\frac{1}{2}}$. Conse-
quently, we can derive another new preconditioner $\mathcal{C}_c$, that is spectral equivalent to the interpolated
preconditioner $\tilde{\mathcal{C}}$. Again, by using the spectral inequality (6.32), we obtain

$$\begin{aligned}
\mathbf{x}^T[\mathbf{M}, \mathbf{G}]_{\frac{1}{2}}\mathbf{x} &= \mathbf{x}^T[\mathbf{M}, (\lambda^{-1} + \omega^2\sigma^2)\mathbf{M} + \mathbf{K}_{\boldsymbol{\nu}}\mathbf{M}^{-1}\mathbf{K}_{\boldsymbol{\nu}}]_{\frac{1}{2}}\mathbf{x} \\
&\leq \mathbf{x}^T \left(\sqrt{\lambda^{-1} + \omega^2\sigma^2}\mathbf{M} + [\mathbf{M}, \mathbf{K}_{\boldsymbol{\nu}}\mathbf{M}^{-1}\mathbf{K}_{\boldsymbol{\nu}}]_{\frac{1}{2}} \right) \mathbf{x} \\
&= \mathbf{x}^T \left(\sqrt{\lambda^{-1} + \omega^2\sigma^2}\mathbf{M} + \mathbf{M}^{\frac{1}{2}} \left(\mathbf{M}^{-\frac{1}{2}}\mathbf{K}_{\boldsymbol{\nu}}\mathbf{M}^{-1}\mathbf{K}_{\boldsymbol{\nu}}\mathbf{M}^{-\frac{1}{2}} \right)^{\frac{1}{2}} \mathbf{M}^{\frac{1}{2}} \right) \mathbf{x} \\
&= \mathbf{x}^T \left(\sqrt{\lambda^{-1} + \omega^2\sigma^2}\mathbf{M} + \mathbf{M}^{\frac{1}{2}} \left(\mathbf{M}^{-\frac{1}{2}}\mathbf{K}_{\boldsymbol{\nu}}\mathbf{M}^{-\frac{1}{2}} \right) \mathbf{M}^{\frac{1}{2}} \right) \mathbf{x} \\
&= \mathbf{x}^T \left(\sqrt{\lambda^{-1} + \omega^2\sigma^2}\mathbf{M} + \mathbf{K}_{\boldsymbol{\nu}} \right) \mathbf{x}, \quad \forall\, \mathbf{x} \in (\ker \mathbf{K}_{\boldsymbol{\nu}})^{\perp}
\end{aligned}$$

and

$$\begin{aligned}
\mathbf{x}^T[\mathbf{M}, \mathbf{G}]_{\frac{1}{2}}\mathbf{x} &= \mathbf{x}^T[\mathbf{M}, (\lambda^{-1} + \omega^2\sigma^2)\mathbf{M} + \mathbf{K}_{\boldsymbol{\nu}}\mathbf{M}^{-1}\mathbf{K}_{\boldsymbol{\nu}}]_{\frac{1}{2}}\mathbf{x} \\
&\geq \frac{1}{\sqrt{2}}\mathbf{x}^T \left(\sqrt{\lambda^{-1} + \omega^2\sigma^2}\mathbf{M} + [\mathbf{M}, \mathbf{K}_{\boldsymbol{\nu}}\mathbf{M}^{-1}\mathbf{K}_{\boldsymbol{\nu}}]_{\frac{1}{2}} \right) \mathbf{x} \\
&= \frac{1}{\sqrt{2}}\mathbf{x}^T \left(\sqrt{\lambda^{-1} + \omega^2\sigma^2}\mathbf{M} + \mathbf{M}^{\frac{1}{2}} \left(\mathbf{M}^{-\frac{1}{2}}\mathbf{K}_{\boldsymbol{\nu}}\mathbf{M}^{-1}\mathbf{K}_{\boldsymbol{\nu}}\mathbf{M}^{-\frac{1}{2}} \right)^{\frac{1}{2}} \mathbf{M}^{\frac{1}{2}} \right) \mathbf{x} \\
&= \frac{1}{\sqrt{2}}\mathbf{x}^T \left(\sqrt{\lambda^{-1} + \omega^2\sigma^2}\mathbf{M} + \mathbf{M}^{\frac{1}{2}} \left(\mathbf{M}^{-\frac{1}{2}}\mathbf{K}_{\boldsymbol{\nu}}\mathbf{M}^{-\frac{1}{2}} \right) \mathbf{M}^{\frac{1}{2}} \right) \mathbf{x} \\
&= \frac{1}{\sqrt{2}}\mathbf{x}^T \left(\sqrt{\lambda^{-1} + \omega^2\sigma^2}\mathbf{M} + \mathbf{K}_{\boldsymbol{\nu}} \right) \mathbf{x}, \quad \forall\, \mathbf{x} \in (\ker \mathbf{K}_{\boldsymbol{\nu}})^{\perp}.
\end{aligned}$$

Furthermore, using the simpler diagonal block $\mathbf{F_c} = (1/\sqrt{\lambda} + \omega\sigma)\mathbf{M} + \mathbf{K}_{\boldsymbol{\nu}}$, we immediately obtain the spectral inequality

$$\frac{1}{2}\mathbf{x}^T\mathbf{F_c}\mathbf{x} \leq \mathbf{x}^T[\mathbf{M},\mathbf{G}]_{\frac{1}{2}}\mathbf{x} \leq \mathbf{x}^T\mathbf{F_c}\mathbf{x}, \quad \forall\,\mathbf{x} \in (\ker\mathbf{K}_{\boldsymbol{\nu}})^{\perp}.$$

Hence, from Subsection 5.2.4, we have, that the preconditioner $\mathcal{C}_c$, given by the block-diagonal matrix

$$\mathcal{C}_c = \operatorname{diag}\left(\sqrt{\lambda}\mathbf{F_c}, \sqrt{\lambda}\mathbf{F_c}, \frac{1}{\sqrt{\lambda}}\mathbf{F_c}, \frac{1}{\sqrt{\lambda}}\mathbf{F_c}\right) \tag{7.15}$$

is a candidate for a parameter-robust preconditioner. In the subspace $\left[(\ker\mathbf{K}_{\boldsymbol{\nu}})^{\perp}\right]^4 \subset \mathbb{R}^{4N_h}$, we immediately obtain the condition number estimate

$$\kappa_{\mathcal{C}_c}(\mathcal{C}_c^{-1}\mathcal{B}) := \|\mathcal{C}_c^{-1}\mathcal{B}\|_{\mathcal{C}_c}\|\mathcal{B}^{-1}\mathcal{C}_c\|_{\mathcal{C}_c} \leq \frac{2(\sqrt{5}+1)}{\sqrt{5}-1} \approx 5.235.$$

In the next step, we extend the qualitative estimate of the condition number to the full vector space $\mathbb{R}^{4N_h}$ and to the case of piecewise constant conductivity σ. Exploring the structural similarities to $\mathcal{C}_c$, our guess for the block-diagonal preconditioner is

$$\mathcal{C} := \operatorname{diag}\left(\sqrt{\lambda}\mathbf{F}, \sqrt{\lambda}\mathbf{F}, \frac{1}{\sqrt{\lambda}}\mathbf{F}, \frac{1}{\sqrt{\lambda}}\mathbf{F}\right), \tag{7.16}$$

with the block $\mathbf{F} = \mathbf{K}_{\boldsymbol{\nu}} + \mathbf{M}_{\boldsymbol{\sigma},\boldsymbol{\omega}} + 1/\sqrt{\lambda}\mathbf{M}$. We mention that for the case $\sigma \in \mathbb{R}^+$ we have $\mathbf{F} = \mathbf{F_c}$. Inspired by the structure of the preconditioner (7.16), we introduce the non-standard norm $\|\cdot\|_{\mathcal{C}}$ in $\mathbf{H_0}(\mathbf{curl},\Omega_1)^4$ by

$$\|(\mathbf{y^c},\mathbf{y^s},\mathbf{p^c},\mathbf{p^s})\|_{\mathcal{C}}^2 = \sqrt{\lambda}\|\mathbf{y^c}\|_{\mathcal{C}_1}^2 + \sqrt{\lambda}\|\mathbf{y^s}\|_{\mathcal{C}_1}^2 + \frac{1}{\sqrt{\lambda}}\|\mathbf{p^c}\|_{\mathcal{C}_1}^2 + \frac{1}{\sqrt{\lambda}}\|\mathbf{p^s}\|_{\mathcal{C}_1}^2,$$

where the non-standard norm $\|\cdot\|_{\mathcal{C}_1}$ in $\mathbf{H_0}(\mathbf{curl},\Omega_1)$ is given by

$$\|\mathbf{y}\|_{\mathcal{C}_1}^2 = (\nu\,\mathbf{curl}\,\mathbf{y},\mathbf{curl}\,\mathbf{y})_{\mathbf{0},\Omega_1} + \omega(\sigma\mathbf{y},\mathbf{y})_{\mathbf{0},\Omega_1} + \frac{1}{\sqrt{\lambda}}(\mathbf{y},\mathbf{y})_{\mathbf{0},\Omega_1}.$$

The main result is summarized in the following lemma, that claims that an inf-sup and a sup-sup condition are fulfilled with parameter-independent constants, namely $1/\sqrt{3}$ and 1.

Lemma 7.3. *We have*

$$\begin{aligned}\frac{1}{\sqrt{3}}\|(\mathbf{y^c},\mathbf{y^s},\mathbf{p^c},\mathbf{p^s})\|_{\mathcal{C}} &\leq \sup_{0\neq(\mathbf{v^c},\mathbf{v^s},\mathbf{q^c},\mathbf{q^s})}\frac{\mathcal{B}((\mathbf{y^c},\mathbf{y^s},\mathbf{p^c},\mathbf{p^s}),(\mathbf{v^c},\mathbf{v^s},\mathbf{q^c},\mathbf{q^s}))}{\|(\mathbf{v^c},\mathbf{v^s},\mathbf{q^c},\mathbf{q^s})\|_{\mathcal{C}}} \\ \|(\mathbf{y^c},\mathbf{y^s},\mathbf{p^c},\mathbf{p^s})\|_{\mathcal{C}} &\geq \sup_{0\neq(\mathbf{v^s},\mathbf{v^c},\mathbf{q^s},\mathbf{q^c})}\frac{\mathcal{B}((\mathbf{y^c},\mathbf{y^s},\mathbf{p^c},\mathbf{p^s}),(\mathbf{v^c},\mathbf{v^s},\mathbf{q^c},\mathbf{q^s}))}{\|(\mathbf{v^c},\mathbf{v^s},\mathbf{q^c},\mathbf{q^s})\|_{\mathcal{C}}}\end{aligned} \tag{7.17}$$

for all $(\mathbf{y^c},\mathbf{y^s},\mathbf{p^c},\mathbf{p^s}) \in \mathbf{H_0}(\mathbf{curl},\Omega_1)^4$.

Proof. Boundedness follows from reapplication of Cauchy's inequality with appropriate scaling of the parameter λ. The lower estimate can be attained by choosing $\mathbf{v^c} = \mathbf{y^c} + \frac{1}{\sqrt{\lambda}}\mathbf{p^c} - \frac{1}{\sqrt{\lambda}}\mathbf{p^s}$, $\mathbf{v^s} = \mathbf{y^s} + \frac{1}{\sqrt{\lambda}}\mathbf{p^s} + \frac{1}{\sqrt{\lambda}}\mathbf{p^c}$, $\mathbf{q^c} = -\mathbf{p^c} + \sqrt{\lambda}\mathbf{y^c} + \sqrt{\lambda}\mathbf{y^s}$ and $\mathbf{q^s} = -\mathbf{p^s} + \sqrt{\lambda}\mathbf{y^s} - \sqrt{\lambda}\mathbf{y^c}$. Note that, for the special choice of the test functions, we have $\|(\mathbf{v^c},\mathbf{v^s},\mathbf{q^c},\mathbf{q^s})\|_{\mathcal{C}} = \sqrt{3}\|(\mathbf{y^c},\mathbf{y^s},\mathbf{p^c},\mathbf{p^s})\|_{\mathcal{C}}$. $\square$

In general, an inf-sup bound for $\mathbf{H_0}(\mathbf{curl},\Omega_1)^4$ does not imply such a lower bound on the finite element subspace $\mathcal{ND}_0^0(\mathcal{T}_h)^4$. However, in this case the inequalities (7.17) remain also valid for the Nédélec finite element subspace $\mathcal{ND}_0^0(\mathcal{T}_h)^4$, since the proof can be repeated for the finite element functions step by step. Therefore, we obtain the improved condition number estimate

$$\kappa_{\mathcal{C}}(\mathcal{C}^{-1}\mathcal{B}) := \|\mathcal{C}^{-1}\mathcal{B}\|_{\mathcal{C}}\|\mathcal{B}^{-1}\mathcal{C}\|_{\mathcal{C}} \leq \sqrt{3} \approx 1.732.$$

Formulation OC-FEM 2   Since we already have a robust preconditioner for $\mathcal{B}$, we pursue the strategy of inexact Schur complement preconditioning, cf. Subsection 5.2.3. Therefore, we propose the following block-diagonal inexact Schur complement preconditioner

$$\mathcal{C}_M = \operatorname{diag}\left(\sqrt{\lambda}\mathbf{F}, \sqrt{\lambda}\mathbf{F}, \frac{1}{\sqrt{\lambda}}\mathbf{F}, \frac{1}{\sqrt{\lambda}}\mathbf{F}, \frac{1}{\sqrt{\lambda}}\mathbf{S_J}, \frac{1}{\sqrt{\lambda}}\mathbf{S_J}, \sqrt{\lambda}\mathbf{S_J}, \sqrt{\lambda}\mathbf{S_J}\right), \tag{7.18}$$

where $\mathbf{S_J} = \mathbf{D_{\sigma,\omega}}^T\mathbf{F}^{-1}\mathbf{D_{\sigma,\omega}}$. Since the matrix $\mathbf{D_{\sigma,\omega}}$ has full rank, the block $\mathbf{S_J}$ is positive definite and therefore the whole preconditioner $\mathcal{C}_M$ is positive definite. According to the choice of the block-diagonal preconditioner (7.18), we introduce the non-standard norm $\|\cdot\|_{\mathcal{C}_M}$ in the product space $\mathbf{H_0}(\mathbf{curl}, \Omega_1)^4 \times H_0^1(\Omega_1)^2$ by

$$\|(\Upsilon, \Psi)\|_{\mathcal{C}_M}^2 := \|\Upsilon\|_{\mathcal{C}}^2 + \left(\sup_{\Phi \in \mathbf{H_0}(\mathbf{curl},\Omega_1)^4} \frac{b(\Phi, \Psi)}{\|\Phi\|_{\mathcal{C}}}\right)^2.$$

The main result is summarized in the following Lemma, that claims that an inf-sup condition and a sup-sup condition are fulfilled in the non-standard norm with constants $\frac{1}{2\sqrt{3}}$ and $\frac{1+\sqrt{5}}{2}$.

Lemma 7.4.   *We have*

$$\frac{1}{2\sqrt{3}}\|(\Upsilon, \Psi)\|_{\mathcal{C}_M} \leq \sup_{(\Phi,\Theta)\neq 0} \frac{\mathcal{B}_M((\Upsilon, \Psi), (\Phi, \Theta))}{\|(\Phi, \Theta)\|_{\mathcal{C}_M}} \leq \frac{1 + \sqrt{5}}{2}\|(\Upsilon, \Psi)\|_{\mathcal{C}_M} \tag{7.19}$$

for all $(\Upsilon, \Psi) \in \mathbf{H_0}(\mathbf{curl}, \Omega_1)^4 \times H_0^1(\Omega_1)^4$.

Proof. From Lemma 7.3 we obtain, that the bilinear form $\mathcal{B}(\cdot, \cdot)$ is bounded with constant 1 and satisfies an inf-sup condition on the kernel of $b(\cdot, \cdot)$ with constant $1/\sqrt{3}$. Boundedness of $b(\cdot, \cdot)$ easily follows with constant 1. Finally, by definition of $\|\cdot\|_{\mathcal{C}_M}$, the bilinear form $b(\cdot, \cdot)$ satisfies an inf-sup condition with constant 1. Consequently the lower and upper bound follow from Theorem 2.3. $\square$

Furthermore, the inequalities (7.19) remain valid for the finite element subspace $\mathcal{ND}_0^0(\mathcal{T}_h)^4 \times \mathcal{S}_0^1(\mathcal{T}_h)^4$, since the proof can be repeated for the finite element functions step by step. Therefore, we obtain the condition number estimate

$$\kappa_{\mathcal{C}_M}(\mathcal{C}_M^{-1}\mathcal{B}_M) := \|\mathcal{C}_M^{-1}\mathcal{B}_M\|_{\mathcal{C}_M}\|\mathcal{B}_M^{-1}\mathcal{C}_M\|_{\mathcal{C}_M} \leq \sqrt{3}(1 + \sqrt{5}) \approx 5.605.$$

7.1.5   Summary

We table the condition number κ and the theoretical number of MinRes iterations *maxiter* needed, for reducing the initial error by a factor of 10^{-8}. Furthermore, we collect the diagonal blocks, that are needed to apply the block-diagonal preconditioner.

	κ	maxiter	diagonal blocks
Formulation OC-FEM 1	1.732	30	$\mathbf{F}$
Formulation OC-FEM 2	5.605	106	$\mathbf{F}$, $\mathbf{S_J}$

The realization of the diagonal blocks $\mathbf{F}$ and $\mathbf{S_J}$ is discussed in Chapter 8.

7.1.6   Numerics

In order to confirm our theoretical results numerically, we report on our first numerical tests for an academic example. Therefore, we consider the solution of the system corresponding to the block of the mode $k = 1$. The numerical results presented in this section were attained using ParMax[1]. First, we demonstrate the robustness of the block-diagonal preconditioners with respect to the frequency ω, the

---

[1] `http://www.numa.uni-linz.ac.at/P19255/software.shtml`

conductivity σ and the regularization parameter λ. Therefore, for the solution of the preconditioning equations arising from the diagonal blocks, we use the sparse direct solver UMFPACK[2] that is very efficient for several thousand unknowns in the case of three dimensional problems [45, 46, 47].

In the following numerical experiments, we provide the number of MinRes iterations needed for reducing the initial residual by a factor 10^{-8} for different ω, σ, λ and h for Problem 7.1 and 7.2. These numerical experiments were performed for a three-dimensional linear problem on the unit cube $\Omega_1 = (0, 1)^3$, discretized by tetrahedra. Furthermore the piecewise constant conductivity σ is given by

$$\sigma = \left\{ \begin{array}{ll} \sigma_1 & \text{in } \Omega_a = \{(x, y, z)^T \in [0, 1]^3 : z > 0.5\} \\ \sigma_2 & \text{in } \Omega_b = \{(x, y, z)^T \in [0, 1]^3 : z \leq 0.5\} \end{array} \right. . \tag{7.20}$$

Formulation OC-FEM 1   Table 7.1-7.5 provide the number of MinRes iterations needed for reducing the initial residual by a factor of 10^{-8}. These experiments demonstrate the independence of the MinRes convergence rate of the parameters ω, σ, λ and the mesh size h since the number of iterations is bounded by 28 for all computed constellations. Furthermore, in Table 7.1 and Table 7.2 we also report the number of unpreconditioned MinRes iterations, that are necessary for reducing the initial residual by a factor of 10^{-8}. The large number of iterations in the unpreconditioned case underline the importance of appropriate preconditioning.

Formulation OC-FEM 1 (modified preconditioner)   Table 7.6-7.9 provide the number of MinRes iterations needed for reducing the initial residual by a factor of 10^{-8}, using a modified preconditioner

$$\mathcal{C}_{mod} = \text{diag} \left(\sqrt{\tilde{\lambda}} \mathbf{F}_{mod}, \sqrt{\tilde{\lambda}} \mathbf{F}_{mod}, \frac{1}{\sqrt{\tilde{\lambda}}} \mathbf{F}_{mod}, \frac{1}{\sqrt{\tilde{\lambda}}} \mathbf{F}_{mod} \right), \tag{7.21}$$

with the diagonal block $\mathbf{F}_{mod} = 1/\sqrt{\tilde{\lambda}} \mathbf{M} + \mathbf{M}_{\sigma,\omega} + \mathbf{K}_{\nu}$, where we use the truncated regularization parameter $\tilde{\lambda} = \min(\lambda, 1)$ in the preconditioner. It is clear, that for $\lambda \leq 1$, the modified preconditioner (7.21) is identical to the original one as stated in (7.15). Indeed, this simple modification is suggested in [99], where the usage of (7.21) provides some benefits in the reduction of possible FEM-BEM Schur complements. These experiments demonstrate the independence of the MinRes convergence rate of the parameters ω, σ, λ and the mesh size h since the number of iterations is bounded by 76 for all computed constellations.

Formulation OC-FEM 2   Table 7.10 and Table 7.11 provide the number of MinRes iterations needed for reducing the initial residual by a factor 10^{-8}. These experiments demonstrate the independence of the MinRes convergence rate of the parameters ω, σ, λ and the mesh size h since the number of iterations is bounded by 88 for all computed constellations.

The numerical experiments presented in this section clearly demonstrate the theoretical robustness of the proposed block-diagonal preconditioners. In large-scale applications, the realization of the diagonal preconditioners by using a sparse direct solver like UMFPACK is illusive. The practical realization of our preconditioners is addressed in Chapter 8.

Remark 7.5. *Let us mention, that in order to provide a rigorous numerical verification of the theoretical condition number bounds numerical experiments for the parameter settings $(\omega, \sigma, \nu, \lambda) \in [10^{-10}, 10^{10}]^4$ are required. Indeed, these experiments have to be performed for all the proposed settings and various mesh sizes of h. Since these experiments are too expensive, we just present a selection of results for critical parameter settings and mesh sizes h.*

---

[2] `http://www.cise.ufl.edu/research/sparse/umfpack/`

		ω										
		10^{-10}	10^{-8}	10^{-6}	10^{-4}	10^{-2}	1	10^2	10^4	10^6	10^8	10^{10}
	10^{-10}	7	7	7	7	7	7	7	7	7	6	4
		[587]	[587]	[586]	[587]	[587]	[587]	[587]	[591]	[485]	[263]	[116]
	10^{-8}	11	11	11	11	11	11	11	10	6	4	4
		[481]	[482]	[482]	[481]	[481]	[481]	[482]	[468]	[263]	[116]	[114]
	10^{-6}	21	21	21	21	21	21	20	12	6	4	4
		[373]	[373]	[373]	[373]	[373]	[373]	[373]	[263]	[116]	[114]	[114]
	10^{-4}	19	19	19	19	20	20	22	12	6	4	4
		[719]	[719]	[720]	[720]	[718]	[719]	[534]	[114]	[114]	[114]	[114]
	10^{-2}	20	20	20	20	20	20	20	12	6	4	4
		[1134]	[1134]	[1134]	[1136]	[1135]	[1134]	[227]	[114]	[114]	[114]	[114]
λ	1	10	10	10	10	10	14	20	12	6	4	4
		[2349]	[2351]	[2349]	[2350]	[2350]	[2274]	[222]	[114]	[114]	[114]	[114]
	10^2	6	6	6	6	8	10	20	12	6	4	4
		[2688]	[2681]	[2696]	[2667]	[3291]	[2494]	[224]	[114]	[114]	[114]	[114]
	10^4	4	4	4	6	6	10	20	12	6	4	4
		[2477]	[2500]	[2983]	[3572]	[4641]	[2499]	[224]	[114]	[114]	[114]	[114]
	10^6	4	4	4	6	6	10	20	12	6	4	4
		[1152]	[1159]	[3434]	[4697]	[4867]	[2493]	[222]	[114]	[114]	[114]	[114]
	10^8	2	4	4	6	6	10	20	12	6	4	4
		[1143]	[1162]	[4101]	[5659]	[4810]	[2502]	[222]	[114]	[114]	[114]	[114]
	10^{10}	2	4	4	4	4	10	20	12	6	4	4
		[1157]	[1163]	[4937]	[5881]	[4791]	[2501]	[224]	[114]	[114]	[114]	[114]

Table 7.1: Formulation OC-FEM 1. Number of MinRes iterations for different values of ω and λ using the EXACT version of the preconditioner with UMFPACK for $\mathbf{F}$ ($DOF = 2416$, $\nu = \sigma = 1$), [·] number of MinRes iterations without preconditioner.

		ω										
		10^{-10}	10^{-8}	10^{-6}	10^{-4}	10^{-2}	1	10^2	10^4	10^6	10^8	10^{10}
	10^{-10}	9	9	9	9	9	9	9	10	6	4	4
		[708]	[708]	[708]	[708]	[708]	[708]	[708]	[711]	[578]	[308]	[134]
	10^{-8}	17	17	17	17	17	17	18	15	6	4	4
		[575]	[575]	[575]	[575]	[575]	[575]	[575]	[557]	[308]	[134]	[132]
	10^{-6}	21	21	21	21	21	21	20	18	6	4	4
		[825]	[824]	[825]	[825]	[825]	[825]	[824]	[307]	[134]	[132]	[132]
	10^{-4}	20	20	20	20	20	21	26	20	6	4	4
		[2536]	[2535]	[2535]	[2536]	[2536]	[2536]	[1848]	[133]	[132]	[132]	[132]
	10^{-2}	18	18	18	18	18	20	22	20	6	4	4
		[6698]	[6669]	[6696]	[6698]	[6690]	[6676]	[1095]	[132]	[132]	[132]	[132]
λ	1	10	10	10	10	10	14	22	20	6	4	4
		[-]	[-]	[-]	[-]	[-]	[-]	[1094]	[132]	[132]	[132]	[132]
	10^2	6	6	6	6	8	10	22	20	6	4	4
		[-]	[-]	[-]	[-]	[-]	[-]	[1094]	[132]	[132]	[132]	[132]
	10^4	4	4	4	6	6	10	22	20	6	4	4
		[-]	[-]	[-]	[-]	[-]	[-]	[1094]	[132]	[132]	[132]	[132]
	10^6	4	4	4	6	6	10	22	20	6	4	4
		[7365]	[7547]	[-]	[-]	[-]	[-]	[1094]	[132]	[132]	[132]	[132]
	10^8	2	4	4	4	6	10	22	20	6	4	4
		[7391]	[7552]	[-]	[-]	[-]	[-]	[1094]	[132]	[132]	[132]	[132]
	10^{10}	2	4	4	4	4	10	22	20	6	4	4
		[7381]	[1545]	[-]	[-]	[-]	[-]	[1094]	[132]	[132]	[132]	[132]

Table 7.2: Formulation OC-FEM 1. Number of MinRes iterations for different values of ω and λ using the EXACT version of the preconditioner with UMFPACK for $\mathbf{F}$ ($DOF = 16736$, $\nu = \sigma = 1$), [·] number of MinRes iterations without preconditioner. [-] indicates that MinRes did not converge within 10000 iterations.

		ω										
		10^{-10}	10^{-8}	10^{-6}	10^{-4}	10^{-2}	1	10^{2}	10^{4}	10^{6}	10^{8}	10^{10}
	10^{-10}	13	13	13	13	13	13	13	13	8	4	4
	10^{-8}	21	21	21	21	21	21	21	17	8	4	4
	10^{-6}	21	21	21	21	21	21	21	20	8	4	4
	10^{-4}	20	20	20	20	20	20	28	22	8	4	4
	10^{-2}	16	16	16	16	16	18	22	22	8	4	4
λ	1	10	10	10	10	10	12	20	22	8	4	4
	10^{2}	6	6	6	6	8	10	20	22	8	4	4
	10^{4}	4	4	4	6	6	10	20	22	8	4	4
	10^{6}	4	4	4	4	6	10	20	22	8	4	4
	10^{8}	2	4	4	4	6	10	20	22	8	4	4
	10^{10}	3	4	4	4	4	10	20	22	8	4	4

Table 7.3: Formulation OC-FEM 1. Number of MinRes iterations for different values of ω and λ using the EXACT version of the preconditioner with UMFPACK for $\mathbf{F}$ ($DOF = 124096$, $\nu = \sigma = 1$).

		ν										
		10^{-10}	10^{-8}	10^{-6}	10^{-4}	10^{-2}	1	10^{2}	10^{4}	10^{6}	10^{8}	10^{10}
	10^{-10}	2	2	3	3	5	13	21	16	6	4	3
	10^{-8}	2	2	3	4	7	21	20	10	4	4	3
	10^{-6}	2	3	3	5	13	21	16	6	4	4	4
	10^{-4}	2	3	4	7	21	20	10	6	4	4	4
	10^{-2}	3	4	6	13	21	18	8	4	4	6	6
λ	1	4	4	8	17	28	12	6	4	6	6	9
	10^{2}	4	4	8	20	22	10	6	4	6	6	8
	10^{4}	4	4	8	22	20	10	6	4	4	4	8
	10^{6}	4	4	8	22	20	10	4	4	4	4	8
	10^{8}	4	4	8	22	20	10	4	4	4	4	8
	10^{10}	4	4	8	22	20	10	4	2	4	4	8

Table 7.4: Formulation OC-FEM 1. Number of MinRes iterations for different values of ν and λ using the EXACT version of the preconditioner with UMFPACK for $\mathbf{F}$ ($DOF = 124096$, $\omega = \sigma = 1$).

		σ_2										
		10^{-10}	10^{-8}	10^{-6}	10^{-4}	10^{-2}	1	10^{2}	10^{4}	10^{6}	10^{8}	10^{10}
	10^{-10}	13	13	13	13	13	13	13	17	16	13	13
	10^{-8}	21	21	21	21	21	21	21	28	21	21	21
	10^{-6}	21	21	21	21	21	21	22	26	22	21	21
	10^{-4}	21	21	21	21	21	20	28	22	20	20	20
	10^{-2}	18	18	18	18	18	18	24	20	16	16	16
λ	1	18	18	18	18	18	12	20	18	12	12	12
	10^{2}	14	14	14	14	14	10	18	18	10	10	10
	10^{4}	8	8	8	8	10	10	18	18	8	8	8
	10^{6}	8	8	8	8	8	10	18	18	8	8	8
	10^{8}	6	6	6	8	8	10	18	18	8	8	8
	10^{10}	6	6	8	8	8	10	18	18	8	8	8

Table 7.5: Formulation OC-FEM 1. Number of MinRes iterations for different values of σ_2 and λ using the EXACT version of the preconditioner with UMFPACK for $\mathbf{F}$ ($DOF = 124096$, $\nu = \omega = 1$, $\sigma_1 = 1$).

		ω										
		10^{-10}	10^{-8}	10^{-6}	10^{-4}	10^{-2}	1	10^2	10^4	10^6	10^8	10^{10}
λ	1	10	10	10	10	10	14	22	20	6	4	4
	10^2	9	11	12	12	12	13	22	20	6	4	4
	10^4	9	11	15	15	14	13	22	20	6	4	4
	10^6	9	11	17	17	15	13	22	20	6	4	4
	10^8	9	11	19	19	15	13	22	20	6	4	4
	10^{10}	9	11	21	19	15	13	22	20	6	4	4

Table 7.6: Formulation OC-FEM 1 with modified preconditioner. Number of MinRes iterations for different values of ω and λ using the EXACT version of the preconditioner with UMFPACK for $\mathbf{F}_{mod}$ ($DOF = 16736$, $\nu = \sigma = 1$).

		ω										
		10^{-10}	10^{-8}	10^{-6}	10^{-4}	10^{-2}	1	10^2	10^4	10^6	10^8	10^{10}
λ	1	10	10	10	10	10	12	20	22	8	4	4
	10^2	9	9	12	12	12	13	20	22	8	4	4
	10^4	9	11	14	14	14	13	20	22	8	4	4
	10^6	9	11	16	16	14	13	20	22	8	4	4
	10^8	9	11	19	18	14	13	20	22	8	4	4
	10^{10}	9	11	21	19	14	13	20	22	8	4	4

Table 7.7: Formulation OC-FEM 1 with modified preconditioner. Number of MinRes iterations for different values of ω and λ using the EXACT version of the preconditioner with UMFPACK for $\mathbf{F}_{mod}$ ($DOF = 124096$, $\nu = \sigma = 1$).

		σ_2										
		10^{-10}	10^{-8}	10^{-6}	10^{-4}	10^{-2}	1	10^2	10^4	10^6	10^8	10^{10}
λ	1	18	18	18	18	18	14	20	18	12	12	12
	10^2	34	34	40	40	40	13	23	19	13	13	13
	10^4	34	35	50	50	47	13	23	19	13	13	13
	10^6	34	35	57	57	48	13	23	19	13	13	13
	10^8	34	35	64	63	48	13	23	19	13	13	13
	10^{10}	34	35	71	64	48	13	23	19	13	13	13

Table 7.8: Formulation OC-FEM 1 with modified preconditioner. Number of MinRes iterations for different values of σ_2 and λ using the EXACT version of the preconditioner with UMFPACK for $\mathbf{F}_{mod}$ ($DOF = 16736$, $\nu = \omega = 1$, $\sigma_1 = 1$).

		σ_2										
		10^{-10}	10^{-8}	10^{-6}	10^{-4}	10^{-2}	1	10^2	10^4	10^6	10^8	10^{10}
λ	1	18	18	18	18	18	12	20	18	12	12	12
	10^2	34	34	41	41	41	13	21	21	13	13	13
	10^4	35	35	50	50	49	13	21	21	13	13	13
	10^6	35	35	60	60	50	13	21	21	13	13	13
	10^8	35	35	68	66	50	13	21	21	13	13	13
	10^{10}	35	35	76	68	50	13	21	21	13	13	13

Table 7.9: Formulation OC-FEM 1 with modified preconditioner. Number of MinRes iterations for different values of ω and λ using the EXACT version of the preconditioner with UMFPACK for $\mathbf{F}_{mod}$ ($DOF = 124096$, $\nu = \omega = 1$, $\sigma_1 = 1$).

		ω										
		10^{-10}	10^{-8}	10^{-6}	10^{-4}	10^{-2}	1	10^2	10^4	10^6	10^8	10^{10}
λ	10^{-10}	21	19	19	17	17	17	17	17	12	8	10
	10^{-8}	29	29	29	29	29	29	29	24	12	8	8
	10^{-6}	33	33	33	33	33	33	29	33	10	8	8
	10^{-4}	28	28	28	28	28	28	36	42	18	12	10
	10^{-2}	22	22	22	22	26	31	34	32	14	12	10
	1	12	13	14	14	14	14	24	22	10	8	8
	10^2	11	11	13	13	13	18	34	32	14	12	10
	10^4	11	11	11	14	16	24	44	40	18	12	10
	10^6	13	13	13	17	21	28	56	50	22	14	14
	10^8	15	15	18	21	25	36	68	62	24	18	16
	10^{10}	31	34	34	23	33	42	80	78	30	20	16

Table 7.10: Formulation OC-FEM 2. Number of MinRes iterations for different values of ω and λ using the EXACT version of the preconditioner with UMFPACK for $\mathbf{F}$ ($DOF = 19652$, $\nu = \sigma = 1$).

		ω										
		10^{-10}	10^{-8}	10^{-6}	10^{-4}	10^{-2}	1	10^2	10^4	10^6	10^8	10^{10}
λ	10^{-10}	27	27	25	25	25	25	25	25	16	8	10
	10^{-8}	35	35	35	35	35	35	35	29	16	8	8
	10^{-6}	32	32	32	32	32	32	33	35	14	8	8
	10^{-4}	28	28	28	28	28	28	38	48	20	12	10
	10^{-2}	20	20	20	20	23	29	35	34	16	12	10
	1	12	12	14	14	14	14	24	26	12	8	8
	10^2	11	11	13	13	13	18	34	34	16	12	10
	10^4	11	11	11	14	16	24	44	46	20	12	10
	10^6	13	13	15	17	21	30	58	60	24	16	14
	10^8	24	17	18	21	27	36	70	72	32	18	16
	10^{10}	46	61	65	23	33	42	88	88	38	24	16

Table 7.11: Formulation OC-FEM 2. Number of MinRes iterations for different values of ω and λ using the EXACT version of the preconditioner with UMFPACK for $\mathbf{F}$ ($DOF = 143748$, $\nu = \sigma = 1$).

7.2   Symmetric FEM-BEM couplings

In the previous section, we have investigated the optimality systems stemming from different variational formulations of the state equation, that all aim a FEM discretization. Therefore, in all these cases, we restricted the analysis to the bounded domain Ω_1. In this section, we consider the state equation in the full computational domain $\mathbb{R}^3$. Therefore, we consider equation (6.47) as a PDE constraint in (7.1). Again, we are dealing with the special regime, that the observation and control domain coincide with the conducting domain Ω_1.

7.2.1   Multiharmonic discretization

Following Chapter 4, we assume that the desired state $\mathbf{y_d}$ is given by a multiharmonic excitation in terms of a truncated Fourier series, cf. (7.3). Consequently, we have, that the periodic state $\mathbf{y}$ and the periodic control $\mathbf{u}$, also can be expressed in terms of the same frequency ω, cf. (7.4).

7.2.2   Symmetric variational formulations for FEM-BEM

In order to solve the minimization problem in the frequency domain, we compute the corresponding optimality system. Therefore, we consider the variational formulations for the state equation *Formulation FEM-BEM 1*, derived in Subsection 6.2.2. Since for each mode $k = 0, \ldots, N$, the optimality systems have the same structure, we concentrate on the time-harmonic case, i.e., $k = 1$. The analysis for the remaining modes can be deduced by formally setting $\omega = k\omega$. In contrast to the forward problem, in the optimal control setting, the analysis for the mode $k = 0$ can also be deduced from the analysis for the mode $k = 1$, by setting $k = 0$ and dropping the two equations, that correspond to the sine parts of the state and the co-state.

Introducing the Neumann data of the Fourier coefficients $\mathbf{y^c}$, $\mathbf{y^s}$ of the state, and the Neumann data of the Fourier coefficients $\mathbf{p^c}$, $\mathbf{p^s}$ of the co-state as additional unknowns, i.e.,

$$\boldsymbol{\lambda^c} := \boldsymbol{\gamma_N} \mathbf{y^c}, \quad \boldsymbol{\lambda^s} := \boldsymbol{\gamma_N} \mathbf{y^s}, \quad \boldsymbol{\eta^c} := \boldsymbol{\gamma_N} \mathbf{p^c} \quad \text{and} \quad \boldsymbol{\eta^s} := \boldsymbol{\gamma_N} \mathbf{p^s},$$

and using the Calderon projection (2.22) for all four, the cosine and the sine component of the state and the co-state, allow to state the optimality system in a framework, that is suited for a FEM-BEM discretization.

For simplicity, we introduce the abbreviation

$$\Upsilon := (\mathbf{y^c}, \boldsymbol{\lambda^c}, \mathbf{y^s}, \boldsymbol{\lambda^s}) \quad \text{and} \quad \Psi := (\mathbf{p^c}, \boldsymbol{\eta^c}, \mathbf{p^s}, \boldsymbol{\eta^s}),$$
$$\Phi := (\mathbf{w^c}, \boldsymbol{\rho^c}, \mathbf{w^s}, \boldsymbol{\rho^s}) \quad \text{and} \quad \Theta := (\mathbf{v^c}, \boldsymbol{\mu^c}, \mathbf{v^s}, \boldsymbol{\mu^s}).$$

We mention, that Υ represents the variables corresponding to the state $\mathbf{y}$, Ψ represents the variables corresponding to the co-state $\mathbf{p}$ and Φ and Θ are the corresponding test functions, respectively. According to the definition of Υ and Ψ, we introduce the appropriate product space

$$\mathcal{W} := \mathbf{H}(\mathbf{curl}, \Omega_1) \times \mathbf{H}_{\|}^{-\frac{1}{2}}(\operatorname{div}_\Gamma 0, \Gamma) \times \mathbf{H}(\mathbf{curl}, \Omega_1) \times \mathbf{H}_{\|}^{-\frac{1}{2}}(\operatorname{div}_\Gamma 0, \Gamma).$$

Therefore, we end up with the weak formulation of the reduced symmetric coupled optimality system:

Find $(\Upsilon, \Psi) \in \mathcal{W}^2$, such that

$$
\begin{cases}
-\omega(\sigma \mathbf{p^s}, \mathbf{w^c})_{\mathbf{0},\Omega_1} + (\nu \, \mathbf{curl} \, \mathbf{p^c}, \mathbf{curl} \, \mathbf{w^c})_{\mathbf{0},\Omega_1} + (\mathbf{y^c}, \mathbf{w^c})_{\mathbf{0},\Omega_1} \\
\qquad\qquad - \langle \mathbf{N}(\gamma_{\mathbf{D}} \mathbf{p^c}), \gamma_{\mathbf{D}} \mathbf{w^c} \rangle_\tau + \langle \mathbf{B}(\boldsymbol{\eta^c}), \gamma_{\mathbf{D}} \mathbf{w^c} \rangle_\tau = (\mathbf{y_d^c}, \mathbf{w^c})_{\mathbf{0},\Omega_1}, \\
\qquad\qquad\quad \langle \boldsymbol{\rho^c}, (\mathbf{C} - \mathbf{Id})(\gamma_{\mathbf{D}} \mathbf{p^c}) \rangle_\tau - \langle \boldsymbol{\rho^c}, \mathbf{A}(\boldsymbol{\eta^c}) \rangle_\tau = 0, \\
\omega(\sigma \mathbf{p^c}, \mathbf{w^s})_{\mathbf{0},\Omega_1} + (\nu \, \mathbf{curl} \, \mathbf{p^s}, \mathbf{curl} \, \mathbf{w^s})_{\mathbf{0},\Omega_1} + (\mathbf{y^s}, \mathbf{w^s})_{\mathbf{0},\Omega_1} \\
\qquad\qquad - \langle \mathbf{N}(\gamma_{\mathbf{D}} \mathbf{p^s}), \gamma_{\mathbf{D}} \mathbf{w^s} \rangle_\tau + \langle \mathbf{B}(\boldsymbol{\eta^s}), \gamma_{\mathbf{D}} \mathbf{w^s} \rangle_\tau = (\mathbf{y_d^s}, \mathbf{w^s})_{\mathbf{0},\Omega_1}, \\
\qquad\qquad\quad \langle \boldsymbol{\rho^s}, (\mathbf{C} - \mathbf{Id})(\gamma_{\mathbf{D}} \mathbf{p^s}) \rangle_\tau - \langle \boldsymbol{\rho^s}, \mathbf{A}(\boldsymbol{\eta^s}) \rangle_\tau = 0, \\
\omega(\sigma \mathbf{y^s}, \mathbf{v^c})_{\mathbf{0},\Omega_1} + (\nu \, \mathbf{curl} \, \mathbf{y^c}, \mathbf{curl} \, \mathbf{v^c})_{\mathbf{0},\Omega_1} - \lambda^{-1}(\mathbf{p^c}, \mathbf{v^c})_{\mathbf{0},\Omega_1} \\
\qquad\qquad - \langle \mathbf{N}(\gamma_{\mathbf{D}} \mathbf{y^c}), \gamma_{\mathbf{D}} \mathbf{v^c} \rangle_\tau + \langle \mathbf{B}(\boldsymbol{\lambda^c}), \gamma_{\mathbf{D}} \mathbf{v^c} \rangle_\tau = 0, \\
\qquad\qquad\quad \langle \boldsymbol{\mu^c}, (\mathbf{C} - \mathbf{Id})(\gamma_{\mathbf{D}} \mathbf{y^c}) \rangle_\tau - \langle \boldsymbol{\mu^c}, \mathbf{A}(\boldsymbol{\lambda^c}) \rangle_\tau = 0, \\
-\omega(\sigma \mathbf{y^c}, \mathbf{v^s})_{\mathbf{0},\Omega_1} + (\nu \, \mathbf{curl} \, \mathbf{y^s}, \mathbf{curl} \, \mathbf{v^s})_{\mathbf{0},\Omega_1} - \lambda^{-1}(\mathbf{p^s}, \mathbf{v^s})_{\mathbf{0},\Omega_1} \\
\qquad\qquad - \langle \mathbf{N}(\gamma_{\mathbf{D}} \mathbf{y^s}), \gamma_{\mathbf{D}} \mathbf{v^s} \rangle_\tau + \langle \mathbf{B}(\boldsymbol{\lambda^s}), \gamma_{\mathbf{D}} \mathbf{v^s} \rangle_\tau = 0, \\
\qquad\qquad\quad \langle \boldsymbol{\mu^s}, (\mathbf{C} - \mathbf{Id})(\gamma_{\mathbf{D}} \mathbf{y^s}) \rangle_\tau - \langle \boldsymbol{\mu^s}, \mathbf{A}(\boldsymbol{\lambda^s}) \rangle_\tau = 0,
\end{cases}
\tag{7.22}
$$

for all test functions $(\Phi, \Theta) \in \mathcal{W}^2$. For simplicity, we introduce the bilinear form $\mathcal{B}_B$, representing the latter variational problem by

$$
\mathcal{B}_B((\Upsilon, \Psi), (\Phi, \Theta)) := a(\Upsilon, \Phi) + b(\Phi, \Psi) + b(\Upsilon, \Theta) - c(\Psi, \Theta),
$$

where the bilinear forms a, b and c are given by

$$
a(\Upsilon, \Phi) = (\mathbf{y^c}, \mathbf{w^c})_{\mathbf{0},\Omega_1} + (\mathbf{y^s}, \mathbf{w^s})_{\mathbf{0},\Omega_1},
$$

$$
b(\Upsilon, \Theta) = \omega(\sigma \mathbf{y^s}, \mathbf{v^c})_{\mathbf{0},\Omega_1} - \omega(\sigma \mathbf{y^c}, \mathbf{v^s})_{\mathbf{0},\Omega_1} + \sum_{j \in \{c,s\}} (\nu \, \mathbf{curl} \, \mathbf{y^j}, \mathbf{curl} \, \mathbf{v^j})_{\mathbf{0},\Omega_1}
$$

$$
- \langle \mathbf{N}(\gamma_{\mathbf{D}} \mathbf{y^j}), \gamma_{\mathbf{D}} \mathbf{v^j} \rangle_\tau + \langle \mathbf{B}(\boldsymbol{\lambda^j}), \gamma_{\mathbf{D}} \mathbf{v^j} \rangle_\tau + \langle \boldsymbol{\mu^j}, (\mathbf{C} - \mathbf{Id})(\gamma_{\mathbf{D}} \mathbf{y^j}) \rangle_\tau - \langle \boldsymbol{\mu^j}, \mathbf{A}(\boldsymbol{\lambda^j}) \rangle_\tau,
$$

$$
c(\Psi, \Theta) = \lambda^{-1}(\mathbf{p^c}, \mathbf{v^c})_{\mathbf{0},\Omega_1} + \lambda^{-1}(\mathbf{p^s}, \mathbf{v^s})_{\mathbf{0},\Omega_1}.
$$

Using this notation, we can state (7.22) in the abstract form:

Problem 7.6. *Find* $(\Upsilon, \Psi) \in \mathcal{W}^2$, *such that*

$$
\mathcal{B}_B((\Upsilon, \Psi), (\Phi, \Theta)) = \sum_{j \in \{c,s\}} (\mathbf{y_d^j}, \mathbf{w^j})_{\mathbf{0},\Omega_1},
\tag{7.23}
$$

for all test functions $(\Phi, \Theta) \in \mathcal{W}^2$.

Problem 7.6 has a unique solution $(\Upsilon, \Psi) \in \mathcal{W}^2$, cf. Lemma 7.7.

7.2.3 Discretization

For discretization we use $\mathcal{ND}^0(\mathcal{T}_h)$, a conforming finite element subspace of $\mathbf{H}(\mathbf{curl}, \Omega_1)$, and $\mathcal{RT}_0^0(\mathcal{K}_h)$, a conforming finite element subspace of $\mathbf{H}_\|^{-\frac{1}{2}}(\mathrm{div}_\Gamma \, 0, \Gamma)$, cf. Section 2.4. Furthermore, we define the finite element product space $\mathcal{W}_h$, given by

$$
\mathcal{W}_h := \mathcal{ND}^0(\mathcal{T}_h) \times \mathcal{RT}_0^0(\mathcal{K}_h) \times \mathcal{ND}^0(\mathcal{T}_h) \times \mathcal{RT}_0^0(\mathcal{K}_h).
$$

Using the definition of the FEM and BEM matrices, cf. (6.62) and (7.12), allows to state the resulting system of finite and boundary element equations.

Formulation OC-FEM-BEM 1   Find $(\mathbf{y}_\mathbf{h}^\mathbf{c}, \boldsymbol{\lambda}_\mathbf{h}^\mathbf{c}, \mathbf{y}_\mathbf{h}^\mathbf{s}, \boldsymbol{\lambda}_\mathbf{h}^\mathbf{s}, \mathbf{p}_\mathbf{h}^\mathbf{c}, \boldsymbol{\eta}_\mathbf{h}^\mathbf{c}, \mathbf{p}_\mathbf{h}^\mathbf{s}, \boldsymbol{\eta}_\mathbf{h}^\mathbf{s})^T \in \mathbb{R}^{4(N_h + L_h)}$:

$$
\underbrace{\begin{pmatrix}
\mathbf{M} & \cdot & \cdot & \cdot & \tilde{\mathbf{K}}_{\boldsymbol{\nu}} & \mathbf{B} & -\mathbf{M}_{\boldsymbol{\sigma},\boldsymbol{\omega}} & \cdot \\
\cdot & \cdot & \cdot & \cdot & \mathbf{B}^T & -\mathbf{A} & \cdot & \cdot \\
\cdot & \cdot & \mathbf{M} & \cdot & \mathbf{M}_{\boldsymbol{\sigma},\boldsymbol{\omega}} & \cdot & \tilde{\mathbf{K}}_{\boldsymbol{\nu}} & \mathbf{B} \\
\cdot & \cdot & \cdot & \cdot & \cdot & \cdot & \mathbf{B}^T & -\mathbf{A} \\
\tilde{\mathbf{K}}_{\boldsymbol{\nu}} & \mathbf{B} & \mathbf{M}_{\boldsymbol{\sigma},\boldsymbol{\omega}} & \cdot & -\lambda^{-1}\mathbf{M} & \cdot & \cdot & \cdot \\
\mathbf{B}^T & -\mathbf{A} & \cdot & \cdot & \cdot & \cdot & \cdot & \cdot \\
-\mathbf{M}_{\boldsymbol{\sigma},\boldsymbol{\omega}} & \cdot & \tilde{\mathbf{K}}_{\boldsymbol{\nu}} & \mathbf{B} & \cdot & \cdot & -\lambda^{-1}\mathbf{M} & \cdot \\
\cdot & \cdot & \mathbf{B}^T & -\mathbf{A} & \cdot & \cdot & \cdot & \cdot
\end{pmatrix}}_{=:\mathcal{B}_B}
\begin{pmatrix}
\mathbf{y}_\mathbf{h}^\mathbf{c} \\
\boldsymbol{\lambda}_\mathbf{h}^\mathbf{c} \\
\mathbf{y}_\mathbf{h}^\mathbf{s} \\
\boldsymbol{\lambda}_\mathbf{h}^\mathbf{s} \\
\mathbf{p}_\mathbf{h}^\mathbf{c} \\
\boldsymbol{\eta}_\mathbf{h}^\mathbf{c} \\
\mathbf{p}_\mathbf{h}^\mathbf{s} \\
\boldsymbol{\eta}_\mathbf{h}^\mathbf{s}
\end{pmatrix}
=
\begin{pmatrix}
\mathbf{y}_{\mathbf{d},\mathbf{h}}^\mathbf{c} \\
\mathbf{0} \\
\mathbf{y}_{\mathbf{d},\mathbf{h}}^\mathbf{s} \\
\mathbf{0} \\
\mathbf{0} \\
\mathbf{0} \\
\mathbf{0} \\
\mathbf{0}
\end{pmatrix}.
$$

7.2.4   Block-diagonal preconditioners

This subsection is devoted to the construction of parameter-robust preconditioners for the systems of linear equations of the last subsection. For the proposed formulation, we investigate its structure to construct a preconditioner by the technique of inexact Schur complement preconditioning, cf. Subsection 5.2.3. Furthermore, we provide condition number bounds for the resulting preconditioned systems of linear equations, by showing well-posedness of the underlying systems of partial differential equations in non-standard norms.

Formulation OC-FEM-BEM 1   We explore the structure of the system matrix $\mathcal{B}_B$. Since we already have a robust preconditioner for the part of $\mathcal{B}_B$, corresponding to the interior, i.e., $\mathcal{B}$, we pursue the strategy of inexact Schur complement preconditioning, cf. Subsection 5.2.3. The contribution from the boundary is taken into account by forming the Schur complements. Therefore, we propose the following block-diagonal inexact Schur complement preconditioner

$$
\mathcal{C}_B = \operatorname{diag}\left(\sqrt{\lambda}\mathbf{S_B}, \sqrt{\lambda}\mathbf{A}, \sqrt{\lambda}\mathbf{S_B}, \sqrt{\lambda}\mathbf{A}, \frac{1}{\sqrt{\lambda}}\mathbf{S_B}, \frac{1}{\sqrt{\lambda}}\mathbf{A}, \frac{1}{\sqrt{\lambda}}\mathbf{S_B}, \frac{1}{\sqrt{\lambda}}\mathbf{A}\right), \tag{7.24}
$$

where $\mathbf{S_B} = \tilde{\mathbf{K}}_{\boldsymbol{\nu}} + \mathbf{M}_{\boldsymbol{\sigma},\boldsymbol{\omega}} + \frac{1}{\sqrt{\lambda}}\mathbf{M} - \mathbf{N} + \mathbf{B}^T\mathbf{A}^{-1}\mathbf{B}$. According to the choice of the block-diagonal preconditioner $\mathcal{C}_B$, we introduce the non-standard norm $\|\cdot\|_{\mathcal{C}_B}$ in the product space $\mathcal{W}^2$:

$$
\|(\Upsilon, \Psi)\|_{\mathcal{C}_B}^2 := \sqrt{\lambda}\left[\|\Upsilon\|_{\mathcal{P}_{B1}}^2 + \sum_{j\in\{c,s\}}\frac{1}{\sqrt{\lambda}}\|\mathbf{y}^\mathbf{j}\|_{\mathbf{0},\Omega_1}^2\right] + \frac{1}{\sqrt{\lambda}}\left[\|\Psi\|_{\mathcal{P}_{B1}}^2 + \sum_{j\in\{c,s\}}\frac{1}{\sqrt{\lambda}}\|\mathbf{p}^\mathbf{j}\|_{\mathbf{0},\Omega_1}^2\right]. \tag{7.25}
$$

The main result is summarized in the following lemma, that claims that an inf-sup and a sup-sup condition are fulfilled with parameter-independent constants, namely $\frac{1}{4}$ and 2.

Lemma 7.7. *We have*

$$
\frac{1}{4}\|(\Upsilon, \Psi)\|_{\mathcal{C}_B} \leq \sup_{(\Phi,\Theta)\neq 0}\frac{\mathcal{B}_B((\Upsilon,\Psi),(\Phi,\Theta))}{\|(\Phi,\Theta)\|_{\mathcal{C}_B}} \leq 2\|(\Upsilon,\Psi)\|_{\mathcal{C}_B} \tag{7.26}
$$

for all $(\Upsilon, \Psi) \in \mathcal{W}^2$.

Proof. By an appropriate distribution of the regularization parameter λ and application of Cauchy's inequality several times, the sup-sup condition follows with constant 2. For the special choices of the

test functions

$$
(\Phi_1, \Theta_1) := (\Upsilon, -\Psi),
$$
$$
(\Phi_2, \Theta_2) := \left(\frac{1}{\sqrt{\lambda}} \mathbf{p^c}, -\frac{1}{\sqrt{\lambda}} \boldsymbol{\eta^c}, \frac{1}{\sqrt{\lambda}} \mathbf{p^s}, -\frac{1}{\sqrt{\lambda}} \boldsymbol{\eta^s}, \sqrt{\lambda} \mathbf{y^c}, -\sqrt{\lambda} \boldsymbol{\lambda^c}, \sqrt{\lambda} \mathbf{y^s}, -\sqrt{\lambda} \boldsymbol{\lambda^s} \right),
$$
$$
(\Phi_3, \Theta_3) := \left(-\frac{1}{\sqrt{\lambda}} \mathbf{p^s}, -\frac{1}{\sqrt{\lambda}} \boldsymbol{\eta^s}, \frac{1}{\sqrt{\lambda}} \mathbf{p^c}, \frac{1}{\sqrt{\lambda}} \boldsymbol{\eta^c}, \sqrt{\lambda} \mathbf{y^s}, \sqrt{\lambda} \boldsymbol{\lambda^s}, -\sqrt{\lambda} \mathbf{y^c}, -\sqrt{\lambda} \boldsymbol{\lambda^c} \right),
$$

we have

$$
\mathcal{B}_B((\Upsilon, \Psi), (\Phi_1, \Theta_1)) = \sum_{j \in \{c,s\}} \left[\|\mathbf{y^j}\|^2_{\mathbf{0},\Omega_1} + \frac{1}{\lambda} \|\mathbf{p^j}\|^2_{\mathbf{0},\Omega_1} \right],
$$
$$
\mathcal{B}_B((\Upsilon, \Psi), (\Phi_2, \Theta_2)) = \sqrt{\lambda} \sum_{j \in \{c,s\}} \left[(\nu \operatorname{\mathbf{curl}} \mathbf{y^j}, \operatorname{\mathbf{curl}} \mathbf{y^j})_{0,\Omega_1} - \langle \mathbf{N}(\gamma_{\mathbf{D}} \mathbf{y^j}), \gamma_{\mathbf{D}} \mathbf{y^j} \rangle_\tau + \langle \boldsymbol{\lambda^j}, \mathbf{A}(\boldsymbol{\lambda^j}) \rangle_\tau \right]
$$
$$
\qquad + \frac{1}{\sqrt{\lambda}} \sum_{j \in \{c,s\}} \left[(\nu \operatorname{\mathbf{curl}} \mathbf{p^j}, \operatorname{\mathbf{curl}} \mathbf{p^j})_{0,\Omega_1} - \langle \mathbf{N}(\gamma_{\mathbf{D}} \mathbf{p^j}), \gamma_{\mathbf{D}} \mathbf{p^j} \rangle_\tau + \langle \boldsymbol{\eta^j}, \mathbf{A}(\boldsymbol{\eta^j}) \rangle_\tau \right],
$$
$$
\mathcal{B}_B((\Upsilon, \Psi), (\Phi_3, \Theta_3)) = \sum_{j \in \{c,s\}} \left[\sqrt{\lambda} \omega (\sigma \mathbf{y}^j, \mathbf{y}^j)_{\mathbf{0},\Omega_1} + \frac{1}{\sqrt{\lambda}} \omega (\sigma \mathbf{p}^j, \mathbf{p}^j)_{\mathbf{0},\Omega_1} \right],
$$

and therefore

$$
\sup_{(\Phi,\Theta) \in \mathcal{W}^2} \frac{\mathcal{B}_B((\Upsilon, \Psi), (\Phi, \Theta))}{\|(\Phi, \Theta)\|_{\mathcal{C}_B}} \geq \frac{\mathcal{B}_B((\Upsilon, \Psi), (\Phi_1 + 2\Phi_2 + \Phi_3, \Theta_1 + 2\Theta_2 + \Theta_3))}{\|(\Phi_1 + 2\Phi_2 + \Phi_3, \Theta_1 + 2\Theta_2 + \Theta_3)\|_{\mathcal{C}_B}}
$$
$$
\geq \frac{\|(\mathbf{y^c}, \mathbf{y^s}, \mathbf{p^c}, \mathbf{p^s})\|^2_{\mathcal{C}} + \sqrt{\lambda} \sum_{j \in \{c,s\}} -\langle \mathbf{N}(\gamma_{\mathbf{D}} \mathbf{y^j}), \gamma_{\mathbf{D}} \mathbf{y^j} \rangle_\tau + \langle \boldsymbol{\lambda^j}, \mathbf{A}(\boldsymbol{\lambda^j}) \rangle_\tau}{2 \|(\Upsilon, \Psi)\|_{\mathcal{C}_B}}
$$
$$
+ \frac{\frac{1}{\sqrt{\lambda}} \sum_{j \in \{c,s\}} -\langle \mathbf{N}(\gamma_{\mathbf{D}} \mathbf{p^j}), \gamma_{\mathbf{D}} \mathbf{p^j} \rangle_\tau + \langle \boldsymbol{\eta^j}, \mathbf{A}(\boldsymbol{\eta^j}) \rangle_\tau}{2 \|(\Upsilon, \Psi)\|_{\mathcal{C}_B}}.
$$

Furthermore, for the choice

$$
(\Phi_4, \Theta_4) := \left(\mathbf{0}, \frac{1}{\sqrt{\lambda}} \boldsymbol{\lambda^c}, \mathbf{0}, \frac{1}{\sqrt{\lambda}} \boldsymbol{\lambda^s}, \mathbf{0}, \sqrt{\lambda} \boldsymbol{\eta^c}, \mathbf{0}, \sqrt{\lambda} \boldsymbol{\eta^s} \right),
$$

we have

$$
\sup_{(\Phi,\Theta) \in \mathcal{W}^2} \frac{\mathcal{B}_B((\Upsilon, \Psi), (\Phi, \Theta))}{\|(\Phi, \Theta)\|_{\mathcal{C}_B}} \geq \sqrt{\lambda} \frac{\sum_{j \in \{c,s\}} \sup_{\boldsymbol{\mu^j}} \frac{\langle \mathbf{B}(\boldsymbol{\mu^j}), \gamma_{\mathbf{D}} \mathbf{y^j} \rangle^2_\tau}{\langle \boldsymbol{\mu^j}, \mathbf{A}(\boldsymbol{\mu^j}) \rangle_\tau} - \langle \boldsymbol{\lambda^j}, \mathbf{A}(\boldsymbol{\lambda^j}) \rangle_\tau}{\sqrt{2} \|(\Upsilon, \Psi)\|_{\mathcal{C}_B}}
$$
$$
+ \frac{1}{\sqrt{\lambda}} \frac{\sum_{j \in \{c,s\}} \sup_{\boldsymbol{\mu^j}} \frac{\langle \mathbf{B}(\boldsymbol{\mu^j}), \gamma_{\mathbf{D}} \mathbf{p^j} \rangle^2_\tau}{\langle \boldsymbol{\mu^j}, \mathbf{A}(\boldsymbol{\mu^j}) \rangle_\tau} - \langle \boldsymbol{\eta^j}, \mathbf{A}(\boldsymbol{\eta^j}) \rangle_\tau}{\sqrt{2} \|(\Upsilon, \Psi)\|_{\mathcal{C}_B}},
$$

cf. (6.65). Combining these two estimates, we obtain the inf-sup bound with constant $1/4$. $\qquad \square$

Furthermore, the inequalities (7.26) remain valid for the finite element subspace $\mathcal{W}^2_h$, since the proof can be repeated for the finite element functions step by step. Therefore, we obtain the condition number estimate

$$
\kappa_{\mathcal{C}_B}(\mathcal{C}_B^{-1} \mathcal{B}_B) := \|\mathcal{C}_B^{-1} \mathcal{B}_B\|_{\mathcal{C}_B} \|\mathcal{B}_B^{-1} \mathcal{C}_B\|_{\mathcal{C}_B} \leq 8.
$$

7.3   Various constraints yielding a decoupling nature

In Section 7.1 and Section 7.2 time-periodic eddy current optimal control problems with distributed control are analyzed and a preconditioned MinRes solver is constructed, that yields parameter-independent convergence rates. Indeed, the applicability of this approach to time-periodic eddy current optimal control problems is shown with some eminent restrictions, that limits the applicability of this solver to general problems in the engineering practice:

1) The observation domain and the control domain have to be equal to the computational domain, i.e., $\Omega_a = \Omega_b = \Omega_1$ (cf. (7.30)).

2) The observation is restricted to be done in a $\mathbf{L_2}$-type norm.

3) There are no control constraints involved.

4) There are no state constraints involved.

Therefore, in this section we extend the basic model problem (7.1)-(7.2) step by step to problems as required in practical applications. For simplicity, we only consider the bounded domain Ω_1, where the conductivity is strictly positive. Therefore, in all these cases, the resulting system matrices obtain high structural similarities to $\mathcal{B}_M$ and $\mathcal{B}$ as in (7.13) and (7.14), respectively. We mention, that the case of domains consisting of both, conducting and non-conducting regions can be dealt with in terms of a FEM-BEM coupling method.

Anyhow, the construction of parameter-robust solvers taking into account modifications of 1) - 4) is not straightforward, since we have to cope with various discretization and model parameters, that impinge upon the convergence rate of any iterative method. Anyhow, in all these cases an efficient preconditioned MinRes method can be constructed, that is robust at least in the space and time discretization parameters. Moreover, in some cases we are able to prove robustness with respect to some more involved model parameters. In fact, the aim of these work is to generalize and extend the ideas derived in [94] for simple parabolic optimal control problems to eddy current optimal control problems. Therefore, we treat the modification of each issue 1) - 4) separately and provide the dependence of the convergence rate on the model parameters, if our solver is applied to the resulting system of equations. Furthermore, we explore the decoupling with respect to the modes of the Fourier coefficients in 1)- 4).

In some applications, it is reasonable to impose control constraints to the individual Fourier coefficients of the control $\mathbf{u}$. Therefore, we analyze this specific case. Pointwise state constraints are of importance for instance to avoid undesired singularities in the optimal state. This issue can also be achieved by adding pointwise state constraints to the Fourier coefficients of the state $\mathbf{y}$. Following [159] and [73], we use a Moreau Yosida regularization to incorporate these pointwise state constraints to the Fourier coefficients. Since even linear inequality constraints give rise to nonlinear optimality systems, we apply a Newton-type approach for their solution, cf. [25, 26, 76]. At every Newton step a saddle point problem has to be solved, that obtains high structural similarities with the linear problems. Therefore in these nonlinear cases, our focus is on the efficient solution of these linear systems arising at each Newton step, cf. [73].

It turns out, that we have to pay a price in the sense, that we lose robustness with respect to specific model or regularization parameters in order to get robustness with respect to modifications in the cost functional and/or the state equation. The idea is to use the same block-diagonal preconditioners $\mathcal{C}$ and $\mathcal{C}_M$, given in (7.16) and (7.18), as for the optimal control problem with distributed control. The crucial point is, that in order to provide theoretical results, it is essential to have a Friedrichs' inequality in some of the cases, especially if 1) - 3) are modified. While the existence of a Friedrichs' inequality in a $H^1(\Omega_1)$ setting only requires a non-empty Dirichlet boundary, cf. Lemma 2.7, in the $\mathbf{H}(\mathbf{curl}, \Omega_1)$ setting a Friedrichs' inequality is only available for weakly divergence-free functions, cf. Lemma 2.8. In fact this is a strong limitation, since we want to use the full $\mathbf{H}(\mathbf{curl}, \Omega_1)$ space in our computations. Therefore, we have to incorporate the weakly divergence-free condition in terms of additional Lagrange multipliers in a weak setting. Consequently, in these cases, we rely

on *Formulation OC-FEM 2*. For modifications in the case 4), it is sufficient to rely on *Formulation OC-FEM 1*.

Before we start with the analysis, we prepare some technical tools and notations that simplify the subsequent analysis. We recall the definition of the bilinear form $\mathcal{B}_M$:

$$\mathcal{B}_M((\Upsilon, \Psi), (\Phi, \Theta)) := a(\Upsilon, \Phi) + b(\Phi, \Psi) + b(\Upsilon, \Theta),$$

with the bilinear forms

$$\begin{aligned} a(\Upsilon, \Phi) := {} & a_a((\mathbf{y^c}, \mathbf{y^s}), (\mathbf{v^c}, \mathbf{v^s})) + a_b((\mathbf{v^c}, \mathbf{v^s}), (\mathbf{p^c}, \mathbf{p^s})) \\ & + a_b((\mathbf{y^c}, \mathbf{y^s}), (\mathbf{q^c}, \mathbf{q^s})) - a_c((\mathbf{p^c}, \mathbf{p^s}), (\mathbf{q^c}, \mathbf{q^s})), \end{aligned} \tag{7.27}$$

that are further decomposed into

$$a_a((\mathbf{y^c}, \mathbf{y^s}), (\mathbf{v^c}, \mathbf{v^s})) := \sum_{j \in \{c,s\}} (\mathbf{y^j}, \mathbf{v^j})_{\mathbf{0}, \Omega_1},$$

$$a_b((\mathbf{y^c}, \mathbf{y^s}), (\mathbf{q^c}, \mathbf{q^s})) := \omega \left[(\sigma \mathbf{y^s}, \mathbf{q^c})_{\mathbf{0}, \Omega_1} - (\sigma \mathbf{y^c}, \mathbf{q^s})_{\mathbf{0}, \Omega_1} \right] + \sum_{j \in \{c,s\}} (\nu \operatorname{\mathbf{curl}} \mathbf{y^j}, \operatorname{\mathbf{curl}} \mathbf{q^j})_{\mathbf{0}, \Omega_1},$$

$$a_c((\mathbf{p^c}, \mathbf{p^s}), (\mathbf{q^c}, \mathbf{q^s})) := \sum_{j \in \{c,s\}} \lambda^{-1} (\mathbf{p^j}, \mathbf{q^j})_{\mathbf{0}, \Omega_1}.$$

Furthermore, we use the following splitting of the $\mathcal{C}$-norm.

$$\|\Upsilon\|_{\mathcal{C}}^2 := \|(\mathbf{y^c}, \mathbf{y^s})\|_{\mathcal{C}_1}^2 + \|(\mathbf{p^c}, \mathbf{p^s})\|_{\mathcal{C}_2}^2, \tag{7.28}$$

with

$$\|(\mathbf{y^c}, \mathbf{y^s})\|_{\mathcal{C}_1}^2 := \sqrt{\lambda} \sum_{j \in \{c,s\}} \|\mathbf{y^j}\|_{\mathcal{C}_1}^2 \quad \text{and} \quad \|(\mathbf{p^c}, \mathbf{p^s})\|_{\mathcal{C}_2}^2 := \frac{1}{\sqrt{\lambda}} \sum_{j \in \{c,s\}} \|\mathbf{p^j}\|_{\mathcal{C}_1}^2. \tag{7.29}$$

In the following, we use Lemma 2.9 (weighted Friedrichs' inequality in $\mathbf{H}(\operatorname{\mathbf{curl}}, \Omega_1)$) in a very specific style.

Corollary 7.8. *For any* $\mathbf{v} \in \mathbf{H_0}(\operatorname{\mathbf{curl}}, \Omega_1)$ *which satisfies*

$$(\sigma \mathbf{v}, \nabla q)_{\mathbf{0}, \Omega_1} = 0, \quad \forall q \in H_0^1(\Omega_1),$$

we have

$$\|\mathbf{v}\|_{\mathbf{0}, \Omega_1} \leq C_{\sigma, \nu} \|\nu^{1/2} \operatorname{\mathbf{curl}} \mathbf{v}\|_{\mathbf{0}, \Omega_1},$$

where $C_{\sigma, \nu} = C_2^F \sqrt{\frac{\overline{\sigma}}{\underline{\sigma}\, \underline{\nu}}}$.

Proof. Using Lemma 2.9, we obtain

$$\begin{aligned} \|\mathbf{v}\|_{\mathbf{0}, \Omega_1}^2 = (\mathbf{v}, \mathbf{v})_{\mathbf{0}, \Omega_1} &\leq \frac{1}{\underline{\sigma}} (\sigma \mathbf{v}, \mathbf{v})_{\mathbf{0}, \Omega_1} \leq \frac{(C_2^F)^2}{\underline{\sigma}} (\sigma \operatorname{\mathbf{curl}} \mathbf{v}, \operatorname{\mathbf{curl}} \mathbf{v})_{\mathbf{0}, \Omega_1} \\ &\leq \frac{(C_2^F)^2 \, \overline{\sigma}}{\underline{\sigma}} (\operatorname{\mathbf{curl}} \mathbf{v}, \operatorname{\mathbf{curl}} \mathbf{v})_{\mathbf{0}, \Omega_1} \leq \frac{(C_2^F)^2 \, \overline{\sigma}}{\underline{\sigma}\, \underline{\nu}} (\nu \operatorname{\mathbf{curl}} \mathbf{v}, \operatorname{\mathbf{curl}} \mathbf{v})_{\mathbf{0}, \Omega_1} = C_{\sigma, \nu}^2 \|\nu^{1/2} \operatorname{\mathbf{curl}} \mathbf{v}\|_{\mathbf{0}, \Omega_1}^2. \end{aligned}$$

$\square$

Note, that for constant conductivity, i.e., $\sigma \in \mathbb{R}^+$, $C_{\sigma, \nu}$ does not depend on σ. Hence, we have the important property, that in the space of weakly divergence-free functions, the mass matrix is basically dominated by the stiffness matrix, with a constant independent of any involved discretization parameters (h, ω, N). Hence, Corollary 7.8 allows us to derive a very specific inf-sup and sup-sup bound for $a_b(\cdot, \cdot)$.

Lemma 7.9. *We have*

$$\underline{c}_b \|(\mathbf{y^c}, \mathbf{y^s})\|_{\mathcal{C}_1} \leq \sup_{(\mathbf{y^c},\mathbf{y^s})\in \mathbf{H_0}(\mathbf{curl},\Omega_1)^2} \frac{a_b((\mathbf{y^c}, \mathbf{y^s}),(\mathbf{q^c},\mathbf{q^s}))}{\|(\mathbf{q^c},\mathbf{q^s})\|_{\mathcal{C}_2}} \leq \overline{c}_b \|(\mathbf{y^c}, \mathbf{y^s})\|_{\mathcal{C}_1}$$

and

$$\underline{c}_b \|(\mathbf{y^c}, \mathbf{y^s})\|_{\mathcal{C}_2} \leq \sup_{(\mathbf{q^c},\mathbf{q^s})\in \mathbf{H_0}(\mathbf{curl},\Omega_1)^2} \frac{a_b((\mathbf{q^c}, \mathbf{q^s}),(\mathbf{y^c},\mathbf{y^s}))}{\|(\mathbf{q^c},\mathbf{q^s})\|_{\mathcal{C}_1}} \leq \overline{c}_b \|(\mathbf{y^c}, \mathbf{y^s})\|_{\mathcal{C}_2}$$

for all $(\mathbf{y^c}, \mathbf{y^s}) \in \mathbf{H_0}(\mathbf{curl}, \Omega_1)^2$ *fulfilling* $(\sigma\mathbf{y^c}, \nabla p)_{0,\Omega_1} = 0$ *and* $(\sigma\mathbf{y^s}, \nabla p)_{\mathbf{0},\Omega_1} = 0$, *for all* $p \in H_0^1(\Omega_1)$. *Here* $\underline{c}_b$ *and* $\overline{c}_b$ *are constants that depend on* λ, σ *and* ν, *but are independent of* h, ω *and* N.

Proof. First we show boundedness of $a_b(\cdot, \cdot)$, indeed

$$a_b((\mathbf{y^c}, \mathbf{y^s}),(\mathbf{q^c},\mathbf{q^s})) \leq \|(\mathbf{y^c},\mathbf{y^s})\|_{\mathcal{C}_1}\|(\mathbf{q^c},\mathbf{q^s})\|_{\mathcal{C}_2}.$$

In order to verify the inf-sup condition of $a_b(\cdot, \cdot)$, we use the special choice $(\mathbf{q^c}, \mathbf{q^s}) = (\mathbf{y^c}+\mathbf{y^s}, \mathbf{y^s}-\mathbf{y^c})$ for the test functions. Due to the restriction on $\mathbf{y^c}$ and $\mathbf{y^s}$ to be weakly divergence-free, we can use Corollary 7.8:

$$\begin{aligned}a_b((\mathbf{y^c}, \mathbf{y^s}),(\mathbf{y^c},\mathbf{y^s})) &+ a_b((\mathbf{y^c},\mathbf{y^s}),(\mathbf{y^s},-\mathbf{y^c})) \geq \\ &\geq \sum_{j\in\{c,s\}} \left[(\nu\,\mathbf{curl}\,\mathbf{y^j}, \mathbf{curl}\,\mathbf{y^j})_{\mathbf{0},\Omega_1} + k\omega(\sigma\mathbf{y^j}, \mathbf{y^j})_{\mathbf{0},\Omega_1}\right]\\ &\geq \sum_{j\in\{c,s\}}\left[\frac{1}{2}(\nu\,\mathbf{curl}\,\mathbf{u^j}, \mathbf{curl}\,\mathbf{u^j})_{\mathbf{0},\Omega_1} + \frac{1}{2C_{\sigma,\nu}}(\mathbf{y^j},\mathbf{y^j})_{\mathbf{0},\Omega_1} + k\omega(\sigma\mathbf{y^j},\mathbf{y^j})_{\mathbf{0},\Omega_1}\right]\\ &\geq c\,\|(\mathbf{y^c},\mathbf{y^s})\|_{\mathcal{C}_2}^2.\end{aligned}$$

Note, that for this special choice we have $\|(\mathbf{v^c}, \mathbf{v^s})\|_{\mathcal{C}_2} = \sqrt{2}\|(\mathbf{y^c},\mathbf{y^s})\|_{\mathcal{C}_2}$. Therefore the first result follows. Since $a_b(\cdot, \cdot)$ is skew symmetric, the same estimate can be obtained for the adjoint setting. □

Indeed, in the following subsections we will consider different minimization functionals, that in particular effect the specific structure of the parts $a_a(\cdot, \cdot)$ and $a_c(\cdot, \cdot)$ of $\mathcal{A}$. In all the considered settings, the bilinear form $a_b(\cdot, \cdot)$ stays the same, and therefore Lemma 7.9 plays the following important role: As long as the bounds

$$0 \leq a_i((\mathbf{y^c}, \mathbf{y^s}),(\mathbf{y^c},\mathbf{y^s})) \leq c_i\|(\mathbf{y^c},\mathbf{y^s})\|_{\mathcal{C}_1}, \quad \text{for } i \in \{a, c\},$$

can be verified with constants c_i, that are independent of h, ω and N, Theorem 2.3 and Theorem 2.4 in combination with Lemma 7.9 can be used to provide well-posedness results for the resulting bilinear form $\mathcal{B}_{M,\cdot}$ in the non-standard norm $\|\cdot\|_{\mathcal{C}_M}$ that are uniform in h, ω and N. At that point it can clearly be seen, that in these settings it is essential to work with the divergence constrained formulation *Formulation OC-FEM 2* instead of *Formulation OC-FEM 1*, since Lemma 7.9 is only true in the space of weakly divergence-free functions.

7.3.1   Different control and observation domains

In many practical applications, it makes no sense to locate the observation and/or control in the full computational domain Ω_1, since the computational domain consists of conducting and non-conducting regions. Typically, some electrical current is prescribed in a coil and the magnetic potential is tracked in some other predefined region, cf. [152].

Therefore, we assume that the observation and control domains Ω_a and Ω_b are non-empty, simply connected subdomains of the computational domain Ω_1, i.e., $\Omega_a \subset \Omega_1$ and $\Omega_b \subset \Omega_1$. In order to deal

with the different support of the observation and control, we define the prolongation operators $\mathbf{P_i}$, $i \in \{a, b\}$, by

$$\mathbf{P_i} : \mathbf{L_2}(\Omega_i) \to \mathbf{L_2}(\Omega_1),$$
$$(\mathbf{P_i u}, \mathbf{v})_{\mathbf{0}, \Omega_1} = (\mathbf{u}, \mathbf{v})_{\mathbf{0}, \Omega_i}, \quad \forall \mathbf{u} \in \mathbf{L_2}(\Omega_i), \ \forall \mathbf{v} \in \mathbf{L_2}(\Omega_1),$$

and the appropriate restriction operators $\mathbf{P_i^*}$, $i \in \{a, b\}$, by

$$\mathbf{P_i^*} : \mathbf{L_2}(\Omega_1) \to \mathbf{L_2}(\Omega_i),$$
$$(\mathbf{P_i u}, \mathbf{v})_{\mathbf{0}, \Omega_1} = (\mathbf{u}, \mathbf{P_i^* v})_{\mathbf{0}, \Omega_i}, \quad \forall \mathbf{u} \in \mathbf{L_2}(\Omega_i), \ \forall \mathbf{v} \in \mathbf{L_2}(\Omega_1).$$

We obtain the following minimization problem:

$$\min_{\mathbf{y}, \mathbf{u}} J(\mathbf{y}, \mathbf{u}) = \frac{1}{2} \int_{\Omega_a \times (0,T)} |\mathbf{P_a}^*[\mathbf{y} - \mathbf{y_d}]|^2 \, \mathrm{d}\mathbf{x}\,\mathrm{dt} + \frac{\lambda}{2} \int_{\Omega_b \times (0,T)} |\mathbf{u}|^2 \mathrm{d}\mathbf{x}\,\mathrm{dt}, \tag{7.30}$$

subject to the state equation

$$\begin{cases} \sigma \dfrac{\partial \mathbf{y}}{\partial t} + \mathbf{curl}(\nu \, \mathbf{curl}\, \mathbf{y}) = \mathbf{P_b u}, & \text{in } \Omega_1 \times (0,T), \\[2mm] \mathrm{div}(\sigma \mathbf{y}) = 0, & \text{in } \Omega_1 \times (0,T), \\[2mm] \mathbf{y} \times \mathbf{n} = \mathbf{0}, & \text{on } \partial\Omega_1 \times (0,T), \\[2mm] \mathbf{y}(0) = \mathbf{y}(T), & \text{on } \Omega_1 \times \{0\}. \end{cases} \tag{7.31}$$

In this setting we have

$$\mathcal{B}_{M,1}((\Upsilon, \Psi), (\Phi, \Theta)) := a^1(\Upsilon, \Phi) + b(\Phi, \Psi) + b(\Upsilon, \Theta)$$

with

$$a^1((\mathbf{y^c}, \mathbf{y^s}, \mathbf{p^c}, \mathbf{p^s}), (\mathbf{v^c}, \mathbf{v^s}, \mathbf{q^c}, \mathbf{q^s})) := a_a^1((\mathbf{y^c}, \mathbf{y^s}), (\mathbf{v^c}, \mathbf{v^s}))$$
$$+ a_b((\mathbf{v^c}, \mathbf{v^s}), (\mathbf{p^c}, \mathbf{p^s})) + a_b((\mathbf{y^c}, \mathbf{y^s}), (\mathbf{q^c}, \mathbf{q^s})) - a_c^1((\mathbf{p^c}, \mathbf{p^s}), (\mathbf{q^c}, \mathbf{q^s})),$$

and the new bilinear forms

$$a_a^1((\mathbf{y^c}, \mathbf{y^s}), (\mathbf{v^c}, \mathbf{v^s})) := \sum_{j \in \{c,s\}} (\mathbf{y^j}, \mathbf{v^j})_{\mathbf{0}, \Omega_a} \quad \text{and} \quad a_c^1((\mathbf{p^c}, \mathbf{p^s}), (\mathbf{q^c}, \mathbf{q^s})) := \sum_{j \in \{c,s\}} \lambda^{-1} (\mathbf{p^j}, \mathbf{q^j})_{\mathbf{0}, \Omega_b}.$$

The main result is summarized in the following Lemma, that claims that an inf-sup condition and a sup-sup condition are fulfilled, where the constants are independent of h, N and ω.

Lemma 7.10. *We have*

$$\underline{c}_1 \|(\Upsilon, \Psi)\|_{\mathcal{C}_M} \le \sup_{(\Phi, \Theta) \ne \mathbf{0}} \frac{\mathcal{B}_{M,1}((\Upsilon, \Psi), (\Phi, \Theta))}{\|(\Phi, \Theta)\|_{\mathcal{C}_M}} \le \bar{c}_1 \|(\Upsilon, \Psi)\|_{\mathcal{C}_M}$$

for all $(\Upsilon, \Psi) \in \mathbf{H_0}(\mathbf{curl}, \Omega_1)^4 \times H_0^1(\Omega_1)^4$. *Here the constants* $\underline{c}_1$, $\bar{c}_1$ *are independent of h, N and ω.*

Proof. In order to proof boundedness and the inf-sup condition of $a(\cdot, \cdot)$ on the kernel of $b(\cdot, \cdot)$, we use Theorem 2.4. We have to verify the lower and upper bounds for $a_a^1(\cdot, \cdot)$ and $a_c^1(\cdot, \cdot)$. Indeed, we have

$$0 \le a_a^1((\mathbf{y^c}, \mathbf{y^s}), (\mathbf{y^c}, \mathbf{y^s})) \le a_a((\mathbf{y^c}, \mathbf{y^s}), (\mathbf{y^c}, \mathbf{y^s})) \le \|(\mathbf{y^c}, \mathbf{y^s})\|_{\mathcal{C}_1}^2$$

and

$$0 \le a_c^1((\mathbf{p^c}, \mathbf{p^s}), (\mathbf{p^c}, \mathbf{p^s})) \le a_c((\mathbf{p^c}, \mathbf{p^s}), (\mathbf{p^c}, \mathbf{p^s})) \le \|(\mathbf{p^c}, \mathbf{p^s})\|_{\mathcal{C}_2}^2.$$

Furthermore we use the result of Lemma 7.9 to obtain the inf-sup conditions for $a_b(\cdot, \cdot)$. Therefore, combining the last estimates yields

$$c\|(\mathbf{y^c}, \mathbf{y^s})\|_{\mathcal{C}_2}^2 \leq a_a((\mathbf{y^c}, \mathbf{y^s}), (\mathbf{y^c}, \mathbf{y^s})) + \left(\sup_{0 \neq (\mathbf{q^c}, \mathbf{q^s})} \frac{a_b((\mathbf{y^c}, \mathbf{y^s}), (\mathbf{q^c}, \mathbf{q^s}))}{\|(\mathbf{q^c}, \mathbf{q^s})\|_{\mathcal{C}_2}} \right)^2 \leq \|(\mathbf{y^c}, \mathbf{y^s})\|_{\mathcal{C}_2}^2,$$

$$c\|(\mathbf{p^c}, \mathbf{p^s})\|_{\mathcal{C}_2}^2 \leq a_c((\mathbf{p^c}, \mathbf{p^s}), (\mathbf{p^c}, \mathbf{p^s})) + \left(\sup_{0 \neq (\mathbf{v^c}, \mathbf{v^s})} \frac{a_b((\mathbf{v^c}, \mathbf{v^s}), (\mathbf{p^c}, \mathbf{p^s}))}{\|(\mathbf{v^c}, \mathbf{v^s})\|_{\mathcal{C}_2}} \right)^2 \leq \|(\mathbf{p^c}, \mathbf{p^s})\|_{\mathcal{C}_2}^2,$$

for all $(\mathbf{y^c}, \mathbf{y^s}, \mathbf{p^c}, \mathbf{p^s})$ in the kernel of $b(\cdot, \cdot)$, where c is some generic constant, independent of h, ω and N. Now with Theorem 2.4, we obtain that the inf-sup condition of $a(\cdot, \cdot)$ on the kernel of $b(\cdot, \cdot)$ is satisfied. Boundedness of $a(\cdot, \cdot)$ follows easily with constant 1. Furthermore boundedness and the inf-sup condition of $b(\cdot, \cdot)$ can be done analogously to Lemma 7.4. Therefore, by Theorem 2.3, the desired result follows. $\qquad\square$

Due to Lemma 7.10 the preconditioner $\mathcal{C}_M$, that was derived for *Formulation OC-FEM 2*, can be reused in the setting, where the observation domain differs from the control domain. Furthermore, we immediately obtain that the condition number of the preconditioned system can be estimated by a constant, i.e.,

$$\kappa_{\mathcal{C}_M}(\mathcal{C}_M^{-1} \mathcal{B}_{M,1}) := \|\mathcal{C}_M^{-1} \mathcal{B}_{M,1}\|_{\mathcal{C}_M} \|\mathcal{B}_{M,1}^{-1} \mathcal{C}_M\|_{\mathcal{C}_M} \leq c_1,$$

where the constant c_1 is independent of the mesh size h, the frequency ω and the total number of modes N.

7.3.2   Observation of the magnetic flux density B

Instead of the vector potential $\mathbf{y}$, we want to observe the magnetic flux density $\mathbf{B} = \mathbf{curl}\,\mathbf{y}$. Therefore we obtain the following minimization problem:

$$\min_{\mathbf{y}, \mathbf{u}} J(\mathbf{y}, \mathbf{u}) = \frac{1}{2} \int_{\Omega_1 \times (0,T)} |\mathbf{curl}\,\mathbf{y} - \mathbf{y_c}|^2 \, \mathrm{d}\mathbf{x}\,\mathrm{d}t + \frac{\lambda}{2} \int_{\Omega_1 \times (0,T)} |\mathbf{u}|^2 \mathrm{d}\mathbf{x}\,\mathrm{d}t, \qquad (7.32)$$

subject to the state equation

$$\begin{cases} \sigma \dfrac{\partial \mathbf{y}}{\partial t} + \mathbf{curl}(\nu\,\mathbf{curl}\,\mathbf{y}) = \mathbf{u}, & \text{in } \Omega_1 \times (0,T), \\ \operatorname{div}(\sigma \mathbf{y}) = 0, & \text{in } \Omega_1 \times (0,T), \\ \mathbf{y} \times \mathbf{n} = \mathbf{0}, & \text{on } \partial\Omega_1 \times (0,T), \\ \mathbf{y}(0) = \mathbf{y}(T), & \text{on } \Omega_1 \times \{0\}. \end{cases} \qquad (7.33)$$

Here $\mathbf{y_c} \in L_2((0,T), \mathbf{L_2}(\Omega_1))$ is some prescribed desired state of the magnetic flux density $\mathbf{curl}\,\mathbf{y}$. In this setting we have

$$\mathcal{B}_{M,2}((\Upsilon, \Psi), (\Phi, \Theta)) := a^2(\Upsilon, \Phi) + b(\Phi, \Psi) + b(\Upsilon, \Theta),$$

with

$$a^2((\mathbf{y^c}, \mathbf{y^s}, \mathbf{p^c}, \mathbf{p^s}), (\mathbf{v^c}, \mathbf{v^s}, \mathbf{q^c}, \mathbf{q^s})) := a_a^2((\mathbf{y^c}, \mathbf{y^s}), (\mathbf{v^c}, \mathbf{v^s})) + a_b((\mathbf{v^c}, \mathbf{v^s}), (\mathbf{p^c}, \mathbf{p^s}))$$
$$+ a_b((\mathbf{y^c}, \mathbf{y^s}), (\mathbf{q^c}, \mathbf{q^s})) - a_c((\mathbf{p^c}, \mathbf{p^s}), (\mathbf{q^c}, \mathbf{q^s})),$$

and the new bilinear form

$$a_a^2((\mathbf{y^c}, \mathbf{y^s}), (\mathbf{v^c}, \mathbf{v^s})) := \sum_{j \in \{c,s\}} (\mathbf{curl}\,\mathbf{y^j}, \mathbf{curl}\,\mathbf{v^j})_{\mathbf{0}, \Omega_1}.$$

The main result is summarized in the following Lemma, that claims that an inf-sup condition and a sup-sup condition are fulfilled, where the constants are independent of h, N and ω.

Lemma 7.11. *We have*

$$\underline{c}_2\|(\Upsilon,\Psi)\|_{\mathcal{C}_M} \leq \sup_{(\Phi,\Theta)\neq\mathbf{0}} \frac{\mathcal{B}_{M,2}((\Upsilon,\Psi),(\Phi,\Theta))}{\|(\Phi,\Theta)\|_{\mathcal{C}_M}} \leq \overline{c}_2\|(\Upsilon,\Psi)\|_{\mathcal{C}_M},$$

for all $(\Upsilon,\Psi) \in \mathbf{H_0}(\mathbf{curl},\Omega_1)^4 \times H_0^1(\Omega_1)$. *Here the constants* $\underline{c}_2$, $\overline{c}_2$ *are independent of* h, N *and* ω.

Proof. The proof is basically the same as the proof of Lemma 7.10. The main differences are the lower and upper bounds for $a_a^2(\cdot,\cdot)$ and $a_c^2(\cdot,\cdot)$. We have

$$0 \leq a_a^2((\mathbf{y^c},\mathbf{y^s}),(\mathbf{y^c},\mathbf{y^s})) \leq \frac{1}{\underline{\nu}}\|(\mathbf{y^c},\mathbf{y^s})\|_{\mathcal{C}_2}^2$$

and

$$0 \leq a_c^2((\mathbf{p^c},\mathbf{p^s}),(\mathbf{p^c},\mathbf{p^s})) \leq \|(\mathbf{p^c},\mathbf{p^s})\|_{\mathcal{C}_2}^2.$$

This completes the proof. □

Due to Lemma 7.11 the preconditioner $\mathcal{C}_M$, that was derived for *Formulation OC-FEM 2*, can be reused in the setting, where the $\mathbf{B}$ filed is observed. Furthermore, we immediately obtain that the condition number of the preconditioned system can be estimated by a constant, i.e.,

$$\kappa_{\mathcal{C}_M}(\mathcal{C}_M^{-1}\mathcal{B}_{M,2}) := \|\mathcal{C}_M^{-1}\mathcal{B}_{M,2}\|_{\mathcal{C}_M}\|\mathcal{B}_{M,2}^{-1}\mathcal{C}_M\|_{\mathcal{C}_M} \leq c_2,$$

where the constant c_2 is independent of the mesh size h, the frequency ω and the total number of modes N.

7.3.3 Control constraints to the Fourier coefficients

In some practical applications it is reasonable to add box constraints for the control $\mathbf{u}$. Indeed, this approach is reasonable, if the amplitudes of the individual modes are intended to be bounded individually. We mention, that in this setting also the special case is included, that the exciting current is of the form $\mathbf{u}(\mathbf{x},t) = \mathbf{u^c}(\mathbf{x})\cos(\omega t)$, cf. [17]. In this case, it is reasonable to add box constraints to the Fourier coefficient $\mathbf{u^c}$.

Therefore in this subsection, we consider the case where the control constraints are associated to the Fourier coefficients of the control $\mathbf{u}$ for all modes $k = 0,\ldots,N$, i.e.,

$$\underline{\mathbf{u_k^c}} \leq \mathbf{u_k^c} \leq \overline{\mathbf{u_k^c}}, \quad \text{a.e. in } \Omega_1, \ k = 0,1,\ldots,N,$$
$$\underline{\mathbf{u_k^s}} \leq \mathbf{u_k^s} \leq \overline{\mathbf{u_k^s}}, \quad \text{a.e. in } \Omega_1, \ k = 1,\ldots,N.$$

Here $\underline{\mathbf{u_k^c}},\underline{\mathbf{u_k^s}},\overline{\mathbf{u_k^c}},\overline{\mathbf{u_k^s}} \in \mathbf{L_2}(\Omega_1)$ are given data and furthermore $\underline{\mathbf{u_k^c}} \leq \overline{\mathbf{u_k^c}}$ and $\underline{\mathbf{u_k^s}} \leq \overline{\mathbf{u_k^s}}$ holds a.e. in Ω_1. Since the problem decouples with respect to the modes k, we again concentrate on one block for a fixed mode k. For simplicity we drop the subindex k. Therefore we consider the following problem: Minimize the functional

$$J(\mathbf{y^c},\mathbf{y^s},\mathbf{u^c},\mathbf{u^c}) = \frac{1}{2}\sum_{j\in\{c,s\}}\int_{\Omega_1}|\mathbf{y^j} - \mathbf{y_d^j}|^2\mathrm{d}\mathbf{x} + \frac{\lambda}{2}\sum_{j\in\{c,s\}}\int_{\Omega_1}|\mathbf{u^j}|^2\mathrm{d}\mathbf{x},$$

subject to the state equation

$$\begin{cases} \omega\sigma\,\mathbf{y^s} + \mathbf{curl}(\nu\,\mathbf{curl}\,\mathbf{y^c}) = \mathbf{u^c}, & \text{in } \Omega_1, \\ -\omega\sigma\,\mathbf{y^c} + \mathbf{curl}(\nu\,\mathbf{curl}\,\mathbf{y^s}) = \mathbf{u^s}, & \text{in } \Omega_1, \\ \mathrm{div}(\sigma\mathbf{y^c}) = 0, & \text{in } \Omega_1, \\ \mathrm{div}(\sigma\mathbf{y^s}) = 0, & \text{in } \Omega_1, \\ \mathbf{y^c}\times\mathbf{n} = \mathbf{y^s}\times\mathbf{n} = \mathbf{0}, & \text{on } \partial\Omega_1, \end{cases} \qquad (7.34)$$

with the control constraints associated to the Fourier coefficients

$$\underline{\mathbf{u}}^{\mathbf{c}} \le \mathbf{u}^{\mathbf{c}} \le \overline{\mathbf{u}}^{\mathbf{c}}, \quad \text{a.e. in } \Omega_1,$$
$$\underline{\mathbf{u}}^{\mathbf{s}} \le \mathbf{u}^{\mathbf{s}} \le \overline{\mathbf{u}}^{\mathbf{s}}, \quad \text{a.e. in } \Omega_1.$$

The first order system of necessary and sufficient optimality conditions can be expressed as follows:

$$
\begin{cases}
-\omega(\sigma\mathbf{p}^{\mathbf{s}}, \mathbf{v}^{\mathbf{c}})_{\mathbf{0},\Omega_1} + (\nu\,\mathbf{curl}\,\mathbf{p}^{\mathbf{c}}, \mathbf{curl}\,\mathbf{v}^{\mathbf{c}})_{\mathbf{0},\Omega_1} + (\mathbf{y}^{\mathbf{c}}, \mathbf{v}^{\mathbf{c}})_{\mathbf{0},\Omega_1} + \omega(\sigma\mathbf{v}^{\mathbf{c}}, \nabla\rho^c)_{\mathbf{0},\Omega_1} = (\mathbf{y}_{\mathbf{d}}^{\mathbf{c}}, \mathbf{v}^{\mathbf{c}})_{\mathbf{0},\Omega_1}, \\
\qquad\qquad\qquad\qquad\qquad\qquad\qquad\qquad\qquad\qquad\qquad \omega(\sigma\mathbf{p}^{\mathbf{c}}, \nabla\eta^c)_{\mathbf{0},\Omega_1} = 0, \\
\omega(\sigma\mathbf{p}^{\mathbf{c}}, \mathbf{v}^{\mathbf{s}})_{\mathbf{0},\Omega_1} + (\nu\,\mathbf{curl}\,\mathbf{p}^{\mathbf{s}}, \mathbf{curl}\,\mathbf{v}^{\mathbf{s}})_{\mathbf{0},\Omega_1} + (\mathbf{y}^{\mathbf{s}}, \mathbf{v}^{\mathbf{s}})_{\mathbf{0},\Omega_1} + \omega(\sigma\mathbf{v}^{\mathbf{s}}, \nabla\rho^s)_{\mathbf{0},\Omega_1} = (\mathbf{y}_{\mathbf{d}}^{\mathbf{s}}, \mathbf{v}^{\mathbf{s}})_{\mathbf{0},\Omega_1}, \\
\qquad\qquad\qquad\qquad\qquad\qquad\qquad\qquad\qquad\qquad\qquad \omega(\sigma\mathbf{p}^{\mathbf{s}}, \nabla\eta^s)_{\mathbf{0},\Omega_1} = 0, \\
\lambda(\mathbf{u}^{\mathbf{c}}, \mathbf{w}^{\mathbf{c}})_{\mathbf{0},\Omega_1} - (\mathbf{p}^{\mathbf{c}}, \mathbf{w}^{\mathbf{c}})_{\mathbf{0},\Omega_1} + (\boldsymbol{\xi}^{\mathbf{c}}, \mathbf{w}^{\mathbf{c}})_{\mathbf{0},\Omega_1} = 0, \\
\lambda(\mathbf{u}^{\mathbf{s}}, \mathbf{w}^{\mathbf{s}})_{\mathbf{0},\Omega_1} - (\mathbf{p}^{\mathbf{s}}, \mathbf{w}^{\mathbf{s}})_{\mathbf{0},\Omega_1} + (\boldsymbol{\xi}^{\mathbf{s}}, \mathbf{w}^{\mathbf{s}})_{\mathbf{0},\Omega_1} = 0, \\
\omega(\sigma\mathbf{y}^{\mathbf{s}}, \mathbf{q}^{\mathbf{c}})_{\mathbf{0},\Omega_1} + (\nu\,\mathbf{curl}\,\mathbf{y}^{\mathbf{c}}, \mathbf{curl}\,\mathbf{q}^{\mathbf{c}})_{\mathbf{0},\Omega_1} - (\mathbf{u}^{\mathbf{c}}, \mathbf{q}^{\mathbf{c}})_{\mathbf{0},\Omega_1} + \omega(\sigma\mathbf{q}^{\mathbf{c}}, \nabla\mu^c)_{\mathbf{0},\Omega_1} = 0, \\
\qquad\qquad\qquad\qquad\qquad\qquad\qquad\qquad\qquad\qquad\qquad \omega(\sigma\mathbf{y}^{\mathbf{c}}, \nabla\theta^c)_{\mathbf{0},\Omega_1} = 0, \\
-\omega(\sigma\mathbf{y}^{\mathbf{c}}, \mathbf{q}^{\mathbf{s}})_{\mathbf{0},\Omega_1} + (\nu\,\mathbf{curl}\,\mathbf{y}^{\mathbf{s}}, \mathbf{curl}\,\mathbf{q}^{\mathbf{s}})_{\mathbf{0},\Omega_1} - (\mathbf{u}^{\mathbf{s}}, \mathbf{q}^{\mathbf{s}})_{\mathbf{0},\Omega_1} + \omega(\sigma\mathbf{q}^{\mathbf{s}}, \nabla\mu^s)_{\mathbf{0},\Omega_1} = 0, \\
\qquad\qquad\qquad\qquad\qquad\qquad\qquad\qquad\qquad\qquad\qquad \omega(\sigma\mathbf{y}^{\mathbf{s}}, \nabla\theta^s)_{\mathbf{0},\Omega_1} = 0, \\
\boldsymbol{\xi}^{\mathbf{c}} - \mathbf{max}(\mathbf{0}, \boldsymbol{\xi}^{\mathbf{c}} + C(\mathbf{u}^{\mathbf{c}} - \overline{\mathbf{u}}^{\mathbf{c}})) - \mathbf{min}(\mathbf{0}, \boldsymbol{\xi}^{\mathbf{c}} + C(\underline{\mathbf{u}}^{\mathbf{c}} - \mathbf{u}^{\mathbf{c}})) = \mathbf{0}, \\
\boldsymbol{\xi}^{\mathbf{s}} - \mathbf{max}(\mathbf{0}, \boldsymbol{\xi}^{\mathbf{s}} + C(\mathbf{u}^{\mathbf{s}} - \overline{\mathbf{u}}^{\mathbf{s}})) - \mathbf{min}(\mathbf{0}, \boldsymbol{\xi}^{\mathbf{s}} + C(\underline{\mathbf{u}}^{\mathbf{s}} - \mathbf{u}^{\mathbf{s}})) = \mathbf{0},
\end{cases}
$$
$$(7.35)$$

with the Lagrange multipliers $\mathbf{p}^{\mathbf{j}}, \rho^j, \boldsymbol{\xi}^{\mathbf{j}}, j \in \{c, s\}$. Here, for any three-dimensional vector function $\mathbf{y}$, $\mathbf{max}(\mathbf{0}, \mathbf{y})$ is the component wise application of max in the pointwise sense. Furthermore C is some positive constant. Due to the last two equations, this system is nonlinear, but due to [76] the last two equations enjoy the Newton differentiability, at least for $C = \lambda$. In order to solve this system, we use the primal-dual active set method as introduced in [76]. This method is equivalent to a semi-smooth Newton method. The strategy proceeds as follows: At each Newton iterate l for $j \in \{c, s\}$ the active sets are determined by

$$\mathcal{E}_l^{j,+} = \{\mathbf{x} \in \Omega_1 : \boldsymbol{\xi}_{\mathbf{l}}^{\mathbf{j}} + C(\mathbf{u}_{\mathbf{l}}^{\mathbf{j}} - \overline{\mathbf{u}}^{\mathbf{j}}) > 0\},$$
$$\mathcal{E}_l^{j,-} = \{\mathbf{x} \in \Omega_1 : \boldsymbol{\xi}_{\mathbf{l}}^{\mathbf{j}} - C(\underline{\mathbf{u}}^{\mathbf{j}} - \mathbf{u}^{\mathbf{j}}) < 0\},$$

and the inactive sets are $\mathcal{I}_l^j = \Omega_1 \backslash \mathcal{E}_l^j$, where $\mathcal{E}_l^j = \mathcal{E}_l^{j,+} \cup \mathcal{E}_l^{j,-}$. Consequently, the Newton step for the solution of (7.35), given in terms of the new iterate, reads as follows (for simplicity the index for the Newton iteration is dropped):

$$
\begin{cases}
-\omega(\sigma\mathbf{p}^{\mathbf{s}}, \mathbf{v}^{\mathbf{c}})_{\mathbf{0},\Omega_1} + (\nu\,\mathbf{curl}\,\mathbf{p}^{\mathbf{c}}, \mathbf{curl}\,\mathbf{v}^{\mathbf{c}})_{\mathbf{0},\Omega_1} + (\mathbf{y}^{\mathbf{c}}, \mathbf{v}^{\mathbf{c}})_{\mathbf{0},\Omega_1} + \omega(\sigma\mathbf{v}^{\mathbf{c}}, \nabla\rho^c)_{\mathbf{0},\Omega_1} = (\mathbf{y}_{\mathbf{d}}^{\mathbf{c}}, \mathbf{v}^{\mathbf{c}})_{\mathbf{0},\Omega_1}, \\
\qquad\qquad\qquad\qquad\qquad\qquad\qquad\qquad\qquad\qquad\qquad \omega(\sigma\mathbf{p}^{\mathbf{c}}, \nabla\eta^c)_{\mathbf{0},\Omega_1} = 0, \\
\omega(\sigma\mathbf{p}^{\mathbf{c}}, \mathbf{v}^{\mathbf{s}})_{\mathbf{0},\Omega_1} + (\nu\,\mathbf{curl}\,\mathbf{p}^{\mathbf{s}}, \mathbf{curl}\,\mathbf{v}^{\mathbf{s}})_{\mathbf{0},\Omega_1} + (\mathbf{y}^{\mathbf{s}}, \mathbf{v}^{\mathbf{s}})_{\mathbf{0},\Omega_1} + \omega(\sigma\mathbf{v}^{\mathbf{s}}, \nabla\rho^s)_{\mathbf{0},\Omega_1} = (\mathbf{y}_{\mathbf{d}}^{\mathbf{s}}, \mathbf{v}^{\mathbf{s}})_{\mathbf{0},\Omega_1}, \\
\qquad\qquad\qquad\qquad\qquad\qquad\qquad\qquad\qquad\qquad\qquad \omega(\sigma\mathbf{p}^{\mathbf{s}}, \nabla\eta^s)_{\mathbf{0},\Omega_1} = 0, \\
\lambda(\mathbf{u}^{\mathbf{c}}, \mathbf{w}^{\mathbf{c}})_{\mathbf{0},\Omega_1} - (\mathbf{p}^{\mathbf{c}}, \mathbf{w}^{\mathbf{c}})_{\mathbf{0},\Omega_1} + (\boldsymbol{\xi}^{\mathbf{c}}, \mathbf{w}^{\mathbf{c}})_{\mathbf{0},\Omega_1} = 0, \\
\lambda(\mathbf{u}^{\mathbf{s}}, \mathbf{w}^{\mathbf{s}})_{\mathbf{0},\Omega_1} - (\mathbf{p}^{\mathbf{s}}, \mathbf{w}^{\mathbf{s}})_{\mathbf{0},\Omega_1} + (\boldsymbol{\xi}^{\mathbf{s}}, \mathbf{w}^{\mathbf{s}})_{\mathbf{0},\Omega_1} = 0, \\
\omega(\sigma\mathbf{y}^{\mathbf{s}}, \mathbf{q}^{\mathbf{c}})_{\mathbf{0},\Omega_1} + (\nu\,\mathbf{curl}\,\mathbf{y}^{\mathbf{c}}, \mathbf{curl}\,\mathbf{q}^{\mathbf{c}})_{\mathbf{0},\Omega_1} - (\mathbf{u}^{\mathbf{c}}, \mathbf{q}^{\mathbf{c}})_{\mathbf{0},\Omega_1} + \omega(\sigma\mathbf{q}^{\mathbf{c}}, \nabla\mu^c)_{\mathbf{0},\Omega_1} = 0, \\
\qquad\qquad\qquad\qquad\qquad\qquad\qquad\qquad\qquad\qquad\qquad \omega(\sigma\mathbf{y}^{\mathbf{c}}, \nabla\theta^c)_{\mathbf{0},\Omega_1} = 0, \\
-\omega(\sigma\mathbf{y}^{\mathbf{c}}, \mathbf{q}^{\mathbf{s}})_{\mathbf{0},\Omega_1} + (\nu\,\mathbf{curl}\,\mathbf{y}^{\mathbf{s}}, \mathbf{curl}\,\mathbf{q}^{\mathbf{s}})_{\mathbf{0},\Omega_1} - (\mathbf{u}^{\mathbf{s}}, \mathbf{q}^{\mathbf{s}})_{\mathbf{0},\Omega_1} + \omega(\sigma\mathbf{q}^{\mathbf{s}}, \nabla\mu^s)_{\mathbf{0},\Omega_1} = 0, \\
\qquad\qquad\qquad\qquad\qquad\qquad\qquad\qquad\qquad\qquad\qquad \omega(\sigma\mathbf{y}^{\mathbf{s}}, \nabla\theta^s)_{\mathbf{0},\Omega_1} = 0, \\
C\chi_{\mathcal{E}^c}\mathbf{u}^{\mathbf{c}} + \chi_{\mathcal{I}^c}\boldsymbol{\xi}^{\mathbf{c}} - C(\chi_{\mathcal{E}^{c,+}}\overline{\mathbf{u}}^{\mathbf{c}} + \chi_{\mathcal{E}^{c,-}}\underline{\mathbf{u}}^{\mathbf{c}}) = \mathbf{0}, \\
C\chi_{\mathcal{E}^s}\mathbf{u}^{\mathbf{s}} + \chi_{\mathcal{I}^s}\boldsymbol{\xi}^{\mathbf{s}} - C(\chi_{\mathcal{E}^{s,+}}\overline{\mathbf{u}}^{\mathbf{s}} + \chi_{\mathcal{E}^{s,-}}\underline{\mathbf{u}}^{\mathbf{s}}) = \mathbf{0}.
\end{cases}
$$

The symbol χ denotes the characteristic function with respect to the set denoted in the subscript. Next we use, that the restriction of $\boldsymbol{\xi}^{\mathbf{j}}$, $j \in \{c, s\}$, to the inactive sets $\mathcal{I}^j$ is zero, and hence this variable can be eliminated from the system. Therefore, we introduce the new variables $\boldsymbol{\xi}_{\boldsymbol{\mathcal{E}}}^{\mathbf{j}}$, namely the restriction of $\boldsymbol{\xi}^{\mathbf{j}}$ to the active set $\mathcal{E}^j$. Furthermore, we derive the weak formulation of the last two equations by multiplying with test functions $\mathbf{z}_{\boldsymbol{\mathcal{E}}}^{\mathbf{j}} \in \mathbf{L_2}(\mathcal{E}^j)$. Consequently, we are dealing with the following variational problem:

$$
\left\{
\begin{aligned}
&-\omega(\sigma \mathbf{p^s}, \mathbf{v^c})_{\mathbf{0},\Omega_1} + (\nu \operatorname{\mathbf{curl}} \mathbf{p^c}, \operatorname{\mathbf{curl}} \mathbf{v^c})_{\mathbf{0},\Omega_1} + (\mathbf{y^c}, \mathbf{v^c})_{\mathbf{0},\Omega_1} + \omega(\sigma \mathbf{v^c}, \nabla \rho^c)_{\mathbf{0},\Omega_1} = (\mathbf{y_d^c}, \mathbf{v^c})_{\mathbf{0},\Omega_1}, \\
&\hspace{8.5cm} \omega(\sigma \mathbf{p^c}, \nabla \eta^c)_{\mathbf{0},\Omega_1} = 0, \\
&\omega(\sigma \mathbf{p^c}, \mathbf{v^s})_{\mathbf{0},\Omega_1} + (\nu \operatorname{\mathbf{curl}} \mathbf{p^s}, \operatorname{\mathbf{curl}} \mathbf{v^s})_{\mathbf{0},\Omega_1} + (\mathbf{y^s}, \mathbf{v^s})_{\mathbf{0},\Omega_1} + \omega(\sigma \mathbf{v^s}, \nabla \rho^s)_{\mathbf{0},\Omega_1} = (\mathbf{y_d^s}, \mathbf{v^s})_{\mathbf{0},\Omega_1}, \\
&\hspace{8.5cm} \omega(\sigma \mathbf{p^s}, \nabla \eta^s)_{\mathbf{0},\Omega_1} = 0, \\
&\hspace{2.2cm} \lambda(\mathbf{u^c}, \mathbf{w^c})_{\mathbf{0},\Omega_1} - (\mathbf{p^c}, \mathbf{w^c})_{\mathbf{0},\Omega_1} + (\boldsymbol{\xi}_{\boldsymbol{\mathcal{E}}}^{\mathbf{c}}, \mathcal{P}_{\mathcal{E}^c} \mathbf{w^c})_{\mathbf{0},\mathcal{E}^c} = 0, \\
&\hspace{2.2cm} \lambda(\mathbf{u^s}, \mathbf{w^s})_{\mathbf{0},\Omega_1} - (\mathbf{p^s}, \mathbf{w^s})_{\mathbf{0},\Omega_1} + (\boldsymbol{\xi}_{\boldsymbol{\mathcal{E}}}^{\mathbf{s}}, \mathcal{P}_{\mathcal{E}^s} \mathbf{w^s})_{\mathbf{0},\mathcal{E}^s} = 0, \\
&\omega(\sigma \mathbf{y^s}, \mathbf{q^c})_{\mathbf{0},\Omega_1} + (\nu \operatorname{\mathbf{curl}} \mathbf{y^c}, \operatorname{\mathbf{curl}} \mathbf{q^c})_{\mathbf{0},\Omega_1} - (\mathbf{u^c}, \mathbf{q^c})_{\mathbf{0},\Omega_1} + \omega(\sigma \mathbf{q^c}, \nabla \mu^c)_{\mathbf{0},\Omega_1} = 0, \\
&\hspace{8.5cm} \omega(\sigma \mathbf{y^c}, \nabla \theta^c)_{\mathbf{0},\Omega_1} = 0, \\
&-\omega(\sigma \mathbf{y^c}, \mathbf{q^s})_{\mathbf{0},\Omega_1} + (\nu \operatorname{\mathbf{curl}} \mathbf{y^s}, \operatorname{\mathbf{curl}} \mathbf{q^s})_{\mathbf{0},\Omega_1} - (\mathbf{u^s}, \mathbf{q^s})_{\mathbf{0},\Omega_1} + \omega(\sigma \mathbf{q^s}, \nabla \mu^s)_{\mathbf{0},\Omega_1} = 0, \\
&\hspace{8.5cm} \omega(\sigma \mathbf{y^s}, \nabla \theta^s)_{\mathbf{0},\Omega_1} = 0, \\
&\hspace{1.5cm} (\mathcal{P}_{\mathcal{E}^c} \mathbf{u^c}, \mathbf{z}_{\boldsymbol{\mathcal{E}}}^{\mathbf{c}})_{\mathbf{0},\mathcal{E}^c} - (\mathcal{P}_{\mathcal{E}^{c,+}} \overline{\mathbf{u}}^{\mathbf{c}} + \mathcal{P}_{\mathcal{E}^{c,-}} \underline{\mathbf{u}}^{\mathbf{c}}, \mathbf{z}_{\boldsymbol{\mathcal{E}}}^{\mathbf{c}})_{\mathbf{0},\mathcal{E}^c} = 0, \\
&\hspace{1.5cm} (\mathcal{P}_{\mathcal{E}^s} \mathbf{u^s}, \mathbf{z}_{\boldsymbol{\mathcal{E}}}^{\mathbf{s}})_{\mathbf{0},\mathcal{E}^s} - (\mathcal{P}_{\mathcal{E}^{s,+}} \overline{\mathbf{u}}^{\mathbf{s}} + \mathcal{P}_{\mathcal{E}^{s,-}} \underline{\mathbf{u}}^{\mathbf{s}}, \mathbf{z}_{\boldsymbol{\mathcal{E}}}^{\mathbf{s}})_{\mathbf{0},\mathcal{E}^s} = 0.
\end{aligned}
\right.
$$

Here the projections $\mathcal{P}_{\mathcal{X}}$, $\mathcal{X} \in \{\mathcal{E}^{c,+}, \mathcal{E}^{c,-}, \mathcal{E}^c, \mathcal{E}^{s,+}, \mathcal{E}^{s,-}, \mathcal{E}^s\}$, are defined by

$$
\begin{aligned}
&\mathcal{P}_{\mathcal{X}} : \mathbf{L_2}(\Omega_1) \to \mathbf{L_2}(\mathcal{X}), \\
&(\mathcal{P}_{\mathcal{X}} \mathbf{u}, \mathbf{v})_{\mathbf{0},\mathcal{X}} = (\mathbf{u}, \mathbf{v})_{\mathbf{0},\mathcal{X}}, \quad \forall \mathbf{u} \in \mathbf{L_2}(\Omega_1), \mathbf{v} \in \mathbf{L_2}(\mathcal{X}).
\end{aligned}
$$

The adjoint operators $\mathcal{P}_{\mathcal{X}}^*$ are defined by

$$
\begin{aligned}
&\mathcal{P}_{\mathcal{X}}^* : \mathbf{L_2}(\mathcal{X}) \to \mathbf{L_2}(\Omega_1), \\
&(\mathbf{u}, \mathcal{P}_{\mathcal{X}}^* \mathbf{v})_{\mathbf{0},\Omega_1} = (\mathcal{P}_{\mathcal{X}} \mathbf{u}, \mathbf{v})_{\mathbf{0},\mathcal{X}}, \quad \forall \mathbf{u} \in \mathbf{L_2}(\Omega_1), \mathbf{v} \in \mathbf{L_2}(\mathcal{X}).
\end{aligned}
$$

In the usual manner, the control variables $\mathbf{u^c}$ and $\mathbf{u^s}$ can be eliminated, using the fifth and the sixth equation. Finally, we eliminate $\boldsymbol{\xi}_{\boldsymbol{\mathcal{E}}}^{\mathbf{c}}$ and $\boldsymbol{\xi}_{\boldsymbol{\mathcal{E}}}^{\mathbf{s}}$ and end up with the reduced optimality system: Find $(\Upsilon, \Psi) \in \mathbf{H_0}(\operatorname{\mathbf{curl}}, \Omega_1)^4 \times H_0^1(\Omega_1)^4$, such that

$$
\left\{
\begin{aligned}
&-\omega(\sigma \mathbf{p^s}, \mathbf{v^c})_{\mathbf{0},\Omega_1} + (\nu \operatorname{\mathbf{curl}} \mathbf{p^c}, \operatorname{\mathbf{curl}} \mathbf{v^c})_{\mathbf{0},\Omega_1} \\
&\hspace{2cm} + (\mathbf{y^c}, \mathbf{v^c})_{\mathbf{0},\Omega_1} + \omega(\sigma \mathbf{v^c}, \nabla \rho^c)_{\mathbf{0},\Omega_1} = (\mathbf{y_d^c}, \mathbf{v^c})_{\mathbf{0},\Omega_1}, \\
&\hspace{5cm} \omega(\sigma \mathbf{p^c}, \nabla \eta^c)_{\mathbf{0},\Omega_1} = 0, \\
&\omega(\sigma \mathbf{p^c}, \mathbf{v^s})_{\mathbf{0},\Omega_1} + (\nu \operatorname{\mathbf{curl}} \mathbf{p^s}, \operatorname{\mathbf{curl}} \mathbf{v^s})_{\mathbf{0},\Omega_1} \\
&\hspace{2cm} + (\mathbf{y^s}, \mathbf{v^s})_{\mathbf{0},\Omega_1} + \omega(\sigma \mathbf{v^s}, \nabla \rho^s)_{\mathbf{0},\Omega_1} = (\mathbf{y_d^s}, \mathbf{v^s})_{\mathbf{0},\Omega_1}, \\
&\hspace{5cm} \omega(\sigma \mathbf{p^s}, \nabla \eta^s)_{\mathbf{0},\Omega_1} = 0, \\
&\omega(\sigma \mathbf{y^s}, \mathbf{q^c})_{\mathbf{0},\Omega_1} + (\nu \operatorname{\mathbf{curl}} \mathbf{y^c}, \operatorname{\mathbf{curl}} \mathbf{q^c})_{\mathbf{0},\Omega_1} \\
&\hspace{0.5cm} - \frac{1}{\lambda} [(\mathbf{p^c}, \mathbf{q^c})_{\mathbf{0},\Omega_1} - (\mathcal{P}_{\mathcal{E}^c}^* \mathcal{P}_{\mathcal{E}^c} \mathbf{p^c}, \mathbf{q^c})_{\mathbf{0},\Omega_1}] + \omega(\sigma \mathbf{q^c}, \nabla \mu^c)_{\mathbf{0},\Omega_1} = (\mathbf{f^c}, \mathbf{q^c})_{\mathbf{0},\Omega_1}, \\
&\hspace{5cm} \omega(\sigma \mathbf{y^c}, \nabla \theta^c)_{\mathbf{0},\Omega_1} = 0, \\
&-\omega(\sigma \mathbf{y^c}, \mathbf{q^s})_{\mathbf{0},\Omega_1} + (\nu \operatorname{\mathbf{curl}} \mathbf{y^s}, \operatorname{\mathbf{curl}} \mathbf{q^s})_{\mathbf{0},\Omega_1} \\
&\hspace{0.5cm} - \frac{1}{\lambda} [(\mathbf{p^s}, \mathbf{q^s})_{\mathbf{0},\Omega_1} - (\mathcal{P}_{\mathcal{E}^s}^* \mathcal{P}_{\mathcal{E}^s} \mathbf{p^s}, \mathbf{q^s})_{\mathbf{0},\Omega_1}] + \omega(\sigma \mathbf{q^s}, \nabla \mu^s)_{\mathbf{0},\Omega_1} = (\mathbf{f^s}, \mathbf{q^s})_{\mathbf{0},\Omega_1}, \\
&\hspace{5cm} \omega(\sigma \mathbf{y^s}, \nabla \theta^s)_{\mathbf{0},\Omega_1} = 0,
\end{aligned}
\right.
$$

for all $(\Phi, \Theta) \in \mathbf{H_0}(\mathbf{curl}, \Omega_1)^4 \times H_0^1(\Omega_1)^4$. Here $\mathbf{f^j}$, for $j \in \{c, s\}$, is given by

$$\mathbf{f^j} = \mathcal{P}_{\mathcal{E}^j}^* (\mathcal{P}_{\mathcal{E}^{j,+}} \overline{\mathbf{u}}^{\mathbf{j}} + \mathcal{P}_{\mathcal{E}^{j,-}} \underline{\mathbf{u}}^{\mathbf{j}}).$$

In this setting we have

$$\mathcal{B}_{M,3}((\Upsilon, \Psi), (\Phi, \Theta)) := a^3(\Upsilon, \Phi) + b(\Phi, \Psi) + b(\Upsilon, \Theta)$$

with

$$a^3((\mathbf{y^c}, \mathbf{y^s}, \mathbf{p^c}, \mathbf{p^s}), (\mathbf{v^c}, \mathbf{v^s}, \mathbf{q^c}, \mathbf{q^s})) := a_a((\mathbf{y^c}, \mathbf{y^s}), (\mathbf{v^c}, \mathbf{v^s}))$$
$$+ a_b((\mathbf{v^c}, \mathbf{v^s}), (\mathbf{p^c}, \mathbf{p^s})) + a_b((\mathbf{y^c}, \mathbf{y^s}), (\mathbf{q^c}, \mathbf{q^s})) - a_c^3((\mathbf{p^c}, \mathbf{p^s}), (\mathbf{q^c}, \mathbf{q^s}))$$

and the new bilinear form

$$a_c^3((\mathbf{y^c}, \mathbf{y^s}), (\mathbf{v^c}, \mathbf{v^s})) := \sum_{j \in \{c,s\}} (\mathbf{p^j}, \mathbf{q^j})_{\mathbf{0}, \Omega_1} - (\mathcal{P}_{\mathcal{E}^j}^* \mathcal{P}_{\mathcal{E}^j} \mathbf{p^j}, \mathbf{q^j})_{\mathbf{0}, \Omega_1}.$$

The main result is summarized in the following Lemma, that claims that an inf-sup condition and a sup-sup condition are fulfilled, where the constants are independent of h, N and ω.

Lemma 7.12. *We have*

$$\underline{c}_3 \|(\Upsilon, \Psi)\|_{\mathcal{C}_M} \leq \sup_{(\Phi, \Theta) \neq \mathbf{0}} \frac{\mathcal{B}_{M,3}((\Upsilon, \Psi), (\Phi, \Theta))}{\|(\Phi, \Theta)\|_{\mathcal{C}_M}} \leq \overline{c}_3 \|(\Upsilon, \Psi)\|_{\mathcal{C}_M}$$

for all $(\Upsilon, \Psi) \in \mathbf{H_0}(\mathbf{curl}, \Omega_1)^4 \times H_0^1(\Omega_1)$. Here the constants $\underline{c}_3$, $\overline{c}_3$ are independent of h, N, ω and the active sets $\mathcal{E}^c$ and $\mathcal{E}^s$.

Proof. The proof is basically the same as the proof of Lemma 7.10. The main differences are the lower and upper bounds for $a_c^3(\cdot, \cdot)$. We have

$$0 \leq a_c^3((\mathbf{p^c}, \mathbf{p^s}), (\mathbf{p^c}, \mathbf{p^s})) \leq 2 \|(\mathbf{p^c}, \mathbf{p^s})\|_{\mathcal{C}_2}^2.$$

This completes the proof. $\qquad\qquad\qquad\qquad\qquad\qquad\qquad\qquad\qquad\qquad\qquad\qquad\square$

Due to Lemma 7.12 the preconditioner $\mathcal{C}_M$, that was derived for *Formulation OC-FEM 2*, can be reused in the setting, where control constraints are added to the Fourier coefficient. Furthermore, we immediately obtain that the condition number of the preconditioned system can be estimated by a constant, i.e.,

$$\kappa_{\mathcal{C}_M}(\mathcal{C}_M^{-1} \mathcal{B}_{M,3}) := \|\mathcal{C}_M^{-1} \mathcal{B}_{M,3}\|_{\mathcal{C}_M} \|\mathcal{B}_{M,3}^{-1} \mathcal{C}_M\|_{\mathcal{C}_M} \leq c_3,$$

where the constant c_3 is independent of the mesh size h, the frequency ω, the total number of modes N and the active sets $\mathcal{E}^c$, $\mathcal{E}^s$.

7.3.4   State constraints to the Fourier coefficients

In some practical applications it is reasonable to add box constraints for the state $\mathbf{y}$. For example, constraints imposed on the state $\mathbf{y}$ are important to filter out undesired singularities in the solution $\mathbf{y}$ of the eddy current problem. Indeed, this can already be achieved by imposing box constraints on the Fourier coefficients of the state $\mathbf{y}$, i.e.,

$$\underline{\mathbf{y}}_{\mathbf{k}}^{\mathbf{c}} \leq \mathbf{y}_{\mathbf{k}}^{\mathbf{c}} \leq \overline{\mathbf{y}}_{\mathbf{k}}^{\mathbf{c}}, \quad \text{a.e. in } \Omega_1, \ k = 0, 1, \dots, N,$$
$$\underline{\mathbf{y}}_{\mathbf{k}}^{\mathbf{s}} \leq \mathbf{y}_{\mathbf{k}}^{\mathbf{s}} \leq \overline{\mathbf{y}}_{\mathbf{k}}^{\mathbf{s}}, \quad \text{a.e. in } \Omega_1, \ k = 1, \dots, N.$$

Here $\underline{\mathbf{y}}_{\mathbf{k}}^{\mathbf{c}}, \underline{\mathbf{y}}_{\mathbf{k}}^{\mathbf{s}}, \overline{\mathbf{y}}_{\mathbf{k}}^{\mathbf{c}}, \overline{\mathbf{y}}_{\mathbf{k}}^{\mathbf{s}} \in \mathbf{L_2}(\Omega_1)$ are given data and furthermore $\underline{\mathbf{y}}_{\mathbf{k}}^{\mathbf{c}} \leq \overline{\mathbf{y}}_{\mathbf{k}}^{\mathbf{c}}$ and $\underline{\mathbf{y}}_{\mathbf{k}}^{\mathbf{s}} \leq \overline{\mathbf{y}}_{\mathbf{k}}^{\mathbf{s}}$ holds a.e. in Ω_1. In this setting we rely on *Formulation OC-FEM 1*, cf. Problem 7.1 and Remark 7.14. Again we

observe a decoupling with respect to the modes k, and therefore drop the mode subindex $k = 0, \dots, N$. In order to incorporate the state constraints, we follow the analytical framework presented in [159]. Due to the lack of regularity of the *control-to-state* map, a penalization method, that is also called Moreau-Yosida regularization, is used. Therefore the regularized problem reads as follows: Minimize the functional

$$
\begin{aligned}
J^{\varepsilon}(\mathbf{y^c}, \mathbf{y^s}, \mathbf{u^c}, \mathbf{u^c}) = {} & \frac{1}{2} \sum_{j \in \{c,s\}} \int_{\Omega_1} |\mathbf{y^j} - \mathbf{y_d^j}|^2 \mathrm{d}\mathbf{x} + \frac{\lambda}{2} \sum_{j \in \{c,s\}} \int_{\Omega_1} |\mathbf{u^j}|^2 \mathrm{d}\mathbf{x} \\
& + \frac{1}{2\varepsilon} \sum_{j \in \{c,s\}} \left(\|\mathbf{max}(\mathbf{0}, \mathbf{y^j} - \overline{\mathbf{y}}^{\mathbf{j}})\|^2_{\mathbf{0},\Omega_1} + \|\mathbf{min}(\mathbf{0}, \mathbf{y^j} - \underline{\mathbf{y}}^{\mathbf{j}})\|^2_{\mathbf{0},\Omega_1} \right),
\end{aligned}
\tag{7.36}
$$

subject to the state equation

$$
\begin{cases}
\omega \sigma \, \mathbf{y^s} + \mathbf{curl}(\nu \, \mathbf{curl} \, \mathbf{y^c}) = \mathbf{u^c}, & \text{in } \Omega_1, \\
-\omega \sigma \, \mathbf{y^c} + \mathbf{curl}(\nu \, \mathbf{curl} \, \mathbf{y^s}) = \mathbf{u^s}, & \text{in } \Omega_1, \\
\mathbf{y^c} \times \mathbf{n} = \mathbf{y^s} \times \mathbf{n} = \mathbf{0}, & \text{on } \partial\Omega_1.
\end{cases}
\tag{7.37}
$$

Here ε is an additional regularization parameter. The first order system of necessary and sufficient optimality conditions of (7.36)-(7.37) can be expressed as follows

$$
\begin{cases}
-\omega(\sigma \mathbf{p^s}, \mathbf{v^c})_{\mathbf{0},\Omega_1} + (\nu \, \mathbf{curl} \, \mathbf{p^c}, \mathbf{curl} \, \mathbf{v^c})_{\mathbf{0},\Omega_1} + (\mathbf{y^c}, \mathbf{v^c})_{\mathbf{0},\Omega_1} + (\boldsymbol{\xi^c}, \mathbf{v^c})_{\mathbf{0},\Omega_1} = (\mathbf{y_d^c}, \mathbf{v^c})_{\mathbf{0},\Omega_1}, \\
\omega(\sigma \mathbf{p^c}, \mathbf{v^s})_{\mathbf{0},\Omega_1} + (\nu \, \mathbf{curl} \, \mathbf{p^s}, \mathbf{curl} \, \mathbf{v^s})_{\mathbf{0},\Omega_1} + (\mathbf{y^s}, \mathbf{v^s})_{\mathbf{0},\Omega_1} + (\boldsymbol{\xi^s}, \mathbf{v^s})_{\mathbf{0},\Omega_1} = (\mathbf{y_d^s}, \mathbf{v^s})_{\mathbf{0},\Omega_1}, \\
\omega(\sigma \mathbf{y^s}, \mathbf{q^c})_{\mathbf{0},\Omega_1} + (\nu \, \mathbf{curl} \, \mathbf{y^c}, \mathbf{curl} \, \mathbf{q^c})_{\mathbf{0},\Omega_1} - \lambda^{-1}(\mathbf{p^c}, \mathbf{q^c})_{\mathbf{0},\Omega_1} = 0, \\
-\omega(\sigma \mathbf{y^c}, \mathbf{q^s})_{\mathbf{0},\Omega_1} + (\nu \, \mathbf{curl} \, \mathbf{y^s}, \mathbf{curl} \, \mathbf{q^s})_{\mathbf{0},\Omega_1} - \lambda^{-1}(\mathbf{p^s}, \mathbf{q^s})_{\mathbf{0},\Omega_1} = 0, \\
\boldsymbol{\xi^c} - \dfrac{1}{\varepsilon}\mathbf{max}(\mathbf{0}, \mathbf{y^c} - \overline{\mathbf{y}}^{\mathbf{c}}) + \dfrac{1}{\varepsilon}\mathbf{min}(\mathbf{0}, \underline{\mathbf{y}}^{\mathbf{c}} - \mathbf{y^c}) = \mathbf{0}, \\
\boldsymbol{\xi^s} - \dfrac{1}{\varepsilon}\mathbf{max}(\mathbf{0}, \mathbf{y^s} - \overline{\mathbf{y}}^{\mathbf{s}}) + \dfrac{1}{\varepsilon}\mathbf{min}(\mathbf{0}, \underline{\mathbf{y}}^{\mathbf{s}} - \mathbf{y^s}) = \mathbf{0}.
\end{cases}
$$

Again, we use a primal-dual active set strategy. Therefore, at each Newton step (for simplicity the index for the Newton iteration is skipped), we have to solve the variational problem: Find $(\Upsilon, \Psi) \in \mathbf{H_0}(\mathbf{curl}, \Omega_1)^4 \times H_0^1(\Omega_1)^4$, such that

$$
\begin{cases}
-\omega(\sigma \mathbf{p^s}, \mathbf{v^c})_{\mathbf{0},\Omega_1} + (\nu \, \mathbf{curl} \, \mathbf{p^c}, \mathbf{curl} \, \mathbf{v^c})_{\mathbf{0},\Omega_1} + (\mathbf{y^c}, \mathbf{v^c})_{\mathbf{0},\Omega_1} + \dfrac{1}{\varepsilon}(\mathbf{y^c}, \mathbf{v^c})_{\mathbf{0},\mathcal{E}^c} \\
\qquad = (\mathbf{y_d^c}, \mathbf{v^c})_{\mathbf{0},\Omega_1} + \dfrac{1}{\varepsilon}\left(\chi_{\mathcal{E}^{c,+}}\overline{\mathbf{y}}^{\mathbf{c}} + \chi_{\mathcal{E}^{c,-}}\underline{\mathbf{y}}^{\mathbf{c}}, \mathbf{v^c} \right)_{\mathbf{0},\Omega_1}, \\
\omega(\sigma \mathbf{p^c}, \mathbf{v^s})_{\mathbf{0},\Omega_1} + (\nu \, \mathbf{curl} \, \mathbf{p^s}, \mathbf{curl} \, \mathbf{v^s})_{\mathbf{0},\Omega_1} + (\mathbf{y^s}, \mathbf{v^s})_{\mathbf{0},\Omega_1} + \dfrac{1}{\varepsilon}(\mathbf{y^s}, \mathbf{v^s})_{\mathbf{0},\mathcal{E}^s} \\
\qquad = (\mathbf{y_d^s}, \mathbf{v^s})_{\mathbf{0},\Omega_1} + \dfrac{1}{\varepsilon}\left(\chi_{\mathcal{E}^{s,+}}\overline{\mathbf{y}}^{\mathbf{s}} + \chi_{\mathcal{E}^{s,-}}\underline{\mathbf{y}}^{\mathbf{s}}, \mathbf{v^s} \right)_{\mathbf{0},\Omega_1}, \\
\omega(\sigma \mathbf{y^s}, \mathbf{q^c})_{\mathbf{0},\Omega_1} + (\nu \, \mathbf{curl} \, \mathbf{y^c}, \mathbf{curl} \, \mathbf{q^c})_{\mathbf{0},\Omega_1} - \lambda^{-1}(\mathbf{p^c}, \mathbf{q^c})_{\mathbf{0},\Omega_1} = 0, \\
-\omega(\sigma \mathbf{y^c}, \mathbf{q^s})_{\mathbf{0},\Omega_1} + (\nu \, \mathbf{curl} \, \mathbf{y^s}, \mathbf{curl} \, \mathbf{q^s})_{\mathbf{0},\Omega_1} - \lambda^{-1}(\mathbf{p^s}, \mathbf{q^s})_{\mathbf{0},\Omega_1} = 0,
\end{cases}
$$

for all $(\Phi, \Theta) \in \mathbf{H_0}(\mathbf{curl}, \Omega_1)^4 \times H_0^1(\Omega_1)^4$. Here the active sets for the cosine and the sine components, i.e., $j \in \{c, s\}$, are given by

$$
\mathcal{E}^{j,+} = \{\mathbf{x} \in \Omega_1 : \mathbf{y^j} - \overline{\mathbf{y}}^{\mathbf{j}} > 0\} \quad \text{and} \quad \mathcal{E}^{j,-} = \{\mathbf{x} \in \Omega_1 : \underline{\mathbf{y}}^{\mathbf{j}} - \mathbf{y^j} < 0\}.
$$

The full active sets for $j \in \{c, s\}$ are denoted by $\mathcal{E}^j = \mathcal{E}^{j,+} \cup \mathcal{E}^{j,-}$. Again, we use a common notation and introduce the bilinear form

$$
\begin{aligned}
\mathcal{B}_4(\Upsilon, \Phi) := {} & a_a^4((\mathbf{y^c}, \mathbf{y^s}), (\mathbf{v^c}, \mathbf{v^s})) + a_b((\mathbf{v^c}, \mathbf{v^s}), (\mathbf{p^c}, \mathbf{p^s})) \\
& + a_b((\mathbf{y^c}, \mathbf{y^s}), (\mathbf{q^c}, \mathbf{q^s})) - a_c((\mathbf{p^c}, \mathbf{p^s}), (\mathbf{q^c}, \mathbf{q^s}))
\end{aligned}
$$

with $a_b(\cdot, \cdot)$ and $a_c(\cdot, \cdot)$ defined as in (7.27) and $a_a^4(\cdot, \cdot)$ given by

$$a_a^4((\mathbf{y^c}, \mathbf{y^s}), (\mathbf{v^c}, \mathbf{v^s})) := \sum_{j \in \{c,s\}} (\mathbf{y^j}, \mathbf{v^j})_{\mathbf{0}, \Omega_1} + \frac{1}{\varepsilon}(\mathbf{y^j}, \mathbf{v^j})_{\mathbf{0}, \mathcal{E}^j}.$$

The main result is summarized in the following Lemma, that claims that an inf-sup condition and a sup-sup condition are fulfilled, where the constants are independent of h, N and ω.

Lemma 7.13. *We have*

$$\underline{c_4}\|\Upsilon\|_{\mathcal{C}} \le \sup_{\Phi \ne 0} \frac{\mathcal{B}_4(\Upsilon, \Phi)}{\|\Phi\|_{\mathcal{C}}} \le \overline{c}_4\|\Upsilon\|_{\mathcal{C}},$$

for all $\Upsilon \in \mathbf{H_0}(\mathbf{curl}, \Omega_1)^4$. Here the constants $\underline{c_4}$, $\overline{c}_4$ are independent of h, N, ω, σ, ν, λ and the active sets $\mathcal{E}^c$ and $\mathcal{E}^s$.

Proof. From Lemma 7.3 we obtain that the bilinear form $a(\cdot, \cdot)$ is bounded with constant 1 and satisfies an inf-sup condition on the kernel of $b(\cdot, \cdot)$ with constant $1/\sqrt{3}$. Therefore for $a(\cdot, \cdot)$, the two conditions (2.8) and (2.9) of Theorem 2.4 are fulfilled. Now the proof for $\mathcal{B}_4(\cdot, \cdot)$ immediately follows, since

$$a_a^4((\mathbf{y^c}, \mathbf{y^s}), (\mathbf{v^c}, \mathbf{v^s})) = a_a((\mathbf{y^c}, \mathbf{y^s}), (\mathbf{v^c}, \mathbf{v^s})) + \frac{1}{\varepsilon} \sum_{j \in \{c,s\}} (\mathbf{y^j}, \mathbf{v^j})_{\mathbf{0}, \mathcal{E}^j},$$

and

$$a_a((\mathbf{y^c}, \mathbf{y^s}), (\mathbf{y^c}, \mathbf{y^s})) \le a_a^4((\mathbf{y^c}, \mathbf{y^s}), (\mathbf{y^c}, \mathbf{y^s})) \le (1 + \frac{1}{\varepsilon})a_a((\mathbf{y^c}, \mathbf{y^s}), (\mathbf{y^c}, \mathbf{y^s})).$$

Indeed, since the conditions (2.8) and (2.8) are necessary and sufficient, the desired result follows. □

Due to Lemma 7.13 the preconditioner $\mathcal{C}$, that was derived for *Formulation OC-FEM 1*, can be reused in the setting, where state constraints are added to the Fourier coefficients. Furthermore, we immediately obtain that the condition number of the preconditioned system can be estimated by a constant, i.e.,

$$\kappa_{\mathcal{C}}(\mathcal{C}^{-1}\mathcal{B}_4) := \|\mathcal{C}^{-1}\mathcal{B}_4\|_{\mathcal{C}}\|\mathcal{B}_4^{-1}\mathcal{C}\|_{\mathcal{C}} \le c_4,$$

where the constant c_4 is independent of the mesh size h, the frequency ω, the total number of modes N and the active sets $\mathcal{E}^c$, $\mathcal{E}^s$, as well as the model parameters σ, ν, and the regularization parameter λ.

Remark 7.14. *In principal, for the case of state constraints imposed on the Fourier coefficients, the same analysis relying on* Formulation OC-FEM 2 *can be carried out. Anyhow, in this setting, it turns out, that at least from the theoretical point of view, no Friedrichs' inequality is needed to provide theoretical results yielding a condition number bound, that is uniform in the discretization parameters h, ω and N. Therefore, we rely on* Formulation OC-FEM 1*, cf. Problem 7.1.*

7.3.5   Summary

Lemma 7.10-7.13 are also valid in the corresponding finite element subspace, since the setup and the proofs can be repeated step by step for the finite element functions. Therefore, for the corresponding system matrices $\mathcal{B}_{M,1}$, $\mathcal{B}_{M,2}$, $\mathcal{B}_{M,3}$ and $\mathcal{B}_4$, given by

$$\mathcal{B}_{M,1} = \begin{pmatrix}
\mathbf{K} & \mathbf{0} & \mathbf{K}_{\nu} & -\mathbf{M}_{\sigma,\omega} & \mathbf{0} & \mathbf{0} & \mathbf{D}_{\sigma,\omega}^T & \mathbf{0} \\
\mathbf{0} & \mathbf{K} & \mathbf{M}_{\sigma,\omega} & \mathbf{K}_{\nu} & \mathbf{0} & \mathbf{0} & \mathbf{0} & \mathbf{D}_{\sigma,\omega}^T \\
\mathbf{K}_{\nu} & \mathbf{M}_{\sigma,\omega} & -\lambda^{-1}\mathbf{M} & \mathbf{0} & \mathbf{D}_{\sigma,\omega}^T & \mathbf{0} & \mathbf{0} & \mathbf{0} \\
-\mathbf{M}_{\sigma,\omega} & \mathbf{K}_{\nu} & \mathbf{0} & -\lambda^{-1}\mathbf{M} & \mathbf{0} & \mathbf{D}_{\sigma,\omega}^T & \mathbf{0} & \mathbf{0} \\
\mathbf{0} & \mathbf{0} & \mathbf{D}_{\sigma,\omega} & \mathbf{0} & \mathbf{0} & \mathbf{0} & \mathbf{0} & \mathbf{0} \\
\mathbf{0} & \mathbf{0} & \mathbf{0} & \mathbf{D}_{\sigma,\omega} & \mathbf{0} & \mathbf{0} & \mathbf{0} & \mathbf{0} \\
\mathbf{D}_{\sigma,\omega} & \mathbf{0} & \mathbf{0} & \mathbf{0} & \mathbf{0} & \mathbf{0} & \mathbf{0} & \mathbf{0} \\
\mathbf{0} & \mathbf{D}_{\sigma,\omega} & \mathbf{0} & \mathbf{0} & \mathbf{0} & \mathbf{0} & \mathbf{0} & \mathbf{0}
\end{pmatrix},$$

$$\mathcal{B}_{M,2} = \begin{pmatrix} \mathbf{M_a} & \mathbf{0} & \mathbf{K}_\nu & -\mathbf{M}_{\sigma,\omega} & \mathbf{0} & \mathbf{0} & \mathbf{D}_{\sigma,\omega}{}^T & \mathbf{0} \\ \mathbf{0} & \mathbf{M_a} & \mathbf{M}_{\sigma,\omega} & \mathbf{K}_\nu & \mathbf{0} & \mathbf{0} & \mathbf{0} & \mathbf{D}_{\sigma,\omega}{}^T \\ \mathbf{K}_\nu & \mathbf{M}_{\sigma,\omega} & -\lambda^{-1}\mathbf{M_b} & \mathbf{0} & \mathbf{D}_{\sigma,\omega}{}^T & \mathbf{0} & \mathbf{0} & \mathbf{0} \\ -\mathbf{M}_{\sigma,\omega} & \mathbf{K}_\nu & \mathbf{0} & -\lambda^{-1}\mathbf{M_b} & \mathbf{0} & \mathbf{D}_{\sigma,\omega}{}^T & \mathbf{0} & \mathbf{0} \\ \mathbf{0} & \mathbf{0} & \mathbf{D}_{\sigma,\omega} & \mathbf{0} & \mathbf{0} & \mathbf{0} & \mathbf{0} & \mathbf{0} \\ \mathbf{0} & \mathbf{0} & \mathbf{0} & \mathbf{D}_{\sigma,\omega} & \mathbf{0} & \mathbf{0} & \mathbf{0} & \mathbf{0} \\ \mathbf{D}_{\sigma,\omega} & \mathbf{0} & \mathbf{0} & \mathbf{0} & \mathbf{0} & \mathbf{0} & \mathbf{0} & \mathbf{0} \\ \mathbf{0} & \mathbf{D}_{\sigma,\omega} & \mathbf{0} & \mathbf{0} & \mathbf{0} & \mathbf{0} & \mathbf{0} & \mathbf{0} \end{pmatrix},$$

$$\mathcal{B}_{M,3} = \begin{pmatrix} \mathbf{M} & \mathbf{0} & \mathbf{K}_\nu & -\mathbf{M}_{\sigma,\omega} & \mathbf{0} & \mathbf{0} & \mathbf{D}_{\sigma,\omega}{}^T & \mathbf{0} \\ \mathbf{0} & \mathbf{M} & \mathbf{M}_{\sigma,\omega} & \mathbf{K}_\nu & \mathbf{0} & \mathbf{0} & \mathbf{0} & \mathbf{D}_{\sigma,\omega}{}^T \\ \mathbf{K}_\nu & \mathbf{M}_{\sigma,\omega} & -\lambda^{-1}\mathbf{M}_{\mathcal{E}^c} & \mathbf{0} & \mathbf{D}_{\sigma,\omega}{}^T & \mathbf{0} & \mathbf{0} & \mathbf{0} \\ -\mathbf{M}_{\sigma,\omega} & \mathbf{K}_\nu & \mathbf{0} & -\lambda^{-1}\mathbf{M}_{\mathcal{E}^s} & \mathbf{0} & \mathbf{D}_{\sigma,\omega}{}^T & \mathbf{0} & \mathbf{0} \\ \mathbf{0} & \mathbf{0} & \mathbf{D}_{\sigma,\omega} & \mathbf{0} & \mathbf{0} & \mathbf{0} & \mathbf{0} & \mathbf{0} \\ \mathbf{0} & \mathbf{0} & \mathbf{0} & \mathbf{D}_{\sigma,\omega} & \mathbf{0} & \mathbf{0} & \mathbf{0} & \mathbf{0} \\ \mathbf{D}_{\sigma,\omega} & \mathbf{0} & \mathbf{0} & \mathbf{0} & \mathbf{0} & \mathbf{0} & \mathbf{0} & \mathbf{0} \\ \mathbf{0} & \mathbf{D}_{\sigma,\omega} & \mathbf{0} & \mathbf{0} & \mathbf{0} & \mathbf{0} & \mathbf{0} & \mathbf{0} \end{pmatrix},$$

and

$$\mathcal{B}_4 = \begin{pmatrix} \mathbf{M} + \frac{1}{\varepsilon}\mathbf{M}_{\mathcal{E}^c} & \mathbf{0} & \mathbf{K}_\nu & -\mathbf{M}_{\sigma,\omega} \\ \mathbf{0} & \mathbf{M} + \frac{1}{\varepsilon}\mathbf{M}_{\mathcal{E}^s} & \mathbf{M}_{\sigma,\omega} & \mathbf{K}_\nu \\ \mathbf{K}_\nu & \mathbf{M}_{\sigma,\omega} & -\lambda^{-1}\mathbf{M} & \mathbf{0} \\ -\mathbf{M}_{\sigma,\omega} & \mathbf{K}_\nu & \mathbf{0} & -\lambda^{-1}\mathbf{M} \end{pmatrix},$$

we immediately obtain, that the spectral condition number of the preconditioned systems can be estimated by constants, i.e.,

$$\begin{aligned}
\kappa(\mathcal{P}^{-1}\mathcal{B}_{M,1}) &\leq \bar{c}_1/\underline{c}_1 \neq c_1(h,\omega,N), \\
\kappa(\mathcal{P}^{-1}\mathcal{B}_{M,2}) &\leq \bar{c}_2/\underline{c}_2 \neq c_2(h,\omega,N), \\
\kappa(\mathcal{P}^{-1}\mathcal{B}_{M,3}) &\leq \bar{c}_3/\underline{c}_3 \neq c_3(h,\omega,N,\mathcal{E}^c,\mathcal{E}^s), \\
\kappa(\mathcal{C}^{-1}\mathcal{B}_4) &\leq \bar{c}_4/\underline{c}_4 \neq c_4(h,\omega,N,\nu,\sigma,\lambda,\mathcal{E}^c,\mathcal{E}^s).
\end{aligned} \tag{7.38}$$

Due to the need for the Friedrichs' inequality in the proofs of Lemma 7.10, Lemma 7.11 and Lemma 7.12, we cannot gain a uniform quantitative bound for the condition numbers of the pre-conditioned systems. Typically, the Friedrichs' constant depends on the computational domain Ω_1. Nevertheless, the qualitative estimates provide us the desired robustness properties.

7.3.6 Numerics

This subsection is devoted to the numerical verification of the condition number estimates stated in (7.38). We report on numerical experiments, that were performed for a three-dimensional linear problem on the unit cube $\Omega_1 = (0,1)^3$, discretized by tetrahedra. As in Subsection 7.1.6, we consider the solution of the system corresponding to the block of the mode $k = 1$. We provide the number of MinRes iterations, needed for reducing the initial residual by a factor of 10^{-8} for different problem settings and various parameter constellations.

As exposed in the introduction of Section 7.3, in some constellation it is essential (at least from the theoretical point of view) to work with *Formulation OC-FEM 2* in order to obtain condition number estimates with respect to the preconditioner $\mathcal{C}_M$, that are independent of the frequency ω and the total number of modes N. In order to investigate this claim from the numerical point of view, we also report on results on the basis of *Formulation OC-FEM 1* using the preconditioner $\mathcal{C}$. We will see, that in the latter constellations, robustness with respect to ω is not attained.

7.3.6.1   Different control and observation domains

In this subsection we consider a numerical example with different observation and control domains Ω_a and Ω_b, i.e., $\Omega_a = \Omega_1 = (0,1)^3$ and $\Omega_b = (0.25, 0.75)^3$. Let us mention that we have to ensure, that Ω_a and Ω_b are resolved by the mesh. The corresponding numerical results are documented in Table 7.12-7.16. Robustness with respect to the space and time discretization parameters h and ω is demonstrated in Table 7.12. Table 7.13 describes the behavior with respect to the non-robust parameters λ and ν. Table 7.14 in combination with Table 7.16 indicates, that for *Formulation OC-FEM 1* in combination with the preconditioner $\mathcal{C}$, robustness with respect to the frequency ω, that is related to the time discretization parameters, cannot be obtained. Here, we want to mention, that the good iteration numbers observed in Table 7.14 are caused by the special choice of $\lambda = 1$.

7.3.6.2   Observation of the magnetic flux density B

Numerical results for observation of the magnetic flux density are reported in Table 7.17-7.20. The robustness with respect to the space and time discretization parameters h and ω is demonstrated in Table 7.17. Table 7.18 and Table 7.19 describe the behavior with respect to the non-robust parameters λ and ν. In Table 7.20 we observe that for large mesh sizes, good iteration numbers are observed even for small λ. Nevertheless, for fixed λ, the iteration numbers are growing with respect to the involved degrees of freedom.

The next experiment demonstrates, that robustness with respect to the time discretization parameter ω cannot be achieved by using the $\mathcal{C}$ preconditioner in *Formulation OC-FEM 1*. In Table 7.21 the number of MinRes iteration needed for reducing the initial residual by a factor of 10^{-8} are tabled. In Table 7.22, the same experiment as in Table 7.18 is performed, but using *Formulation OC-FEM 1* instead of *Formulation OC-FEM 2*. Indeed, comparing Table 7.17 with Table 7.21 and Table 7.18 with Table 7.22 clearly shows, that it is essential to work with *Formulation OC-FEM 2*. Beside the robustness with respect to the frequency ω, that is related to the time discretization parameters, we additionally observe better iteration numbers with respect to the regularization parameter λ in the feasible region $\lambda < 1$.

7.3.6.3   State constraints

Numerical results for the case of state constraints imposed on the Fourier coefficients are presented in Table 7.23-7.26. Here we choose 15512 random points as the active sets $\mathcal{E}^c$ and $\mathcal{E}^s$ and solve the resulting Jacobi system with the system matrix $\mathcal{B}_4$. The dependence of the MinRes convergence rate on the Moreau-Yosida regularization parameter ε is demonstrated in Table 7.23 and Table 7.24. Table 7.25 and Table 7.26 clearly demonstrate the robustness with respect to the parameters λ, ω and σ.

Remark 7.15. *As already mentioned in Remark 7.5, a full numerical verification requires computations over the parameter settings $(\omega, \sigma, \nu, \lambda, \varepsilon) \in [10^{-10}, 10^{10}]^5$. Since we only present a selection of these numerical experiments, it may happen that we encounter a two-dimensional hyperplane of $[10^{-10}, 10^{10}]^5$, where robustness qualities of the proposed solvers with respect to certain parameters can be observed, that are not predicted by theory. Let us mention, that from these experiments robustness in the full parameter settings $(\omega, \sigma, \nu, \lambda, \varepsilon)$ cannot be concluded.*

7.4   Various constraints yielding a non-decoupling nature

In this section we discuss the application of the MH-FEM method to problems including end time control. It is clear, that in this setting the advantageous block-diagonal structure is lost. Anyhow, we demonstrate that a generalization of our solver can also be applied in this case.

DOF	ω										
	10^{-10}	10^{-8}	10^{-6}	10^{-4}	10^{-2}	1	10^2	10^4	10^6	10^8	10^{10}
2916	19	19	20	21	23	30	30	22	12	8	8
19652	19	19	20	21	24	30	32	26	12	8	8
143748	19	19	19	21	23	29	32	28	14	10	8

Table 7.12: Different control and observation domains in Formulation OC-FEM 2. Number of MinRes iterations for different values of ω and various DOF using the EXACT version of the preconditioner with UMFPACK for **F** ($\nu = \sigma = \lambda = 1$).

		ν										
		10^{-10}	10^{-8}	10^{-6}	10^{-4}	10^{-2}	1	10^2	10^4	10^6	10^8	10^{10}
	10^{-10}	1038	1006	661	3421	[-]	[-]	[-]	946	49	28	9
	10^{-8}	479	478	497	1091	[-]	[-]	2217	426	37	18	8
	10^{-6}	342	344	363	843	6843	7142	619	256	26	9	8
	10^{-4}	261	261	324	586	4086	769	275	134	39	14	16
	10^{-2}	188	206	209	313	607	204	114	82	79	80	106
λ	1	40	40	41	48	52	30	26	26	26	24	26
	10^2	41	41	42	64	70	40	26	22	22	20	28
	10^4	28	28	30	60	64	34	20	16	22	22	63
	10^6	24	24	30	68	76	38	24	16	26	42	414
	10^8	22	22	30	76	84	42	22	20	28	67	[-]
	10^{10}	22	22	34	88	148	46	44	36	68	276	[-]

Table 7.13: Different control and observation domains in Formulation OC-FEM 2. Number of MinRes iterations for different values of ν and λ using the EXACT version of the preconditioner with UMFPACK for **F** ($DOF = 19652$, $\sigma = \omega = 1$). [-] indicates that MinRes did not converge within 10000 iterations.

DOF	ω										
	10^{-10}	10^{-8}	10^{-6}	10^{-4}	10^{-2}	1	10^2	10^4	10^6	10^8	10^{10}
2416	34	34	67	61	52	30	22	12	6	4	4
16736	32	33	82	67	51	30	22	20	6	4	4
124096	29	31	83	63	48	30	20	22	8	4	4

Table 7.14: Different control and observation domains in Formulation OC-FEM 1. Number of MinRes iterations for different values of ω and various DOF using the EXACT version of the preconditioner with UMFPACK for **F** ($\nu = \sigma = \lambda = 1$). [-] indicates that MinRes did not converge within 10000 iterations.

		ν										
		10^{-10}	10^{-8}	10^{-6}	10^{-4}	10^{-2}	1	10^2	10^4	10^6	10^8	10^{10}
	10^{-10}	34	34	36	66	2701	[-]	983	103	60	47	[-]
	10^{-8}	32	32	34	80	2890	6795	168	67	45	41	[-]
	10^{-6}	31	32	32	87	2630	828	81	46	41	58	73
	10^{-4}	30	30	42	86	1294	139	51	40	38	50	64
	10^{-2}	29	37	37	66	169	61	43	39	37	43	47
λ	1	19	20	22	29	39	30	25	23	22	21	24
	10^2	10	10	11	20	22	13	12	12	11	10	10
	10^4	6	6	8	20	22	10	8	8	8	8	8
	10^6	6	6	6	20	22	10	6	6	6	6	6
	10^8	4	4	6	20	22	10	4	4	4	4	6
	10^{10}	4	4	6	20	22	10	4	4	4	4	6

Table 7.15: Different control and observation domains in Formulation OC-FEM 1. Number of MinRes iterations for different values of ν and λ using the EXACT version of the preconditioner with UMFPACK for **F** ($DOF = 16736$, $\sigma = \omega = 1$). [-] indicates that MinRes did not converge within 10000 iterations.

		ω										
		10^{-10}	10^{-8}	10^{-6}	10^{-4}	10^{-2}	1	10^2	10^4	10^6	10^8	10^{10}
	10^{-10}	9338	9347	9346	9340	[-]	[-]	2630	66	11	6	4
	10^{-8}	4272	4271	4274	4308	8260	6795	1294	29	8	4	4
	10^{-6}	571	571	571	1075	983	828	169	20	6	4	4
	10^{-4}	100	100	103	193	168	139	39	20	6	4	4
	10^{-2}	49	49	122	103	81	61	22	20	6	4	4
λ	1	32	33	82	67	51	30	22	20	6	4	4
	10^2	23	112	60	46	43	13	22	20	6	4	4
	10^4	17	90	45	40	25	10	22	20	6	4	4
	10^6	[-]	46	41	39	12	10	22	20	6	4	4
	10^8	[-]	41	38	23	8	10	22	20	6	4	4
	10^{10}	[-]	58	37	12	6	10	22	20	6	4	4

Table 7.16: Different control and observation domains in Formulation OC-FEM 1. Number of MinRes iterations for different values of ω and λ using the EXACT version of the preconditioner with UMFPACK for $\mathbf{F}$ ($DOF = 16736$, $\sigma = \nu = 1$). [-] indicates that MinRes did not converge within 10000 iterations.

DOF		ω										
		10^{-10}	10^{-8}	10^{-6}	10^{-4}	10^{-2}	1	10^2	10^4	10^6	10^8	10^{10}
500		13	13	14	14	14	16	23	12	9	8	7
2916		11	12	13	13	13	15	29	16	10	8	8
19652		11	11	12	12	12	14	30	21	11	8	8
143748		11	11	12	12	12	14	28	27	13	8	8

Table 7.17: Observation of the magnetic flux density $\mathbf{B}$ in Formulation OC-FEM 2. Number of MinRes iterations for different values of ω and various DOF using the EXACT version of the preconditioner with UMFPACK for $\mathbf{F}$ ($\nu = \sigma = \lambda = 1$).

		ν										
		10^{-10}	10^{-8}	10^{-6}	10^{-4}	10^{-2}	1	10^2	10^4	10^6	10^8	10^{10}
	10^{-10}	174	175	175	176	175	213	290	68	14	10	8
	10^{-8}	155	155	155	154	155	214	257	16	10	6	8
	10^{-6}	146	146	146	146	177	215	58	12	8	6	8
	10^{-4}	147	147	147	176	200	195	13	8	7	7	9
	10^{-2}	272	272	272	289	306	55	13	10	9	10	13
λ	1	290	290	290	292	240	14	8	6	8	10	12
	10^2	475	474	479	448	83	18	12	10	14	14	26
	10^4	757	758	757	703	53	24	14	12	18	20	54
	10^6	193	193	195	179	55	28	18	24	24	26	360
	10^8	57	57	57	61	68	36	20	18	28	64	[-]
	10^{10}	36	38	39	77	84	42	26	36	50	264	[-]

Table 7.18: Observation of the magnetic flux density $\mathbf{B}$ in Formulation OC-FEM 2. Number of MinRes iterations for different values of ν and λ using the EXACT version of the preconditioner with UMFPACK for $\mathbf{F}$ ($DOF = 19652$, $\sigma = \omega = 1$). [-] indicates that MinRes did not converge within 10000 iterations.

		ν										
		10^{-10}	10^{-8}	10^{-6}	10^{-4}	10^{-2}	1	10^{2}	10^{4}	10^{6}	10^{8}	10^{10}
	10^{-10}	325	324	326	326	327	411	505	65	14	10	8
	10^{-8}	289	289	287	289	289	402	352	16	10	6	8
	10^{-6}	289	289	289	289	359	392	53	12	10	6	8
	10^{-4}	292	292	292	348	391	265	15	8	7	9	11
	10^{-2}	543	543	543	561	523	52	13	10	8	11	15
λ	1	543	544	541	564	325	14	8	6	8	10	14
	10^{2}	948	949	941	861	79	18	12	10	14	14	36
	10^{4}	1829	1832	1835	1279	53	24	14	12	18	28	134
	10^{6}	688	688	680	377	55	30	18	22	26	40	[-]
	10^{8}	129	128	192	81	70	36	20	30	42	120	[-]
	10^{10}	56	56	55	91	88	42	26	38	54	[-]	[-]

Table 7.19: Observation of the magnetic flux density **B** in Formulation OC-FEM 2. Number of MinRes iterations for different values of ν and λ using the EXACT version of the preconditioner with UMFPACK for **F** ($DOF = 143748$, $\sigma = \omega = 1$). [-] indicates that MinRes did not converge within 10000 iterations.

DOF	λ										
	10^{-10}	10^{-8}	10^{-6}	10^{-4}	10^{-2}	1	10^{2}	10^{4}	10^{6}	10^{8}	10^{10}
500	36	36	37	39	40	16	19	26	30	36	44
2916	115	113	121	121	55	15	18	24	28	38	44
19652	213	214	215	195	55	14	18	24	28	36	42
143748	411	402	392	265	52	14	18	24	30	36	42

Table 7.20: Observation of the magnetic flux density **B** in Formulation OC-FEM 2. Number of MinRes iterations for different values of λ and various DOF using the EXACT version of the preconditioner with UMFPACK for **F** ($\nu = \sigma = \lambda = 1$).

DOF	ω										
	10^{-10}	10^{-8}	10^{-6}	10^{-4}	10^{-2}	1	10^{2}	10^{4}	10^{6}	10^{8}	10^{10}
392	4133	[-]	46	20	16	15	21	9	5	4	3
2416	[-]	[-]	64	29	15	13	27	12	6	4	4
16736	[-]	[-]	102	28	15	13	26	18	7	4	4
124096	[-]	[-]	28	13	12	26	24	9	5	4	4

Table 7.21: Observation of the magnetic flux density **B** in Formulation OC-FEM 1. Number of MinRes iterations for different values of ω and various DOF using the EXACT version of the preconditioner with UMFPACK for **F** ($\nu = \sigma = \lambda = 1$). [-] indicates that MinRes did not converge within 10000 iterations.

		ν										
		10^{-10}	10^{-8}	10^{-6}	10^{-4}	10^{-2}	1	10^{2}	10^{4}	10^{6}	10^{8}	10^{10}
	10^{-10}	739	901	1073	1140	1462	1153	1548	182	32	19	[-]
	10^{-8}	515	533	534	577	641	918	589	28	16	15	21
	10^{-6}	357	361	357	385	478	607	96	17	10	9	18
	10^{-4}	316	316	233	253	318	272	15	8	9	8	13
	10^{-2}	234	234	234	253	279	50	9	6	7	6	9
λ	1	260	260	260	259	214	13	7	5	6	6	8
	10^{2}	462	462	469	440	76	11	6	4	6	6	7
	10^{4}	524	524	523	489	26	10	6	4	4	4	6
	10^{6}	79	79	79	73	21	10	4	4	4	4	6
	10^{8}	17	17	17	18	22	10	4	4	4	4	6
	10^{10}	10	10	9	19	22	10	4	3	4	4	6

Table 7.22: Observation of the magnetic flux density **B** in Formulation OC-FEM 1. Number of MinRes iterations for different values of ν and λ using the EXACT version of the preconditioner with UMFPACK for **F** ($DOF = 16736$, $\sigma = \omega = 1$). [-] indicates that MinRes did not converge within 10000 iterations.

		ϵ										
		10^{-10}	10^{-8}	10^{-6}	10^{-4}	10^{-2}	1	10^2	10^4	10^6	10^8	10^{10}
	10^{-10}	88	74	59	45	31	17	9	9	9	9	9
	10^{-8}	217	179	142	104	66	29	19	17	17	17	17
	10^{-6}	992	801	612	421	220	36	21	21	21	21	21
	10^{-4}	6184	4874	3558	2131	416	35	22	21	21	21	21
	10^{-2}	[-]	[-]	[-]	3259	351	29	20	20	20	20	20
λ	1	[-]	[-]	[-]	3795	191	24	16	16	14	14	14
	10^2	[-]	[-]	[-]	1619	120	13	12	10	10	10	10
	10^4	[-]	[-]	8588	727	26	10	10	10	10	10	10
	10^6	[-]	[-]	5852	160	12	10	10	10	10	10	10
	10^8	[-]	[-]	924	26	10	10	10	10	10	10	10
	10^{10}	[-]	7681	162	12	10	10	10	10	10	10	10

Table 7.23: State constraints in Formulation OC-FEM 1. Number of MinRes iterations for different values of ε and λ using the EXACT version of the preconditioner with UMFPACK for $\mathbf{F}$ ($DOF = 16736$, $\nu = \sigma = \omega = 1$). [-] indicates that MinRes did not converge within 10000 iterations.

		ϵ										
		10^{-10}	10^{-8}	10^{-6}	10^{-4}	10^{-2}	1	10^2	10^4	10^6	10^8	10^{10}
	10^{-10}	142	118	94	70	46	22	13	13	13	13	13
	10^{-8}	532	434	335	236	137	36	21	21	21	21	21
	10^{-6}	3275	2602	1930	1241	372	35	21	21	21	21	21
	10^{-4}	[-]	[-]	[-]	4360	460	34	21	20	20	20	20
	10^{-2}	[-]	[-]	[-]	5482	383	29	18	18	18	18	18
λ	1	[-]	[-]	[-]	5443	206	24	16	14	13	12	12
	10^2	[-]	[-]	[-]	1836	124	13	12	10	10	10	10
	10^4	[-]	[-]	[-]	830	26	10	10	10	10	10	10
	10^6	[-]	[-]	6619	167	11	10	10	10	10	10	10
	10^8	[-]	[-]	1080	26	10	10	10	10	10	10	10
	10^{10}	[-]	8883	167	11	10	10	10	10	10	10	10

Table 7.24: State constraints in Formulation OC-FEM 1. Number of MinRes iterations for different values of ε and λ using the EXACT version of the preconditioner with UMFPACK for $\mathbf{F}$ ($DOF = 124096$, $\nu = \sigma = \omega = 1$). [-] indicates that MinRes did not converge within 10000 iterations.

		ω										
		10^{-10}	10^{-8}	10^{-6}	10^{-4}	10^{-2}	1	10^2	10^4	10^6	10^8	10^{10}
	10^{-10}	22	22	22	22	22	22	22	22	12	6	4
	10^{-8}	36	36	36	36	36	36	36	27	10	6	4
	10^{-6}	35	35	35	35	35	35	35	22	8	4	4
	10^{-4}	33	33	33	33	33	34	32	22	8	4	4
	10^{-2}	30	30	30	30	30	29	22	22	8	4	4
λ	1	20	20	20	20	20	24	20	22	8	4	4
	10^2	16	16	16	16	18	13	20	22	8	4	4
	10^4	15	15	15	15	21	10	20	22	8	4	4
	10^6	13	13	14	18	12	10	20	22	8	4	4
	10^8	13	13	15	20	8	10	20	22	8	4	4
	10^{10}	13	13	16	12	6	10	20	22	8	4	4

Table 7.25: State constraints in Formulation OC-FEM 1. Number of MinRes iterations for different values of ω and λ using the EXACT version of the preconditioner with UMFPACK for $\mathbf{F}$ ($DOF = 124096$, $\nu = \sigma = \varepsilon = 1$).

		σ_2										
		10^{-10}	10^{-8}	10^{-6}	10^{-4}	10^{-2}	1	10^2	10^4	10^6	10^8	10^{10}
	10^{-10}	17	17	17	17	17	17	17	21	25	16	16
	10^{-8}	29	29	29	29	29	29	29	41	29	29	29
	10^{-6}	36	36	36	36	36	36	37	40	36	36	36
	10^{-4}	35	35	35	35	35	35	42	34	34	34	34
	10^{-2}	30	30	30	30	30	29	34	28	25	25	25
λ	1	33	33	33	33	33	24	23	23	21	21	21
	10^2	28	28	28	28	26	13	20	18	13	13	13
	10^4	18	18	18	18	23	10	20	18	10	10	10
	10^6	17	17	17	19	13	10	20	18	10	10	10
	10^8	17	17	17	21	8	10	20	18	10	10	10
	10^{10}	17	17	18	12	8	10	20	18	10	10	10

Table 7.26: State constraints in Formulation OC-FEM 1. Number of MinRes iterations for different values of σ_2 and λ using the EXACT version of the preconditioner with UMFPACK for $\mathbf{F}$ ($DOF = 16736$, $\nu = \omega = \varepsilon = \sigma_1 = 1$).

		σ_2										
		10^{-10}	10^{-8}	10^{-6}	10^{-4}	10^{-2}	1	10^2	10^4	10^6	10^8	10^{10}
	10^{-10}	22	22	22	22	22	22	22	25	28	22	22
	10^{-8}	36	36	36	36	36	36	36	46	36	36	36
	10^{-6}	35	35	35	35	35	35	36	42	35	35	35
	10^{-4}	35	35	35	35	35	34	42	34	34	34	32
	10^{-2}	30	30	30	30	30	29	33	29	25	25	25
λ	1	33	33	33	33	33	24	23	23	21	21	21
	10^2	28	28	28	28	27	13	20	18	12	12	12
	10^4	18	18	18	18	22	10	18	18	10	10	10
	10^6	17	17	17	19	12	10	18	18	8	8	8
	10^8	17	17	17	21	8	10	18	18	8	8	8
	10^{10}	17	17	18	12	8	10	18	18	8	8	8

Table 7.27: State constraints in Formulation OC-FEM 1. Number of MinRes iterations for different values of σ_2 and λ using the EXACT version of the preconditioner with UMFPACK for $\mathbf{F}$ ($DOF = 124096$, $\nu = \omega = \varepsilon = \sigma_1 = 1$).

7.4.1   End time control

In this section, we additionally want to control the end time of the state $\mathbf{y}$. Consequently, we obtain the following minimization problem: Minimize the functional

$$J(\mathbf{y}, \mathbf{u}) = \frac{1}{2} \int_{\Omega_1 \times (0,T)} |\mathbf{y} - \mathbf{y_d}|^2 \mathrm{d}\mathbf{x} \, \mathrm{dt} + \frac{\alpha}{2} \int_{\Omega_1} |\mathbf{y}(T) - \mathbf{y_T}|^2 \mathrm{d}\mathbf{x} + \frac{\lambda}{2} \int_{\Omega_1 \times (0,T)} |\mathbf{u}|^2 \mathrm{d}\mathbf{x} \, \mathrm{dt}, \qquad (7.39)$$

subject to the state equation

$$\begin{cases} \sigma \dfrac{\partial \mathbf{y}}{\partial t} + \mathbf{curl}(\nu \, \mathbf{curl} \, \mathbf{y}) = \mathbf{u}, & \text{in } \Omega_1 \times (0,T), \\[2mm] \mathbf{y} \times \mathbf{n} = \mathbf{0}, & \text{on } \partial\Omega_1 \times (0,T), \\[2mm] \mathbf{y}(0) = \mathbf{y}(T), & \text{in } \Omega_1. \end{cases} \qquad (7.40)$$

Here the additional weight parameter $\alpha > 0$ and $\mathbf{y_T} \in \mathbf{L_2}(\Omega_1)$ are given data, where $\mathbf{y_T}$ represents the desired state at the end time T. Using the multiharmonic representation of the state $\mathbf{y}$, the desired state $\mathbf{y_d}$ and the control $\mathbf{u}$, we can state the minimization problem in the frequency domain: Minimize the functional

$$J_N(\mathbf{y}, \mathbf{u}) = \sum_{j \in \{c,s\}} \sum_{k=0}^{N} \left[\frac{1}{2} \int_{\Omega_1} |\mathbf{y_k^j} - \mathbf{y_{d,k}^j}|^2 \mathrm{d}\mathbf{x} + \frac{\lambda}{2} \int_{\Omega_1} |\mathbf{u_k^j}|^2 \mathrm{d}\mathbf{x} \right] + \frac{\alpha}{2} \int_{\Omega_1} |\sum_{k=0}^{N} \mathbf{y_k^c} - \mathbf{y_T}|^2 \mathrm{d}\mathbf{x}, \quad (7.41)$$

subject to the state equation

$$\text{for } k = 0, \ldots, N: \begin{cases} k\omega\sigma \, \mathbf{y_k^s} + \mathbf{curl}(\nu \, \mathbf{curl} \, \mathbf{y_k^c}) = \mathbf{u_k^c}, & \text{in } \Omega_1 \times (0,T), \\[2mm] -k\omega\sigma \, \mathbf{y_k^c} + \mathbf{curl}(\nu \, \mathbf{curl} \, \mathbf{y_k^s}) = \mathbf{u_k^s}, & \text{in } \Omega_1 \times (0,T), \\[2mm] \mathbf{y_k^c} \times \mathbf{n} = \mathbf{y_k^s} \times \mathbf{n} = \mathbf{0}, & \text{on } \partial\Omega_1 \times (0,T). \end{cases} \qquad (7.42)$$

The reduced optimality system of (7.41)-(7.42) is given by: For each mode $k = 0, 1, \ldots, N$, find the Fourier coefficients $(\mathbf{y_k^c}, \mathbf{y_k^s}, \mathbf{p_k^c}, \mathbf{p_k^s}) \in \mathbf{H_0}(\mathbf{curl}, \Omega_1)^4$, such that

$$\begin{cases} (1+\alpha)(\mathbf{y_k^c}, \mathbf{v_k^c})_{\mathbf{0},\Omega_1} - \omega(\sigma\mathbf{p_k^s}, \mathbf{v_k^c})_{\mathbf{0},\Omega_1} + (\nu \, \mathbf{curl} \, \mathbf{p_k^c}, \mathbf{curl} \, \mathbf{v_k^c})_{\mathbf{0},\Omega_1} \\[2mm] \qquad\qquad + \alpha \sum_{l \neq k} (\mathbf{y_l^c}, \mathbf{v_k^c})_{\mathbf{0},\Omega_1} = (\mathbf{y_{d,k}^c}, \mathbf{v_k^c})_{\mathbf{0},\Omega_1} + \alpha(\mathbf{y_T}, \mathbf{v_k^c})_{\mathbf{0},\Omega_1}, \\[3mm] (\mathbf{y_k^s}, \mathbf{v_k^s})_{\mathbf{0},\Omega_1} + \omega(\sigma\mathbf{p_k^c}, \mathbf{v_k^s})_{\mathbf{0},\Omega_1} + (\nu \, \mathbf{curl} \, \mathbf{p_k^s}, \mathbf{curl} \, \mathbf{v_k^s})_{\mathbf{0},\Omega_1} = (\mathbf{y_{d,k}^s}, \mathbf{v_k^s})_{\mathbf{0},\Omega_1}, \\[3mm] \omega(\sigma\mathbf{y_k^s}, \mathbf{q_k^c})_{\mathbf{0},\Omega_1} + (\nu \, \mathbf{curl} \, \mathbf{y_k^c}, \mathbf{curl} \, \mathbf{q_k^c})_{\mathbf{0},\Omega_1} - \dfrac{1}{\lambda}(\mathbf{p_k^c}, \mathbf{q_k^c})_{\mathbf{0},\Omega_1} = 0, \\[3mm] -\omega(\sigma\mathbf{y_k^c}, \mathbf{q_k^s})_{\mathbf{0},\Omega_1} + (\nu \, \mathbf{curl} \, \mathbf{y_k^s}, \mathbf{curl} \, \mathbf{q_k^s})_{\mathbf{0},\Omega_1} - \dfrac{1}{\lambda}(\mathbf{p_k^s}, \mathbf{q_k^s})_{\mathbf{0},\Omega_1} = 0, \end{cases}$$

for all test functions $(\mathbf{v_k^c}, \mathbf{v_k^s}, \mathbf{q_k^c}, \mathbf{q_k^s}) \in \mathbf{H_0}(\mathbf{curl}, \Omega_1)^4$. Due to the control of the final time, there is a coupling through the cosine terms $\mathbf{y_k^c}$ of the state. Nevertheless, the resulting system of equations fits into our framework. We end up with the variational formulation: Find $\mathbf{\Upsilon} = (\Upsilon_0, \ldots, \Upsilon_N) \in \mathbf{H_0}(\mathbf{curl}, \Omega_1)^{4N+2}$, such that

$$\mathcal{A}_5(\mathbf{\Upsilon}, \mathbf{\Phi}) = \mathcal{F}_5(\mathbf{\Phi}), \qquad (7.43)$$

for all $\mathbf{\Phi} = (\Phi_0, \ldots, \Phi_N) \in \mathbf{H_0}(\mathbf{curl}, \Omega_1)^{4N+2}$, where the left hand side $\mathcal{A}_5$ is given by

$$\mathcal{A}_5(\mathbf{\Upsilon}, \mathbf{\Phi}) := a(\mathbf{\Upsilon_y}, \mathbf{\Phi_v}) + b(\mathbf{\Phi_v}, \mathbf{\Upsilon_p}) + b(\mathbf{\Upsilon_y}, \mathbf{\Phi_q}) + c(\mathbf{\Upsilon_p}, \mathbf{\Phi_q})$$

with the bilinear forms

$$a(\mathbf{\Upsilon_y}, \mathbf{\Phi_v}) := \sum_{k=0}^{N} (1+\alpha)(\mathbf{y_k^c}, \mathbf{v_k^c})_{\mathbf{0}, \Omega_1} + (\mathbf{y_k^s}, \mathbf{v_k^s})_{\mathbf{0}, \Omega_1} + \alpha \sum_{k \neq l} (\mathbf{y_l^c}, \mathbf{v_k^c})_{\mathbf{0}, \Omega_1},$$

$$c(\mathbf{\Upsilon_p}, \mathbf{\Phi_q}) := \frac{1}{\lambda} \sum_{j \in \{c,s\}} \sum_{k=0}^{N} (\mathbf{p_k^j}, \mathbf{q_k^j})_{\mathbf{0}, \Omega_1},$$

$$b(\mathbf{\Upsilon_y}, \mathbf{\Phi_q}) := \sum_{k=0}^{N} \omega k \left[(\sigma \mathbf{y_k^s}, \mathbf{q_k^c})_{\mathbf{0}, \Omega_1} - (\sigma \mathbf{y_k^c}, \mathbf{q_k^s})_{\mathbf{0}, \Omega_1} \right] + \sum_{j \in \{c,s\}} (\nu \, \mathbf{curl} \, \mathbf{y_k^j}, \mathbf{curl} \, \mathbf{q_k^j})_{\mathbf{0}, \Omega_1}.$$

Therein we used the following notations

$$\mathbf{\Upsilon_y} = (\mathbf{y_0^c}, \mathbf{y_1^c}, \mathbf{y_1^s}, \dots, \mathbf{y_N^c}, \mathbf{y_N^s}) \quad \text{and} \quad \mathbf{\Upsilon_p} = (\mathbf{p_0^c}, \mathbf{p_1^c}, \mathbf{p_1^s}, \dots, \mathbf{p_N^c}, \mathbf{p_N^s}),$$
$$\mathbf{\Phi_v} = (\mathbf{v_0^c}, \mathbf{v_1^c}, \mathbf{v_1^s}, \dots, \mathbf{v_N^c}, \mathbf{u_N^s}) \quad \text{and} \quad \mathbf{\Phi_q} = (\mathbf{q_0^c}, \mathbf{q_1^c}, \mathbf{q_1^s}, \dots, \mathbf{q_N^c}, \mathbf{p_N^s}).$$

The right hand side $\mathcal{F}_5$ is given by

$$\mathcal{F}_5(\mathbf{\Phi}) := \sum_{k=0}^{N} (\mathbf{y_{d,k}^c}, \mathbf{v_k^c})_{\mathbf{0}, \Omega_1} + (\mathbf{y_{d,k}^s}, \mathbf{v_k^s})_{\mathbf{0}, \Omega_1} + \alpha (\mathbf{y_T}, \mathbf{v_k^c})_{\mathbf{0}, \Omega_1}.$$

Furthermore, we introduce a non-standard norm in the product space $\mathbf{H_0}(\mathbf{curl}, \Omega_1)^{4N+2}$. In principal, we reuse the definition of the norm (7.28) for each mode k, but for technical reasons, we define a different splitting by

$$\|\mathbf{\Upsilon}\|_{\mathcal{C}_N}^2 = \|\mathbf{\Upsilon_y}\|_{\mathcal{C}_{N,1}}^2 + \|\mathbf{\Upsilon_p}\|_{\mathcal{C}_{N,2}}^2,$$

where the two components are given by

$$\|\mathbf{\Upsilon_y}\|_{\mathcal{C}_{N,1}}^2 = \sum_{k=0}^{N} \|(\mathbf{y_k^c}, \mathbf{y_k^s})\|_{\mathcal{C}_1}^2 \quad \text{and} \quad \|\mathbf{\Upsilon_p}\|_{\mathcal{C}_{N,2}}^2 = \sum_{k=0}^{N} \|(\mathbf{y_k^c}, \mathbf{y_k^s})\|_{\mathcal{C}_2}^2.$$

Here we use $\|(\cdot, \cdot)\|_{\mathcal{C}_1}$ and $\|(\cdot, \cdot)\|_{\mathcal{C}_2}$ as defined in (7.29) with ω replaced by ωk. The main result is summarized in the following lemma, that claims that an inf-sup condition and a sup-sup condition are fulfilled, where the constants are independent of h, ω, σ, ν and λ.

Lemma 7.16. *We have*

$$\underline{c}_5 \|(\mathbf{\Upsilon})\|_{\mathcal{C}_N} \leq \sup_{\mathbf{\Phi} \neq \mathbf{0}} \frac{\mathcal{A}_5(\mathbf{\Upsilon}, \mathbf{\Phi})}{\|\mathbf{\Phi}\|_{\mathcal{C}_N}} \leq \overline{c}_5 \|\mathbf{\Upsilon}\|_{\mathcal{C}_N}, \tag{7.44}$$

for all $\mathbf{\Upsilon} \in \mathbf{H_0}(\mathbf{curl}, \Omega_1)^{4N+2}$. *Here the constants* $\underline{c}_5$, $\overline{c}_5$ *are independent of* h, ω, ν, σ *and* λ.

Proof. In order to show the inf-sup and the sup-sup condition for $\mathcal{A}_5$, we use Theorem 2.4. By definition of $c(\cdot, \cdot)$, we have

$$c(\mathbf{\Upsilon_p}, \mathbf{\Upsilon_p}) = \frac{1}{\lambda} \sum_{j \in \{c,s\}} \sum_{k=0}^{N} \|\mathbf{p_k^j}\|_{\mathbf{0}, \Omega_1}^2.$$

Furthermore, using Cauchy's inequality and the definition of $\|\cdot\|_{\mathcal{C}_{N,2}}$, we obtain

$$\sup_{\mathbf{\Phi_q} \neq \mathbf{0}} \frac{b(\mathbf{\Upsilon_y}, \mathbf{\Phi_q})}{\|\mathbf{\Phi_q}\|_{\mathcal{C}_{N,2}}} \leq \sqrt{\lambda} \sum_{j \in \{c,s\}} \sum_{k=0}^{N} \omega k (\sigma \mathbf{y_k^j}, \mathbf{y_k^j})_{\mathbf{0}, \Omega_1} + (\nu \, \mathbf{curl} \, \mathbf{y_k^j}, \mathbf{curl} \, \mathbf{y_k^j})_{\mathbf{0}, \Omega_1}.$$

It remains to show the inf-sup condition for $b(\cdot,\cdot)$. Using the idea of Lemma 7.9, we can derive

$$\sup_{\mathbf{\Phi_q}\neq\mathbf{0}}\frac{b(\mathbf{\Upsilon_y},\mathbf{\Phi_q})}{\|\mathbf{\Phi_q}\|_{\mathcal{C}_{N,2}}}\geq\frac{1}{\sqrt{2}}\frac{\sum_{j\in\{c,s\}}\sum_{k=0}^{N}\omega k(\sigma\mathbf{y_k^j},\mathbf{y_p^j})_{\mathbf{0},\Omega_1}+(\nu\,\mathbf{curl\,y_k^j},\mathbf{curl\,y_k^j})_{\mathbf{0},\Omega_1}}{\|\mathbf{\Upsilon_y}\|_{\mathcal{C}_{N,2}}}.$$

Since $b(\cdot,\cdot)$ is skew symmetric, the same estimate can be obtained for the adjoint setting. Finally, it remains to estimate $a(\cdot,\cdot)$. Since we have

$$\sum_{k=0}^{N}\left[\|\mathbf{y_k^c}\|_{\mathbf{0},\Omega_1}^2+\sum_{l\neq k}(\mathbf{y_l^c},\mathbf{y_k^c})_{\mathbf{0},\Omega_1}\right]=\sum_{l,k=0}^{N}(\mathbf{y_l^c},\mathbf{y_k^c})_{\mathbf{0},\Omega_1}=(\sum_{l=0}^{N}\mathbf{y_l^c},\sum_{k=0}^{N}\mathbf{y_k^c})_{\mathbf{0},\Omega_1}\geq0,$$

the lower bound follows. The upper bound can be derived by applying Cauchy's inequality several times:

$$\sum_{j\in\{c,s\}}\sum_{k=0}^{N}\|\mathbf{y_k^j}\|_{\mathbf{0},\Omega_1}^2\leq a(\mathbf{\Upsilon_y},\mathbf{\Upsilon_y})\leq(1+\alpha)N\sum_{j\in\{c,s\}}\sum_{k=0}^{N}\|\mathbf{y_k^j}\|_{\mathbf{0},\Omega_1}^2.$$

Combining the estimates according to Theorem 2.4 yields the desired result.   □

Furthermore, the inequalities (7.44) remain valid for the finite element subspace $\mathcal{ND}_0^0(\mathcal{T}_h)^{4N+2}$, since the proof can be repeated for the finite element functions step by step. Hence, we immediately obtain that the condition number of the preconditioned system can be estimated by a constant, i.e.,

$$\kappa_{\mathcal{C}_N}(\mathcal{C}_N^{-1}\mathcal{A}_5):=\|\mathcal{C}_N^{-1}\mathcal{A}_5\|_{\mathcal{C}_N}\|\mathcal{A}_5^{-1}\mathcal{C}_N\|_{\mathcal{C}_N}\leq c_5,$$

where the constant c_5 is independent of the mesh size h, the frequency ω, the regularization parameter λ and the model parameters ν and σ.

7.5   Summary

In order to keep the presentation clear, we give an overview of the results obtained in this chapter. We established the multiharmonic discretization technique as an adequate tool to discretize time-periodic eddy current optimal control problems in various constrained settings. We explored the decoupling structure of the resulting frequency domain equations and analyzed numerous FEM and FEM-BEM formulations for the continuous and discrete settings. For the unconstrained optimization problems we constructed parameter-robust preconditioned iterative solvers for the discretized optimality system and provided quantitative bounds for the condition numbers, that are independent of the discretization parameters h, ω and N, the model parameters σ and ν and the regularization parameter λ. For the constrained optimization problems, we obtain qualitative bounds for the condition number estimates. In the following table, we summarize the robustness results. Note that the notation (σ) denotes robustness for $\sigma\in\mathbb{R}^+$.

setting							robust parameters	
1) different control and observation domains	h	ω	N	(σ)			$\Omega_a,\,\Omega_b$	
2) desired curl state	h	ω	N	(σ)				
3) desired final state	h	ω		σ	ν	λ		
4) control constraints (Fourier coefficients)	h	ω	N	(σ)			active index sets	
5) state constraints (Fourier coefficients)	h	ω	N	σ	ν	λ	active index sets	
distributed control (model problem)	h	ω	N	σ	ν	λ		

For the problem settings, that obtain a structure, that decouples with respect to the modes $k=0,\ldots,N$, we were able to construct solvers, that are a least robust with respect to the space and time discretization parameters ω, N and h. For the problem settings with non-decoupling structure, the

block-diagonal preconditioning technique does not lead to a solver, that is robust with respect to the time discretization parameter N.

Using the proposed preconditioners, the convergence rate deteriorates with respect to small λ. Furthermore, the dependence on the model parameters σ and ν is also a delicate issue, since in practice these parameters are typically piecewise constant and may have large jumps. Indeed, in the case of simple H^1 parabolic problems, the estimates can be improved, cf. [94]. Another possibility to tackle the robustness with respect to the remaining parameters is to develop all-at-once multigrid methods, cf. [142, 145, 146].

One of the big advantages of our block-diagonal preconditioning technique is, that for the realization of the diagonal blocks, only solvers for *standard* problems, that for example also appear in the magnetostatic case, are needed. Indeed, we are dealing with the following four fundamental kinds of problems:

FEM	$\mathbf{F} = \mathbf{K}_{\boldsymbol{\nu}} + \mathbf{M}_{\boldsymbol{\sigma},\boldsymbol{\omega}} + \frac{1}{\sqrt{\lambda}}\mathbf{M}$	$\mathbf{H}(\mathbf{curl}, \Omega_1)$ inner product
FEM	$\mathbf{D}_{\boldsymbol{\sigma},\boldsymbol{\omega}}{}^T \mathbf{F}^{-1} \mathbf{D}_{\boldsymbol{\sigma},\boldsymbol{\omega}}$	$H_0^1(\Omega_1)$ inner product
BEM	$\mathbf{A}$	$\mathbf{H}_{\parallel}^{-1/2}(\mathrm{div}_\Gamma, \Gamma)$ inner product
FEM-BEM	$\mathbf{F} - \mathbf{N} + \mathbf{B}^T \mathbf{A}^{-1} \mathbf{B}$	$\mathbf{H}(\mathbf{curl}, \Omega_1)$ inner product

The efficient realization of these diagonal blocks is discussed in Chapter 8.

The analysis presented in Section 7.3 and Section 7.4 is limited to the case of uniform positive conductivity. Anyhow, the non-conducting parts can be taken into account either by performing an inexact regularization technique, cf. Section 6.1, or by a symmetrical FEM-BEM coupling method, cf. Section 7.2. Parameter-robust solvers for the resulting FEM-BEM systems can be obtained by combining the analysis of Section 7.2-7.4.

Finally, we briefly summarize the most important benefits of the proposed method:

- The periodic structure of our problem is treated by a natural approach in terms of a Fourier approximation. Therefore, the computations can be done in the frequency domain, where we can benefit from the full decoupling with respect to the individual modes.

- Inequality constraints imposed on the Fourier coefficients preserve the decoupling structure.

- Unbounded domains are treated by means of a FEM-BEM method.

- Parameter-robust solvers for the resulting systems of linear equations in the frequency domain guarantee competitiveness of the proposed method not only in theory but also in practice.

- The proposed solvers are applicable to a full range of practical relevant settings for optimal control problems.

- Due to the decoupling nature of the frequency domain equations with respect to the individual modes, a parallelization of the proposed method is straightforward.

- Since, our proposed solver just relies on solvers or preconditioners for *standard* problems, any further improvements in these solvers or preconditioners will lead to additional improvements in our solver as well.

Chapter 8

Preconditioners for the diagonal blocks

This chapter is devoted to stable and efficient solution strategies for linear systems arising from the space and time discretization technique as presented in the previous chapters. So far we have seen, that the solution procedure can be accelerated in a robust way by using preconditioned iterative methods, whereas the preconditioners obtain block-diagonal structures. Anyhow, the application of the proposed block-diagonal preconditioners involves the solution of systems with certain diagonal blocks. In large-scale computations the exact inversion of these diagonal blocks is still illusive, and therefore these have to be replaced by easy "invertible" symmetric and positive definite preconditioners. Following Subsection 5.2.4, the quality of these new preconditioners, directly enters the condition number estimate of the preconditioned systems. Therefore, the accurate choice of the preconditioners for the diagonal blocks is a delicate issue.

In the following, we list the matrices, that have to be *inverted* in order to apply the theoretical preconditioners. Indeed, the efficient and robust application of the inverse to a given vector is sufficient for the application of the preconditioners.

I	FEM	$\mathbf{K}_{\boldsymbol{\nu}} + \mathbf{M}_{\boldsymbol{\sigma},\boldsymbol{\omega}}$	$\mathbf{H}(\mathbf{curl}, \Omega_1)$ inner product
II	FEM	$\mathbf{K}_{\boldsymbol{\nu}} + \mathbf{M}_{\boldsymbol{\sigma},\boldsymbol{\omega}} + \frac{1}{\sqrt{\lambda}}\mathbf{M}$	$\mathbf{H}(\mathbf{curl}, \Omega_1)$ inner product
III	FEM	$\mathbf{K}_{\boldsymbol{\nu}} + \mathbf{D}_{\boldsymbol{\sigma}}\mathbf{L}_{\boldsymbol{\sigma}}^{-1}\mathbf{D}_{\boldsymbol{\sigma}}^{T}$	$\mathbf{H}(\mathbf{curl}, \Omega_1)$ inner product
IV	FEM	$\mathbf{D}_{\boldsymbol{\sigma},\boldsymbol{\omega}}^{T}(\mathbf{K}_{\boldsymbol{\nu}} + \mathbf{M}_{\boldsymbol{\sigma},\boldsymbol{\omega}} + \frac{1}{\sqrt{\lambda}}\mathbf{M})^{-1}\mathbf{D}_{\boldsymbol{\sigma},\boldsymbol{\omega}}$	$H_0^1(\Omega_1)$ inner product
V	FEM	$\mathbf{L}_{\boldsymbol{\sigma},\boldsymbol{\omega}}$	$H_0^1(\Omega_1)$ inner product
VI	BEM	$\mathbf{A}$	$\mathbf{H}_{\parallel}^{-1/2}(\mathrm{div}_{\Gamma}, \Gamma)$ inner product
VII	FEM-BEM	$\mathbf{K}_{\boldsymbol{\nu}} + \mathbf{M}_{\boldsymbol{\sigma},\boldsymbol{\omega}} - \mathbf{N} + \mathbf{B}^{T}\mathbf{A}^{-1}\mathbf{B}$	$\mathbf{H}(\mathbf{curl}, \Omega_1)$ inner product
VIII	FEM-BEM	$\mathbf{K}_{\boldsymbol{\nu}} + \mathbf{M}_{\boldsymbol{\sigma},\boldsymbol{\omega}} + \frac{1}{\sqrt{\lambda}}\mathbf{M} - \mathbf{N} + \mathbf{B}^{T}\mathbf{A}^{-1}\mathbf{B}$	$\mathbf{H}(\mathbf{curl}, \Omega_1)$ inner product
IX	FEM-BEM	$\mathbf{A} + \mathbf{B}(\mathbf{K}_{\boldsymbol{\nu}} + \mathbf{M}_{\boldsymbol{\sigma},\boldsymbol{\omega}} - \mathbf{N})^{-1}\mathbf{B}^{T}$	$\mathbf{H}_{\parallel}^{-1/2}(\mathrm{div}_{\Gamma}, \Gamma)$ inner product

All these matrices are not severally, but they are related with the underlying Hilbert spaces and therefore correspond to standard problem settings in computational electromagnetics. Therefore, in the remainder of this chapter, we discuss already existing solvers and/or preconditioners for these kinds of systems.

8.1   FEM preconditioners for H^1 and $\mathbf{H}(\mathbf{curl})$

The cases IV and V correspond to system matrices of the bilinear form

$$(\alpha \nabla p, \nabla q)_{\mathbf{0}, \Omega_1} + (\beta p, q)_{0, \Omega_1}, \tag{8.1}$$

with respect to the space $\mathcal{S}^1(\mathcal{T}_h)$. These kinds of problems are well studied in literature. Candidates for (almost) optimal and robust preconditioners can be found among the following list of references (this list is not exhaustive).

Multigrid and multilevel methods	Bramble	[29]
	Vassilevski et al.	[31, 55]
	Hackbusch	[68]
	Henson, Yang	[72][1]
	Kraus et al.	[104, 105, 106]
	Olshanski, Reusken	[125]
	Ruge, Stüben	[138]
Domain decomposition methods	Pechstein	[130, 131]
	Toselli, Widlund	[149]
$\mathcal{H}$-matrices	Hackbusch	[69, 70]

The cases I, II and III correspond to system matrices of the bilinear form

$$(\alpha \, \mathbf{curl}\, \mathbf{u}, \mathbf{curl}\, \mathbf{v})_{\mathbf{0}, \Omega_1} + (\beta \mathbf{u}, \mathbf{v})_{\mathbf{0}, \Omega_1}, \tag{8.2}$$

with respect to the space $\mathcal{ND}^0(\mathcal{T}_h)$. The development of fast solvers for these kinds of problems is a hot topic in actual research. Candidates for (almost) optimal and robust preconditioners are listed in the following table (this list is not exhaustive).

Multigrid methods	Arnold, Falk, Winther	[9]
	Hiptmair	[78]
Algebraic multigrid methods	Bochev et al.	[28]
	Jones, Lee	[90]
	Schöberl, Reitzinger	[136]
Auxiliary space methods	Hiptmair, Xu	[85]
	Kolev, Vassilevksi	[93][2]
	Xu, Zhu	[154]
Domain decomposition methods	Dohrmann, Widlund	[50]
	Hu, Zou	[87, 88]
	Toselli	[147, 148]
	Toselli, Widlund	[149]
$\mathcal{H}$-matrices	Bebendorf, Hiptmair	[21, 127]

Depending on the robustness and optimality qualities of the chosen preconditioner for the diagonal blocks, a robust and optimal solver is obtained.

8.2   BEM preconditioners for $\mathbf{H}(\mathbf{curl})$ and H^1

In contrast to finite element methods, the operators involved in boundary element methods are nonlocal and therefore lead to dense populated matrices. This issue clearly indicates the need for fast implementations of boundary element methods with low memory consumption.

---

[1]Implementation of [138] BoomerAMG in software library *hypre*.
[2]Implementation of [85] AMS (Auxiliary-space Maxwell Solver) in software library *hypre*.

Efficient techniques for the assembling of the system matrices and the evaluation of the matrix-vector products for boundary integral equations are well developed and one could use $\mathcal{H}$-matrices [69, 70], multilevel methods [75, 150], multipole methods [62, 63] or adaptive cross approximation methods [19] to reduce the memory cost and speed up the assembly procedure and the evaluation of the matrix-vector product.

The case VI corresponds to the system matrix of the bilinear form

$$\langle \mathbf{A}\boldsymbol{\lambda}, \boldsymbol{\mu} \rangle_\tau \tag{8.3}$$

with respect to the space $\mathcal{RT}_0^0(\mathcal{K}_h)$. In practice, it is more convenient to use the space $\mathbf{curl}_\Gamma \, \mathcal{S}^1(\mathcal{K}_h)$ and utilize the identity

$$\langle D\,\varphi, \psi \rangle_{1/2} = \langle \mathbf{A}\,\mathbf{curl}_\Gamma \, \varphi, \mathbf{curl}_\Gamma \, \psi \rangle_\tau, \quad \forall \phi, \psi \in \mathcal{S}^1(\mathcal{K}_h), \tag{8.4}$$

where $D : H^{1/2}(\Gamma) \to H^{-1/2}(\Gamma)$ is the hypersingular operator for the Laplacian, cf. [44]. Hence, in order to tackle this problem, any tools from the Galerkin boundary element method for the Laplacian problem can be used.

8.3 Preconditioners for the FEM-BEM Schur complement

In this section we discuss the realization of the diagonal blocks VII-IX, that indeed correspond to FEM-BEM Schur complements of standard $\mathbf{H}(\mathbf{curl})$ problems.

In [57] block-diagonal preconditioners for a FEM-BEM coupled system are proposed, that are based on multigrid solvers for the individual blocks. Indeed, the proposed preconditioners are spectral equivalent to a Schur complement preconditioner, where the spectral constants are independent of the mesh size h. Indeed, this approach leads to an efficient method, but robustness of the proposed method with respect to the involved model parameters is not clear at the first glance.

A block-diagonal preconditioning technique for FEM-BEM systems arising in computational electromagnetics was developed in [116] as a generalization of the method proposed in [57]. Therein the resulting solver is based on domain decomposition methods applied to the FEM-part and the BEM-part separately. It is shown, that the resulting method is efficient in the sense that it only depends on the ratio of the coarse grid mesh size and the overlap. The dependence on the involved model parameters is not addressed. Indeed, these two approaches exactly fit into the framework mentioned in Remark 6.29. Consequently, we can say, that optimal or almost optimal (with respect to the mesh size h) solvers or preconditioners are provided by existing solvers or preconditioners discussed in Section 8.1. Nevertheless, the robustness with respect to the remaining parameters is a delicate issue and calls for a careful study. So far it seems to be essential to work with the full FEM-BEM Schur complements in order to obtain (theoretical) parameter-robust solvers for the MH-FEM-BEM matrices.

8.4 Numerical validation of inexact solvers and preconditioners

In this section we demonstrate, that our proposed block-diagonal preconditioners can efficiently be combined with the preconditioners for the diagonal blocks. In our application we choose the algebraic multigrid solver [138] (BOOMERAMG) and the auxiliary space solver [85] (AMG) for the $H_0^1(\Omega_1)$ and $\mathbf{H_0}(\mathbf{curl}, \Omega_1)$ problems, respectively. For both, we rely on the implementation in the library *hypre*[3]. Indeed, therein the implementation of AMG employs hypre's BOOMERAMG solver. The choice of algebraic multigrid solvers is justified, since those can be applied to systems stemming from the finite element discretization of unstructured meshes, where only fine grid information is employed. This allows a great flexibility in the discretization of the computational domain, since no mesh hierarchies have to be constructed explicitly.

---

[3]`https://computation.llnl.gov/casc/hypre/software.html`

8.4.1 Time-periodic eddy current problems

Formulation FEM 2 For numerical validation of a candidate for a *robust* and *optimal* preconditioner, we consider Problem 6.2. In this setting, we again address the setup used in Subsection 6.1.6. Lemma 6.11 suggests to choose the block-diagonal preconditioning matrix as

$$\mathcal{P} = \text{diag } (\mathbf{M}_{\sigma,\omega} + \mathbf{K}_{\nu}, \mathbf{M}_{\sigma,\omega} + \mathbf{K}_{\nu}) = \text{diag } (\mathbf{P_1}, \mathbf{P_1}).$$

That is, that the preconditioning matrix $\mathbf{M}_{\sigma,\omega} + \mathbf{K}_{\nu}$ is chosen as the finite element discretization of (8.2) with $\alpha = \nu$ and $\beta = \sigma\omega$. According to Subsection 5.2.4 the application of $(\mathbf{M}_{\sigma,\omega} + \mathbf{K}_{\nu})^{-1}$ is replaced by $\tilde{\mathbf{P}}_{\mathbf{1}}^{-1}$, the application of one V-cycle of AMG as implemented in *hypre* with standard parameter settings, cf. [93]. This results in the block-diagonal preconditioning matrix

$$\tilde{\mathcal{P}} = \text{diag } \left(\tilde{\mathbf{P}}_{\mathbf{1}}, \tilde{\mathbf{P}}_{\mathbf{1}}\right).$$

For this example the condition number of the preconditioned diagonal matrix $\tilde{\mathcal{P}}^{-1}\mathcal{P}$ is computed numerically and is listed in the following table. Furthermore, we table the resulting estimate of the condition number of the preconditioned system $\tilde{\mathcal{P}}^{-1}\mathcal{A}_{F2}$ and the resulting upper bound for the number of MinRes iteration for reducing the initial residual by a factor of 10^{-8} for various sizes of the system matrix $\mathcal{A}_{F2}$.

DOF	196	1208	8368	62048	477376	3744128
computed $\kappa(\tilde{\mathcal{P}}^{-1}\mathcal{P})$	1.16	1.37	1.81	2.52	3.87	5.58
bound for $\kappa(\tilde{\mathcal{P}}^{-1}\mathcal{A}_{F2})$	1.64	1.94	2.58	3.56	5.46	7.87
resulting bound for maxiter	28	34	48	68	104	150

In the following numerical experiments, we provide the number of MinRes iterations needed for reducing the initial residual by a factor 10^{-8} for different ω, σ and h. Table 8.1 and Table 8.2 provide experiments for *Formulation FEM 2*. Again, the numerical results show robustness of our preconditioner, since the number of iterations is bounded by the predicted bound derived in the previous table for all computed constellations.

DOF	ω										
	10^{-10}	10^{-8}	10^{-6}	10^{-4}	10^{-2}	1	10^2	10^4	10^6	10^8	10^{10}
196	4	6	8	8	10	13	18	10	8	8	8
1208	30	30	30	30	30	19	22	14	12	12	12
8368	26	26	26	24	26	24	24	20	12	12	12
62048	34	36	38	38	38	42	36	22	12	12	12
477376	46	54	45	52	62	66	53	22	14	12	12
3744128	100	78	78	76	90	96	75	24	18	12	12

Table 8.1: Formulation FEM 2. Number of MinRes iterations for various ω and various DOF using the INEXACT version of the preconditioner with one V-cycle of AMG for $\mathbf{P_1}$ ($\nu = 1$, $\sigma = 1$).

DOF	σ_2										
	10^{-10}	10^{-8}	10^{-6}	10^{-4}	10^{-2}	1	10^2	10^4	10^6	10^8	10^{10}
196	12	12	12	12	12	13	20	12	11	11	11
1208	8	10	10	12	14	19	22	19	20	20	20
8368	22	22	24	22	26	24	28	28	28	36	27
62048	32	32	34	36	40	42	47	46	46	44	44
477376	42	48	46	54	62	66	70	69	64	62	64
3744128	78	70	78	78	92	96	100	100	92	90	90

Table 8.2: Formulation FEM 2. Number of MinRes iterations for various σ_2 and various DOF using the INEXACT version of the preconditioner with one V-cycle of AMG for $\mathbf{P_1}$ ($\nu = 1$, $\sigma_1 = 1$, $\omega = 1$).

Formulation FEM 4 For numerical validation of a candidate for a *robust* and *optimal* preconditioner, we consider Problem 6.4. In this setting, we again address the setup used in Subsection 6.1.6. Lemma 6.13 suggests to choose the block-diagonal preconditioning matrix as

$$\mathcal{P}_M = \mathrm{diag}\ (\mathbf{M}_{\sigma,\omega} + \mathbf{K}_\nu, \mathbf{M}_{\sigma,\omega} + \mathbf{K}_\nu, \mathbf{L}_{\sigma,\omega}, \mathbf{L}_{\sigma,\omega}) = \mathrm{diag}\ (\mathbf{P_1}, \mathbf{P_1}, \mathbf{P_2}, \mathbf{P_2}).$$

That is, that the first preconditioning matrix $\mathbf{M}_{\sigma,\omega} + \mathbf{K}_\nu$ is chosen as the finite element discretization of (8.2) with $\alpha = \nu$ and $\beta = \sigma\omega$, and the second preconditioning matrix $\mathbf{L}_{\sigma,\omega}$ is chosen as the finite element discretization of (8.1) with $\alpha = \sigma\omega$ and $\beta = 0$. According to Subsection 5.2.4 the application of $(\mathbf{M}_{\sigma,\omega} + \mathbf{K}_\nu)^{-1}$ is replaced by $\tilde{\mathbf{P}}_1^{-1}$, the application of one V-cycle of AMG as implemented in *hypre* with standard parameter settings, cf. [93], and the application of $\mathbf{L}_{\sigma,\omega}^{-1}$ is replaced by $\tilde{\mathbf{P}}_2^{-1}$, the application of one V-cycle of BOOMERAMG as implemented in *hypre* with standard parameter settings, cf. [72]. This results in the block-diagonal preconditioning matrix

$$\tilde{\mathcal{P}}_M = \mathrm{diag}\ \left(\tilde{\mathbf{P}}_1, \tilde{\mathbf{P}}_1, \tilde{\mathbf{P}}_2, \tilde{\mathbf{P}}_2\right).$$

For this example the condition number of the preconditioned diagonal matrix $\tilde{\mathcal{P}}_M^{-1}\mathcal{P}_M$ is computed numerically and is listed in the following table. Furthermore, we table the resulting estimate of the condition number of the preconditioned system $\tilde{\mathcal{P}}_M^{-1}\mathcal{A}_{M2}$ and the resulting upper bound for the number of MinRes iteration for reducing the initial residual by a factor of 10^{-8} for various sizes of the system matrix $\mathcal{A}_{M2}$.

DOF	250	1458	9826	71874	549250	4293378
computed $\kappa(\tilde{\mathcal{P}}_M^{-1}\mathcal{P}_M)$	1.06	1.22	1.43	2.22	3.37	4.84
bound for $\kappa(\tilde{\mathcal{P}}_M^{-1}\mathcal{A}_{M2})$	3.01	3.45	4.04	6.28	9.52	13.68
resulting bound for maxiter	56	66	76	120	182	262

In the following numerical experiments, we provide the number of MinRes iterations needed for reducing the initial residual by a factor 10^{-8} for different ω, σ and h. Table 8.3 and Table 8.4 provide experiments for *Formulation FEM 4*. Again, the numerical results show robustness of our preconditioner, since the number of iterations is bounded by the predicted bound derived in the previous table for all computed constellations.

DOF	ω										
	10^{-10}	10^{-8}	10^{-6}	10^{-4}	10^{-2}	1	10^2	10^4	10^6	10^8	10^{10}
250	12	12	10	14	18	22	22	16	15	16	16
1458	28	28	31	32	34	32	32	25	25	25	25
9826	45	45	43	45	47	48	37	31	29	29	29
71874	61	61	64	65	67	74	55	37	33	33	33
549250	79	89	80	91	103	113	83	41	41	39	39
4293378	139	119	127	128	145	161	123	50	49	47	47

Table 8.3: Formulation FEM 4. Number of MinRes iterations for various ω and various DOF using the INEXACT version of the preconditioner with one V-cycle of AMG for $\mathbf{P_1}$ and one V-cycle of BOOMERAMG for $\mathbf{P_2}$ ($\nu = 1$, $\sigma = 1$).

8.4.2 Time-periodic eddy current optimal control problems

Formulation OC-FEM 1 In Table 8.5-8.7 we provide iteration numbers and CPU times for a time-harmonic eddy current optimal control problem with a typical parameter setting for λ and ω. Therein we present three different kinds for the realization of the block-diagonal preconditioner:

1. Realization of the diagonal blocks using the exact solver UMFPACK.

2. Realization of the diagonal blocks using the CG method preconditioned by one V-cycle of AMG. Therein the CG solves up to a relative tolerance of 10^{-8}. We mention, that here we are using a nonlinear preconditioner.

DOF	σ_2										
	10^{-10}	10^{-8}	10^{-6}	10^{-4}	10^{-2}	1	10^2	10^4	10^6	10^8	10^{10}
250	23	23	23	23	23	22	26	19	18	18	18
1458	22	24	25	28	30	32	36	32	32	32	32
9826	36	34	43	40	50	48	46	49	47	58	48
71874	55	53	57	62	67	74	78	74	73	71	73
549250	73	79	79	91	103	113	117	113	103	103	105
4293378	119	113	123	129	147	161	167	163	149	149	149

Table 8.4: Formulation FEM 4. Number of MinRes iterations for various σ_2 and various DOF using the INEXACT version of the preconditioner with one V-cycle of AMG for $\mathbf{P_1}$ and one V-cycle of BOOMERAMG for $\mathbf{P_2}$ ($\nu = 1$, $\sigma_1 = 1$, $\omega = 1$).

3. Realization of the diagonal blocks using one V-cycle of AMG.

In all the three considered settings, we clearly see the optimality of the solver, since the CPU times only grow linearly with respect to the involved degrees of freedom. We also observe, that variant 3 is almost as fast as variant 1, but due to the *cheap* preconditioner also higher numbers of degrees of freedom can be treated efficiently. Furthermore, from Table 8.6 it turns out that a CG acceleration for the diagonal blocks does not pay off in the total CPU time (even if the CG tolerance is reduced). Anyhow, in the case of strongly varying piecewise constant coefficients σ and ν, the CG acceleration might help, since the AMG may not be able to efficiently treat these strong discontinuities. Another thing that catches our eyes are the slightly growing iteration numbers in Table 8.7. In light of the theory presented in Subsection 5.2.4, the growing iteration numbers in Table 8.7 are certainly below the bound $\sqrt{3}\kappa(\tilde{\mathcal{C}}^{-1}\mathcal{C})$ and therefore perfectly fit into the developed framework.

DOF	iter	CPU time
392	14	0.04s
2416	22	0.36s
16736	22	3.04s
124096	20	27.95s
954752	[-]	[-]
7488256	[-]	[-]

Table 8.5: Formulation OC-FEM 1. Number of MinRes iterations for $\omega = 1000$, $\lambda = 10^{-3}$ and various DOF using the EXACT version of the preconditioner with UMFPACK for $\mathbf{F}$, cf. (7.16) ($\nu = \sigma = 1$). [-] indicates that UMFPACK ran out of memory.

DOF	iter	CPU time
392	14	0.06s
2416	22	0.69s
16736	22	5.54s
124096	20	44.38s
954752	22	441.61s
7488256	22	4344.16s

Table 8.6: Formulation OC-FEM 1. Number of MinRes iterations for $\omega = 1000$, $\lambda = 10^{-3}$ and various DOF using the INEXACT version of the preconditioner with CG preconditioned by one V-cycle of AMG for $\mathbf{F}$ ($\nu = \sigma = 1$).

DOF	iter	$\kappa(\tilde{\mathcal{C}}^{-1}\mathcal{C})$	CPU time
392	15	1.01	0.04s
2416	23	1.03	0.38s
16736	27	1.09	3.22s
124096	33	1.22	30.94s
954752	39	2.51	289.11s
7488256	62	8.05	3663.97s

Table 8.7: Formulation OC-FEM 1. Number of MinRes iterations for $\omega = 1000$, $\lambda = 10^{-3}$ and various DOF using the INEXACT version of the preconditioner with one V-cycle of AMG for $\mathbf{F}$ ($\nu = \sigma = 1$).

Chapter 9

Software development and numerical experiments

9.1 Software development

For our numerical experiments we used the framework ParMax[1]. ParMax is a C++ research code developed at the Institute of Computational Mathematics at the Johannes Kepler University Linz in the research project *"Data-sparse Boundary and Finite Element Domain Decomposition Methods in Electromagnetics"* (FWF-Project P19255) under the main developer Dr. Clemens Pechstein. Indeed, ParMax provides a unified framework for developing finite element research codes and has successfully been used for a wide range of FEM, FETI, BEM-based-FEM or optimal control applications in computational electromagnetics, elasticity or biomechanical applications.

In order to capture the theory developed in this thesis and perform numerical tests, we were required to extend ParMax to master the following main tasks:

1. Implementation of $\mathbf{H}(\mathbf{curl})$ conforming finite elements in 3D, i.e., Nédélec elements of lowest order.

2. Implementation of assembling procedure for the MH-FEM block matrices.

3. Implementation of solution algorithms including Krylov subspace methods and block-diagonal preconditioners.

4. Implementation of solution or preconditioning algorithms for the diagonal blocks.

5. Visualization of the solution.

While tasks 1-3 were directly incorporated into the ParMax framework, for the last two tasks, we relied on external libraries. Indeed, for task 4, i.e., for the solution or preconditioning of the diagonal blocks, we used two fundamentally different kinds of approaches:

Sparse direct solvers: In order to verify the condition number bounds for the theoretical robust block-diagonal preconditioners, the diagonal blocks were realized exactly by using sparse direct solvers. Of course, the development of direct solvers for three dimensional problems are a delicate issue. Therefore, our software relies on already existing software packages and an interface to PARDISO[2] and UMFPACK[3] was implemented.[4]

---

[1] http://www.numa.uni-linz.ac.at/P19255/software.shtml

[2] http://www.pardiso-project.org/

[3] http://www.cise.ufl.edu/research/sparse/umfpack/

[4] Unfortunately, during this work the developers of PARDISO changed their licensing policy to restricting the free-academic access. Therefore, we decided to change to the free package UMFPACK.

Iterative solvers: In practical applications, especially in large scale applications, direct solvers are illusive. Hence, iterative solution or preconditioning algorithms have to be taken into account. Indeed, there exists a full range of candidates for preconditioners for the diagonal blocks, cf. Chapter 8. Our choice fell on the family of algebraic multigrid methods, since they can be applied directly to the system matrices with hardly any additional informations about the underlying partial differential equations, the discretization or mesh hierarchies. Therefore, an interface to *hypre*[5] was implemented, where especially for $\mathbf{H}(\mathbf{curl})$ problems we used AMG and for the H^1 problems we used BOOMERAMG, cf. Section 8.4.

Combining the individual software fragments leads to a robust and optimal (or at least almost optimal) solver for MH-FEM discretized time-periodic eddy current problems and eddy current optimal control problems. Furthermore, for task 5, i.e., the visualization of the solution, we relied on the open-source data analysis and visualization application ParaView[6].

Additionally, we mention, that all the experiments described in Chapter 6-9 were performed on a PC with Intel(R) Core(TM) i7-2600 CPU @3.40GHz.

9.2 Numerical experiments including visualization of the solution

In order to validate the proposed solving algorithms and their implementation, we use a series of problems for both, the eddy current problem and the eddy current optimal control problem. Therein we put the main emphasis on eddy current optimal control computations. Throughout this section, we restrict the computational domain to be given by the unit cube $\Omega_1 = (0,1)^3$ and solve for the fixed time-period $(0,1)$. For the discretization of Ω_1 we use tetrahedral elements whereas the corresponding finite element space has $DOF = 238688$ degrees of freedom. Therefore, the resulting systems of equations have size $(2N+1)DOF$ or $(4N+2)DOF$ for eddy current problems or eddy current optimal control problems, respectively. In all the considered constellations, the systems of linear equations are solved up to a relative accuracy of 10^{-8}.

9.2.1 Eddy current problems

For the eddy current problem, we consider a test example with known analytic solution in order to demonstrate, that our algorithm converges to the correct solution. Let us consider the following time-periodic test problem:

$$\begin{cases} \dfrac{\partial \mathbf{y}}{\partial t} + \mathbf{curl}(\mathbf{curl}\,\mathbf{y}) = \mathbf{u}, & \text{in } \Omega_1 \times (0,1), \\[2mm] \mathbf{y} \times \mathbf{n} = \mathbf{0}, & \text{on } \partial\Omega_1 \times (0,1) \\[2mm] \mathbf{y}(0) = \mathbf{y}(T), & \text{on } \Omega_1. \end{cases} \tag{9.1}$$

Here $\mathbf{u} \in L_2((0,1), \mathbf{L_2}(\Omega_1))$ is given by the time-harmonic excitation

$$\mathbf{u}((x,y,z),t) = 800\pi^2 \begin{pmatrix} \sin(2\pi y)\sin(2\pi z) \\ \sin(2\pi x)\sin(2\pi z) \\ \sin(2\pi x)\sin(2\pi y) \end{pmatrix} \cos(t) - 100 \begin{pmatrix} \sin(2\pi y)\sin(2\pi z) \\ \sin(2\pi x)\sin(2\pi z) \\ \sin(2\pi x)\sin(2\pi y) \end{pmatrix} \sin(t),$$

satisfying $\mathrm{div}(\mathbf{u}) = 0$. The exact unique solution of the test problem (9.1) is given by

$$\mathbf{y}((x,y,z),t) = 100 \begin{pmatrix} \sin(2\pi y)\sin(2\pi z) \\ \sin(2\pi x)\sin(2\pi z) \\ \sin(2\pi x)\sin(2\pi y) \end{pmatrix} \cos(t),$$

---

[5]`https://computation.llnl.gov/casc/hypre/software.html`
[6]`http://www.paraview.org/`

and obviously fulfills $\text{div}(\mathbf{y}) = 0$. W mention, that due to the specific design of the test example, we have $\mathbf{y}((x,y,z),0) = 8\pi^2\mathbf{u}((x,y,z),0)$. The numerical solution, computed by using our MH-FEM MinRes solver, can be seen in Figure 9.1 and Figure 9.2. Due to the knowledge of the exact solution $\mathbf{y}$, it is easy to see, that we have computed a correct approximation.

(a) Norm of the vector field $\mathbf{y}(\cdot, 0)$. (b) Vector field $\mathbf{y}(\cdot, 0)$.
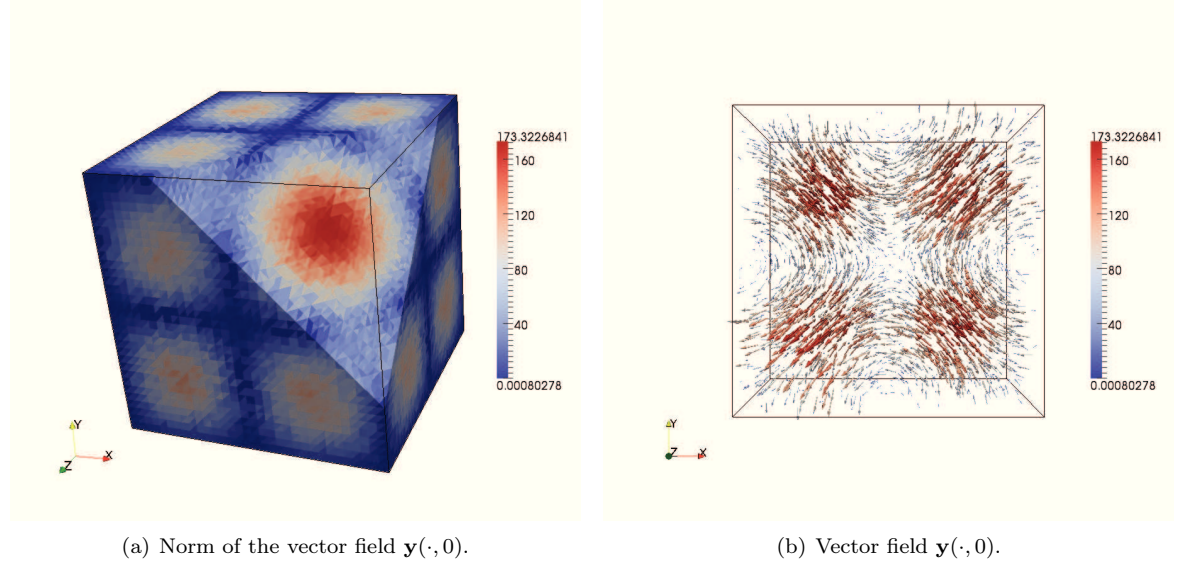
Figure 9.1: 3D-visualization of the solution $\mathbf{y}$ at $t = 0$.

9.2.2 Eddy current optimal control problems

This subsection is devoted to the numerical validation of the algorithms developed for the eddy current optimal control problem. Therefore, we consider the following test problem: Minimize the functional

$$\mathcal{J}(\mathbf{y}, \mathbf{u}) = \frac{1}{2} \int_{\Omega_1 \times (0,1)} |\mathbf{y} - \mathbf{y_d}|^2 \mathrm{d}\mathbf{x}\,\mathrm{d}t + \frac{\lambda}{2} \int_{\Omega_1 \times (0,1)} |\mathbf{u}|^2 \mathrm{d}\mathbf{x}\,\mathrm{d}t. \tag{9.2}$$

subject to the state equation (9.1) for a prescribed desired state $\mathbf{y_d} \in L_2((0,T), \mathbf{L_2}(\Omega_1))$. In particular we present three examples, whereas the desired state $\mathbf{y_d}$ is

1. analytic in time,

2. non-differentiable in time,

3. a characteristic function in time.

For all these settings, we derive a time-periodic solution using the MH-FEM MinRes solver and demonstrate the convergence with respect to the discretization parameters.
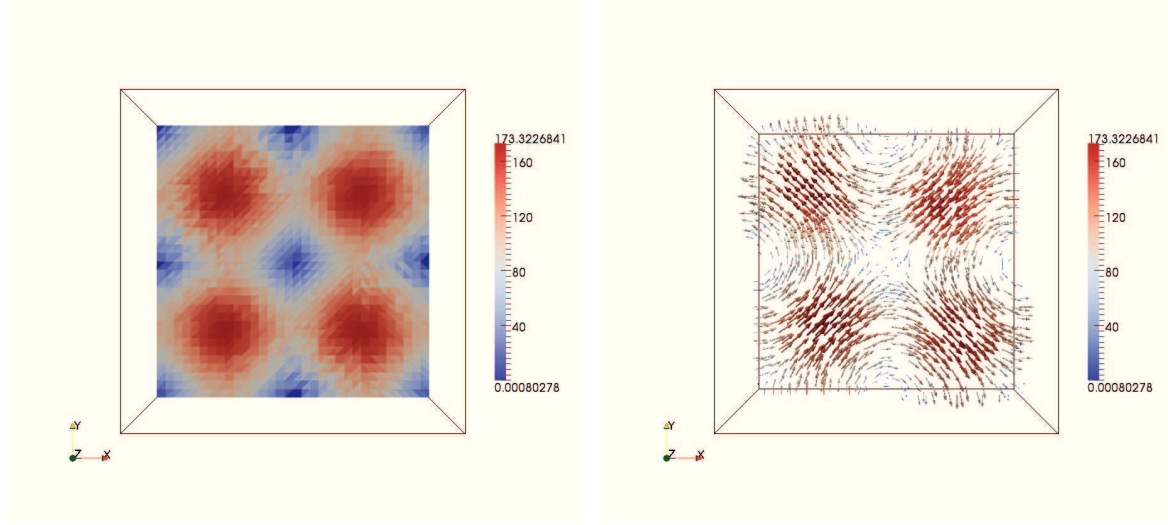
(a) Norm of the vector field $\mathbf{y}((\cdot, \cdot, 0.25), 0)$.   (b) Vector field $\mathbf{y}((\cdot, \cdot, 0.25), 0)$.

Figure 9.2: 2D-visualization of the solution $\mathbf{y}$ at $t = 0$ and $z = 0.25$.

Example 1

We start by considering the time-harmonic desired state

$$
\mathbf{y_d}((x, y, z), t) = \begin{cases} \begin{pmatrix} 100 \\ 0 \\ 0 \end{pmatrix} \cos(t), & \text{in } \left(\tfrac{1}{4}, \tfrac{3}{4}\right)^3 \times (0, 1), \\[2ex] \begin{pmatrix} 0 \\ 0 \\ 0 \end{pmatrix}, & \text{else,} \end{cases}
$$

that is obviously analytic in time. We mention, that here we are dealing with a desired state, that is not weakly divergence-free. The numerical solution, computed by using our MH-FEM MinRes solver, can be seen in Figure 9.3-9.6. While in Figure 9.3 and Figure 9.4 we use the regularization parameter $\lambda = 10^{-4}$, in Figure 9.5 and Figure 9.6 the choice $\lambda = 10^{-8}$ is used. Therein the colored contour visualizes the norm of the state $\mathbf{y}$ and the control $\mathbf{u}$, respectively. We observe, that for the choice $\lambda = 10^{-8}$ the state $\mathbf{y}$ is a better approximation to the desired state $\mathbf{y_d}$, than for the choice $\lambda = 10^{-4}$.

Furthermore we mention, that $\mathbf{y_d} \notin L_2((0, T), \mathbf{H_0}(\mathbf{curl}, \Omega_1)$ since there is no tangential continuity over the boundary of the interior cube $(1/4, 3/4)^3$. Therefore, the desired state is not reachable. Indeed, in the visualization of the computed state $\mathbf{y}$ this issue can be observed by the frayed contour at the boundary of $(1/4, 3/4)^3$. Furthermore we mention, that the tangential continuity of the desired state $\mathbf{y_d}$ in the x-direction is recovered by the computed state $\mathbf{y}$.

For completeness, we mention, that due to the exact representation of the desired state as a Fourier series ($N = 1$), there is no discretization error in time.

(a) State $\mathbf{y}((\cdot, \cdot, 0.5), 0)$.
(b) Control $\mathbf{u}((\cdot, \cdot, 0.5), 0)$.

Figure 9.3: Example 1: 2D-visualization of the state $\mathbf{y}$ and the control $\mathbf{u}$ at $t = 0$ and $z = 0.5$ ($\lambda = 10^{-4}$).

Example 2

As a second example we consider a continuous, but non-differentiable desired state $\mathbf{y_d}$, given by

$$\mathbf{y_d}((x,y,z),t) = \begin{cases} \begin{pmatrix} 100 \\ 0 \\ 0 \end{pmatrix} (1 - |t - 0.5|) & \text{in } \left(\frac{1}{4}, \frac{3}{4}\right)^3 \times (0,1), \\ \begin{pmatrix} 0 \\ 0 \\ 0 \end{pmatrix}, & \text{else.} \end{cases}$$

Since $\mathbf{y_d}$ has no multiharmonic representation, we use an approximation of $\mathbf{y_d}$ in terms of a truncated Fourier series $\mathbf{y_{d,N}}$ with frequency $\omega = 2\pi$ and N modes, i.e.,

$$\mathbf{y_{d,N}}((x,y,z),t) = \begin{cases} \begin{pmatrix} 100 \\ 0 \\ 0 \end{pmatrix} \left(\frac{3}{4} - \frac{2}{\pi^2} \sum_{k=1}^{N} \frac{\text{sign}(k(\text{mod } 2))}{k^2} \cos(2\pi k t)\right) & \text{in } \left(\frac{1}{4}, \frac{3}{4}\right)^3 \times (0,1), \\ \begin{pmatrix} 0 \\ 0 \\ 0 \end{pmatrix}, & \text{else.} \end{cases}$$

The numerical solution of the state $\mathbf{y}$ and the corresponding control $\mathbf{u}$, computed by using our MH-FEM MinRes solver with $N = 5$ modes, can be seen in Figure 9.7 and Figure 9.8. We clearly observe the linear increase/decrease of the magnitude of the state $\mathbf{y}$ with respect to the time t. The approximation due to the truncation of the Fourier series is displayed in Figure 9.9. By taking into account only a few modes ($N < 10$), we already observe a good approximation of the desired state.

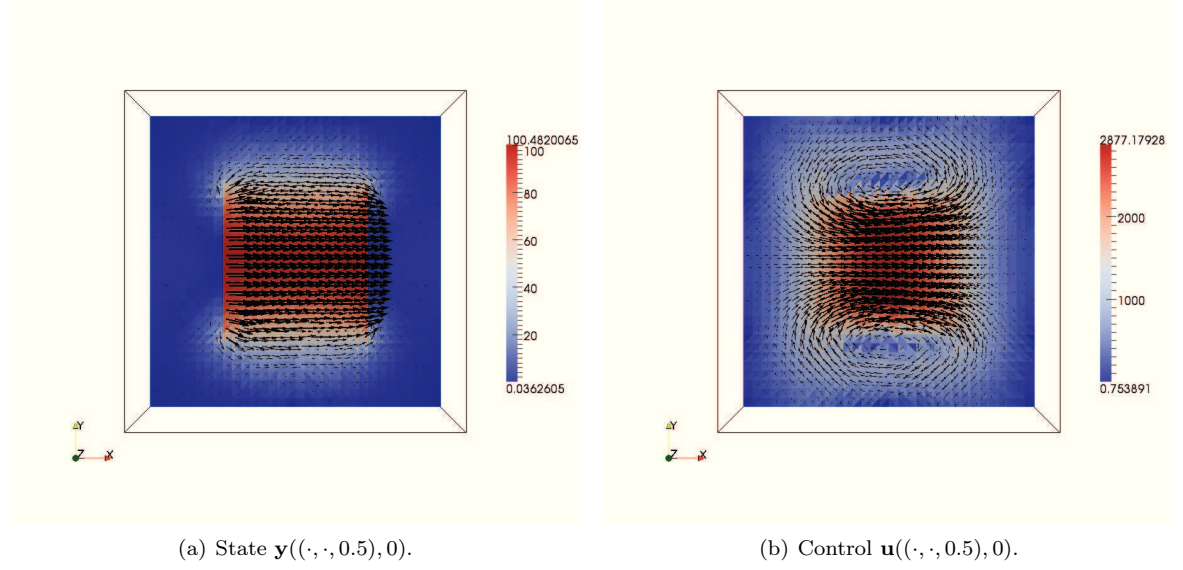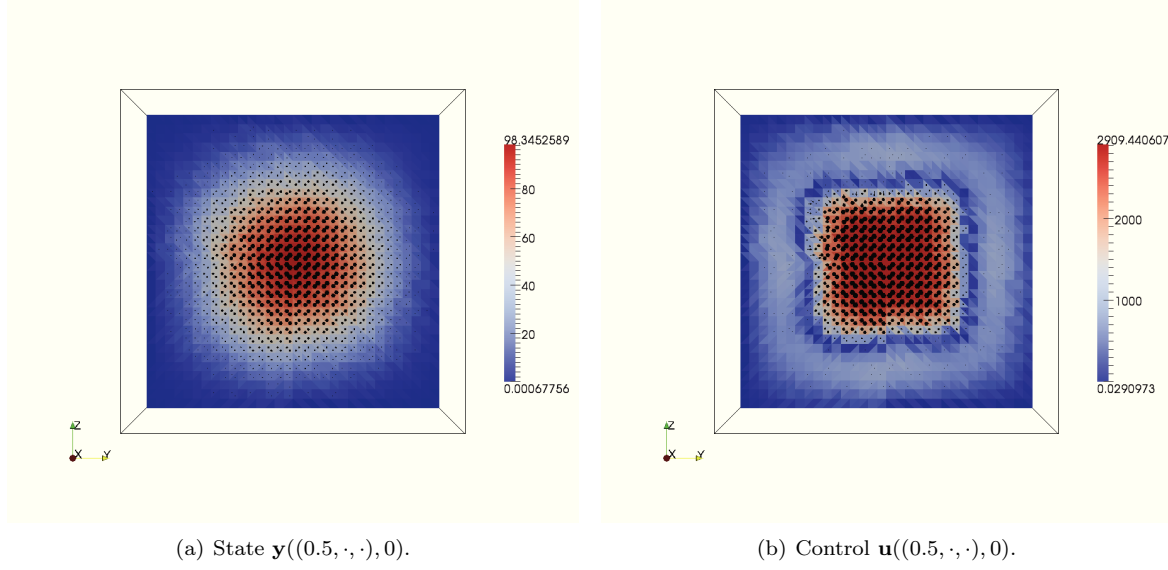(a) State $\mathbf{y}((0.5, \cdot, \cdot), 0)$.   (b) Control $\mathbf{u}((0.5, \cdot, \cdot), 0)$.

Figure 9.4: Example 1: 2D-visualization of the state $\mathbf{y}$ and the control $\mathbf{u}$ at $t = 0$ and $x = 0.5$ ($\lambda = 10^{-4}$).

Example 3

Finally, we consider a non-continuous desired state, given by

$$
\mathbf{y_d}((x, y, z), t) = \begin{cases} \begin{pmatrix} 100 \\ 0 \\ 0 \end{pmatrix} & \text{in } \left(\frac{1}{4}, \frac{3}{4}\right)^3 \times (1/3, 2/3), \\ \begin{pmatrix} 0 \\ 0 \\ 0 \end{pmatrix} & \text{else.} \end{cases}
$$

Again, we use an approximation of $\mathbf{y_d}$ in terms of the truncated Fourier series $\mathbf{y_{d,N}}$ with frequency $\omega = 2\pi$ and N modes, i.e.,

$$
\mathbf{y_{d,N}}((x, y, z), t) = \begin{cases} \begin{pmatrix} 100 \\ 0 \\ 0 \end{pmatrix} \left(\frac{1}{3} + \frac{\sqrt{3}}{\pi} \sum_{k=1}^{N} (-1)^{k(\text{mod }3)} \frac{\text{sign}(k(\text{mod }3))}{k} \cos(2\pi k t) \right) & \text{in } \left(\frac{1}{4}, \frac{3}{4}\right)^3 \times (0, 1), \\ \begin{pmatrix} 0 \\ 0 \\ 0 \end{pmatrix} & \text{else.} \end{cases}
$$

The numerical solution, computed by using our MH-FEM MinRes solver with $N = 50$ modes, can be seen in Figure 9.10 and Figure 9.11. The approximation due to the truncation of the Fourier series is displayed in Figure 9.12. Furthermore, we also observe the well known Gibbs phenomenon, in terms of oscillations near the jump at $t = 1/3$ and $t = 2/3$. In contrast to the previous example, we require a higher number of modes N (in our numerical example $N = 50$) in order to obtain an accurate approximation in time. Again, we want to point out, that the computations corresponding to the individual modes can be done total in parallel. Therefore, on a machine with $N \geq 50$ cores, all the computations with respect to the individual modes can be done total in parallel; i.e., on such

(a) State $\mathbf{y}((\cdot, \cdot, 0.5), 0)$.
(b) Control $\mathbf{u}((\cdot, \cdot, 0.5), 0)$.
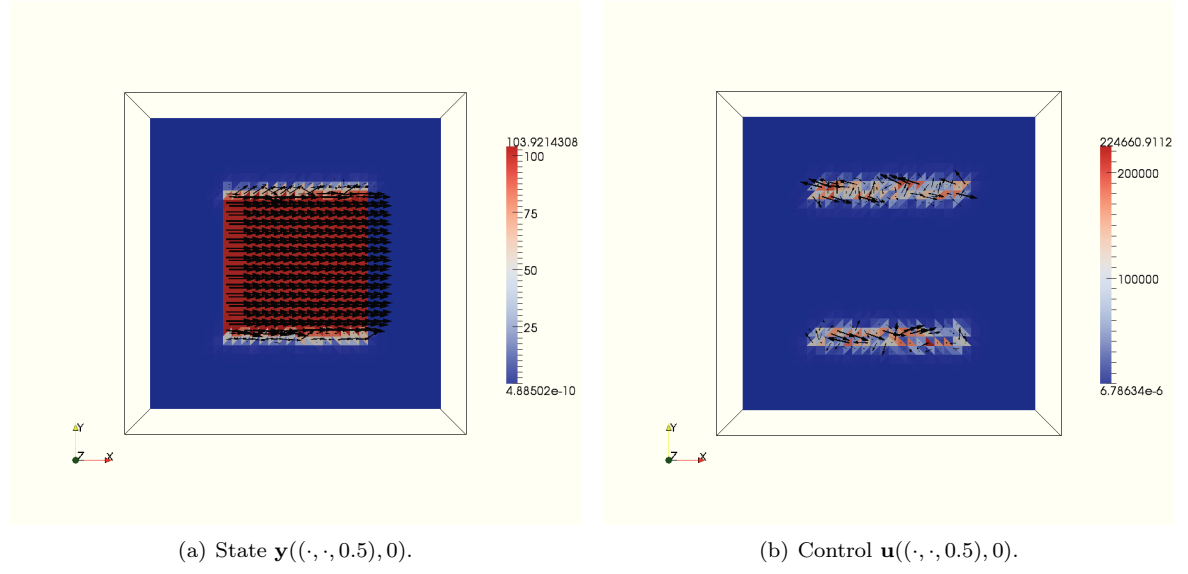
Figure 9.5: Example 1: 2D-visualization of the state $\mathbf{y}$ and the control $\mathbf{u}$ at $t = 0$ and $z = 0.5$ ($\lambda = 10^{-8}$).

a parallel machine, the total CPU time is basically defined by the CPU time that is needed for one mode, which corresponds to one time-harmonic optimal control problem.
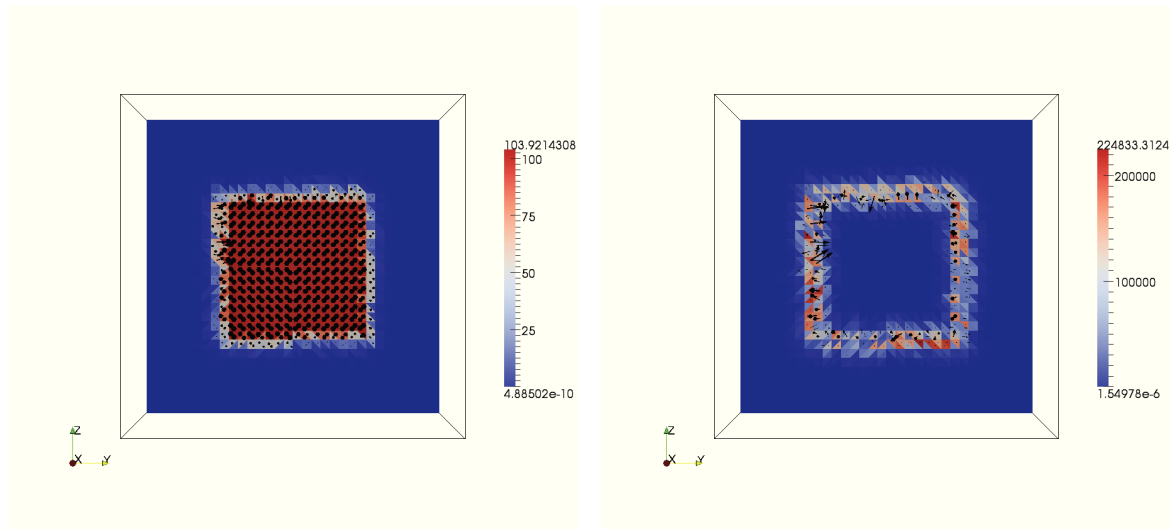
(a) State $\mathbf{y}((0.5, \cdot, \cdot), 0)$.

(b) Control $\mathbf{u}((0.5, \cdot, \cdot), 0)$.

Figure 9.6: Example 1: 2D-visualization of the state $\mathbf{y}$ and the control $\mathbf{u}$ at $t = 0$ and $x = 0.5$ ($\lambda = 10^{-8}$).

(a) State $\mathbf{y}((\cdot,\cdot,0.5),0)$.

(b) State $\mathbf{y}((\cdot,\cdot,0.5),0.125)$.

(c) State $\mathbf{y}((\cdot,\cdot,0.5),0.25)$.

(d) State $\mathbf{y}((\cdot,\cdot,0.5),0.375)$.

(e) State $\mathbf{y}((\cdot,\cdot,0.5),0.5)$.

(f) State $\mathbf{y}((\cdot,\cdot,0.5),0.625)$.

(g) State $\mathbf{y}((\cdot,\cdot,0.5),0.75)$.

(h) State $\mathbf{y}((\cdot,\cdot,0.5),0.875)$.

(i) State $\mathbf{y}((\cdot,\cdot,0.5),1)$.

Figure 9.7: Example 2: 2D-visualization of the x-component of the state $\mathbf{y}$ at $z = 0.5$ ($\lambda = 10^{-6}$, $N = 5$).

(a) Control $\mathbf{u}((\cdot,\cdot,0.5),0)$.

(b) Control $\mathbf{u}((\cdot,\cdot,0.5),0.125)$.

(c) Control $\mathbf{u}((\cdot,\cdot,0.5),0.25)$.

(d) Control $\mathbf{u}((\cdot,\cdot,0.5),0.375)$.

(e) Control $\mathbf{u}((\cdot,\cdot,0.5),0.5)$.

(f) Control $\mathbf{u}((\cdot,\cdot,0.5),0.625)$.

(g) Control $\mathbf{u}((\cdot,\cdot,0.5),0.75)$.

(h) Control $\mathbf{u}((\cdot,\cdot,0.5),0.875)$.

(i) Control $\mathbf{u}((\cdot,\cdot,0.5),1)$.
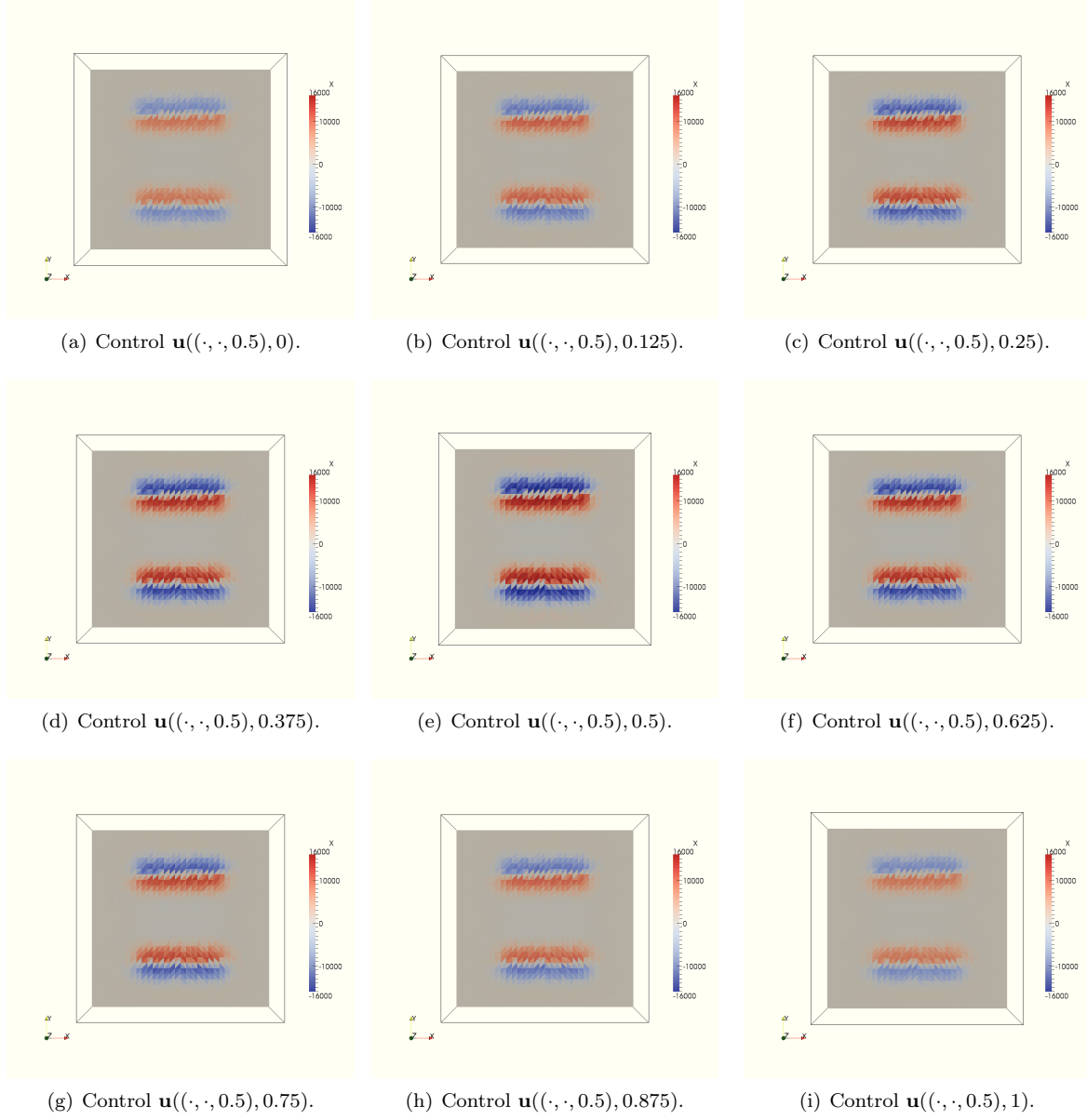
Figure 9.8: Example 2: 2D-visualization of the x-component of the control $\mathbf{u}$ at $z = 0.5$ ($\lambda = 10^{-6}$, $N = 5$).

(a) $N = 1$.

(b) $N = 3$.

(c) $N = 5$.

(d) $N = 7$.

(e) $N = 9$.
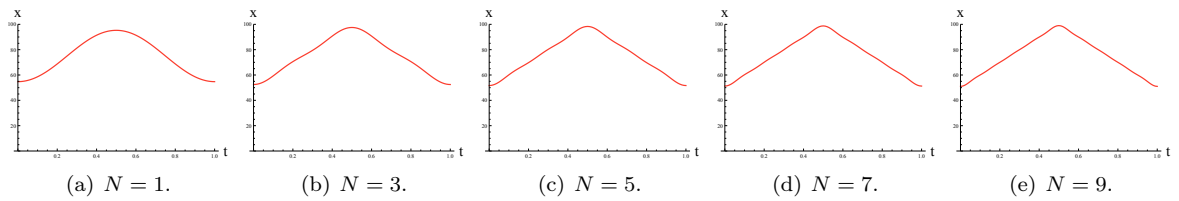
Figure 9.9: Example 2: 1D-visualization of the x component of the state $\mathbf{y}((0,5,0.5,0.5),\cdot)$ ($\lambda = 10^{-8}$).

(a) State $\mathbf{y}((\cdot,\cdot,0.5),0)$.   (b) State $\mathbf{y}((\cdot,\cdot,0.5),0.5)$.   (c) State $\mathbf{y}((\cdot,\cdot,0.5),1)$.

Figure 9.10: Example 2: 2D-visualization of the x-component of the state $\mathbf{y}$ at $z = 0.5$ ($\lambda = 10^{-8}$, $N = 50$).
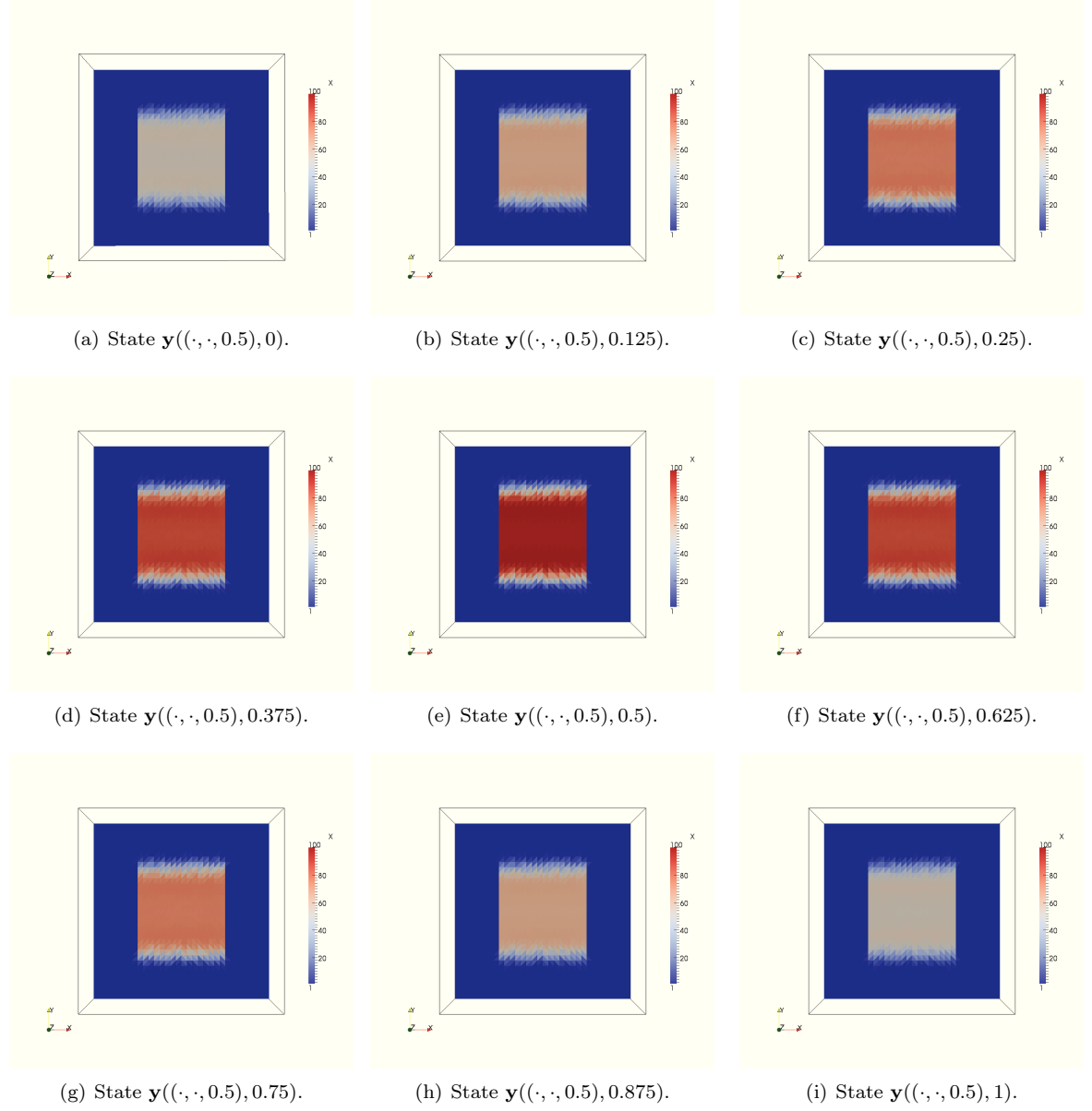

(a) State $\mathbf{u}((\cdot,\cdot,0.5),0)$.   (b) State $\mathbf{u}((\cdot,\cdot,0.5),0.5)$.   (c) State $\mathbf{u}((\cdot,\cdot,0.5),1)$.
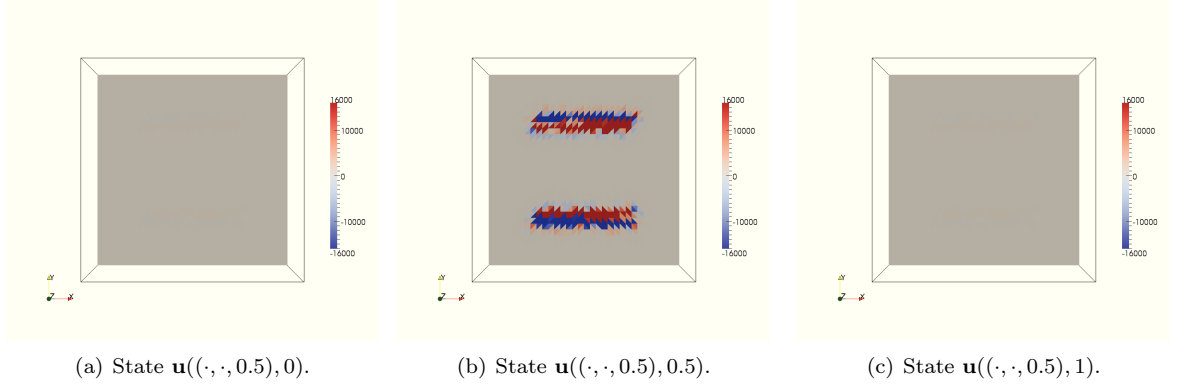
Figure 9.11: Example 2: 2D-visualization of the x-component of the control $\mathbf{u}$ at $z = 0.5$ ($\lambda = 10^{-8}$, $N = 50$).

(a) $N = 10$.   (b) $N = 20$.   (c) $N = 30$.   (d) $N = 40$.   (e) $N = 50$.

(f) $N = 60$.   (g) $N = 70$.   (h) $N = 80$.   (i) $N = 90$.   (j) $N = 100$.

Figure 9.12: Example 3: 1D-visualization of the x component of the state $\mathbf{y}((0.5, 0.5, 0.5), \cdot)$ ($\lambda = 10^{-8}$).
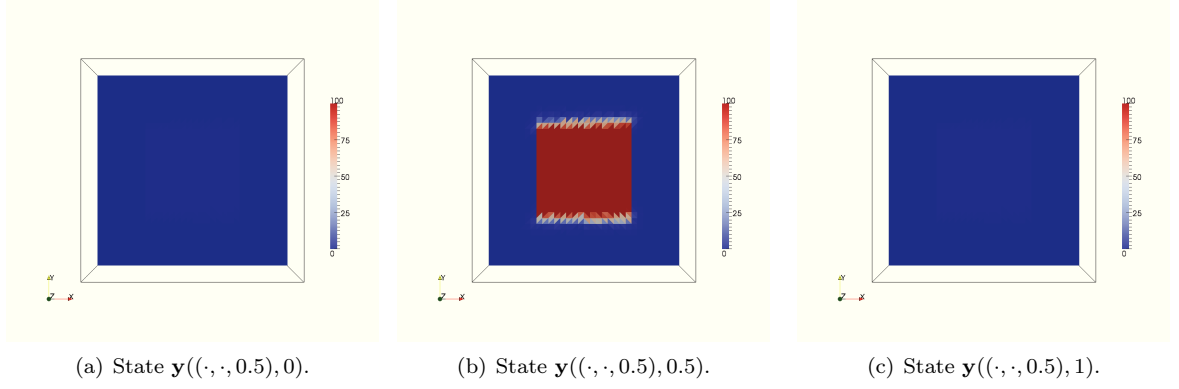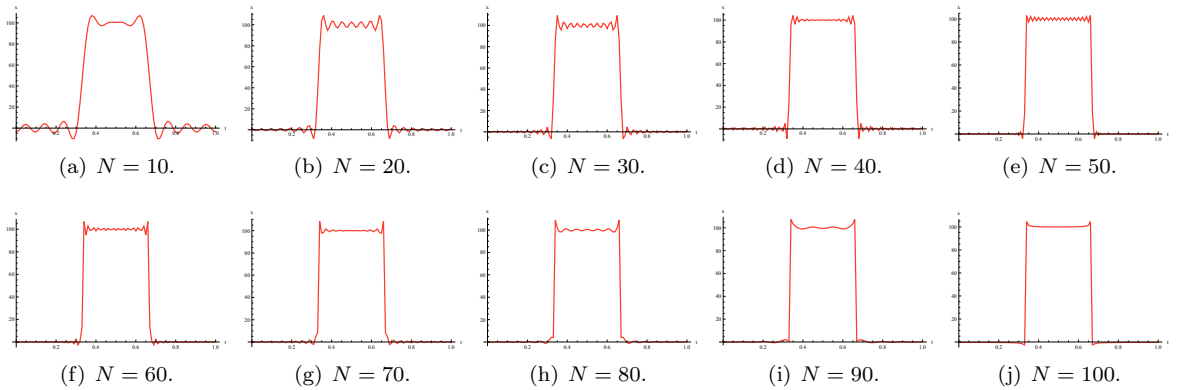
Chapter 10

Conclusion and outlook

10.1 Conclusion

We established the MH-FEM and MH-FEM-BEM method as powerful tools for solving both, time-periodic eddy current problems and time-periodic eddy current optimal control problems. We demonstrated, that appropriate discretization techniques in combination with efficient and parameter-robust solvers lead to a very competitive method.

Therefore, the key points of our method were the usage of

- a non-standard time discretization technique in terms of a truncated Fourier series in order to capture the time-periodic structure of the solution,

- a FEM-BEM coupling method in order to capture the different physical behavior of the underlying possible unbounded domain

- and the construction of parameter-robust solvers for the resulting systems of equations in the frequency domain.

We devoted special attendance to the development of efficient and parameter-robust solvers on a theoretical basement. Hence, the solvers were constructed and analyzed in the following fashion:

- Construct candidates for block-diagonal preconditioners via a matrix interpolation technique or a Schur complement approach for special regimes.

- Based on these special regimes, introduce non-standard norms in the underlying Hilbert spaces and show well-posedness of the variational problems in these norms.

- Transfer these well-posedness results to the discrete system by using a stable discretization and derive uniform condition number estimates.

- Replace the non-standard norms by appropriate well-known preconditioners.

Indeed, this approach has been applied to a full range of problems in our computational setting.

10.2 Outlook

Further work

- The theoretical results obtained for the MH-FEM-BEM approach have to be validated numerically. While the theory developed for the MH-FEM discretization is fully confirmed by numerical experiments, the preconditioners developed for the MH-FEM-BEM discretization are still of theoretical nature and therefore have to be verified numerically. Hence, a fast boundary element method has to be implemented in our research code ParMax.

155

- Another issue concerning software development is the optimization and parallelization of our algorithm. Improvements in the efficiency of the method could dramatically decrease the total computational time. So far, the implementation of the solution algorithm in ParMax is not parallel. Indeed, the proposed solution technique offers a full range of starting points for a parallelization of the solution procedure. Indeed, the new super computer MACH[1] at the Johannes Kepler University Linz offers the unique possibility to test the algorithms on a parallel machine.

- This work covers the analysis and solution of linear eddy current problems. In real life applications, one is often faced with nonlinear problems. As already addressed in Section 6.3, solvers for the nonlinear systems of equations, stemming from the MH-FEM approximation of the nonlinear eddy current problem, should be analysed.

Open questions   The following questions concerning eddy current optimal control problems remain open:

- As outlined in Subsection 3.2.2, one crucial point in the optimal control of Maxwell's equations is to enforce the conservation of charges law in the state equation. So far, our analysis only covers the case of constant conductivity. Extending this analysis also to the case of piecewise constant conductivity is a delicate issue.

- Another way of dealing with the conservation of charges law is described in Remark 3.11. In this setting, the conservation of charges is even fulfilled for piecewise constant conductivity. Nevertheless, due to the vector potential ansatz for $\mathbf{u}$, the construction of parameter-robust solvers is not straightforward. It turns out, that for the construction of parameter-robust solvers, different scalings with respect to the regularization parameter λ of the gradient and divergence-free parts appearing in the Helmholtz decomposition have to be taken into account. The approach of Hiptmair and Xu [85] is certainly one candidate to tackle this kind of problem.

- So far our analysis covers the case of box constraints imposed on the Fourier coefficients of the control and the state. The efficient treatment of full box constraints in the minimization problem (7.1) for the control and the state is much harder. The inclusion of such inequality constraints into the cost functional as a penalty term is one technique to handle this problem, cf. [59]. Another possibility is to use barrier methods, cf. [140]. However, this adds another nonlinear, non-quadratic term to the quadratic cost functional. In the case of nonlinear problems caused by the penalty technique or other nonlinearities in the state equation, we lose the decoupling of the optimality system with respect to the Fourier coefficients.

- In some of the considered optimal control settings, it was necessary to incorporate the divergence constraints in an explicit manner, in order to be able to provide theoretical condition number estimates. Anyhow, numerical experiments indicate, that in some settings the incorporation is not needed in practice.

Possible continuations

- The efficient and parameter-robust evaluation of the FEM-BEM Schur complement $\mathbf{K}_\nu + \mathbf{M}_{\sigma,\omega} - \mathbf{N} + \mathbf{B}^T \mathbf{A}^{-1} \mathbf{B}$ is a delicate task. Indeed, this issue is also relevant for a full range of computations in the electromagnetic regime, cf. [57].

- In Section 7.3 and Section 7.4, we discussed the application of our solver to optimal control problems with various constraints. Due to these additional modifications, robustness with respect to certain regularization or model parameters is lost. The application of the technique of block-diagonal preconditioning is limited in these settings. Hence other preconditioning

---

[1]SGI Altix UltraViolet 1000, 256 processors, 16 TB shared memory.

techniques should be investigated to obtain full parameter-robust solvers. Possible continuations are offered by recent investigations of the research groups around Anton Schiela, Andy Wathen and Walter Zulehner.

- Another issue is the improvement of the error estimate corresponding to the time-discretization error. Indeed, for functions that are analytic in time, one may expect exponential convergence with respect to the number of Fourier modes N.

- Investigating other types of time discretization methods. Instead of an approximation in time by means of a Fourier series, other spectral methods can be used. Therein, one of the crucial points is to use spectral methods, that allow the incorporation of initial conditions. Candidates are orthogonal polynomials like Legendre polynomials or integrated Legendre polynomials.

- Another possibility is to use a full space-time discretization of a four-dimensional space-time cylinder into finite elements, which also allows a rather general and flexible discretization in time. Starting points for this approach are provided by Neumüller and Steinbach in [122, 123].

Bibliography

[1] D. Abbeloos, M. Diehl, M. Hinze, and S. Vandewalle. Nested multigrid methods for time-periodic, parabolic optimal control problems. *Computing and Visualization in Science*, 14:27–38, 2011.

[2] R. Acevedo and S. Meddahi. An E-based mixed FEM and BEM coupling for a time-dependent eddy current problem. *IMA J. Numer. Anal.*, 31(2):667–697, 2011.

[3] R. Acevedo, S. Meddahi, and R. Rodríguez. An E-based mixed formulation for a time-dependent eddy current problem. *Math. Comp.*, 78(268):1929–1949, 2009.

[4] R. Adams and J. Fournier. *Sobolev spaces. Second Edition.* Academic Press, 2008. Volume 140 in the Pure and Applied Mathematics series, Elsevier.

[5] A. Alonso Rodríguez, P. Fernandes, and A. Valli. Weak and strong formulations for the time-harmonic eddy-current problem in general multi-connected domains. *European J. Appl. Math.*, 14(4):387–406, 2003.

[6] A. Alonso Rodríguez and A. Valli. *Eddy current approximation of Maxwell equations*, volume 4 of *MS&A. Modeling, Simulation and Applications.* Springer-Verlag Italia, Milan, 2010.

[7] H. Ammari, A. Buffa, and J.-C. Nédélec. A justification of eddy currents model for the Maxwell equations. *SIAM J. Appl. Math.*, 60(5):1805–1823, 2000.

[8] D. N. Arnold, R. S. Falk, and R. Winther. Preconditioning in $H(\mathrm{div})$ and applications. *Math. Comp.*, 66(219):957–984, 1997.

[9] D. N. Arnold, R. S. Falk, and R. Winther. Multigrid in $H(\mathrm{div})$ and $H(\mathrm{curl})$. *Numer. Math.*, 85(2):197–217, 2000.

[10] L. Arnold and B. Harrach. A unified variational formulation for the parabolic-elliptic eddy current equations. *SIAM Journal on Applied Mathematics*, 72(2):558–576, 2012.

[11] S. Ausserhofer, O. Biro, and K. Preis. An efficient harmonic balance method for nonlinear eddy current problems. In *Electromagnetic Field Computation, 2006 12th Biennial IEEE Conference on*, pages 22 –22, 2006.

[12] S. Ausserhofer, O. Biro, and K. Preis. An efficient harmonic balance method for nonlinear eddy-current problems. *Magnetics, IEEE Transactions on*, 43(4):1229 –1232, April 2007.

[13] S. Ausserhofer, O. Biro, and K. Preis. Frequency and time domain analysis of nonlinear periodic electromagnetic problems. In *Electromagnetics in Advanced Applications, 2007. ICEAA 2007. International Conference on*, pages 229 –232, sep. 2007.

[14] I. Babuška. Error-bounds for finite element method. *Numer. Math.*, 16(4):322–333, 1971.

[15] F. Bachinger. Multigrid solvers for 3D multiharmonic nonlinear magnetic field computations. Master's thesis, Johannes Kepler University, Linz, October 2003.

[16] F. Bachinger, M. Kaltenbacher, and S. Reitzinger. An Efficient Solution Strategy for the HBFE Method. In *Proceedings of the IGTE '02 Symposium Graz, Austria*, pages 385–389, 2002.

[17] F. Bachinger, U. Langer, and J. Schöberl. Numerical analysis of nonlinear multiharmonic eddy current problems. *Numer. Math.*, 100(4):593–616, 2005.

[18] F. Bachinger, U. Langer, and J. Schöberl. Efficient solvers for nonlinear time-periodic eddy current problems. *Comput. Vis. Sci.*, 9(4):197–207, 2006.

[19] M. Bebendorf. Approximation of boundary element matrices. *Numer. Math.*, 86(4):565–589, 2000.

[20] M. Bebendorf. *Hierarchical matrices*, volume 63 of *Lecture Notes in Computational Science and Engineering*. Springer-Verlag, Berlin, 2008.

[21] M. Bebendorf and J. Ostrowski. Parallel hierachical matrix preconditioners for the curl-curl operator. *J. Comput. Math.*, 27(5):624–641, 2009.

[22] Z. Belhachmi, C. Bernardi, S. Deparis, and F. Hecht. A truncated Fourier/finite element discretization of the Stokes equations in an axisymmetric domain. *Math. Models Methods Appl. Sci.*, 16(2):233–263, 2006.

[23] M. Benzi, G. H. Golub, and J. Liesen. Numerical solution of saddle point problems. *Acta Numer.*, 14:1–137, 2005.

[24] J. Bergh and J. Löfström. *Interpolation spaces: An introduction.* Springer-Verlag, Berlin-Heidelberg-New York, 1976.

[25] M. Bergounioux, K. Ito, and K. Kunisch. Primal-dual strategy for constrained optimal control problems. *SIAM J. Control Optim.*, 37(4):1176–1194, 1999.

[26] M. Bergounioux and K. Kunisch. Primal-dual strategy for state-constrained optimal control problems. *Comput. Optim. Appl.*, 22(2):193–224, 2002.

[27] C. Bernardi, M. Dauge, and Y. Maday. *Spectral methods for axisymmetric domains*, volume 3 of *Series in Applied Mathematics (Paris)*. Gauthier-Villars, Éditions Scientifiques et Médicales Elsevier, Paris, 1999.

[28] P. B. Bochev, C. J. Garasi, J. J. Hu, A. C. Robinson, and R. S. Tuminaro. An improved algebraic multigrid method for solving Maxwell's equations. *SIAM J. Sci. Comput.*, 25(2):623–642, 2003.

[29] J. H. Bramble. *Multigrid methods*, volume 294 of *Pitman Research Notes in Mathematics Series*. Longman Scientific & Technical, Harlow, 1993.

[30] J. H. Bramble and J. E. Pasciak. A preconditioning technique for indefinite systems resulting from mixed approximations of elliptic problems. *Math. Comp.*, 50(181):1–17, 1988.

[31] J. H. Bramble, J. E. Pasciak, and P. S. Vassilevski. Computational scales of Sobolev norms with application to preconditioning. *Math. Comp.*, 69(230):463–480, 2000.

[32] F. Brezzi. On the existence, uniqueness and approximation of saddle-point problems arising from Lagrangian multipliers. *Rev. Française Automat. Informat. Recherche Opérationnelle Sér. Rouge*, 8(R-2):129–151, 1974.

[33] A. Buffa and P. Ciarlet, Jr. On traces for functional spaces related to Maxwell's equations. I. An integration by parts formula in Lipschitz polyhedra. *Math. Methods Appl. Sci.*, 24(1):9–30, 2001.

[34] A. Buffa and P. Ciarlet, Jr. On traces for functional spaces related to Maxwell's equations. II. Hodge decompositions on the boundary of Lipschitz polyhedra and applications. *Math. Methods Appl. Sci.*, 24(1):31–48, 2001.

[35] A. Buffa, M. Costabel, and C. Schwab. Boundary element methods for Maxwell's equations on non-smooth domains. *Numer. Math.*, 92(4):679–710, 2002.

[36] A. Buffa and R. Hiptmair. Galerkin boundary element methods for electromagnetic scattering. In *Topics in computational wave propagation*, volume 31 of *Lect. Notes Comput. Sci. Eng.*, pages 83–124. Springer, Berlin, 2003.

[37] A. Buffa, R. Hiptmair, T. von Petersdorff, and C. Schwab. Boundary element methods for Maxwell transmission problems in Lipschitz domains. *Numer. Math.*, 95(3):459–485, 2003.

[38] J. Chen, Z. Chen, T. Cui, and L.-B. Zhang. An adaptive finite element method for the eddy current model with circuit/field couplings. *SIAM J. Sci. Comput.*, 32(2):1020–1042, 2010.

[39] P. Ciarlet, Jr. and J. Zou. Fully discrete finite element approaches for time-dependent Maxwell's equations. *Numer. Math.*, 82(2):193–219, 1999.

[40] D. Copeland, M. Kolmbauer, and U. Langer. Domain Decomposition Solvers for Frequency-Domain Finite Element Equations. In *Domain Decomposition Methods in Science and Engineering XIX*, volume 78 of *Lecture Notes in Computational Science and Engineering*, pages 301–308. Springer, 2011.

[41] D. Copeland and U. Langer. Domain Decomposition Solvers for Nonlinear Multiharmonic Finite Element Equations. *J. Numer. Math.*, 18(3):157–175, 2010.

[42] M. Costabel. Symmetric methods for the coupling of finite elements and boundary elements (invited contribution). In *Boundary elements IX, Vol. 1 (Stuttgart, 1987)*, pages 411–420. Comput. Mech., Southampton, 1987.

[43] W. J. Cunningham. *Introduction to nonlinear analysis.* McGraw-Hill Electrical and Electronic Engineering Series. McGraw-Hill Book Co., Inc., New York, 1958.

[44] R. Dautray and J.-L. Lions. *Mathematical analysis and numerical methods for science and technology. Vol. 4.* Springer-Verlag, Berlin, 1990.

[45] T. A. Davis. Algorithm 832: Umfpack v4.3—an unsymmetric-pattern multifrontal method. *ACM Trans. Math. Softw.*, 30:196–199, June 2004.

[46] T. A. Davis. A column pre-ordering strategy for the unsymmetric-pattern multifrontal method. *ACM Trans. Math. Softw.*, 30:165–195, June 2004.

[47] T. A. Davis and I. S. Duff. A combined unifrontal/multifrontal method for unsymmetric sparse matrices. *ACM Trans. Math. Softw.*, 25:1–20, March 1999.

[48] H. De Gersem, S. Vandewalle, and K. Hameyer. Krylov subspace methods for harmonic balanced finite element methods. In *Lecture Notes in Computational Science and Engineering*, pages 387 – 396, 2001.

[49] L. Demkowicz, J. Kurtz, D. Pardo, M. Paszyński, W. Rachowicz, and A. Zdunek. *Computing with hp-adaptive finite elements. Vol. 2.* Chapman & Hall/CRC Applied Mathematics and Nonlinear Science Series. Chapman & Hall/CRC, Boca Raton, FL, 2008.

[50] C. Dohrmann and O. Widlund. Some recent tools and a BDDC algorithm for 3D problems in **H(curl)**. In *Domain Decomposition Methods in Science and Engineering XX*, Lecture Notes in Computational Science and Engineering. Springer, 2012. (to appear).

[51] J. Driesen, G. Deliege, T. Van Craenenbroeck, and H. K. Implementation of the harmonic balance FEM method for large-scale saturated electromagnetic devices. In *Proceedings of ELECTROSOFT 99 conference, Sevilla, Spain*, pages 75 – 84, 1999.

[52] P.-É. Druet, O. Klein, J. Sprekels, F. Tröltzsch, and I. Yousept. Optimal control of three-dimensional state-constrained induction heating problems with nonlocal radiation effects. *SIAM J. Control Optim.*, 49(4):1707–1736, 2011.

[53] H. C. Elman, D. J. Silvester, and A. J. Wathen. *Finite elements and fast iterative solvers: with applications in incompressible fluid dynamics*. Numerical Mathematics and Scientific Computation. Oxford University Press, New York, 2005.

[54] L. C. Evans. *Partial differential equations*, volume 19 of *Graduate Studies in Mathematics*. American Mathematical Society, Providence, RI, second edition, 2010.

[55] R. D. Falgout and P. S. Vassilevski. On generalizing the algebraic multigrid framework. *SIAM J. Numer. Anal.*, 42(4):1669–1693, 2004.

[56] R. W. Freund and N. M. Nachtigal. QMR: a quasi-minimal residual method for non-Hermitian linear systems. *Numer. Math.*, 60(3):315–339, 1991.

[57] S. A. Funken and E. P. Stephan. Fast solvers with block-diagonal preconditioners for linear FEM-BEM coupling. *Numer. Linear Algebra Appl.*, 16(5):365–395, 2009.

[58] H. D. Gersem., H. V. Sande, and K. Hameyer. Strong coupled multi-harmonic finite element simulation package. *COMPEL*, 20:535 –546, 2001.

[59] H. Gfrerer. Generalized penalty methods for a class of convex optimization problems with pointwise inequality constraints. NuMa-Report 07, Institute of Computational Mathematics, Linz, 2009.

[60] V. Girault and P.-A. Raviart. *Finite element methods for Navier-Stokes equations*, volume 5 of *Springer Series in Computational Mathematics*. Springer-Verlag, Berlin, 1986.

[61] A. Greenbaum. *Iterative methods for solving linear systems*, volume 17 of *Frontiers in Applied Mathematics*. Society for Industrial and Applied Mathematics (SIAM), Philadelphia, PA, 1997.

[62] L. Greengard. *The rapid evaluation of potential fields in particle systems*. ACM Distinguished Dissertations. MIT Press, Cambridge, MA, 1988.

[63] L. Greengard and V. Rokhlin. The rapid evaluation of potential fields in three dimensions. In *Vortex methods (Los Angeles, CA, 1987)*, volume 1360 of *Lecture Notes in Math.*, pages 121–141. Springer, Berlin, 1988.

[64] R. Griesse and K. Kunisch. Optimal control for a stationary MHD system in velocity-current formulation. *SIAM J. Control Optim.*, 45(5):1822–1845, 2006.

[65] M. Gunzburger and C. Trenchea. Analysis and discretization of an optimal control problem for the time-periodic MHD equations. *J. Math. Anal. Appl.*, 308(2):440–466, 2005.

[66] J. Gyselinck, P. Dular, C. Geuzaine, and W. Legros. Harmonic-balance finite-element modeling of electromagnetic devices: a novel approach. *Magnetics, IEEE Transactions on*, 38(2):521 –524, March 2002.

[67] J. Gyselinck, P. Dular, C. Geuzaine, and W. Legros. 2D harmonic balance FE modelling of electromagnetic devices coupled to nonlinear circuits. *COMPEL*, 23(3):800–812, 2004.

[68] W. Hackbusch. *Multigrid methods and applications*, volume 4 of *Springer Series in Computational Mathematics*. Springer-Verlag, Berlin, 1985.

[69] W. Hackbusch. A sparse matrix arithmetic based on $\mathcal{H}$-matrices. I. Introduction to $\mathcal{H}$-matrices. *Computing*, 62(2):89–108, 1999.

[70] W. Hackbusch and B. N. Khoromskij. A sparse $\mathcal{H}$-matrix arithmetic. II. Application to multi-dimensional problems. *Computing*, 64(1):21–47, 2000.

[71] B. Heinrich. The Fourier-finite-element method for Poisson's equation in axisymmetric domains with edges. *SIAM J. Numer. Anal.*, 33(5):1885–1911, 1996.

[72] V. E. Henson and U. M. Yang. BoomerAMG: a parallel algebraic multigrid solver and preconditioner. *Appl. Numer. Math.*, 41(1):155–177, 2002.

[73] R. Herzog and E. Sachs. Preconditioned conjugate gradient method for optimal control problems with control and state constraints. *SIAM J. Matrix Anal. Appl.*, 31(5):2291–2317, 2010.

[74] M. R. Hestenes and E. Stiefel. Methods of conjugate gradients for solving linear systems. *J. Research Nat. Bur. Standards*, 49:409–436 (1953), 1952.

[75] N. Heuer and E. P. Stephan. Iterative substructuring for hypersingular integral equations in $\mathbb{R}^3$. *SIAM J. Sci. Comput.*, 20(2):739–749, 1998.

[76] M. Hintermüller, K. Ito, and K. Kunisch. The primal-dual active set strategy as a semismooth Newton method. *SIAM J. Optim.*, 13(3):865–888, 2002.

[77] R. Hiptmair. Canonical construction of finite elements. *Math. Comp.*, 68(228):1325–1346, 1999.

[78] R. Hiptmair. Multigrid method for Maxwell's equations. *SIAM J. Numer. Anal.*, 36(1):204–225, 1999.

[79] R. Hiptmair. Finite elements in computational electromagnetism. *Acta Numer.*, 11:237–339, 2002.

[80] R. Hiptmair. Symmetric coupling for eddy current problems. *SIAM J. Numer. Anal.*, 40(1):41–65, 2002.

[81] R. Hiptmair. Boundary element methods for eddy current computation. In *Computational electromagnetics (Kiel, 2001)*, volume 28 of *Lect. Notes Comput. Sci. Eng.*, pages 103–126. Springer, Berlin, 2003.

[82] R. Hiptmair. Operator preconditioning. *Comput. Math. Appl.*, 52(5):699–706, 2006.

[83] R. Hiptmair and P. Meury. Stabilized FEM-BEM coupling for Maxwell transmission problems. In *Modeling and computations in electromagnetics*, volume 59 of *Lect. Notes Comput. Sci. Eng.*, pages 1–38. Springer, Berlin, 2008.

[84] R. Hiptmair and J. Ostrowski. Coupled boundary-element scheme for eddy-current computation. *J. Engrg. Math.*, 51(3):231–250, 2005.

[85] R. Hiptmair and J. Xu. Nodal auxiliary space preconditioning in $\mathbf{H}(\mathbf{curl})$ and $\mathbf{H}(\mathrm{div})$ spaces. *SIAM J. Numer. Anal.*, 45(6):2483–2509, 2007.

[86] B. Houska and M. Diehl. Robustness and stability optimization of power generating kite systems in a periodic pumping mode. In *Control Applications (CCA), 2010 IEEE International Conference on*, pages 2172 –2177, September 2010.

[87] Q. Hu and J. Zou. A nonoverlapping domain decomposition method for Maxwell's equations in three dimensions. *SIAM J. Numer. Anal.*, 41(5):1682–1708, 2003.

[88] Q. Hu and J. Zou. A weighted Helmholtz decomposition and application to domain decomposition for saddle-point Maxwell systems. Technical Report 15, CUHK, 2007.

[89] K. Ito and K. Kunisch. Semi-smooth Newton methods for state-constrained optimal control problems. *Systems Control Lett.*, 50(3):221–228, 2003.

[90] J. Jones and B. Lee. A multigrid method for variable coefficient Maxwell's equations. *SIAM J. Sci. Comput.*, 27(5):1689–1708, 2006.

[91] M. Kaltenbacher. *Numerical Simulation of Mechatronic Sensors and Actuators*. Springer Berlin Heidelberg, 2007.

[92] G. Koczka, S. Ausserhofer, O. Biro, and K. Preis. Optimal fixed-point method for solving 3D nonlinear periodic eddy current problems. *COMPEL*, 28(4):1059 – 1067, April 2009.

[93] T. V. Kolev and P. S. Vassilevski. Parallel auxiliary space AMG for H(curl) problems. *J. Comput. Math.*, 27(5):604–623, 2009.

[94] M. Kollmann and M. Kolmbauer. A preconditioned MinRes solver for time-periodic parabolic optimal control problems. *Numer. Linear Algebra Appl.*, 2012. DOI: 10.1002/nla.1842.

[95] M. Kollmann, M. Kolmbauer, U. Langer, M. Wolfmayr, and W. Zulehner. A robust finite element solver for a multiharmonic parabolic optimal control problem. *Computers and Mathematics with Applications*, 2012. DOI: 10.1016/j.camwa.2012.06.012.

[96] M. Kolmbauer. A multiharmonic solver for nonlinear parabolic problems. Master's thesis, Johannes Kepler University, Linz, October 2009.

[97] M. Kolmbauer. Existence and uniqueness of eddy current problems in bounded and unbounded domains. NuMa-Report 03, Johannes Kepler University Linz, Institute of Computational Mathematics, Linz, May 2011.

[98] M. Kolmbauer. Efficient solvers for multiharmonic eddy current optimal control problems with various constraints and their analysis. *IMA J. Numer. Anal.*, 2012. (to appear).

[99] M. Kolmbauer. A robust FEM-BEM MinRes solver for distributed multiharmonic eddy current optimal control problems in unbounded domains. *Electronic Transactions on Numerical Analysis*, 39:231–252, 2012.

[100] M. Kolmbauer and U. Langer. A frequency-robust solver for the time-harmonic eddy current problem. In *Scientific Computing in Electrical Engineering SCEE 2010*, volume 16 of *Mathematics in Industry*, pages 97–106. Springer, 2011.

[101] M. Kolmbauer and U. Langer. A robust preconditioned MinRes solver for distributed time-periodic eddy current optimal control problems. NuMa-Report 2011-04, Institute of Computational Mathematics, Linz, May 2011.

[102] M. Kolmbauer and U. Langer. A robust FEM-BEM solver for time-harmonic eddy current problems. In *Domain Decomposition Methods in Science and Engineering XX*, Lecture Notes in Computational Science and Engineering. Springer, 2012. (to appear).

[103] M. Kolmbauer and U. Langer. A robust preconditioned MinRes solver for time-periodic eddy current problems. *Comput. Methods Appl. Math.*, January 2012. DOI: 10.2478/cmam-2012-0023.

[104] J. Kraus. Algebraic multilevel preconditioning of finite element matrices using local Schur complements. *Numer. Linear Algebra Appl.*, 13(1):49–70, 2006.

[105] J. Kraus. Additive schur complement approximation and application to multilevel preconditioning. RICAM Report 2011-22, Johann Radon Institute for Computational and Applied Mathematics (RICAM) of the Austrian Academy of Sciences, Linz, August 2011.

[106] J. Kraus and S. Margenov. *Robust algebraic multilevel methods and algorithms*. Walter de Gruyter, 2009.

[107] M. Kuhn. *Efficient Parallel Numerical Simulation of Magnetic Field Problems*. PhD thesis, Johannes Kepler University, Linz, 1998.

[108] K. Kunisch and A. Rösch. Primal-dual active set strategy for a general class of constrained optimal control problems. *SIAM J. Optim.*, 13(2):321–334, 2002.

[109] Y. A. Kuznetsov. Efficient iterative solvers for elliptic finite element problems on nonmatching grids. *Russ. J. Numer. Anal. Math. Model.*, 10:187–211, 1995.

[110] P. D. Ledger and S. Zaglmayr. *hp*-finite element simulation of three-dimensional eddy current problems on multiply connected domains. *Comput. Methods Appl. Mech. Engrg.*, 199(49-52):3386–3401, 2010.

[111] F. Leydecker, M. Maischak, E. P. Stephan, and M. Teltscher. Adaptive FE-BE coupling for an electromagnetic problem in $\mathbb{R}^3$—a residual error estimator. *Math. Methods Appl. Sci.*, 33(18):2162–2186, 2010.

[112] D. Loghin and A. J. Wathen. Analysis of preconditioners for saddle-point problems. *SIAM J. Sci. Comput.*, 25(6):2029–2049, 2004.

[113] J. Lu, Y. Li, C. Sun, and S. Yamada. A parallel-computation model for nonlinear electromagnetic field analysis by harmonic balance finite element method. volume 2, pages 780 –787 vol.2, April 1995.

[114] J. Lu, S. Yamada, and K. Bessho. Time-periodic magnetic field analysis with saturation and hysteresis characteristics by harmonic balance finite element method. *Magnetics, IEEE Transactions on*, 26(2):995 –998, March 1990.

[115] J. W. Lu, S. Yamada, and H. Harrison. Application of harmonic balance-finite element method (HBFEM) in the design of switching power supplies. *Power Electronics, IEEE Transactions on*, 11(2):347 –355, March 1996.

[116] M. Maischak and T. Tran. A block preconditioner for an electromagnetic FEM-BEM coupling problem is $\mathbb{R}^3$. In *Proceedings of the 2nd International Conference on Scientific Computing and Partial Differential Equations*, Recent Progress in Scientific Computing, pages 302–318, Beijing, 2007.

[117] K.-A. Mardal and R. Winther. Preconditioning discretizations of systems of partial differential equations. *Numer. Linear Algebra Appl.*, 18(1):1–40, 2011.

[118] P. Monk. *Finite element methods for Maxwell's equations*. Numerical Mathematics and Scientific Computation. Oxford University Press, New York, 2003.

[119] M. F. Murphy, G. H. Golub, and A. J. Wathen. A note on preconditioning for indefinite linear systems. *SIAM J. Sci. Comput.*, 21:1969–1972, 2000.

[120] J.-C. Nédélec. Mixed finite elements in $\mathbf{R}^3$. *Numer. Math.*, 35(3):315–341, 1980.

[121] J.-C. Nédélec. A new family of mixed finite elements in $\mathbf{R}^3$. *Numer. Math.*, 50(1):57–81, 1986.

[122] M. Neumüller and O. Steinbach. Refinement of flexible space-time finite element meshes and discontinuous galerkin methods. *Computing and Visualization in Science*, 14:189–205, 2011.

[123] M. Neumüller. Eine Finite Elemente Methode für optimale Kontrollprobleme mit parabolischen Randwertaufgaben. Master's thesis, Technische Universität Graz, Graz, 2010.

[124] B. F. Nielsen and K.-A. Mardal. Efficient preconditioners for optimality systems arising in connection with inverse problems. *SIAM J. Control Optim.*, 48(8):5143–5177, 2010.

[125] M. A. Olshanskii and A. Reusken. On the convergence of a multigrid method for linear reaction-diffusion problems. *Computing*, 65(3):193–202, 2000.

[126] M. A. Olshanskii and V. Simoncini. Acquired clustering properties and solution of certain saddle point systems. *SIAM J. Matrix Anal. Appl.*, 31(5):2754–2768, 2010.

[127] J. Ostrowski, M. Bebendorf, R. Hiptmair, and F. Krämer. $\mathcal{H}$-matrix-based operator preconditioning for full Maxwell at low frequencies. *Magnetics, IEEE Transactions on*, 46(8):3193 –3196, aug. 2010.

[128] C. C. Paige and M. A. Saunders. Solutions of sparse indefinite systems of linear equations. *SIAM J. Numer. Anal.*, 12(4):617–629, 1975.

[129] G. Paoli, O. Biro, and G. Buchgraber. Complex representation in nonlinear time harmonic eddy current problems. *Magnetics, IEEE Transactions on*, 34(5):2625 –2628, Sep. 1998.

[130] C. Pechstein. *Finite and Boundary Element Tearing and Interconnecting Methods for Multiscale Elliptic Partial Differential Equations*. PhD thesis, Universität Linz, Linz, 2008.

[131] C. Pechstein. *Finite and Boundary Element Tearing and Interconnecting Solvers for Multiscale Problems*, volume 90 of *Lecture Notes in Computational Science and Engineering*. Springer, 2013.

[132] C. Pechstein and B. Jüttler. Monotonicity-preserving interproximation of *B-H*-curves. *J. Comput. Appl. Math.*, 196(1):45–57, 2006.

[133] A. Potschka, M. Mommer, J. Schlöder, and H. Bock. Newton-Picard-based preconditioning for linear-quadratic optimization problems with time-periodic parabolic PDE constraints. *SIAM Journal on Scientific Computing*, 34(2):A1214–A1239, 2012.

[134] R. A. Prato Torres, E. P. Stephan, and F. Leydecker. A FE/BE coupling for the 3D time-dependent eddy current problem. Part I: a priori error estimates. *Computing*, 88(3-4):131–154, 2010.

[135] R. A. Prato Torres, E. P. Stephan, and F. Leydecker. A FE/BE coupling for the 3D time-dependent eddy current problem. Part II: a posteriori error estimates and adaptive computations. *Computing*, 88(3-4):155–172, 2010.

[136] S. Reitzinger and J. Schöberl. An algebraic multigrid method for finite element discretizations with edge elements. *Numer. Linear Algebra Appl.*, 9(3):223–238, 2002.

[137] A. A. Rodríguez and A. Valli. A FEM-BEM approach for electro-magnetostatics and time-harmonic eddy-current problems. *Appl. Numer. Math.*, 59(9):2036–2049, 2009.

[138] J. W. Ruge and K. Stüben. Algebraic multigrid. In *Multigrid methods*, volume 3 of *Frontiers Appl. Math.*, pages 73–130. SIAM, Philadelphia, PA, 1987.

[139] Y. Saad and M. H. Schultz. GMRES: a generalized minimal residual algorithm for solving nonsymmetric linear systems. *SIAM J. Sci. Statist. Comput.*, 7(3):856–869, 1986.

[140] A. Schiela. Barrier methods for optimal control problems with state constraints. *SIAM J. Optim.*, 20(2):1002–1031, 2009.

[141] K. Schmidt, O. Sterz, and R. Hiptmair. Estimating the eddy-current modeling error. *Magnetics, IEEE Transactions on*, 44(6):686 –689, june 2008.

[142] J. Schöberl, R. Simon, and W. Zulehner. A robust multigrid method for elliptic optimal control problems. *SIAM J. Numer. Anal.*, 49(4):1482–1503, 2011.

[143] J. Schöberl and W. Zulehner. Symmetric indefinite preconditioners for saddle point problems with applications to PDE-constrained optimization problems. *SIAM J. Matrix Anal. Appl.*, 29(3):752–773, 2007.

[144] E. P. Stephan and M. Maischak. A posteriori error estimates for FEM-BEM couplings of three-dimensional electromagnetic problems. *Comput. Methods Appl. Mech. Engrg.*, 194(2-5):441–452, 2005.

[145] M. Stoll. One-shot solution of a time-dependent time-periodic PDE-constrained optimization problem. Preprint MPIMD/11-04, Max-Planck-Institut für Dynamik komplexer Technischer Systeme, Magdeburg, July 2011.

[146] S. Takacs and W. Zulehner. Convergence analysis of multigrid methods with collective point smoothers for optimal control problems. *Comput. Vis. Sci.*, 14(3):131–141, 2011.

[147] A. Toselli. Overlapping Schwarz methods for Maxwell's equations in three dimensions. *Numer. Math.*, 86(4):733–752, 2000.

[148] A. Toselli. Dual-primal FETI algorithms for edge finite-element approximations in 3D. *IMA J. Numer. Anal.*, 26(1):96–130, 2006.

[149] A. Toselli and O. Widlund. *Domain decomposition methods—algorithms and theory*, volume 34 of *Springer Series in Computational Mathematics*. Springer-Verlag, Berlin, 2005.

[150] T. Tran and E. P. Stephan. An overlapping additive Schwarz preconditioner for boundary element approximations to the Laplace screen and Lamé crack problems. *J. Numer. Math.*, 12(4):311–330, 2004.

[151] F. Tröltzsch. *Optimal Control of Partial Differential Equations. Theory, Methods and Applications*. Graduate Studies in Mathematics 112, American Mathematical Society (AMS), Providence, RI, 2010.

[152] F. Tröltzsch. Some results in the optimal control of electro-magnetic fields. In *European Multi-Grid Conference EMG 2010*, Ischia, 2010.

[153] U. van Rienen. *Numerical methods in computational electrodynamics*, volume 12 of *Lecture Notes in Computational Science and Engineering*. Springer-Verlag, Berlin, 2001.

[154] J. Xu and Y. Zhu. Robust preconditioner for H(curl) interface problems. In *Domain Decomposition Methods in Science and Engineering XIX*, volume 78 of *LNCSE*, pages 173–180, Heidelberg, 2011. Springer.

[155] S. Yamada and K. Bessho. Harmonic field calculation by the combination of finite element analysis and harmonic balance method. *Magnetics, IEEE Transactions on*, 24(6):2588 –2590, nov. 1988.

[156] S. Yamada, K. Bessho, J. Lu, and K. Hirano. Development and application of harmonic balance finite element method in electromagnetic fields. *International Journal of Applied Electromagnetics in Materials*, 1(1-2):305–312, 1990.

[157] S. Yamada, P. Biringer, and K. Bessho. Calculation of nonlinear eddy-current problems by the harmonic balance finite element method. *Magnetics, IEEE Transactions on*, 27(5):4122 – 4125, sep. 1991.

[158] I. Yousept. Optimal control of a nonlinear coupled electromagnetic induction heating system with pointwise state constraints. *Ann. Acad. Rom. Sci. Ser. Math. Appl.*, 2(1):45–77, 2010.

[159] I. Yousept. Optimal control of Maxwell's equations with regularized state constraints. *Computational Optimization and Applications*, pages 1–23, 2011.

[160] S. Zaglmayr. *High Order Finite Element Methods for Electromagnetic Field Computation.* PhD thesis, Universität Linz, Linz, 2006.

[161] E. Zeidler. *Nonlinear functional analysis and its applications. II/A.* Springer-Verlag, New York, 1990.

[162] E. Zeidler. *Nonlinear functional analysis and its applications. II/B.* Springer-Verlag, New York, 1990.

[163] O. C. Zienkiewicz, D. W. Kelly, and P. Bettess. Marriage à la mode—the best of both worlds (finite elements and boundary integrals). In *Energy methods in finite element analysis*, pages 81–107. Wiley, Chichester, 1979.

[164] W. Zulehner. Nonstandard norms and robust estimates for saddle point problems. *SIAM J. Matrix Anal. Appl.*, 32:536 – 560, 2011.

Eidesstattliche Erklärung

Ich, Michael Kolmbauer, erkläre an Eides statt, dass ich die vorliegende Dissertation selbständig und ohne fremde Hilfe verfasst, andere als die angegebenen Quellen und Hilfsmittel nicht benutzt bzw. die wörtlich oder sinngemäß entnommenen Stellen als solche kenntlich gemacht habe. Die vorliegende Dissertation ist mit dem elektronisch übermittelten Textdokument identisch.

Linz, August 2012

_____

Michael Kolmbauer

Curriculum Vitae

Name: Dipl.-Ing. Michael Kolmbauer Bakk.techn.

Nationality: Austria

Date of Birth: 4th February, 1985

Place of Birth: Linz, Austria

Education:

1995–2003	Öffentliches Gymnasium der Benediktiner in Kremsmünster (secondary comprehensive school).
2003–2004	Basic military service, Kremstalkaserne Kirchdorf.
2004–2008	Studies in Technical Mathematics (Bachelor), JKU Linz.
2008–2009	Studies in Technical Mathematics (Master), JKU Linz.
2009–2012	Studies in Technical Mathematics (PhD), JKU Linz.

Professional Career:

2009-2012	Research Assistant, Institute of Computational Mathematics, JKU Linz. FWF Project P19255 and Doctoral Program DK W1214 (project DK4).